Zeitschrift: IABSE reports = Rapports AIPC = IVBH Berichte
Band: 57/1/57/2 (1989)

Rubrik: Session 2: Influence of material properties on the durability of structures

SESSION 2

INFLUENCE OF MATERIAL PROPERTIES ON THE DURABILITY OF STRUCTURES

Leere Seite
Blank page
Page vide

KEYNOTE LECTURES

Leere Seite
Blank page
Page vide

Durability of Concrete — a Measurable Quantity?

Durabilité du béton — quantité mesurable?

Die Dauerhaftigkeit von Beton — Eine messbare Grösse?

Hubert K. HILSDORF
Univ. Professor Dr.-Ing.
Universität Karlsruhe
Karlsruhe, BR Deutschland

Hubert K. Hilsdorf, geboren 1930, promovierte als Bauingenieur an der Technischen Hochschule München. Er ist seit 1953 in der Baustofforschung in der BRD und den USA tätig. Er befasst sich mit Prüfmethoden, Dauerhaftigkeit und Stoffgesetzen von Beton und Mauerwerk. Seit 1977 ist er Ordinarius für Baustofftechnologie an der Universität Karlsruhe.

SUMMARY

The durability of concrete depends primarily on the resistance of the concrete against the ingress of aggressive substances. Though the transport of such substances may follow different mechanisms, it is investigated if a single parameter, the air permeability of concrete is suitable to characterize concrete durability in a general way. A simple test method to determine this parameter is presented. The effect of water-cement ratio and curing on progress of carbonation and rate of capillary suction can be described with this parameter, however, not the influence of type of cement.

RÉSUMÉ

La durabilité du béton dépend de la résistance du béton à la pénétration de substances agressives. Bien que le transport de telles substances puisse se produire selon des mécanismes différents, nous avons examiné si un seul paramètre, le coefficient de la perméabilité à l'air du béton est apte à caractériser généralement la durabilité du béton. Une méthode d'essai simple pour la détermination du paramètre est présentée. A l'aide de cette valeur, il est possible de décrire l'influence du rapport eau/ciment et de la cure sur le progrès de la carbonatation et sur la succion capillaire, mais il n'est pourtant pas possible de mettre en évidence l'influence du type du ciment.

ZUSAMMENFASSUNG

Die Dauerhaftigkeit von Beton wird von seinem Widerstand gegen das Eindringen aggressiver Substanzen bestimmt. Obwohl der Transport solcher Substanzen nach verschiedenen Mechanismen erfolgt, wird untersucht, ob nur ein Parameter, der Permeabilitätskoeffizient des Betons für Luft geeignet ist, die Dauerhaftigkeit von Beton allgemein zu charakterisieren. Es wird ein einfaches Prüfverfahren zur Bestimmung dieses Parameters vorgestellt. Der Einfluss des Wasserzementwerts und der Nachbehandlung auf die Karbonatisierung und auf das kapillare Saugen können mit diesem Parameter beschrieben werden, nicht jedoch der Einfluss der Zementart.

1. INTRODUCTION

The durability of concrete structures depends both on the resistance of the concrete against physical and chemical attack and on its ability to protect embedded steel reinforcement against corrosion. So far, concrete quality is evaluated primarily on the basis of the compressive strength of standard companion specimens. However, irrespective of differences between the concrete in a structure and in a companion specimen, the parameters controlling strength are not identical to those controlling durability. Furthermore, the compressive strength e.g. of a cube depicts an average property of the entire cross-section whereas durability is governed primarily by the properties of the surface near region of a section exposed to an aggressive environment.

Therefore, certain requirements regarding concrete composition as well as type and quality of concrete making materials are specified in most national and international codes in order to ascertain a sufficient durability of the finished concrete structure. However, concrete composition can be controlled reliably only at the mixer, and with a few exceptions a rapid analysis of the composition of fresh concrete still constitutes an unsolved problem [1].

If we can measure the potential strength of a particular concrete, why can't we measure its potential durability? One reason is that "durability" is a collective term for the resistance against a variety of physical and chemical attacks, whose intensity may vary with time. Thus durability always has to be related to a point in time or to the design life of a structure.

However, also "strength" is not a unique property and varies with time. Nevertheless some mostly empirical relations between the compressive strength of a standard specimen and tensile strength, strength under multiaxial states of stress, sustained load and fatigue strength etc. have been derived, are reasonably reliable and widely accepted.

Though there exists no cube test for concrete durability microstructural and other physical properties of concrete may be used to describe the potential durability of a particular concrete.

2. MICROSTRUCTURAL ASPECTS

Though concrete consists of two major phases, the hydrated cement paste and the aggregates, mechanical properties as well as the durability of concrete are governed primarily but not exclusively by the hydrated cement paste. HCP consists primarily of calcium silicate hydrates, calcium hydroxide, calcium aluminate hydrates and residues of unhydrated cement. Additional compounds which exist in smaller quantities such as calcium sulfates, potassium and sodium hydroxides may play a significant role for the durability of concrete.

The hydrated cement paste contains a system of small gel pores and partially continuous capillary pores. Particularly the capillary pores allow the ingress of water or aggressive media so that the most decisive characteristic of durable concrete is a dense pore structure i.e. a low total porosity and pore diameters as small as possible.

The total volume and the diameters of capillary pores decrease with decreasing water-cement-ratio and increasing degree of hydration which in turn depends on the duration of curing and on the age of the concrete [2]. This can be seen from Figs. 1 and 2 which show the size distribution of capillary pores from approx. 5 to 10^5 nm as determined by mercury intrusion porosimetry. With decreasing water-cement-ratio and increasing duration of curing the total capillary porosity decreases, and the pore size distribution shifts to smaller sizes. As a result the hydrated cement paste exhibits a denser structure. This reflects itself in the air permeability of concrete which decreases with decreasing water-cement-ratio and increasing duration of curing as will be shown in chapter 8.

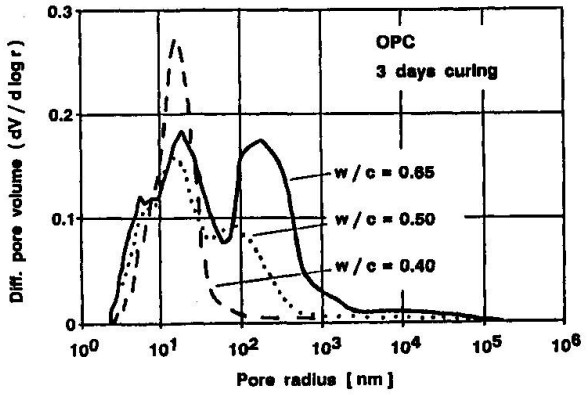

Fig. 1 Effect of water-cement ratio on pore size distribution of hydrated cement paste; ordinary portland cement (OPC); duration of curing: 3 days [3]

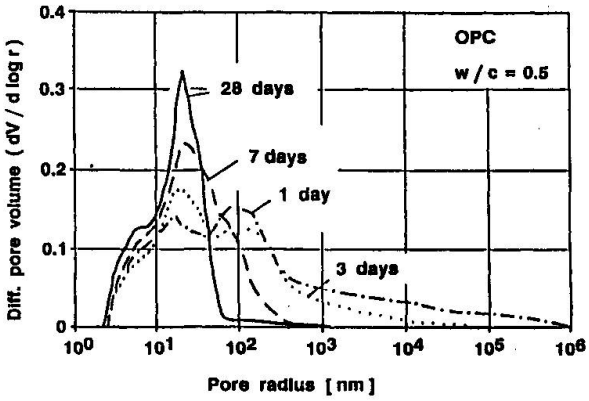

Fig. 2 Effect of duration of curing on pore size distribution of hydrated cement paste; ordinary portland cement OPC; water-cement-ratio = 0.50 [3]

Normal weight aggregates generally have a much lower porosity than the hydrated cement paste and, therefore, play no decisive role for the permeability of a concrete. Though most aggregates are chemically inert some minerals may react with compounds of the hydrated cement paste resulting in concrete deterioration.

The microstructure of the aggregate-cement paste interface generally has a higher porosity and a larger proportion of calcium hydroxide. In addition, microcracks may form at the interface resulting in a higher permeability of concretes compared to that of hydrated cement pastes.

3. SOME MECHANISMS OF PHYSICAL AND CHEMICAL ATTACK OF CONCRETE

The microstructure of concrete may be altered by a variety of external influences which often but not always lead to concrete deterioration. References describing these mechanisms are given e.g. in [2; 3].

Concrete whose pore system is critically water saturated will eventually be destroyed by freezing and thawing. Concrete shows a high resistance to freezing and thawing if the aggregates are frost resistant, if the amount of freezable water in the concrete is low i.e. if the capillary porosity is low and if the paste contains a system of entrained air voids characterized by a spacing factor < 0.20 mm. Such concretes rarely reach a critical degree of saturation. Though the chemical effects of most deicing agents are minor they strengthen the effects of freezing and thawing by increasing the degree saturation and the number of actual freezing and thawing cycles.

Various chemicals such as acids or salt solutions may desolve some compounds of the hydrated cement paste. Chemical reactions may also result in a volume increase of the hydrated cement paste and thus cause disruption of the concrete e.g. if sulfate solutions from the ground water penetrate the concrete and react with the calcium aluminates of the cement to form ettringite.

Some concrete aggregates may contain silicate minerals such as opals or chalcedonites which are partially amorphous and may react with the sodium and potassium hydroxides of the hydrated cement paste. The reaction products form a gel which swells if water is available. As a consequence the concrete may be destroyed due to the swelling pressure.

In all cases of chemical and physical attack the ingress of water into the concrete plays a major role. Therefore, in addition to other measures such as air entrainment or the proper choice of cements, the concrete is the more durable the denser its pore structure.

4. MECHANISMS OF DEPASSIVATION OF STEEL EMBEDDED IN CONCRETE

It is well known that steel embedded in concrete does not corrode even if oxygen and an electrolyte are present. A passive layer is formed on the steel surface in the environment provided by the concrete which is characterized by a pH-value of the pore solution of approx. 12.6. However, under certain circumstances this passive layer may be destroyed resulting in corrosion of the steel.

Many of the durability problems encountered in reinforced concrete structures are caused by carbonation of the concrete. Carbondioxide which occurs in the open air in amounts of approx. 0.03 percent by volume penetrates the dry concrete through the capillary pores and reacts with the calcium hydroxide of the hydrated cement paste and to some extent with calcium silicate hydrates. Calcium carbonate is formed, and the pH-value of the pore solution decreases to values between 8 and 9 so that the passive layer is no longer stable. Carbonation is not necessarily detremental to the mechanical properties of the concrete. Of particular significance in this context is the observation that for concretes made of portland cement carbonation may densify the pore structure, whereas in the case of concretes made of slag cements with a high slag content coarsening of the pore system may occur [2], [4].

Carbonation of the surface near regions of concrete cannot be avoided, however, the rate of carbonation can be kept so low that the carbonation front does not reach the level of reinforcement even after centuries, provided the concrete cover is sufficiently thick.

The progress of carbonation with time can be described on the basis of Fick's first law with sufficient accuracy by eq. 1 [e.g.3]:

$$d_c = \sqrt{2\, D_c \cdot \frac{C_a}{C_c} \cdot t} \qquad (1)$$

where d_c = depth of carbonation [m]
t = duration of carbonation [sec]
D_c = diffusion coefficient of CO_2 through carbonated concrete [m^2/sec]
C_a = concentration of CO_2 in the air [g/m^3]
C_c = amount of CO_2 required for complete carbonation of a unit mass of the concrete [g/m^3].

The term C_c depends on the type of cement as well as on the presence of pozzolans or additions. The diffusion coefficient D_c is controlled primarily by the pore structure and by the moisture content of the concrete. As the relative humidity approaches 100 percent, D_c approaches zero and carbonation seizes. The rate of carbonation is the lower, the lower the capillary porosity of the concrete.

Even if the pH-value of the concrete is high the passive layer on the surface of an embedded steel bar may be locally destroyed by chloride ions penetrating the concrete e.g. by means of sodium chloride solutions used as deicing agents. The prediction of depth of penetration of chloride ions into concrete is difficult because the concentration of chloride ions on the concrete surface is not a constant and because both diffusion and capillary suction may take part in the transport of chloride ions [e.g. 5]. Also the type of cement influences the rate of penetration of chlorides since different types of cement have different binding capacities of chloride ions. Nevertheless, the general rule that dense concrete enhances concrete durability still applies.

5. TEST METHODS TO EVALUATE CONCRETE DURABILITY

Mostly phenomenological test procedures have been developed to estimate the probable behavior of a particular concrete in a given aggressive environment.

Various test methods are described in national and international specifications to determine the freeze-thaw resistance of concrete. In most instances concrete specimens are exposed to cyclic freezing and thawing in water. A decrease in dynamic modulus of elasticity of the concrete or the loss of weight or volume due to surface deterioration of the samples after a given number of freezing and thawing cycles is taken as a measure of the frost resistance of the concrete. Since in such experiments the degree of saturation of the concrete is not a constant but increases with time every concrete will eventually be destroyed once a critical degree of saturation is reached. Therefore, a test method proposed by Fagerlund appears to be the most objective [6]; [7]:

Different concrete specimens of the same mix are brought to different degrees of saturation and exposed to freezing and thawing cycles in a sealed condition. Thus a critical degree of saturation S_{crit} resulting in severe damage after a few freeze-thaw cycles is determined. In additional experiments the uptake of water by capillary suction S_{cap} is determined. Capillary suction-time relationships exhibit two distinct phases: the initial phase during which the water rises up to the top face of the concrete specimen and the second phase during which additional pores such as air voids gradually become water filled. It is the second phase which is of particular significance for the frost resistance of concrete. According to Fagerlund frost resistance F is defined as $F = S_{crit} - S_{cap}$. Thus F depends on the duration of exposure to capillary suction.

To estimate the resistance of concrete against chemical attack generally mortar or concrete samples are placed in solutions of various concentrations. Mostly weight change, change in dynamic modulus of elasticity or length and volume change are taken as relative measures of the resistance of a particular concrete against chemical attack. Deterioration may be accelerated by testing at elevated temperatures. However, the temperature dependence of the various deterioration processes is not well known, and different deterioration mechanisms may take place in different temperature regimes.

The measurement of depth of carbonation using phenolphtaleine as an indicator is well established. However, at least several months are required to estimate the resistance of a particular concrete against carbonation. The use of higher CO_2-concentrations results in an acceleration of carbonation. However, the structure of a concrete after carbonation at e.g. 3 percent CO_2 differs substantially from the structure of a concrete carbonated at 0.03 percent CO_2 [2].

6. TRANSPORT OF LIQUIDS AND GASES IN CONCRETE

The take-up of moisture in the concrete may occur either by permeation of liquid water under an external pressure, by capillary suction of water or by diffusion of water vapor.

Permeation of water through a porous body under a constant pressure gradient is generally described by Darcy's law:

$$Q = K_w \cdot \frac{h}{l} \cdot A \cdot t \qquad (2)$$

where Q = volume of water [m^3] flowing during time t [sec]
$\frac{h}{l}$ = hydraulic gradient in terms of hydraulic head [m/m]
A = penetrated area
K_w = coefficient of permeability of water [m/sec]

The rise of the water level by capillary suction can be expressed in terms of the diameter of the capillaries. However, in hydrated cement paste the pore diameters vary over a range of several orders of magnitude so that capillary suction cannot be expressed on the basis of theoretical considerations. It may be approximated by the following empirical relation [3]:

$$\frac{w}{w_1} = \left(\frac{t}{t_1}\right)^n \tag{3}$$

where w = water absorption at time t
w_1 = water absorption after 1 h
t = time
t_1 = 1 h
n = exponent

For a steady state the transport of water vapor by diffusion can be described by Fick's first law of diffusion. However, in most practical cases a steady state is not reached. Therefore, for transient phenomena Fick's second law of diffusion has to be applied where the diffusion coefficient depends on the moisture concentration:

$$\frac{\partial H}{\partial t} = \frac{\partial}{\partial x}\left[D(H)\frac{\partial H}{\partial x}\right] \tag{4}$$

where H = internal relative humidity at location x
D = Diffusion coefficient [m^2/sec] at relative humidity H

The penetration of gases into concrete by permeation may be expressed by:

$$V = K_v \frac{A}{l}\frac{(p_1 - p_2)}{\eta} \cdot \frac{p^*}{p} \cdot t \tag{5}$$

where V = Volume of gas [m^3] flowing during time t [sec]
p_1-p_2 = pressure difference [N/m^2]
p^* = $p_2 + 0{,}5\,(p_1 - p_2)$
p = local pressure at which V is observed [N/m^2]
l = thickness of member [m]
η = viscosity of the gas [$Nsec/m^2$]
K_v = coefficient of gas permeability [m^2]

The transport of gases by diffusion can be described sufficiently well by Fick's first law. Eq. 1 is an example for the diffusion of CO_2.

From these relations it follows that there is no single materials characteristic to describe the resistance of concrete against the ingress of various aggressive substances. Further research is needed to establish relations e.g. between permeation and diffusion of air and diffusion or capillary suction of water or of aggressive solutions. Nevertheless, an attempt will be made to correlate some durability characteristics with a single concrete parameter, the characteristic air permeability K_{AC} of a concrete disc of given dimensions and age cured and stored in a prescribed way.

7. CONCRETE AIR PERMEABILITY-TEST METHOD

Schönlin developed a test procedure to determine the air permeability of a concrete disc, thickness 40 mm, diameter 150 mm as shown in Fig. 3 [4]; [8]. The concrete sample is cast directly into a rubber ring and is subsequently cured

for 7 days, unless the duration of curing is the variable, and then stored in a constant environment of 20°C, 65 percent RH up to the time of testing at an age of 56 days.

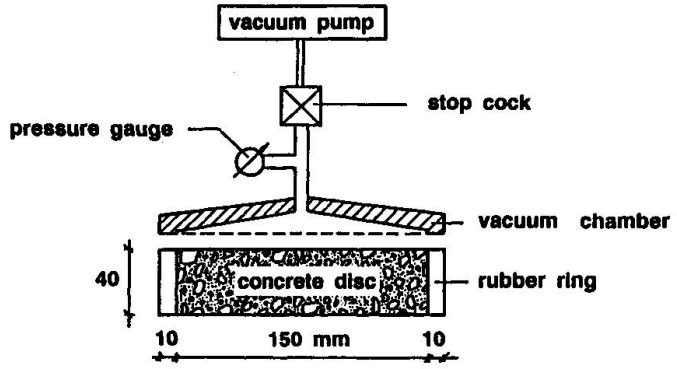

Fig. 3 Apparatus to determine concrete air permeability [3]; [8]

For the test a suction device is placed on one side of the specimen. A vacuum is generated in the space between the specimen and the instrument. After evacuation a stop cock between the vacuum pump and the instrument is closed. The pressure inside the instrument gradually increases and can be read from a pressure gage. A time t_o is taken at the instant the pressure reaches a value of p_o = 20 mbar. The time t_1 corresponds to the time after which p_1 = 50 mbar. The coefficient of permeability of the concrete disc can be calculated from eq. 6 which follows from eq. 5 neglecting the influence of the pressure p and not taking into account the viscosity of air.

$$K_{AC} = \frac{(p_1 - p_o) \cdot V_s}{(t_1 - t_o)\,(p_a - \frac{p_1 + p_o}{2})} \cdot \frac{l}{A} \qquad (6)$$

where
K_{AC} = characteristic air permeability [m^2/sec]
p_1, p_o = pressure inside the suction device at the end and at the beginning of the experiment, respectively
$t_1 - t_o$ = duration of experiment
V_s = Volume of interior of suction device
p_a = atmospheric pressure
l = thickness of the specimen
A = cross-section of the specimen

No special measures are needed to attach the apparatus to the specimen. An experiment takes from a few minutes upt to 60 minutes for very dense concretes. Since the test result depends on the moisture content of the concrete the dimensions as well as the curing and storage conditions have to be kept constant. A similar device has been developed to measure the permeability of the concrete skin of a structure [3]; [9].

8. CONCRETE AIR PERMEABILITY - TEST RESULTS

8.1 Effect of water-cement-ratio and duration of curing

Fig. 4 shows the influence of duration of curing on K_{AC} for concretes made of ordinary portland cement with different water-cement-ratios. Reductions of the

water-cement-ratio or an increase of the duration of curing may lead to a reduction of K_{AC} by more than one order of magnitude.

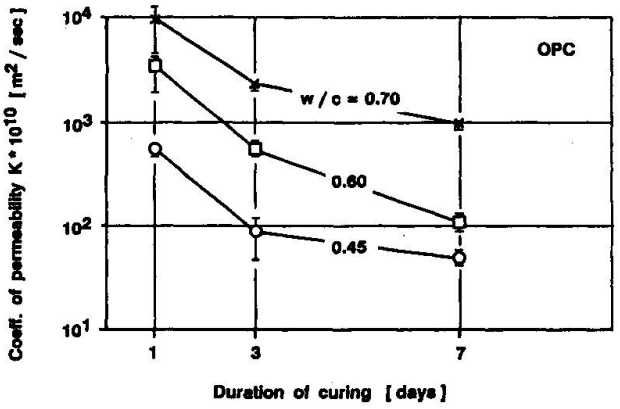

Fig. 4 Effect of duration of curing and water-cement ratio on air permeability of concrete; ordinary portland cement (OPC) [3]

Tests on concretes made of different types of cement with and without additions and cured at different temperatures demonstrated the well known fact that cements containing blast furnace slag or pulverized fuel ash need longer curing periods - other parameters being equal - to reach a certain impermeability [3].

8.2 Permeability and microstructure

There exists a unique relation between the air permeability of the surface near region of a concrete section and microstructural parameters e.g. as given in Figs. 1 and 2 which is independent of type of cement, water-cement-ratio and curing. For further details refer to [3]; [4]; [8].

8.3 Permeability and carbonation

Concrete cubes 150 by 150 by 150 mm, cement content 300 and 360 kg/m^3, respectively, were made of the following types of cement: ordinary portland cement (OPC) with additions of pulverized fly ash (FA) such that 0; 20; 30 or 40 percent of the weight of cement were replaced by FA, and portland blast furnace slag cements (PBFSC) with a slag content of 35 percent and of 65 percent, respectively. Water-cement-ratios of 0.45; 0.60 and 0.70 were employed, and the specimens were cured for 1; 3 or 7 days. After 1 year of storage in air with 0.03 percent CO_2, 65 percent rel. humidity and 20°C the depth of carbonation was determined. For further details refer to [3].

Fig. 5 shows for some of the concretes tested the relation between the square of the depth of carbonation d_c^2 after 1 year and the permeability coefficients K_{AC} on a double logarithmic scale. Two distinct relations exist, one for the concretes made of slag cements with 65 percent slag (PBFSC), the other for the concretes made of portland cement (OPC) with 0 and 20 percent FA replacement and slag cements with 35 percent slag. For the concretes with 30 or 40 percent FA replacement the depth of carbonation for a given permeability K_{AC} increased with increasing FA content.

Eq. 1 in chapter 4 describes the progress of carbonation with time as a function of the diffusion coefficient of carbondioxide through carbonated concrete.

In [10] it is shown that there exists a linear relationship between the logarithms of the diffusion coefficient and of the permeability coefficient of oxygen in non-carbonated concrete. Therefore, it is assumed in the following that a general relation exists also between D_c as defined in eq. 1 and the characteristic permeability coefficient K_{AC}:

$$\frac{D_c}{D_{co}} = \left(\frac{K_{AC}}{K_{ACo}}\right)^m \tag{7}$$

where D_{co}, K_{ACo} = dimensional coefficients

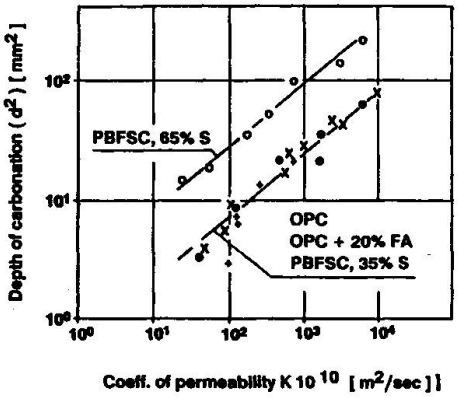

Fig. 5 Air permeability of concrete and depth of carbonation after 1 year at 65 percent rel. humidity and 20° C [3]

From eqs. 1 and 7 the following relation between depth of carbonation d_c at time t for a concrete with a characteristic permeability K_{AC} can be deduced:

$$d_c = d_{co}\sqrt{\frac{(K_{AC})^m}{K_{ACo}} \cdot \frac{t}{t_o}} \tag{8}$$

The depth of carbonation d_c of concretes with different values of K_{AC} exposed to certain environmental conditions after an exposure time $t = t_o$ can be expressed as follows:

$$\log d_c^2 = \log d_{co}^2 + m \cdot \log \frac{K_{AC}}{K_{ACo}} \tag{9}$$

Such relations can be determined from the experimental results presented in Fig. 5 for t_o = 1 year. Apparently, these results closely follow eq. 9. The power m in eqs. 7 through 9 is given by the slope of the streight lines in Fig. 6. It is independent of the type of cement, m = 0.5. If we set K_{AC} = 1, $\log d_{co}^2$ is given by the intersect of the streight lines with the $\log d_c^2$-axis:

$\log d_{co}^2$ = -0.15 for OPC, OPC + 20 % FA and PBFSC, 35 % S

and $\log d_{co}^2$ = +0.45 for PBFSC, 65 % S

The most significant conclusion to be drawn from these experiments is the ob-

servation that for given environmental conditions and a given type of cement there exists a unique relation between the characteristic air permeability K_{AC} and the progress of carbonation which is independent of water-cement ratio, curing and cement content within the range investigated. The reasons why d_{CO} depends on the type of cement may be twofold: C_c in eq. 1 i.e. the amount of CO_2 required to carbonate the concrete is influenced by the type of cement. Furthermore, carbonation itself alters the pore structure of HCP differently depending on the type of cement [2].

It has to be pointed out that the applicability of eq. 8 to carbonation of concrete in a structure still has to be verified by long term observations of concrete with a known K_{AC} under natural exposure conditions. This is particularly true for the values of d_{CO} given above which are valid only for the controlled laboratory environment prevailing during these experiments.

8.4 Permeability and capillary suction

The uptake of water by capillary suction was determined on the same concrete discs, thickness 40 mm, diameter 150 mm, which were used to measure the characteristic air permeability. Concretes made with different types of cement, water-cement-ratios, and durations of curing were investigated. For further details refer to [3]. Immediately after the determination of K_{AC} the specimens were brought into contact with a water bath, and the uptake of water was measured. The results closely followed eq. 3.

It was found that there exists a linear increase of w_1 in eq. 3, the water absorption after 1 hour, with the logarithm of K_{AC}. The relation between the power n in eq. 3 and K_{AC} is given in Fig. 6. Only for rather permeable concretes values of n = 0.5 as reported in [6], [7] were observed. For a given value of K_{AC} concretes made of slag cement with 65 percent slag show a significantly lower value of n and thus absorb water by capillary suction at a slower rate than portland cement concretes. For very low values of K_{AC} the relations between n and K_{AC} approach a horizontal slope. This may be due to differences in the transport of moisture and of air in porous media, a phenomenon which should be studied in more detail in the future.

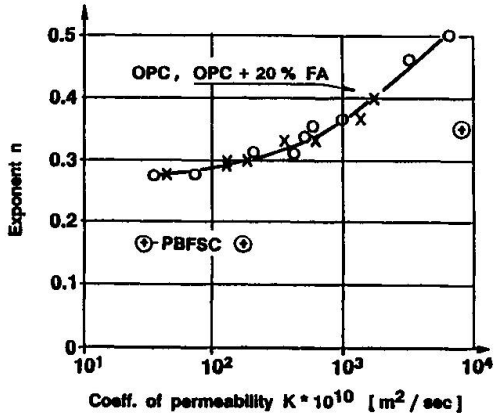

Fig. 6 Air permeability of concrete and rate of water absorption [3]

In these studies only the initial phase of water absorption by capillary suction as referred to in chapter 5 has been observed. So far it is not known if also the point of transition from the first to the second phase and the second phase itself can be described in terms of K_{AC}.

8.5 Permeability and other concrete durability properties

There is no doubt that a reduction in concrete permeability leads to an enhanced frost resistance of the concrete. This is supported by test results described in [3]. However, it is unlikely that a unique relation exists between the critical degree of saturation as defined in chapter 5 and K_{AC}. In particular the effects of air entrainment will not reflect themselves in the characteristic air permeability.

Other parameters being equal concrete resistance to chemical attack will increase as K_{AC} decreases. However, the chemical composition of the cement paste i.e. the type of cement used will in many instances have a dominating effect.

The same is true for the resistance of concrete to chloride penetration. Though in [3] a close relation between depth of penetration of chloride ions due to capillary suction and K_{AC} was found the effect of the binding capacity of the concrete and thus type and amount of cement and additions will be the dominating parameters.

9. CONCLUSIONS

- A characteristic air permeability coefficient K_{AC} of a standard concrete specimen which has been cured and preconditioned in a standardized way can be determined rapidly and reliably with the test procedure developed by Schönlin.

- The characteristic air permeability coefficient K_{AC} correlates well with the progress of carbonation under laboratory conditions. Effects of water-cement ratio and curing reflect themselves in K_{AC}. However, if cements containing larger amounts of components other than portland cement clinker such as pulverized fly ash or slag are used the relation between depth of carbonation and K_{AC} is no longer unique.

- Other parameters being equal concretes absorb water by capillary suction the slower the lower K_{AC}. Consequently they show a higher resistance to freezing and thawing, to chemical attack and to the pentration of chloride ions than concretes with a higher K_{AC}. But other microstructural and chemical aspects which do not reflect themselves in K_{AC} such as air-entrainment or composition of the cement may be of equal significance.

- Thus, concrete air permeability K_{AC} is not the unique parameter to describe concrete durability, and it is unlikely that such a parameter exists. Nevertheless, it is advantageous to characterize concrete not only in terms of its standard compressive strength but also in terms of K_{AC} since together with a knowledge of the type of cement it reveals the effects of several technological parameters such as composition and curing on the potential durability of a particular concrete.

10. REFERENCES

1. NÄGELE E., HILSDORF H.K., Die Frischbetonanalyse auf der Baustelle. Beton, Heft 4, 1980.

2. BIER Th.A., Karbonatisierung und Realkalisierung von Zementstein und Beton. Schriftenreihe des Instituts für Massivbau und Baustofftechnologie, Universität Karlsruhe, Heft 4, 1988.

3. SCHÖNLIN K., Permeabilität als Kennwert der Dauerhaftigkeit von Beton. Schriftenreihe des Instituts für Massivbau und Baustofftechnologie, Universität Karlsrune, Heft 8, 1989.

4. KROPP J., Karbonatisierung und Transportvorgänge in Zementstein. Dissertation, Universität Karlsruhe, 1983.

5. P. JUNGWIRTH, W. BEYER, P. GRÜBL, Dauerhafte Betonbauwerke, Substanzerhaltung und Schadensvermeidung in Forschung und Praxis. Beton-Verlag, Düsseldorf, 1986, pp. 167.

6. FAGERLUND G., The critical degree of saturation method of assessing the freeze-thaw resistance of concrete. Prepared on behalf of RILEM Committee 4DC, Matériaux et Constructions, Vol. 10, 1977, pp. 217.

7. FAGERLUND G., The international cooperative test of the critical degree of saturation method of assessing the freeze-thaw resistance of concrete. Matériaux et Constructions, Vol. 10, 1977, pp. 231.

8. K. SCHÖNLIN, H.K. HILSDORF, The potential durability of concrete. IV European Ready Mixed Concrete Organisation Congress, Stavanger 1989.

9. K. SCHÖNLIN, H.K. HILSDORF, Evaluation of the effectiveness of curing of concrete structures. Concrete Durability, Katharine and Bryant Mather International Conference, American Concrete Institute SP-100, 1987, pp. 207.

10. LAWRENCE C.D., Transport of oxygene through concrete. The British Ceramic Society Meeting - Chemistry and chemically related properties of cement. Imperial College, London, 1984.

Leere Seite
Blank page
Page vide

Influence of Material Properties on the Durability of Structures

Influence des caractéristiques des matériaux sur la durabilité des structures

Einfluss von Materialeigenschaften auf die Dauerhaftigkeit von Bauwerken

Steen ROSTAM
Assoc. Professor
Techn. Univ. of Denmark
Copenhagen, Denmark

Steen Rostam, born 1943. MSc 1969 and PhD in 1978 from the Technical University of Denmark. Employed by COWIconsult since 1972. Head of Development and Coordination of Concrete Technology. Since 1978 Associate Professor in concrete bridge design and durability of concrete structures. Member of the Administrative Council of CEB and Reporter of Task Group Durability.

SUMMARY

The influence of material properties on the durability of structures is an integrated part of the interaction between environmental aggressivity and the resistance of the structure. Durability is treated in a Service Life concept depending on level of modelling of deterioration mechanisms. The Service Life achieved depends on initial decisions, codes and standards and on Management and Maintenance Systems employed. CEB-FIP Model Code 1990 is the first Service Life Code and helps bridge the communication gap between material scientists and structural engineers.

RÉSUMÉ

L'influence des caractéristiques des matériaux sur la durabilité des constructions est une partie intégrante de l'interaction entre l'aggressivité du milieu ambiant et la résistance de la structure. La durabilité est traitée dans le concept Durée de vie dépendant du niveau de détail de la modélisation des mécanismes de détérioration. La Durée de vie dépend des décisions initiales, des codes et des normes et des systèmes de gestion et de maintenance utilisés. Le Code Modèle CEB-FIP 1990 est le premier code de Durée de vie, et permet de rétablir le dialogue entre les spécialistes de la science des matériaux et les ingénieurs civils.

ZUSAMMENFASSUNG

Der Einfluss von Materialeigenschaften auf die Dauerhaftigkeit von Bauwerken ist Bestandteil der Wechselwirkung zwischen der Aggressivität der Umwelt und der Widerstandsfähigkeif des Bauwerks. Die Dauerhaftigkeit wird in einem Nutzungsdauer-Konzept behandelt, welches vom Niveau des Modells für den Alterungsprozess abhängt. Die erreichte Nutzungsdauer ihrerseits hängt ab von anfangs getroffenen Entscheidungen, von Vorschriften und Normen und von den angewandten Verwaltungs- und Unterhaltungssystemen. Der CEB-FIP Model Code 1990 (Mustervorschrift) ist die erste Vorschrift zur Nutzungsdauer, und hilft die Verständigungslücke zwischen Materialforschern und Bauingenieuren zu überbrücken.

0. INTRODUCTION

The influence of material properties on the durability of structures is an integrated part of the overall interaction between the

- aggressivity of the environment, and the
- resistance against premature degradation as provided by the structure.

The environmental aggressivity is determined by the

- moisture availability
- temperature level
- type and amount of aggressive substance in gaseous or dissolved form,

and the concentrations, variations and gradiants of these parametres on a micro-environmental scale determined very locally by the interaction between the environment and the stucture.

The resistance of a structure against premature degradation, when exposed to an aggressive environment, is determined by the combined effect of the

- structural design and layout as fixed by the architect and the engineer,
- building material, or combination of the chosen materials,
- quality of execution, determining if the in-situ material properties are obtained including their variability,
- development of material properties with time, as determined by the physico-chemical micro-environment and type, level and frequency of maintenance performed.

0.1 Building Materials

The most widely used building materials are concrete, steel, wood and masonry, and the aggressivity of an environment differs considerably, depending on which building material that is being employed in the structure.

Our traditional approach in constructing and maintaining buildings differs surprisingly, depending on the chosen building material. In crude form this means that

- **Masonry** is chosen for wall-type structures in compression and is in general considered to be a robust low-maintenance material mainly because of its inorganic nature resembling stone. Its sensitivity to salt bursting caused by crystal growth in a polluted environment, sensitivity to moisture accumulation and freeze-thaw action often comes as a surprise, though these mechanisms are well-known to material scientists.
- **Wood** is a very versatile material, but its organic nature has led to the acceptance, that exposed structures very early need a regular maintenance and supplementary protection in the form of paint and impregnation.
- **Steel** is a high performance refined material threatened only by rusting, so regular re-painting will ensure a long term durability.
- **Concrete** is a unique material due to its as believed very simple production out of domestic materials, and due to its formability. The development of reinforced and prestressed concrete has created an ideal interaction between steel and concrete judged from a load carrying and a

durability point of view. The inorganic nature and the strength levels of concrete, make users believe that this material in all respects is superior to natural stone, and to constitute maintenance-free structures.

The errors in these simplistic characteristics are painfully evident, looking at the durability problems arising in many areas all over the world.

The structural engineer and the user have forgotten the thermodynamic instability inherently associated with these highly energy containing, worked materials. However, the physicists and chemists (material scientists) have had a clear mind on these durability problems for more than a century. This raises the questions:

- Why does this serious knowledge gap prevail today?
- How do we overcome the problems?
- Will theses problems last into the next century?
- Who should lead the way - those who mainly know the answers (material scientists) or those who have realized their own ignorance and ask the questions (structural engineers)?

1. SERVICE LIFE OF STRUCTURES

The natural ageing of building materials renders the concept of "Durable Structures" non-operational in practice because it leaves the questions "How durable?" and "Durable for how long?" unanswered. By considering the associated time scale, a "Service Life Concept" evolves which is directly applicable by the structural engineer when handling design of new structures and when assessing the residual service life of existing structures (1).

These considerations have led to the definition of the Service Life of a structure, as being the time for which the structure satisfies the imposed functional requirements, without needing unforeseen or excessive costs for maintenance and repair.

In this way durability is not merely a technical problem of relevance mainly to the engineer and the scientist, but becomes a combined technical and economic problem, which directly reflects the interest of the user and the owner (2).

1.1 Technical, Economic and Functional Service Life

The Technical Service Life depends on the performance of the materials and the structure in time, when exposed to a given environment.

The Economic and Functional Service Life depends on the economic demands in time, to ensure safe and satisfactory use of the structure.

The Economic and Functional Service Life of structures is a political instrument in the overall economic optimization of costs for creating a structure and keeping it in operation. The required minimum quality of a structure may reflect:

- the condition of structural and non-structural elements,
- the load carrying capacity, or safety, of the structure,

- the geometric restraints such as clearances, construction depths, etc.,
- the aesthetical qualities of the ageing structure.

Political decisions may influence the imposed requirements with respect to

- the safety level required
- the design loads and required clearances (room heights, bridge clearance, etc.)
- the acceptable appearance.

Changes in such requirements will simultaneously change the corresponding residual Economic and Functional Service Life, although the Technical Service Life is kept unaltered. In practice it would be optimal, if the Technical Service Life is longer than or equal to the Economic and Functional Service Life.

The Service Life Concept allows individual design policies to be pursued for each structure, based on an economic sub-optimization of the economy of each individual owner. From society's point of view this will soon become an unacceptable situation, why some uniformity must be ensured. This is mainly achieved through Codes and Regulations which may be tailored such as to ensure a reasonable uniformity in the safety and the serviceability of similar structures over the years, i.e. ensure an acceptable service life of the structures viewed from the point of view of society.

2. CONCRETE STRUCTURES - A LONG TERM CHALLENGE

Out of the previously mentioned four main building materials, concrete and concrete structures, including reinforced and prestressed structures, present probably the most complicated set of problems with respect to the durability and service life of structures.

Concrete is a conglomerate of many different inorganic materials bound together by several types of cementiteous and pozzolanic materials. The size of each particle is several orders of magnitude larger than the individual particles in other materials such as steel, and each particle (aggregate) is in itself a complicated component.

The production of concrete, and the execution of concrete structures, follows very simple procedures compared to the procedures in other structural technologies such as in the airplane, nuclear and electronic industry. Therefore, the influence of workmanship and the conditions of execution has a very pronounced influence on the quality of the outcome of the process.

2.1 "Lab-crete" and "real-crete"

The hardened concrete achieved on site very often differs substantially from the specified concrete, and when quality is to be verified, specially cast and cured cylinders or cubes are produced, and tested for strength. The sometimes humorous differentiation between "lab-crete", representing performance test specimens and specimens for research, and "real-crete", representing the in-situ concrete, is a serious matter when evaluating the durability of structures. A service life design having a reasonable degree of reliability will have to be based on in-situ measurements of the decisive parametres for durability as determined from the deterioration mechanisms which threaten the structures.

The variability of in-situ concrete quality is even more pronounced, when the hardening and curing conditions are taken into account. If the curing does not control the moisture exchange between hardening concrete and the environment, the surface layer - or skin - of concrete will exhibit early micro-cracking and even plastic shrinkage cracking, due to drying out, or may be harmfully porous due to excessive water uptake during the curing process. Similarly, the temperature levels and temperature differences between the newly cast concrete and the surrounding air, or between new and old concrete across a construction joint must be kept below specified values to avoid the early age cracking which will once and for all open up the concrete for penetrating aggressive agents including water.

2.2 Strength versus durability

The traditional 28 day strength requirement for concrete has been a simple and operational means of verifying the strength requirements. With the growing concern for durability, this parameter is not sufficient to reveal the durability characteristics of concrete. Much more involved testing is required in order to clarify if a concrete will be durable in a structure exposed to certain aggressive environments.

2.2.1 Testing for durability

Nearly all deterioration mechanisms depend on some type of aggressive media entering from the surrounding environment through the surface of the concrete and penetrating into the concrete. The one most important substance promoting deterioration is water. In fact only mechanical damage and temperature differences may cause damage without the governing influence of water.

The important rate-determining parameter then becomes the rate of penetration of aggressive substance including water. The permeability and the diffusivity of the concrete becomes decisive, and especially the conditions of the outer concrete layer, i.e. the skin of the concrete, or possibly the concrete cover will be a main controlling factor in the rate of deterioration.

There is no tradition for designing concrete with low permeability nor any well established test methods to verify the permeability of structural concrete. The permeability also differs for the same concrete, depending on the penetrating medium such as gaseous substance (CO_2), water, and chlorides dissolved in water. New concrete mix designs are currently being developed to cope with the service life requirements.

The one well established parameter controlling the permeability and diffusivity of concrete is the W/C-ratio. A very low W/C-ratio, usually achieved by introducing plasticising or superplasticising admixtures, will enhance the durability. Penetration of chlorides is a main governing risk with respect to corrosion of reinforcement. However, pozzolanic admixtures develop their properties at very different rates. Microsilica usually reacts very quickly, and the effect is obtained after just a few days. Contrary to this flyash reacts very slowly, and the effect is usually not traceable at the classical 28 days testing age. After 3 months a considerable improvement in permeability and diffusivity e.g. in connection with chloride penetration, is observed, but the effect may still improve after 1-2 years. Consequently the age at which veryfying tests shall be performed is very difficult to fix, and the 28 days testing age with respect to concrete strength cannot uncritically be maintained when the effects on durability are considered. This has further implications when performing pre-produc-

tion trials and production controls, as the test results are not available until long after production has started or corrective interventions have become very difficult.

2.3 Hazards

Due to the usual progression of deterioration from the surface inwards and due to the composite nature of concrete structures, where concrete is combined with reinforcement, deterioration may have different consequences.

The corresponding hazards may be graded as follows (3):

- local hazards, where the surface of the structure slowly disintegrates and spalls due to cracking of the concrete (freeze/thaw action, Alkali-Silica Reactions etc.) or due to corrosion of the reinforcement. This creates serious hazards for users and bypassers risking being hit by falling debries. In the initial stage of development this does not cause noticeable reductions in overall load carrying capacity, stability and safety of the structure.
- global hazards,where damage has developed to such an extend that the structural integrity, stability and safety is reduced, and parts of or the whole structure may collapse or otherwise become unfit for use.

In this respect the warning associated with initial cracking, miscolouring and spalls are valuable signals of distress which should not be left unattended.

2.4 Concrete is expected to crack

It should be recalled, that concrete structures by virtue of their designed load uptaking mechanics are expected to develop load induced cracks with limited crack widths. For this reason cracking in concrete structures shall not à priori be considered signs of deterioration or malfunction.

3. DETERIORATION MODELLING

In order to understand the mechanisms of deterioration it is essential that physico-chemical models are available explaining how degradation occurs and clarifies which parametres are governing the process. This knowledge is a prerequisite in order to:

- perform a rational assessment into the damage type and the rate of development,
- select correct interventions and remedial measures and avoid aggravating the ongoing degradation, - the latter point unfortunately often being the case when incorrect remedial measures are being employed,
- avoid premature deterioration to develop in future structures,
- perform relevant maintenance during the operation of structures.

Decisions on these aspects are usually taken by structural engineers whereas the deteriorating processes are occurring within the micro-structure of the materials. The problem thus contains an inherent conflict between the level of modelling being directly or indirectly employed.

3.1 Micro, mesa or macro level of modelling

The deep insight into materials behaviour is represented by the materials scientist who naturally bases his models on micro-level materials science models whereas the structural engineer takes decisions based on his understanding of the problem which incorporates macro-level modelling or structural engineering models.

If these two basically different levels of modelling are not fully clarified in the information transfer between the structural engineer and the materials scientist, misunderstandings will occur. They will not speak the same language, and the so called communication gaps develops. The intermediate, or mesa-level modelling, performed by the materials engineer is an attempt to help bridging the main communication gap between micro-level and macro-level approaches.

However, it should be clear, that models on each level have the same degree of validity and are all indispensable. I.e. micro-level models are not necessarily more correct, or better than macro-level models.

3.2 Modelling, credibility and education

The tasks of the scientists and the engineers are to ensure compatibility between models on different levels treating the same phenomena. This is maybe the area most neglected in modern materials science and materials engineering; a communication problem that may well continue to create the most serious conflicts in the building and construction sector, including repair and rehabilitation.

The situation may well remain so well into the next century, if our engineering educational system is not changed. This represents the most serious dilemma of our profession in our relations to society and is contributing to our growing credibility problem. The lack of interdisciplinary understanding (and mutual respect) among engineers makes it especially difficult to cope with the durability problems of our structures, because these problems encompass all the disciplines of the engineer such as

- structural design, statics and mathematics,
- materials and their degradation,
- heat and moisture insulation,
- climatic conditions,
- execution and maintenance,
- repair and strengthening.

Information must be received and transferred between the different levels of detailing. This highlights the true need for a professional and rational interdisciplinary scientifically based engineering curriculum, - a true poly-technical education (4).

4. EXISTING STRUCTURES

4.1 Operation and maintenance strategies

Recent years growing durability problems with part of the existing buildings and structures have emphasized the need to follow a rational operation and maintenance strategy in the upkeep of structures.

These problems have grown to levels where the traditional approach of repairing damaged structures and attempting to bring them back near to initial quality will be exorbitantly expensive. Completely new ways of handling these problems on both structural level, and safety and reliability level have been sought. In the intermediate say 10 years with unclear maintenance and repair strategies the size of the problems have been close to getting out of hand, especially what concerns problems associated to concrete structures, because major parts of concrete problems are rather new and the total number of concrete structures is very large.

Today we have realized the following needs

- Repairs do not necessarily have to re-install initial or near initial quality and performance, a sufficient target quality of the repaired structure must be determined.
- From a service life concept point of view the economic optimization will often lead to the conclusion that repair and upgrading is not optimal, and a decision of non-repair together with an intensified inspection and maintenance routine, e.g. including monitoring, may well be the optimal solution. I.e. degenerate under control.
- The traditional visual inspections of structures may tend to maximize maintenance costs instead of the minimizing effect sought. The reason being that interventions are not made until an active or rapidly propagating deterioration mechanism is in progress. Preventive maintenance is thus not applicable or is of very little value.
- Deterioration mechanisms threatening our building materials in the structures must be clarified, and the main governing - and influenceable parameters must be identified in order to allow for a repair procedure which can slow down or stop an ongoing deterioration.
- Inspection procedures - also so-called superficial inspections - should include on-site testing to determine the degree of break-down of inherent protective effects in the structure. For concrete structures this means determining the current state with regard to e.g. carbonation depth, chloride penetration, electro-chemical potentials, depth of deleterious reactions, residual bar diameter etc.
- Preventive maintenance performed before the onset of rapid propagation of deterioration will be a very cost-effective way of prolonging the service life of structures. This leads to a need to make users and owners of structures much more conscious of the long term economic benefits of such interventions. This task is difficult from a political and psychological point of view, because maintenance activities must be performed on an otherwise intact structure showing no visual signs of distress.
- In order to keep track of the condition of structures and their time-dependent developments, rational management systems should be employed.

Thus the management of structures becomes a major task in the overall optimization of costs and technical efforts in the upkeep of structures (5).

4.2 Structures Management and Maintenance Systems

Structures Management and Maintenance Systems thus performs a rational and systematic administration of structures aiming at:

- maintaining an acceptable performance of each structure
- ensuring an optimum economic service-life of each individual structure.

In doing this, the following factors shall be considered:

- safety, local as well as global,
- current construction and repair technology,
- economic constraints,
- aesthetics,
- social and political aspects.

It shall be noted, that the road and bridge sector has been the forerunners with respect to combined Bridge Management and Maintenance Systems. Much value can be gained by profiting from experience from this field (6).

5. DESIGN OF NEW STRUCTURES

5.1 Codes and standards

Codes and standards constitute the legal technical basis for structural design and execution. They represent the requirements of society towards safety and serviceability in the complex task of creating structures. Thereby codes and standards constitute the most important structural design pre-requisites, and will remain to do so in a foreseeable future. Codes often incorporate centuries of invaluable national or regional experience. As such they may, however, at times be regarded as obstacles towards introducing new technologies.

Recent years' rapid technological development coinciding with the growing awareness to consider the long term durability of structures present a challenge to code writers. Future generations of codes shall focus on formulating basic principles of long term validity and allow freedom and openness in specifying means of fulfilling these principles. Only so can they be sufficiently flexible to profit from new technological achievements and accomodate new techniques without loosing the valuable parts of accumulated experience.

Concrete is - and will continue to be - our most important building material and ongoing international concrete code-writing activities will strongly influence the civil and structural engineering profession and may well set milestones for the code developments for other materials.

5.2 CEB-FIP Model Code 1990

CEB is, in cooperation with FIP, currently preparing a new Model Code for Concrete Structures for the 90'ies, MC 90. The Model Code attempts to incorporate service life design concepts in an operational code-like format penetrating all relevant aspects of safety and serviceability. By avoiding that service life aspects constitute a separate limit state, but are integrated into sections of Ultimate Limit State and Serviceability Limit States, a harmonic evolution of the Model Code is ensured. The Model Code is further supported by a separate Design Guide: "CEB -Guide to Durable Concrete Structures" (7).

MC 90 thus leads towards a new generation of structural Codes of Practice being prepared for concrete structures, but being conceptually adaptable to codes for other building materials. This represents the internationalization of design concepts which is leading to ongoing harmonization of codes

and standards, e.g. as represented by the Eurocodes and Euronorms of the European Community and by the Comecon Codes of the CMEA countries in Eastern Europe.

This valuable achievement can be attributed mainly to the year-long international professional cooperation within private organizations like IABSE, FIP, RILEM and CEB.

5.2.1 Service Life Requirements in CEB-FIP Model Code 1990

The basic requirements in the Draft CEB-FIP Model Code 1990 currently under discussion are (8):

"Concrete structures shall be designed, constructed and operated in such a way that, under the expected environmental influences, they maintain their safety, serviceability and acceptable appearance during an explicit or implicit period of time without requiring unforeseen high costs for maintenance and repair".

In order to fulfil these requirements the Draft - Model Code focus on the whole building process. It is assumed that durability problems only can be avoided if adequate and coordinated efforts are imposed upon all persons involved and upon all phases in the process of defining, planning, building and using the structure until the end of its expected lifetime.

The whole process of creating structures and keeping them in satisfactory use and service requires cooperation between the following four parties:

- The owner, by defining his present and foreseen future demands and wishes.
- The designers (engineers and architects) by preparing design specifications (including quality control schemes) and conditions.
- The contractor who will try to follow these intentions in his construction works. Most commonly also subcontractors are involved.
- The user, who will normally be responsible for the maintenance of the structure during the period of use.

Any of these four parties may - by their actions or lack of actions -contribute to any unsatisfactory state of durability of the structure and thus cause a reduction of the service life. Also interactions between two parties may cause faults which can have an adverse effect on durability and service life.

5.2.2 Decisions on design life and exposure class

The selection of design life and of exposure class constitute the two most important decisions with respect to the resulting long term durability and appearance of the structure.

The required service life should be obtained without relying on special protections needing frequent maintenance or redoing. However, in cases of especially aggressive environments special protective measures may be foreseen.

5.2.3 Service Life Design Strategy

The design strategy should consider possible measures protecting the structure against premature deterioration. A set of appropriate measures (one or more) shall be combined to ensure that the required service life is obtained with a sufficiently high probability.

Protective measures may be established by, i.a.:

- the selected structural form,
- the concrete composition, including special additions or admixtures,
- the reinforcement detailing including cover,
- a special skin concrete quality, including skin reinforcement,
- limiting or avoiding crack development and crack widths by prestressing,
- additional protective measures such as tanking, membranes or coatings, including coating of reinforcement,
- specified inspection and maintenance procedures during in-service operation of the structure, including monitoring procedures,
- special active protective measures such as cathodic protection or warning systems.

A service life design may profit from a multitude of protective measures cooperating simultaneously to ensure the required service life with an acceptable level of reliability.

This design strategy is considered a Multistage Protection Strategy which leaves the selection of individual protective measures to the designer.

6. RESEARCH, DEVELOPMENT AND EDUCATION

The durability problems facing the structural engineer has lead to a dilemma in the research community.

It is a well established procedure in research, that complicated problems are split into more easily defined part-problems. These part-problems are then solved one by one, and the results combined to constitute the answers to the initial and more complicated problems.

However, the durability problems - especially in the field of concrete structures - have proven to be so interdependent that splitting may result in misleading conclusions. The interdisciplinary problems relate partly to macro-level and partly to micro-level problems including physical, chemical, electro-chemical and even biological processes, which complicate the problem solving process even further.

In this connection it should be recalled, that the durability problems in so-called more advanced technologies like the aircraft, space and nuclear industries are faced with only one major problem of durability, being the development and growth of cracks (3). In this way the assessment and maintenance activities are reduces to - crudely speaking - a simple analysis, track recording, and management of crack propagation.

The complexity of the durability problems are in reality shaking the established scientific schooling, and a new multidisciplinary approach must evolve from the turmoil.

Part of the problems may also be related back to our basic education in which two simplifications distort part of our spontaneous understanding of the problems:

- we think in linear scales, both in geometric terms and in time,
- we think in deterministic events.

For reasons above, we are faced with a communication gap between engineers and everyday people not trained in a technical approach to problems.

The technical community should therefore concentrate more effort in presenting and explaining the problems of durability and service life considerations - and the uncertainties associated with our answers - to the users and owners of the structures, including lawyers, politicians and other decision makers. Education is needed on all levels!

7. REFERENCES

(1) FAGERLUND, Göran, "Service Life of Structures", General Report Session 2.3. Proceedings RILEM Symposium: Quality Control of Concrete Structures, June 1979, Stockholm, Sweden.

(2) GOTFREDSEN, Hans-Henrik, "Economic Aspects in Planning of Bridge Rehabilitation and Repair". IABSE Symposium on Bridge Rehabilitation and Repair, Washington, 1982.

(3) ROSTAM, Steen, Report of Discussion Group on Metallic Materials. "Problems in Service Life Prediction of Building and Construction Materials". NATO ASI Series E No. 95, Martinus Nijhoff Publishers, 1985.

(4) HANSEN, Torben C., "Towards a Unified Engieering Education in Concrete Techology", CEB-RILEM International Workshop: Durability of Concrete Structures". CEB-Bulletin d'Information No. 152, 1984.

(5) ROSTAM, Steen, "Bridge Monitoring and Maintenance Strategy". US-European Workshop: Rehabilitation of Bridges. Paris, France, June 1987. Workshop Report.

(6) SØRENSEN, Anders B., DAVIDSEN, Lone, "Micro-Computer Based System for Management of Bridges", IABSE, 13th Congress June 6 - 10, 1988, Prereport.

7) CEB, "Draft - Guide to Durable Concrete Structures." CEB-Bulletin d'information No. 166, May 1985.

(8) CEB-FIP, "Model Code 1990", First Predraft 1988, CEB-Bulletin d'Information No. 190.

PRESENTATIONS

Leere Seite
Blank page
Page vide

Diffusion de gaz et durabilité du béton armé

Gasdiffusion und Dauerhaftigkeit von Stahlbeton

Diffusion of Gas and Durability of Reinforced Concrete

Yves F. HOUST
Chimiste
Ecole Polytechnique Fédérale
Lausanne, Suisse

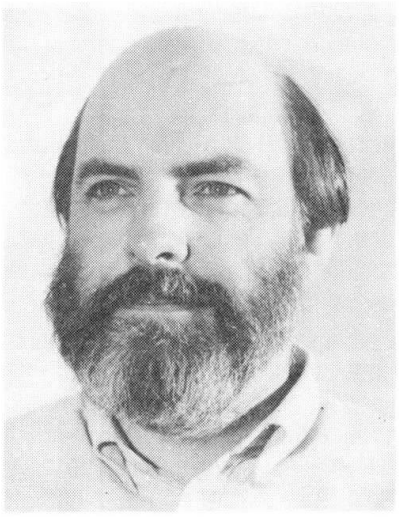

Yves F. Houst, né en 1946, est diplômé de chimie de l'Université de Lausanne. Il travaille dans le domaine des matériaux de construction depuis 16 ans. Il est actuellement chef de la section chimie au Laboratoire des Matériaux de Construction de l'Ecole Polytechnique Fédérale de Lausanne.

Folker H. WITTMANN
Professeur
Ecole Polytechnique Fédérale
Zurich, Suisse

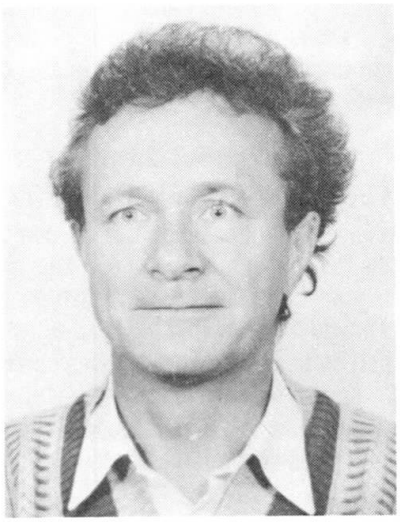

Folker H. Wittmann, né en 1936, est gradué en physique. Il fut 4 ans professeur de matériaux de construction à l'Université technique de Delft (Pays-Bas) et 8 ans à l'Ecole Polytechnique Fédérale de Lausanne. Il est actuellement Professeur ordinaire de matériaux de construction à l'Ecole Polytechnique Fédérale de Zurich.

RÉSUMÉ

Une méthode de mesure du coefficient de diffusion des gaz à travers la pâte de ciment durcie est décrite. On peut surtout étudier l'influence de la teneur en eau et de la porosité sur la diffusion de l'oxygène et du gaz carbonique. Les premiers résultats sont indiqués.

ZUSAMMENFASSUNG

Es wird eine Methode zur Bestimmung der Gasdiffusionskoeffizienten von Zementstein beschrieben. Insbesondere der Einfluss des Feuchtigkeitsgehaltes und der Porosität auf die Diffusion von Sauerstoff und Kohlendioxid kann damit untersucht werden. Über erste Ergebnisse wird berichtet.

SUMMARY

A method to determine the coefficients of gas diffusion in hardened cement paste is described. The influence of moisture content and porosity on diffusion of oxygen and carbon dioxide in particular can be studied. Preliminary results are presented.

1. INTRODUCTION

La carbonatation du béton armé et ses conséquences sur la corrosion des armatures est un phénomène connu depuis longtemps. A titre d'exemple, on peut citer un article de B. Zschokke datant de 1916 [1] qui décrit déjà les causes de carbonatation du béton, la corrosion des armatures et les précautions à prendre pour limiter les dégâts. Jusqu'au moins au début des années soixante, les problèmes liés à la carbonatation du béton et à la corrosion des armatures n'ont que peu touché les ingénieurs constructeurs qui se sont plutôt concentrés sur de nouvelles méthodes de construction. Toutefois, ces deux dernières décennies, l'augmentation très rapide des dégâts, le coût des réparations et de l'entretien [2, 3] ont crû de telle façon que de nombreuses personnes ont commencé à s'occuper du comportement à long terme du béton armé et précontraint.

De nombreuses publications traitent de la carbonatation. Récemment, Parrott [4] a compilé une bibliographie sur la carbonatation du béton armé et recensé 182 articles datant essentiellement des vingt dernières années. Cependant, tous ces efforts ont certainement permis de mieux comprendre le phénomène de la carbonatation et les facteurs qui l'influencent, mais par contre les méthodes de prévision de la durée de vie des constructions nouvelles ou existantes ne sont actuellement pas fiables. Ainsi, il n'est pas possible de concevoir, entretenir ou réparer les structures avec toute l'efficacité souhaitable. Cette situation exige une recherche détaillée des différents processus impliqués.

Jusqu'à maintenant, l'essentiel des recherches a porté sur l'étude phénoménologique et empirique de parties d'un problème très complexe. Les méthodes traditionnelles ne permettent pas de faire la synthèse de toutes les connaissances acquises et de développer ainsi des méthodes capables de prévoir la durée de vie des structures de façon réaliste. Le développement de nouvelles méthodes devrait permettre de décrire quantitativement les effets de l'humidité, de la teneur en dioxyde de carbone, de la température, des chlorures, de la cure, du type de ciment, de la composition du béton, de revêtements protecteurs sur la carbonatation et la vitesse de corrosion de l'acier d'armature.

Actuellement, la simulation numérique permet de traiter quantitativement des processus interactifs complexes. C'est ce que nous allons tenter de montrer dans cet article, en décrivant brièvement quelques modèles. On montrera également qu'il est nécessaire d'étudier certaines propriétés des matériaux et donnera à titre d'exemple, la mesure du coefficient de diffusion de l'oxygène et du dioxyde de carbone à travers des pâtes de ciment en fonction de l'humidité.

2. EFFETS DE LA CARBONATATION SUR LA DURABILITE DU BETON ARME

La carbonatation du ciment est la réaction de neutralisation de ses composés basiques sur le dioxyde de carbone ou gaz carbonique présent dans l'air. Cette réaction atteint tous les composés hydratés à l'exception du gypse. Dans certaines conditions, même les composés anhydres peuvent réagir. Du point de vue pratique, ce sont essentiellement l'hydroxyde de calcium, $Ca(OH)_2$, et les silicates de calcium hydratés qui jouent un rôle important. La carbonatation de ces derniers composés conduit à la formation de carbonate de calcium ($CaCO_3$), de silice (SiO_2) et d'eau. Les mécanismes chimiques sont décrits plus en détail dans une autre communication à ce même symposium [5]. La carbonatation dépend d'un grand nombre de paramètres. Les influences les plus importantes sont décrites dans la publication de Parrott déjà mentionnée [2].

On trouve dans la littérature deux concepts de base qui décrivent mathématiquement l'avancement du processus de carbonatation. La plus ancienne théorie est basée sur une loi en $\sqrt{t}$ qui est une solution de l'équation de diffusion. Les valeurs empiriques montrent toutefois que l'exposant du temps est un peu inférieur à 0.5 et diminue légèrement pour de longues durées. Schiessl [6] a introduit un facteur de retardement qui conduit à un maximum de profondeur de carbonatation fini pour $t = \infty$. Cette conclusion ne peut être absolument correcte. Cette approche peut toutefois être réaliste pour des durées de vie des constructions de 80 à 100 ans.

Lorsque le béton directement en contact avec les armatures se carbonate, l'eau des pores subit une forte baisse du pH. Dans ces conditions nouvelles, l'acier ne bénéficie plus de la protection que lui assurait un pH élevé. Dans certaines conditions, notamment avec une humidité relativement élevée, l'acier peut se corroder

à une vitesse qui dépend de nombreux paramètres [7]. Il faut en particulier avoir à disposition suffisamment d'oxygène qui doit également diffuser depuis la surface du béton en contact avec l'atmosphère. La présence de chlorures, provenant essentiellement des sels de déverglaçage ou d'adjuvants, supprime la protection dont bénéficie l'acier dans un milieu à pH élevé.

3. MODELISATION

La modélisation de problèmes de durabilité a été étudiée au Laboratoire des Matériaux de Construction (LMC) de l'Ecole Polytechnique Fédérale de Lausanne (EPFL) selon plusieurs approches. Denarié [8] a montré comment développer une méthode tenant compte des incertitudes inhérentes au phénomène (approche probabiliste) qui permet d'évaluer l'état présent d'une construction et de calculer sa durée de vie probable. Un processus stochastique a été utilisé pour évaluer la distribution de la profondeur de carbonatation dans le temps et une distribution normale pour la couverture des armatures. La comparaison des résultats obtenus par le calcul de la probabilité de défaillance, à partir des distributions de valeurs théoriques et mesurées, montre le bien fondé des approximations faites. Enfin, cet auteur propose d'utiliser un système expert de diagnostic et d'analyse pour reprendre la démarche effectuée afin de fournir de véritables outils d'étude d'ouvrages endommagés.

Dans une première étude, Brieger et Wittmann [9] ont décrit le processus de carbonatation au moyen d'un système d'équations aux dérivées partielles, qui leur ont permis d'étudier les facteurs les plus importants, ainsi que divers mécanismes. La résolution des équations a été effectuée par voie numérique. Une autre approche a été faite par Brieger et Bonomi [10] qui ont été inspirés de modèles de la dynamique des fluides pour construire un modèle discret en temps et en espace d'automate cellulaire probabiliste. Cette méthode laisse entrevoir d'intéressants développements.

Dans une première tentative, Houst et al. [11] ont tenté d'étudier la carbonatation au moyen d'un modèle numérique. Tous les paramètres utilisés peuvent être reliés à des propriétés mesurables qui sont définies pour une composition du béton et un environnement donnés. Cet exemple nous paraît intéressant, car il permet clairement de montrer le genre de paramètre à déterminer expérimentalement.

Les équations (1), (2) et (3) suivantes permettent d'étudier l'interaction mutuelle du séchage et de la diffusion du dioxyde de carbone sur la carbonatation.

Le béton jeune peut être considéré comme un matériau poreux saturé d'eau. Le séchage peut être décrit par une équation de diffusion. Pour un tel béton, la carbonatation se superpose au séchage. Pendant ce processus de l'eau est libérée dans le béton. Il faut donc ajouter un terme à l'équation de diffusion pour tenir compte de la libération d'eau :

$$\frac{\partial w}{\partial t} = \frac{\partial}{\partial x} D_w \frac{\partial w}{\partial x} + \alpha_1 \frac{\partial c}{\partial t} \qquad (1)$$

Dans cette équation, w représente l'eau évaporable et D_w le coefficient de diffusion de vapeur d'eau. Ce coefficient dépend de la teneur en eau. c représente la quantité de carbonate formé et α_1 est un paramètre du matériau qui tient compte du dosage en ciment et du rapport e/c. Dans l'étape suivante, il faut décrire la pénétration du dioxyde de carbone dans le système poreux du béton. En première approximation, on peut à nouveau utiliser l'équation générale de la diffusion. La réaction de carbonatation consomme du dioxyde de carbone. En tenant compte de cette perte, on peut écrire l'équation différentielle (2) suivante :

$$\frac{\partial g}{\partial t} = \frac{\partial}{\partial x} D_g \frac{\partial g}{\partial x} - \alpha_2 \frac{\partial c}{\partial t} \qquad (2)$$

Dans cette équation, D_g est le coefficient de diffusion du CO_2. Il dépend de la teneur en humidité. α_2 est à nouveau un paramètre du matériau qui dépend essentiellement de la composition du béton.

La vitesse de carbonatation dépend du degré de carbonatation, de la concentration en CO_2 et finalement de la teneur en eau du béton. En admettant que l'on puisse combiner ces trois influences majeures sous forme de facteurs, on obtient :

$$\frac{\partial c}{\partial t} = \alpha_3 \cdot f_1(c) \cdot f_2(g) \cdot f_3(w) \qquad (3)$$

α_3 est à nouveau un paramètre du matériau qui tient compte de la composition du béton et du degré d'hydratation. Un développement plus détaillé de ce modèle est donné dans [11].

En résolvant les équations (1), (2) et (3) on peut étudier l'interaction mutuelle du séchage et de la diffusion du CO_2 sur la carbonatation. Un modèle numérique basé sur ces trois équations a été développé et la méthode des différences finies utilisée pour résoudre les équations du modèle numérique.

Actuellement, les valeurs des paramètres du modèle sont loin d'être toutes connues. L'étude de ces paramètres peut être relativement complexe, comme l'exemple donné dans la partie suivante nous le montre.

Toutefois, soit à l'aide de valeurs de paramètres tirées de la littérature, soit estimées, une solution numérique du système de trois équations différentielles donné précédemment, a permis de déterminer la profondeur de carbonatation de deux types de béton en fonction du temps. Les résultats obtenus à l'aide du modèle montrent qu'après une carbonatation initiale rapide, l'avancement de la carbonatation suit approximativement une loi en $\sqrt{t}$. Ces résultats, comparés à des mesures effectuées in situ, se sont avérés tout à fait réalistes.

4. MESURE DE LA DIFFUSION D'UN GAZ

4.1. Préparation des échantillons

Afin de déterminer le coefficient de diffusion D_g du modèle décrit ci-dessus, nous avons été amené à préparer des échantillons qui devaient être suffisamment minces pour pouvoir être complètement carbonatés et équilibrés à différentes humidités relatives dans un temps relativement court. Pour cela, nous avons confectionné des cylindres de pâte de ciment de diamètre 160 mm qui après au moins six mois de cure dans l'eau ont été coupés en disques de 1 à 2 mm d'épaisseur. Comme il n'est pas possible de varier le rapport eau/ciment de pâtes de ciment de façon notable sans avoir de décantation, nous avons dû maintenir les grains de ciment en suspension en faisant tourner le cylindre jusqu'à ce que la prise évite toute décantation, ce qui nous a permis de varier le rapport e/c entre 0.3 et 0.8. Pour cela, nous nous sommes inspirés de la méthode décrite par Sereda et Swenson [12], mais nous avons dû y apporter certaines modifications étant donné le grand diamètre de nos échantillons par rapport à ceux de Sereda et Swenson (Ø 32 mm). Lors de la carbonatation naturelle le gaz diffuse dans un matériau carbonaté. Nous avons donc carbonaté artificiellement nos échantillons et les avons équilibrés dans le climat correspondant à l'h.r. à laquelle nous effectuons la mesure.

4.2. Mesure des coefficients de diffusion de O_2 et CO_2

Comme la disponibilité d'oxygène à proximité de l'armature susceptible de se corroder est un facteur important et que la mesure de la diffusion d'oxygène n'entraînait pas de complication particulière, nous avons développé un système de mesure. Le coeur de ce système est une cellule de mesure séparée en deux chambres par le disque du matériau à tester. Avant les mesures, on purge les deux chambres avec de l'azote pur contenant la quantité de vapeur d'eau nécessaire à l'obtention de l'h.r. désirée. Au début de la mesure, on fait pénétrer dans la chambre supérieure un mélange de gaz artificiel (78% N_2, 20% O_2, 2% CO_2) dont l'h.r. est la même que celle de l'azote utilisé pour la purge du système. Ce gaz est régulièrement renouvelé dans la chambre supérieure où la concentration des différentes espèces est constante peu après le début des mesures. Au cours du temps, on analyse la concentration en O_2 et CO_2 dans la chambre inférieure par un analyseur en circuit fermé. Dans cette chambre, la concentration en O_2 varie donc de 0 à 20 % et celle en CO_2 de 0 à 2 %. Les coefficients de diffusion de O_2 et CO_2 peuvent être calculés à partir

des courbes de concentration de ces gaz en fonction du temps. Le système a d'abord été testé avec du béton cellulaire autoclavé. Les résultats obtenus, ainsi qu'une description plus détaillée du système de mesure figurent dans [13].

5. RESULTATS ET DISCUSSION

La diffusion des deux gaz a été mesurée à travers des échantillons équilibrés à deux différentes h.r. Les résultats sont donnés dans la table. Les valeurs moyennes et l'écart type y sont indiqués. Le nombre de mesures individuelles est donné par n. Toutes les valeurs sont reprises dans la figure.

Comme on pouvait s'y attendre le coefficient de diffusion augmente sensiblement avec le rapport eau/ciment. Dans le domaine de nos mesures le coefficient de diffusion ne dépend pas de la teneur en eau. Des mesures à des h.r. plus élevées sont maintenant en route. On peut s'attendre à ce que le coefficient de diffusion diminue lorsque les capillaires de la pâte de ciment durcie se remplissent progressivement d'eau.

	e/c = 0.4		e/c = 0.8	
Humidité relative	D_{O2} [$cm^2 \cdot s^{-1}$]	D_{CO2} [$cm^2 \cdot s^{-1}$]	D_{O2} [$cm^2 \cdot s^{-1}$]	D_{CO2} [$cm^2 \cdot s^{-1}$]
48 %	$(7.6 \pm 2.1) \cdot 10^{-5}$ (n = 4)	$(5.8 \pm 2.1) \cdot 10^{-5}$ (n = 4)	$(1.8 \pm 0.5) \cdot 10^{-3}$ (n = 8)	$(1.4 \pm 0.5) \cdot 10^{-3}$ (n = 8)
55 %	$(7.7 \pm 1.9) \cdot 10^{-5}$ (n = 7)	$(5.6 \pm 1.6) \cdot 10^{-5}$ (n = 7)	$(2.1 \pm 0.6) \cdot 10^{-3}$ (n = 6)	$(1.6 \pm 0.5) \cdot 10^{-3}$ (n = 6)

Table : Coefficient de diffusion D de O_2 et CO_2 mesuré sur deux pâtes de ciment (e/c: rapport eau/ciment lors du gâchage, n= nombre de mesures).

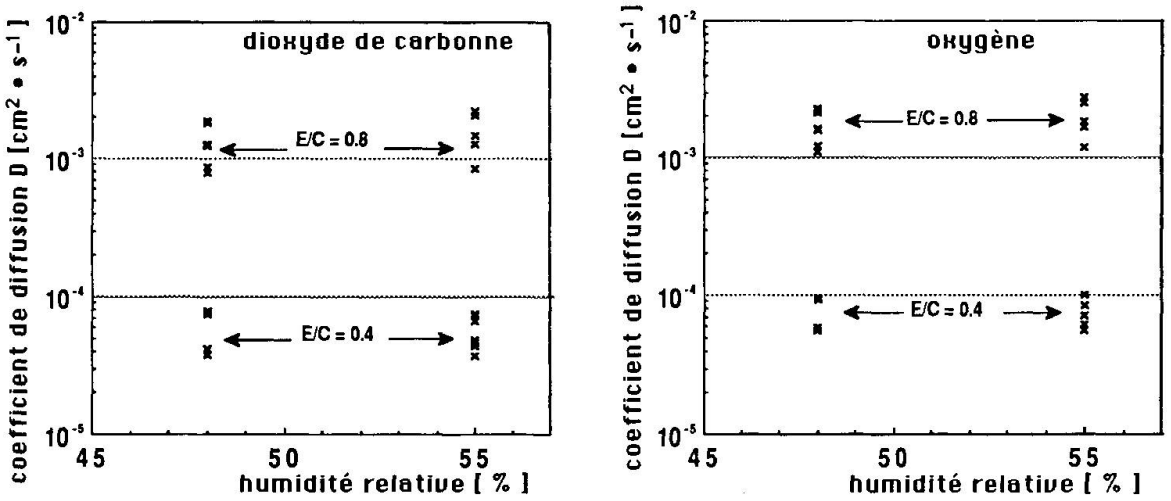

Fig. Coefficients de diffusion de CO2 et O2 dans la pâte de ciment durcie mesurés à 48 et 55 %.

6. CONCLUSIONS

Nous avons développé une méthode qui nous permet de déterminer le coefficient de diffusion du gaz carbonique et de l'oxygène dans la pâte de ciment durcie en fonction de la teneur en eau.

Le coefficient de diffusion dépend fortement du rapport eau/ciment.

Dans le béton ce n'est que la pâte de ciment durcie qui subit la carbonatation. Il est pratiquement impossible cependant de mesurer les coefficients de diffusion directement sur des échantillons en béton. Il faut encore développer un modèle d'un matériau composite qui permette de transposer les résultats obtenus et décrits ici au béton.

BIBLIOGRAPHIE

1. ZSCHOKKE B., Über das Rosten der Eiseneinlagen im Eisenbeton, Schweiz. Bauzeitung, LXVII (1916) 285-289.
2. PARROTT L.J., A review of carbonation in reinforced concrete, Cement and Concrete Association, Wexham Springs (1987).
3. WITTMANN F.H., Structure et durabilité du béton armé in Durabilité du béton armé, documentation SIA 89, SIA, Zürich (1985) pp. 7-14.
4. PARROTT L.J., Carbonation in reinforced concrete: A bibliography, Cement and Concrete Association, Wexham Springs (1987).
5. HOUST Y.F. et WITTMANN F.H., Le retrait de carbonatation, communication à ce symposium.
6. SCHIESSL P., Zur Frage der zulässigen Rissbreite und der erforderlichen Betondeckung im Stahlbetonbau unter besonderer Berücksichtigung der Karbonatisierung des Betons, Deutscher Ausschuss für Stahlbeton, Heft 255, Wilhelm Ernst & Sohn, Berlin-München-Düsseldorf (1976).
7. SCHIESSL P., Korrosion der Bewehrung im Stahlbeton, Bausanierung und Bautenschutz, Sonderheft (1983) pp. 64-71.
8. DENARIE E., Carbonatation - Durée de vie de bâtiments en béton armé, Chantiers/Suisse, 19 (1988) 89-92 et 149-151.
9. BRIEGER L.M., WITTMANN F.H., Numerical simulation of carbonation of concrete, in (F.H. Wittmann Ed.), Material Science and Restoration, Technische Akademie Esslingen, Ostfildern (1986) 635-640.
10. BRIEGER L.M., and BONOMI E., A cellular automaton model of diffusion and reaction in a porous medium: Concrete, Supercomputing Review, november 1988, pp. 3-4.
11. HOUST Y.F., ROELFSTRA P.E., and WITTMANN F.H., A model to predict service life of concrete structures, in (F.H. Wittmann Ed.), Material Science and Restoration, Ed. Lack + Chemie, Filderstadt (1983) 181-186.
12. SEREDA P.J., and SWENSON E.G., Apparatus for preparing portland cement paste of high water-cement ratio, Mat. Res. & Standards, 7 (1967) 152-154.
13. HOUST Y.F., and WITTMANN F.H., The diffusion of carbon dioxide and oxygen in aerated concrete, in (F.H. WITTMANN Ed.) Materials Science and Restoration, Technische Akademie Esslingen, Ostfildern (1986) 629-634.

Evaluation of On-site Conditions and Durability of Concrete Panels Exposed to Weather

Prévision de la durabilité de parois en béton exposées aux intempéries

Vorhersage der Dauerhaftigkeit bewitterter Betonbauten

Ferdinand S. ROSTÁSY
Prof. Dr.-Ing.
TU Braunschweig
Braunschweig, FR Germany

F. S. Rostásy, born 1932, professor for structural materials, at the Institut für Baustoffe, Massivbau und Brandschutz.

Dieter BUNTE
Dipl.-Ing.
TU Braunschweig
Braunschweig, FR Germany

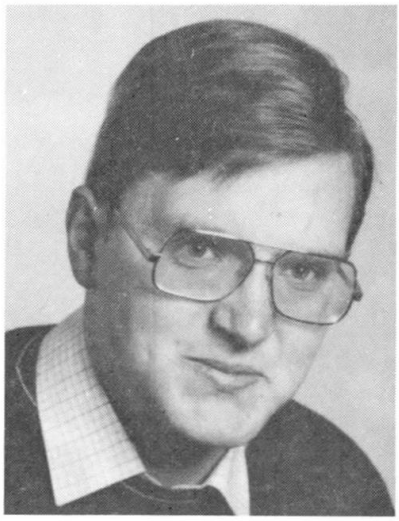

D. Bunte, born 1959, research assistant for structural materials, at the Institut für Baustoffe, Massivbau und Brandschutz.

SUMMARY

A model for the prediction of durability of concrete panels exposed to weather is developed. This model combines a carbonation law derived on basis of the reaction process with on-site non-destructive measurements of the permeability of cover.

RÉSUMÉ

Un modèle pour la prévision de la durabilité de parois en béton exposées aux intempéries est dévoloppé. Ce modèle lie une loi de la carbonatation avec des mesures de la perméabilité du béton d'enrobage.

ZUSAMMENFASSUNG

Zur Vorhersage der Dauerhaftigkeit von Stahlbetonbauten wird ein Modell entwickelt, das einen physikochemisch begründeten Ansatz der Karbonatisierungstiefenberechnung mit Ergebnissen von Dichtigkeitsmessungen am Bauwerk verknüpft.

1. INTRODUCTION

Durability is generally defined as the characteristic property which ensures function, structural safety and adequate appearance of a r/c-member during service life with a minimum of maintenance. For a specific case, however, durability must be defined in terms of environment and potential type of damage. The most common damage is the corrosion of the reinforcement near the surface of the r/c-member. In this case, durability may be regarded as exhausted as soon as peaks of the carbonation front with pH 9 reach - with a certain probability - regions of the steel with a minimum cover. Thus, durability is defined as incubation time of corrosion as a function of depth and tightness of cover. In this report a prediction model is presented which combines a physicochemical law of carbonation with the results of non-destructive on-site permeability tests.

2. MODEL FOR THE PREDICTION OF DURABILITY

2.1 Range of validity of model

The prediction model is valid for r/c-members exposed to normal weather of Central Europe and for essentially vertical surfaces. Concrete with a quality of C 25 to C 35 made with portland cement and frost-resistant natural aggregate is considered; complete compaction is presupposed. The model is valid for any type of curing. The model describes the carbonation progress in uncracked concrete. It is, however, also applicable for cracked r/c-members as long as the 95 %-fractile of the actual, measured crack widths does not exceed 0,25 to 0,30 mm.

2.2 Schießl's carbonation law

The progress of carbonation can be described with Schießl's law [1]. The mean final depth of carbonation is given by

$$\bar{x}_\infty = \frac{D_{co}}{\bar{b}} \Delta c \qquad (1)$$

with

Δc .... difference of CO_2-concentration of air between surface and carbonation front ($\approx 0{,}6^2$ g/m³ in urban and $\approx$ 0,8 - 1,0 g/m³ in polluted industrial areas, 0,54 g/m³ as average value).

D_{co} ... coefficient of CO_2-diffusion through carbonated concrete at the member's surface at the age of about 90 d and for the mean annual moisture content of concrete cover.

$\bar{b}$ ..... coefficient taking into account the realkalization of carbonated concrete by $Ca(OH)_2$-diffusion and the dependence of D_{co} on depth of carbonation, moisture of concrete, etc.

The progress of carbonation is described by:

$$t = -\frac{a}{\bar{b}}\left[x + x_\infty \ln\left(1 - \frac{x}{x_\infty}\right)\right] \qquad (2)$$

with a, content of all relevant alkaline hydration products which can be converted into carbonates.

The Equ.(1) and (2) were derived by idealization of the complex physicochemical reactions of carbonation. For prediction, representative values for the coefficient of Equ.(1) were proposed in [1]. Experiments show their wide range and considerable scatter. Thus, the prediction of durability of a specific structure solely on basis of representative values of D_{co}, $\bar{b}$ and Δc is insecure. Uncertainty can be reduced if the carbonation depth and D_{co} are measured. This, how-

ever, can only be performed in the laboratory, considerable core extraction becomes necessary. Because such procedure is usually impossible, the necessary information on the diffusivity for CO_2 must be acquired by substitutive on-site absorption tests such as ISA [2]. Such tests can be performed non-destructively and repeatedly.

2.3 Combination of carbonation law and ISA test results

By the ISA-test the absorption of water is measured as function of suction time t_s. The ISA-value is related to pore structure data of the first 10 to 20 mm of cover. These date incorporate the influence of compositional parameters of concrete, curing, carbonation, etc. Consequently, they also describe the diffusivity for CO_2 and water vapour. As explained and verified in [2], [3] the ISA-value can be expressed by:

$$ISA(t_s) = \frac{K_2 \sqrt{2r_h}\, \epsilon_{abs}}{2\rho_w a_{Tabs}}\, t_s^{-\frac{1}{2}} \tag{4}$$

Meaning of the parameters in Equ.(4) were defined in [2]. ϵ_{abs} is the effective porosity for absorption ($r \geq 100$ nm). The effective porosity for gas diffusion ϵ_{diff} exceeds ϵ_{abs} because pores with $r \geq 30$ nm become accessible. Tortuosity of diffusion consequently also increases. Acc. to [3], the following relations can be formulated:

$$\begin{aligned} \epsilon_{diff} &\approx 1{,}7\ \epsilon_{abs} \\ a_{Tdiff} &\approx 1{,}5\ a_{Tabs} \end{aligned} \tag{5}$$

The unknown coefficient D_C for CO_2-diffusion can be expressed by:

$$D_C = D_a \frac{\epsilon_{diff}}{a_{Tdiff}} \tag{6}$$

with D_a, the diffusivity of CO_2 through air (0,159 cm^2/s at 20 °C). By insertion of Equ.(4), (5), and (6) into Equ.(1), we obtain the prediction value of the mean, final carbonation depth based on the mean $ISA_{(10\ min.)}$-value:

$$\overline{x}_\infty \approx \frac{D_a \Delta c}{\overline{b}\, K_3} \frac{\overline{ISA}_{10}}{\sqrt{2r_h}} \tag{7}$$

Progress function follows Equ.(2). Fig. 1 shows the evaluation of Equ.(7) for several mean values of ISA_{10} vs. age.

3. APPLICATION

3.1 Variability and durability criterion

The prediction model Equ.(7) contains essentially the same assumptions as Equ.(1). Though, by on-site measurement a realistic assessment of diffusivity becomes possible, the other coefficients must still be chosen within a reasonable range. Thereby, their scatter is taken into account. Furthermore, the ISA-value depends on the moisture and temperature of concrete at test. The effect of the difference between the temperature at test and the mean annual temperature ($\overline{T} \approx 12$ °C) can be taken into account. ISA-tests have to be performed a certain drying time after rainfall. It is assumed, that the moisture of concrete at this state corresponds to the mean annual value. The unknown scatter of the constituents of Equ.(7) is globally satisfied by a coefficient of variation of ≈ 40 % of carbonation depth [1]. Thus, we obtain for the 95 %-fractile of the carbonation depth at any age t:

$$x_{95}(t) \approx 1{,}7\ \overline{x}(t) \tag{8}$$

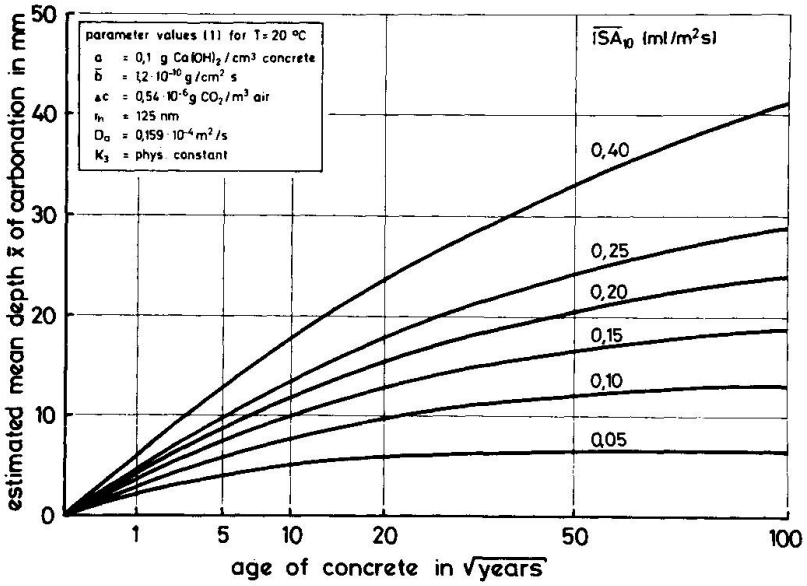

Fig. 1: Mean of carbonation depth dependent on age and ISA_{10}-value (Equ.(2) and (7))

The concrete cover also scatters [3]. Its 5 %-fractile may be expressed by

$$c_5 \approx 0{,}6\ \bar{c} \tag{9}$$

with $\bar{c}$, the nominal cover of bars to be ensured by spacers. Now, the durability criterion is expressed by:

$$x_{95}(t_1) \leq c_5 \tag{10}$$

with t_1, the service life.

This criterion is a rough simplification of reality because it stipulates a probability of 1 for the coincidence of peak values of carbonation depth occurring at the reinforcing bars placed with an unknown, distinct spacing.

3.2 Comparison with test results

Fig. 2 shows the dependence of test results of the mean carbonation depth on age for concrete walls exposed for about 25 years to weather. At the age of 25 years ISA-tests were performed on-site. With Equ.(7), (2) and with the mean experimental ISA-values the prediction curves x(t) and $x_{95}(t)$ can be calculated. For exposure to normal weather the minimum cover which corresponds to c_5 would have to be 25 mm acc. to DIN 1045. The example of Fig. 2 shows that peaks of carbonation would reach the steel's surface after ≈ 90 years.

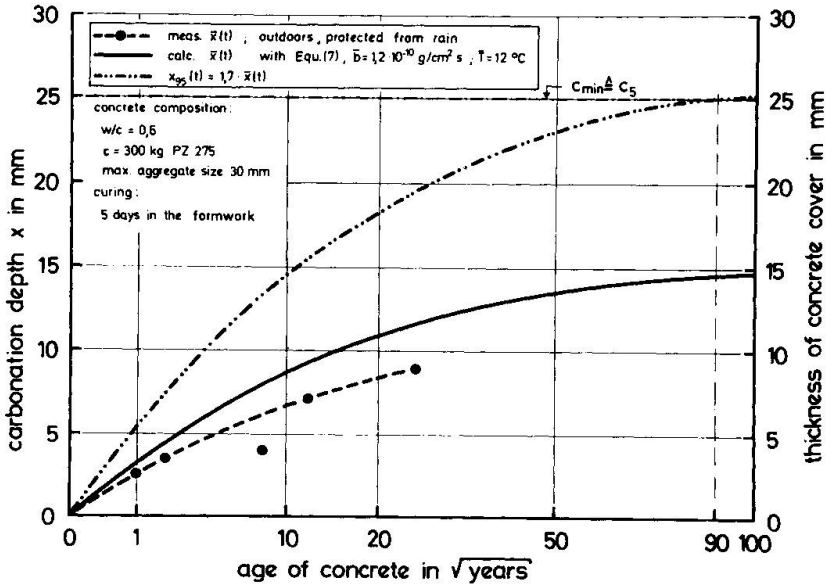

Fig. 2: Comparison of measured and calculated carbonation depth for a 25 years old concrete (calculation with measured ISA_{10}-value at 25 years)

3.3 Use of model in practice

The prediction model in combination with on-site ISA-tests can be used for: a) quality control in course of acceptance of the just completed structure and b) durability assessment of the older structure in course of maintenance. In any case reliable information on concrete cover is necessary.

For quality control certain mean ISA_{10}-values for acceptance must be stipulated which should not be transgressed by the on-site results.

In course of inspection of a structure, ISA-readings can be taken in suitable intervals. On their basis, carbonation can be estimated. By occasional measurement of the carbonation depth the model uncertainty can be reduced.

4. FINAL REMARK

The model presented is yet a tentative one. Several assumptions were necessary in course of its development. Thus, further evaluation is needed for its corroberation.

REFERENCES

[1] Schießl, P.: Zur Frage der zulässigen Rißbreite und der erforderlichen Betonüberdeckung im Stahlbetonbau unter besonderer Berücksichtigung der Karbonatisierung des Betons, DAfStb-Heft 255, 1976

[2] Rostásy, F.S.; Bunte, D.: Test methods for the on-site assessment of reinforced concrete surfaces exposed to normal weather, IABSE-Symposium Durability of Stuctures, Lisbon, 06.09. - 08.09.1989

[3] Stangenberg, F.; Kiefert, H.: Erfahrungen bei der Qualitätskontrolle von Stahlbetonbauwerken, Beton- und Stahlbetonbau 83, 1989, P. 53 - 58

Leere Seite
Blank page
Page vide

Influence of Local Repairs on Corrosion of Steel Reinforcement

Influence des réparations locales sur la corrosion des aciers d'armature

Beeinflussung der Korrosion der Bewehrung durch örtliche Instandsetzungsarbeiten

Joost GULIKERS
Civil Engineer
Univ. of Technology Delft
Delft, The Netherlands

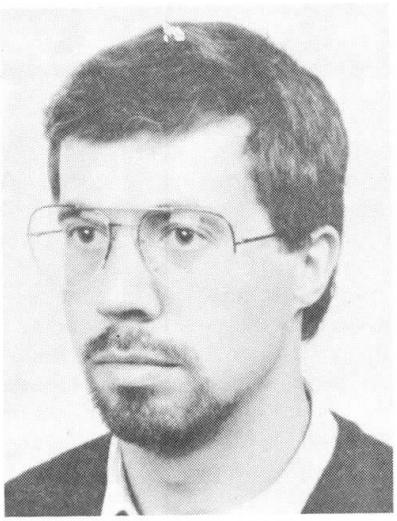

Joost Gulikers received his Master of Science degree at Delft University of Technology, The Netherlands, in 1986. Since then he is a research engineer at the Stevin Laboratory and is involved in research projects on durability of concrete structures.

SUMMARY

In this paper a description is given of a concrete corrosion celle which has been developed to investigate the mutual influence, between rebars in carbonated concrete and rebars embedded in repair mortar, on the corrosion processes. This influence is qualitively analyzed and preliminary test results are presented.

RÉSUMÉ

Une description est donnée d'une cellule d'essais de corrosion de béton permettant d'examiner l'influence mutuelle entre des barres enrobées de béton carbonaté et des barres enrobées de mortier de réparation, sur le processus de corrosion. Cette influence est analysée qualitativement et des résultats préliminaires sont présentés.

ZUSAMMENFASSUNG

Eine Betonkorrosionszelle wird zur Untersuchung der gegenseitigen Beeinflussung zwischen Bewehrung in karbonatisiertem Beton bzw. der Bewehrung umgeben von Reparaturmörtel und dem Korrosionsvorgang beschrieben. Diese Beeinflussung wird qualtitativ erfasst und vorläufige Versuchsergebnisse werden vorgelegt.

1. INTRODUCTION

Non-carbonated and chloride-free concrete normally provides reinforcement with excellent corrosion protection. The high alkalinity of the pore-water in concrete (pH > 12.5) results in the formation of a tightly adhering iron oxide film on the steel surface, preventing the ionic dissolution of iron. Corrosion of steel, however, can occur if the concrete is not of adequate quality, the structure was not properly designed for the service environment, or the environment was not as anticipated or changed during the service life of the concrete. Carbonation of concrete due to the ingress of carbondioxide from the air results in the reduction of the pH-value below 10, thereby permitting corrosion of reinforcing steel. The presence of chloride-ions in concrete can cause severe corrosion to occur when the chloride content at the steel surface exceeds a critical limit. The rate of corrosion is strongly influenced by environmental factors. Both carbonation- and chloride-induced corrosion can occur only if sufficient oxygen and moisture are available.
Because the corrosion products (rust) occupy a greater volume than the steel and exert substantial stresses on the surrounding concrete, corrosion results in deterioration of concrete. At the exterior surface this may demonstrate as staining, spalling and cracking of the concrete. Durability, structural and esthetic aspects can be the reason for repairing the damaged structure. If only a part of the total concrete surface is damaged it may be decided that only those parts should be repaired. In practice it is observed that local repairs can negatively affect the corrosion behaviour of rebars embedded in the non-repaired concrete. The effects of local repairs on the corrosion processes in carbonated concrete are studied by means of a concrete corrosion cell with which the influences of all relevant practical parameters can be quantitatively determined under different conditions. The principles of the corrosion cell will be described and the first results will be presented.

2. ELECTROCHEMICAL PRINCIPLES

Corrosion of steel in concrete is an electrochemical proces which can be divided in an anodic and a cathodic part: at the anode electrochemical oxidation takes place and at the cathode electrochemical reduction occurs. Any metal surface on which corrosion is taking place is a composite of anodes and cathodes being electrically connected through the body of the metal itself. At the anode, which is the negative pole, the dissolution of ferrous ions takes place as a result of the oxidation of iron:

$$Fe \rightarrow Fe^{+2} + 2e \qquad (1)$$

The ferrous ions are subsequently changed to oxides of iron by a number of complex reactions. At the cathode, which is the positive pole, reduction takes place. In a high alkaline environment and an adequate supply of oxygen, as is the case in concrete, the cathodic reaction is represented by:

$$2H_2O + O_2 + 4e \rightarrow 4OH^- \qquad (2)$$

If the cathodic process is the slower process, the corrosion is considered to be cathodically controlled. Conversely, if the anodic process is slower, the corrosion rate is said to be anodically controlled. In concrete, one or two types of corrosion-rate-controlling mechanisms normally dominate. One is cathodic diffusion, where the rate of oxygen diffusion through the concrete determines the rate of corrosion. The other type of controlling mechanism involves the development of a high resistance path. When steel corrodes in concrete, anodic and cathodic areas may be as much of several decimeters apart, therefore the resistance of the concrete may be of great importance [5].
The corrosion process can proceed only if certain conditions are fulfilled. For the situation where depassivation due to carbonation of the concrete has occurred, these principal conditions are shown schematically in fig. 1:
Anodes develop as a result of depassivation; cathodic reactions can occur in both passivated and depassivated areas of the steel surface when sufficient water and oxygen are available. The ferrous and hydroxyl ions dissolute in the pore water; the released electrons travel through the steel from the anode to the cathode nearby.
Depassivation of steel caused by carbonation of concrete leads to the formation of micro

corrosion cells on the steel surface. The cathodic and anodic reactions proceed directly side by side and will cause a uniform corrosion rate along the steel surface. Under certain conditions it may be possible that in carbonated concrete corrosion areas develop where the cathodic reactions dominate the anodic reactions. This overcharge of cathodic activity can support the anodic reactions in corrosion areas nearby.

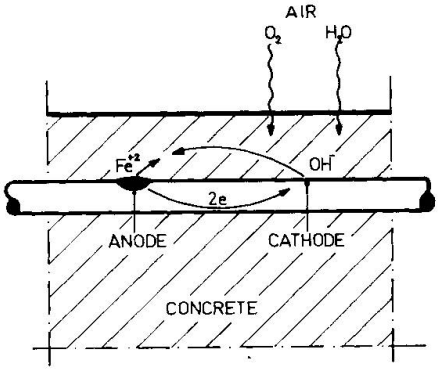

Anodic reaction
(oxidation)

$Fe \longrightarrow Fe^{++} + 2e$

Cathodic reaction
(reduction)

$2H_2O + O_2 + 4e \longrightarrow 4OH^-$

Fig. 1 Schematic representation of corrosion processes after depassivation by carbonation

The presence of chloride-ions in concrete usually gives rise to the formation of a macro-cell, i.e. localized anodic and cathodic regions of the steel surface are seperate from one another. This sitation is especially dangerous when large cathodic regions are opposed to small anodic regions. This so-called pitting corrosion results in a significant dissolution of metal advancing in the interior of the rebar.
In this paper repair of reinforced concrete with carbonation induced corrosion is subject of research.

3. EXPERIMENTS

3.1 Description of the concrete corrosion cell

The concrete corrosion cell is shown in fig. 2; a similar corrosion testing cell was previously developed by Schiessl [1]. Each specimen is made of solid concrete (see Appendix for composition and curing conditions) and contains initially 4 electrodes (steel rebars) at fixed places: 3 electrodes (A, B and D) at the upper surface with a concrete cover of 10mm and an

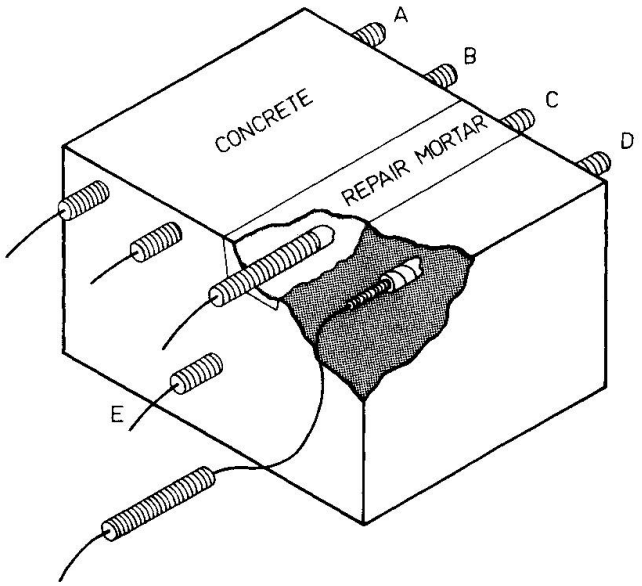

Fig. 2 Concrete corrosion cell

in-between distance of 50mm, and 1 electrode (E) at a distance of 50mm to the basis. At the upper surface a slot is made with a depth of 30mm. All electrodes have an effective corrosion length of 100mm and a surface area of $37.7*10^3 mm^2$. After accelerated carbonation (80 days at 5% (v/v) CO_2 and 50% R.H.) the three upper electrodes are positioned in carbonated concrete and as a consequence they are in a potential state of corrosion. Micro corrosion cells will develop dependent on the environmental conditions, viz. relative humidity and the availability of oxygen. The electrode E is surrounded by non-carbonated concrete and can act only as a cathode (macro cathode); this electrode is used for reference measurements. After accelerated carbonation the four vertical surfaces of the specimen are sealed with a tight epoxy coating permitting access of oxygen and moisture only through the upper and lower surfaces of the specimen. The electrodes are externally conductively connected, enabling the corrosion current to flow. Any corrosion due to micro cell formation cannot be detected until at the end of the test the specimens are split and the weight of rust for each electrode is determined.
In each specimen the electrically conductive connection between the electrodes A - B and D - E was established directly after the period of accelerated carbonation. After three months the fourth electrode (C) at the upper surface is placed in the slot and embedded in repair mortar. Two days after repair the connections between the electrodes A - B and C - D were established.
It is emphasized here that the only purpose of this type of concrete corrosion cell is to measure the mutual influence between rebars embedded in carbonated concrete and rebars embedded in repair mortar on the corrosion processes.

3.2 Description of the measuring system

To determine the very small corrosion currents a special developed measuring system is set up (see fig. 3). Each electrical circuit consists of two electrodes (A - B and C - D) which are continuously interconnected by means of a copper wire through a resistor. The resistance is relatively low to limit any external interference of the natural corrosion process; in the present situation a resistance of 1X is chosen. Between 10 corrosioncircuits and a multimeter (type: Philips PM 2535) 1 multiplexer (type: Philips PM 2121) is placed; in total 60 circuits are monitored. A PC (type: Hewlett Packard Vectra ES) is connected with the multimeter to start the measuring cyclus and to buffer the received corrosion current data.

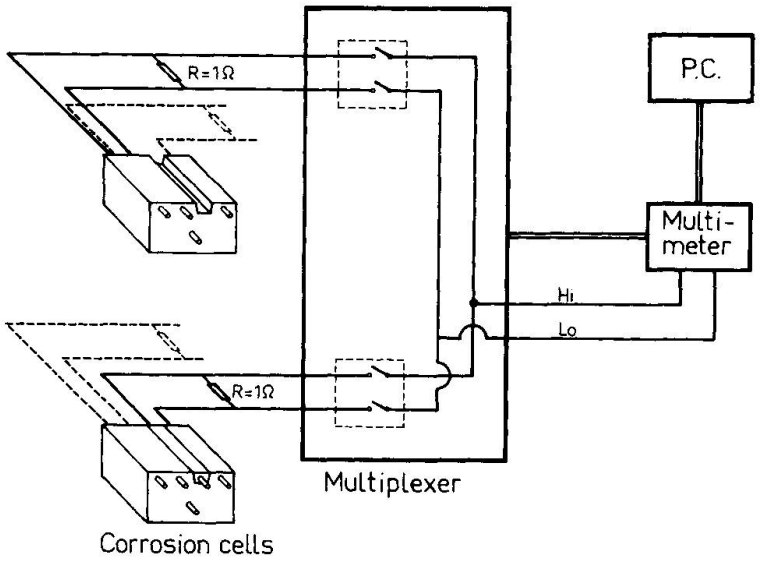

Fig. 3 Measuring system

3.3 Variables

In the first stage of the research program only two parameters are taken into account, viz. the relative humidity of the air and the type of repair mortar:

R.H. : 1) alternating climate : 2 weeks 50% R.H.;
2 weeks 100% R.H.
2) constant climate : continuously 80% R.H.

Repair mortar : 1) CC-mortar;
2) PCC-mortar;
3) PC-mortar.

4. PRELIMINARY EXPERIMENTAL RESULTS

The results of the first three weeks after repair are shown in figs. 4 and 5 for different climate conditions and different types of repair mortar.

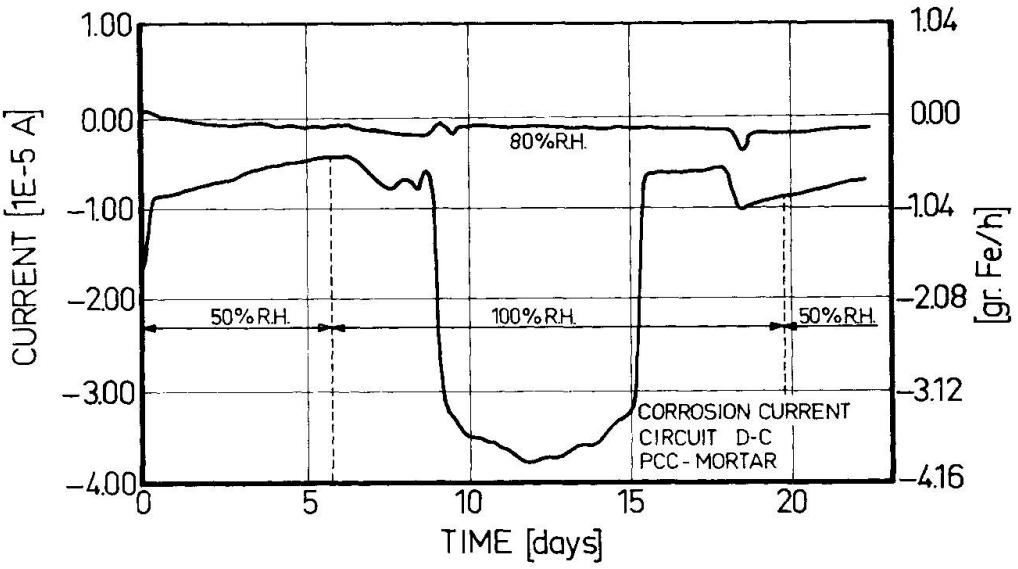

Fig. 4 Corrosion currents for PCC-mortar at 80% R.H. and 50/100% R.H.

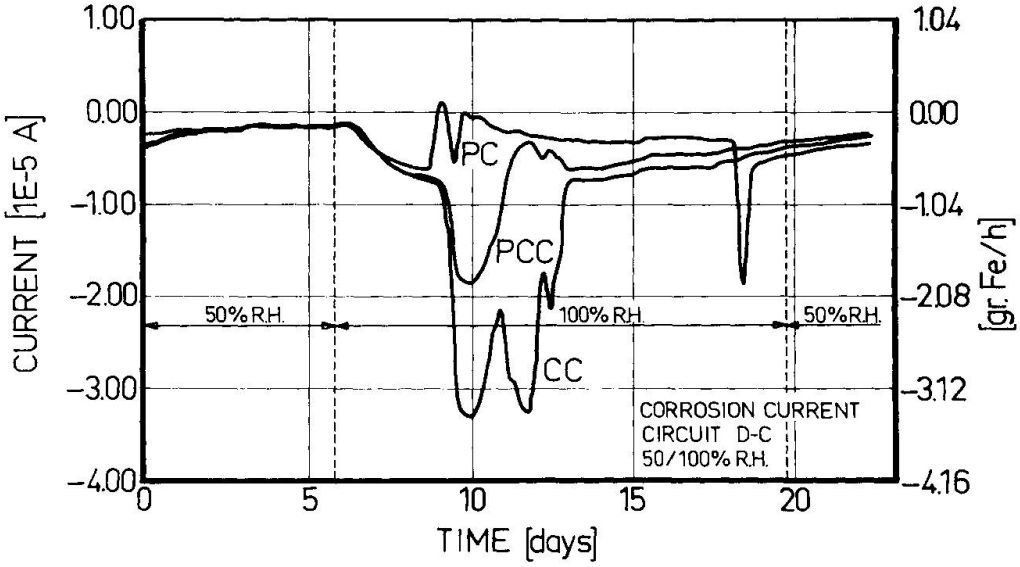

Fig. 5 Corrosion currents for 3 types of repair mortar at 50/100% R.H.

5. DISCUSSION

The steel reinforcement in the carbonated concrete area is in a potential state of corrosion; the steel surrounded by repair mortar cannot corrode i.e. at the steel surface no anodic reactions can proceed. In a mineral mortar (CC- and PCC-mortars) the alkaline environment re-establishes a protective oxide film on the steel surface (repassivation). In a PC-mortar, e.g. epoxy mortar, permeability and porosity are very low and as a result cathodic and anodic reactivity will be very slow. Rebars embedded in mineral mortars can develop into macro cathodes, the rate of their reactivity being mainly determined by the diffusion of oxygen. When these macro cathodes are electrically connected with rebars in carbonated concrete an acceleration of their anodic processes will occur. This can be especially dangerous if the acceleration is concentrated on a small steel area. In that case a situation identical to pitting corrosion is possible. For rebars partly embedded in repair mortar and partly in carbonated concrete it is likely that the small macro anode will occur next to the large macro cathode. Whether cathodic or anodic reactions dominate at steel surfaces of rebars surrounded by PC-mortar mainly depends on the porosity and permeability of the repair mortar and the corrosion controlling factors at the rebars in carbonated concrete nearby.

In the period about which tentative results are presented, the measuring system is tested and further developed; the time period is too short to draw any definite conclusions from the results. The program is continued to investigate the long-term effect of local repairs on corrosion processes; in due time these results will be presented and discussed.

ACKNOWLEDGEMENTS

The experiments in this research project are carried out in the Stevin Laboratory of the Delft University of Technology. Support provided by the CUR (Centre for Civil Engineering Research, Codes and Specifications) is acknowledged with thanks.

REFERENCES

1. SCHIESSL, P.; SCHWARZKOPF M., Chloride-induced corrosion of steel in concrete: Development of a concrete corrosion testing cell. Betonwerk + Fertigteil-Technik, Heft 10/1986.

2. SCHWENK W., Principles of the corrosion-chemical behaviour of structural steel. Betonwerk + Fertigteil-Technik, Heft 4/1985.

3. GONZALEZ J.A.; ALGABA S.; ANDRADE C., Corrosion of reinforcing bars in carbonated concrete. British Corrosion Journal, No.3 1980.

4. HOPE B.; IP A., Corrosion of steel in concrete made with slag cement. ACI Materials Journal, November/December 1987.

5. ACI Committee 222, Corrosion of metals in concrete. ACI Journal, January/February 1985.

6. RILEM Technical Committee 60-CSC, Corrosion of steel in concrete. State of the art report, Final draft, April 1986.

APPENDIX

Concrete composition: 300 kg/m^3 bfsc; wcf = 0.60; aggregate 8-16mm: 24%; 4-8mm: 20%; 2-4mm: 20%; 1-2mm: 10%; 0.5-1mm: 9%; 0.25-0.5mm: 9%; 0.125-0.25mm: 8%.
Curing conditions: 2 weeks 100% R.H.

Surface Shrinkage of Concrete: Evaluation and Modelling

Retrait superficiel du béton: évaluation et modélisation

Oberflächenschwinden des Betons: Ermittlung und Modellierung

Charles ABDUNUR
Docteur es Sciences
LCPC
Paris, France

Paul ACKER
Docteur de l'ENPC
LCPC
Paris, France

Bu-quan MIAO
Docteur de l'ENPC
LCPC
Paris, France

SUMMARY

The mechanical effects of drying shrinkage were investigated in the field and the laboratory, using theoretical, experimental and technological means. Direct stress measurements, by the stress release method, and their numerical analysis gave the stress profiles and the depth of damage for different configurations. Simulation of the drying effects by a stochastic model reproduced the same stress profiles. The explanation and evaluation of these effects should lead to appropriate precautions, for reinforcement protection and a better durability.

RÉSUMÉ

Les effets mécaniques dûs au retrait de dessiccation ont été étudiés, sur ouvrages réels et en laboratoire, associant des moyens théoriques, expérimentaux et technologiques. Des mesures directes de contraintes, par la méthode de libération, et leur analyse numérique ont permis de déterminer les profils de contraintes et la profondeur d'endommagement, pour différents configurations. Une simulation des effets du séchage par un modèle stochastique a reproduit les mêmes profils de contraintes. L'explication et l'évaluation de ces effets devraient faciliter la définition des précautions à prendre, pour la protection des armatures et une meilleure durabilité.

ZUSAMMENFASSUNG

Die Wirkung des Schwindens infolge Austrocknung wurde an Hand von Labor- und Bauwerksuntersuchungen erforscht. Dazu wurden drei verschiedene Studien durchgeführt; experimentelle, theoretische und technologische Studien. Direkte Spannungsmessungen mit flachen Druckmessdosen und ihre numerische Analyse haben die Bestimmung des Schwindens ermöglicht. Eine Simulation des Trocknungsvorganges durch ein stochastisches Modell hat die Ereignisse bestätigt. Durch die nun mögliche Erklärung und daraus resultierende Berechenbarkeit dieser Wirkung kann eine bessere Dauerhaftigkeit gewährleistet werden.

1. INTRODUCTION : EXTENSIVENESS OF CONCRETE SKIN CRACKING

In most concrete formulae, the water quantity necessary for the mix greatly exceeds that needed for the cement hydration. As soon as shuttering is removed, even in humid climates, a part of the water will migrate to the outside. This drying can attain a 5% loss of the total concrete weight and lead to considerable dimensional variations. Drying is never uniform and its effects have three components :

- eigenstresses, due to very slow drying and resulting gradients ;
- skin cracking of evolutive depth ;
- apparent strains, usually known as drying shrinkage.

These depend on the geometry of the sample or structural element. By their intense superficial mechanical effects, both the removal of shuttering and the variation of air humidity are equivalent to a thermal shock. In general, the result is a pattern of very dense, shallow hair cracks which do not always jeopardize the durability of the material. However, under certain conditions, an extensive growth of this cracking can favour reinforcement corrosion, a very frequent type of pathology cases in concrete structures.

To better control this mechanism, it could be helpful to first evaluate the mechanical effects of shrinkage with the utmost possible accuracy.

2. A DOUBLE APPROACH BY EXPERIMENT AND MODELLING

Many authors [1], [2], have given a fair but rather qualitative description of these effects. By thermal analogy, shrinkage strains and eigenstresses cannot be properly calculated from measured water content distributions (fig. 1), owing to the lack of a sufficiently accurate "coefficient of hydric contraction". This can only be obtained on a test sample free from gradients and cracks, which are difficult to avoid, given the excessively slow drying process [3].

For a quantitative analysis of the mechanical effects, we needed an accurate method of direct stress measurement, leading to a more realistic constitutive model. It happens that such a method has already been developed by one of the authors [4], [5], for the assessment of structures. It now offers a suitable means for this quantitative approach.

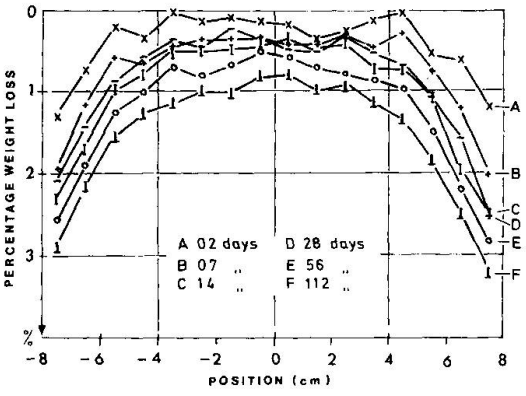

Fig. 1 : Time-dependent distribution curves of water content measured in a 10-cm-diameter, 16-cm long concrete core, laterally coated to represent uniaxial drying in a 16-cm thick infinite slab.

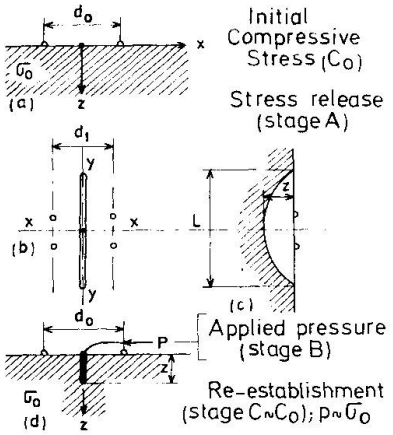

Fig. 2 : Different stages of direct stress measurements, by the release method.

3. DIRECT MEASUREMENT OF STRESS

3.1 - The release method

It is a local and partial release of stress, followed by a controlled pressure compensation [5]. In practice (fig. 2 and 3), a displacement reference field is first set up on the surface ; a tiny slot is then cut in a plane normal to the desired stress direction ; finally, a special very thin flat jack is introduced into the slot and used to restore the initial displacement field. The amount of cancelling pressure gives the absolute compressive stress normal to the slot. In the same way, with the same accuracy, tensile stresses are obtained by a corollary. The stress profile is traced by repeating the operation at closely successive depths of the same slot, then by treating the data numerically. In spite of the minute working scale, the error stays within 0.3 MPa. The depth operating range is 80^{mm}, giving an average stress till 32^{mm}. Measurement is "direct" in the sense that the same physical quantity is involved (pressure for stress) and that none of the material elastic properties are needed. These are even determined in the process. Stress components may sometimes be separated.

3.2 - Applications on site

The first operational field application of the release methode was on a 10-year-old tall concrete column with a box section [6]. It carries two half, simply supported spans of a bridge (equivalent to 2.5 MPa) and undergoes a slow, irregular foundation settlement. On four points of the section, absolute stress profiles were determined through the outside part of wall thicknesses (fig. 4). At all four points, contrary to what is expected from a compression member, high tensile stresses were measured close to the surface, falling sharply with depth.

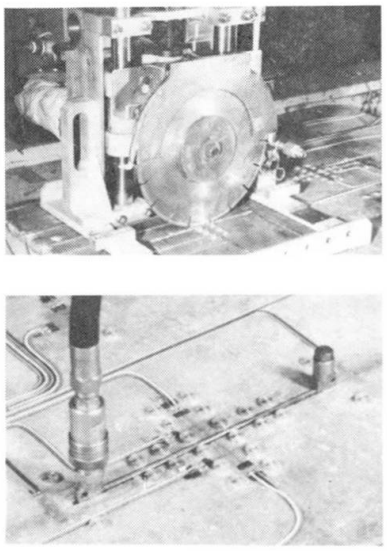

Fig. 3 : (top) Slot cutting machine with 0.1-mm adjustment ;
(bottom) A 0.1 µm-precision displacement measuring apparatus with a 4-mm thick flat jack in the slot.

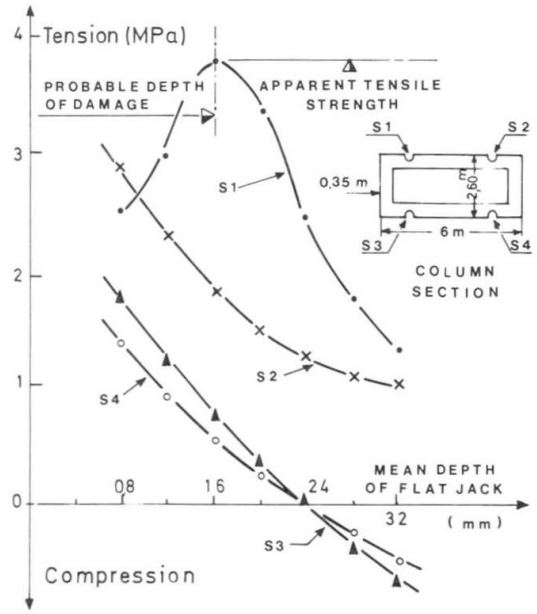

Fig. 4 : Compensating pressures, given by the release method, reflecting the actual stress profiles on a 10-year-old concrete column with a 2.5 MPa external compression. They show the still prevailing superficial tensions and sharp gradients of shrinkage. The relative vertical shift between the curves, illustrates the effect of flexure (confirmed later while completely cutting and shoring the column base).

Shrinkage effect is undoubtedly the cause, running deep with similar gradients and stabilizing beyond the range of measurement. At point S1, the stress curve breaks right below the usual tensile strength of concrete, announcing a softening of stress by superficial cracking. The measured stress at this depth is in fact an average over the area of the flat jack, hence the actual stress distribution should be more pronounced upwards.

Such applications helped to emit basic and realistic assumptions necessary to carry on the research.

4. LABORATORY TESTS AND A MODEL FOR ANALYSIS

Three plain concrete test slabs were casted, 80 x 40 cm, respectively 8, 10, 16 cm thick [7]. The first one had a uniform 12.5 MPa prestress at 7 days. In areas away from edges, stress distribution is assumed to depend exclusively on the distance from the surface.

The release method was used again in all slabs. The displacement field evolution, accurately measured as cutting proceeded, was combined with a specific compliance matrix (F.E.M. 3-D programme CESAR), to obtain a better defined stress profile as a function of depth. In this analysis model, elastic behaviour is assumed, as confirmed by the linear and reversible response of the displacement field to the flat jack pressure, at consecutive slot depths.

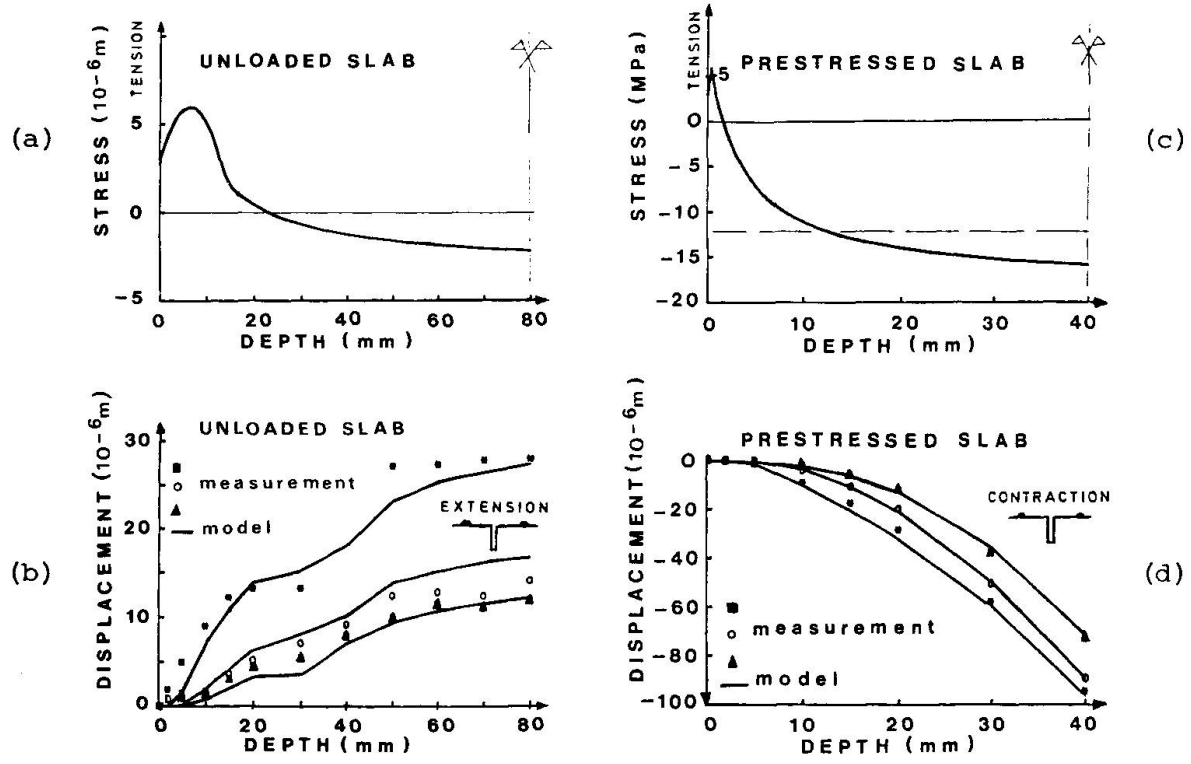

Fig. 5 : (a, c) Stress distribution, in non-loaded and prestressed configurations, estimated by the analysis model, completed by parametric optimization.
(b, d) Respective surface displacements comparing those actually measured by the release method (points), and those deduced from stress distributions (curves). In the two-step evolution observed in (b), the first discontinuity marks a stress fall to zero, the second, an opposite flexure effect of stress redistribution after partial release in a slab of limited cross-section.

5. RESULTS AND DISCUSSION : HIGH STRESSES, SOFTENING AND LOAD COUPLING

The resulting stress profiles and the comparison of measured and computed surface displacements are given in fig. 5. Considerable surface displacements were observed, depending heavily on the external loading configuration.

In the non-loaded slab (fig. 5b), the increasing depth-dependent extension reflects an intense superficial tension of several MPa's. A direct resolution by the above analysis model gave the general form of this tension which rises first with depth, passes by a maximum, then falls to compression, in the central part of the thickness, to sum up the internal forces over the cross-section to zero. The presence of a softening zone confirms earlier stress measurements on structural members with low compression loading (curve S1, fig. 4). The shrinkage stress profile may now be assimilated to a junction of two curves : (i) a parabola, covering the damaged depth, with its vertex on the tensile strength level and (ii) a central curve, proportional to the water content distribution.

Very close to the surface, the analysis model grows too delicate to apply owing to the extremely small compliance coefficients. The damaged depth then becomes the main parameter whose optimum value should fix the stress curve and give the best correlation between the theoretically deduced displacements and those actually measured by the release method (fig. 5b, d). The optimization process yielded a 4.0 and 6.4 mm damage, respectively for the 10 and 16 cm thick non-loaded slabs. It is 0.3 mm only for the prestressed slab. With these additional and consistent data, the stress profiles (fig. 5a, c) were obtained.

The main difficulty of the above approach naturally resides in the lack of a reliable constitutive law for concrete in tension. On this scale, the experimentally observed softening strongly depends on the size of discontinuities [8]. This size effect may be explicitly reproduced in Rossi's stochastic model [9]. Specific, perfect brittle, contact elements are inserted in an elastic F.E.M. model with tensile strength values placed at random according to an experimentally determined statistic distribution. In applying this model to the above example fig. 5 b, the stochastic mean stresses generate a shape similar to the experimental distribution (fig. 6).

At successive drying stages, the model shows a "condensation" process of main crack openings : as damage deepens, fewer cracks propagate giving more concentrated, hence wider, openings.

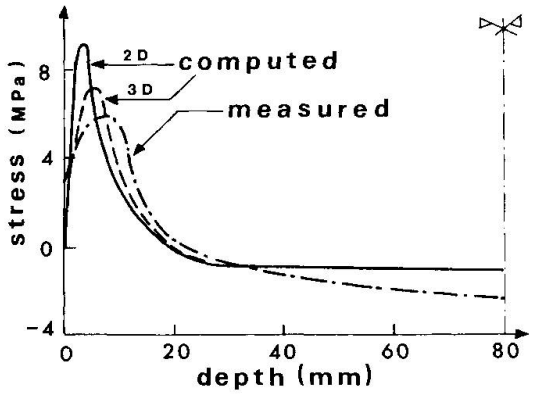

Fig. 6 : Depth-dependent mean stresses, computed by the stochastic model and compared to experimental values for the 16 cm thick test slab.

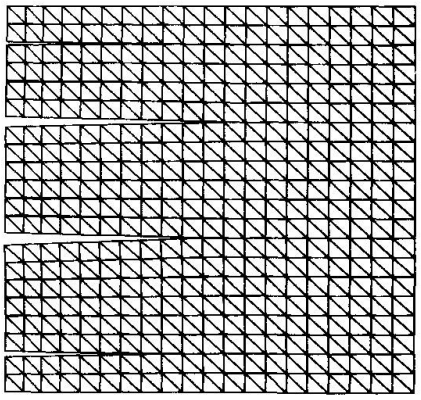

Fig. 7 : Crack pattern obtained by the stochastic model. Cracking depth varies from 5 to 11 mm but only a few cracks appear open.

Finally, in the prestressed slab, even a 12.5 MPa applied compression could not prevent a slight tension damage experimentally observed. However, this loading did favour an almost full development of the intrinsic drying strains. These reflect the water content distribution and proportionally induce the stress profile (fig. 5c) deduced through the release method.

6. CONCLUSIONS

1- The displacements, occuring on the concrete surface while cutting a slot, reflect the high tensile stresses due to drying shrinkage and enable their evaluation.
2- The observed displacement field response to stress release is significantly different according to whether concrete is prestressed or not. In both cases, the response to jack pressure confirmed the linear elastic relationship assumed between drying strains and stresses.
3- A closer scrutiny of the results shows potential tension exceeding the strength of the material through an appreciable depth (5-10 mm), and creating a damage or softening zone.
4- The quantitative analysis of the mechanical damage, actually suffered by the concrete skin layer, confirms the importance and facilitates the optimization of two re-bar parameters : cover and bond. This may contribute to a better control of durability problems linked with the drying of concrete.
5- The stress release method, developed in the LCPC, proved suitable for the analysis of drying effects. The method also enables the access to external load stresses acting on the structure, for a drying depth within the measurement range. For drying beyond this range, other operation ways are now being tested to attain the load stresses.

ACKNOWLEDGEMENTS

Part of this research was supported by AFREM-MRT-DAEI Contract.
The authors thank A. Lelièvre and A. Attolou for the care with which they carried out the tests.

REFERENCES

1. WITTMANN F.H., ROELFSTRA P.E., "Total Deformation of Loaded Drying Concrete", Cement and Concrete Research, Vol. 10, p. 601-610, 1980.
2. BAŽANT Z.P., RAFTSHOL W.J., "Effect of Cracking and Drying in Shrinkage Specimens", Cement and Concrete Research, Vol. 12, n° 2, 1982.
3. MENSI R., ACKER P., ATTOLOU A., "Séchage du béton : analyse et modélisation", Matériaux et Constructions, Vol. 21, p. 3-12, 1988.
4. ABDUNUR C., "Stress and Deformability in Concrete and Masonry", IABSE Symposium, Final Report, p. 123-130, Venezia, 1983.
5. ABDUNUR C., "Mesure de contraintes sur ouvrages d'art par une méthode de libération miniaturisée", Bulletin de Liaison des LPC, n° 138, p. 5-14, 1985.
6. ABDUNUR C., "Mesures directes de contraintes sur une pile du viaduc de Charmaix", Rapport LCPC, 1986.
7. MIAO B., "Effets mécaniques dus au retrait de dessiccation du béton", Thèse de l'ENPC, Paris, 1988.
8. Proc. CNRS-NSF Workshop "Localization, Damage and Size Effect", J. Mazars and Z.P. Bažant Ed., Elsevier Publ., 1989.
9. ROSSI P., PIAU J.M., "The Usefulness of Statistical Models to Describe Damage and Fracture in Concrete", in Workshop ref.8.
10. ACKER P., "Comportement mécanique du béton : apports de l'approche physico-chimique", Rapport de Recherche des LPC, n° 152, 1988.

Thermal Incompatibility of Concrete Components and Durability of Structures

Incompatibilité thermique des composants du béton et durabilité des structures

Thermische Unverträglichkeit der Betonkomponenten und Dauerfestigkeit der Konstruktionen

Srdjan D. VENEČANIN
Docent
University of Beograd
Beograd, Yugoslavia

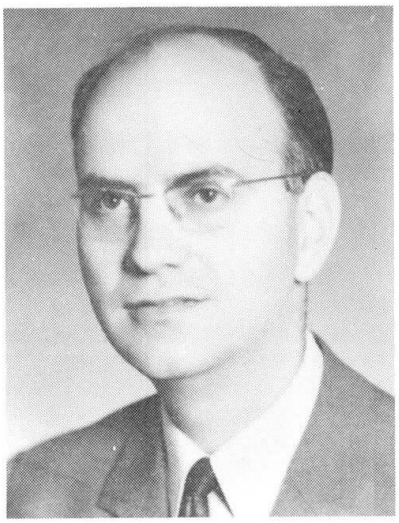

Srdjan Venečanin, born 1930, received his civil engineering degree at the University of Beograd, Beograd, Yugoslavia. He has designed reinforced and prestressed concrete structures. Now he lectures on Concrete Bridges at the Dep. of Civil Eng. of the University of Beograd. His research work is associated with durability of concrete structures.

SUMMARY

Unequal thermal expansions of aggregate and hardened cement paste reduce durability of concrete if it is exposed to temperature changes. Properties of aggregate which affect this phenomenon, and types of structures in which this phenomenon can appear are discussed.

RÉSUMÉ

Les dilatations thermiques différentes des granulats et de la pâte de ciment durcie réduisent la durabilité du béton s'il est exposé à des variations de température. Les propriétés des agrégats influençant ce phénomène ainsi que les types de structures concernés, sont décrits dans l'article.

ZUSAMMENFASSUNG

Die ungleichen Volumenänderungen der Zuschlagstoffe und der Zementkörner infolge von Temperaturänderungen verkleinern die Dauerfestigkeit des Betons. In der vorliegenden Arbeit wird über die Eigenschaften der Zuschlagstoffe, welche diese Phänomene beeinflussen, sowie über die Art der Konstruktionen, bei welchen sich derartige Fragen stellen, diskutiert.

1. INTRODUCTION

Unequal temperature volume changes of concrete components - aggregates and hardened cement paste - cause tensile stresses and cracks in concrete. This does not reduce much compressive strength, but cracks enable penetration of moisture and chlorides into concrete, and durability of such concrete is reduced.

This phenomenon is often called thermal incompatibility of concrete components (TICC). It appears if difference of coefficients of thermal expansion (CTE) of concrete components is sufficiently large, and if such concrete is exposed to sufficiently large temperature changes.

2. SHORT BACKGROUND

One of the first papers on TICC /1/ describes rapid failure of some cast stone steps in the winter 1938-39. An aggregate of unusually low CTE was used. The published discussion /2/ by ten writers was approximately five times as large as the original paper, and it shows the great interest for the theme.

In the last five decades the problem was discussed in journals, but "investigations in the literature and authoritative textbooks on the subject do not present a clear-cut picture of the effects that might be expected and some aspects of the problem are somewhat controversial" /3/. In fact some experiments confirmed theories on TICC, but some did not.

In the last ten years or so, analytical solutions supported the theories on TICC phenomenon /4, 5, 6/, and recent laboratory tests /7, 8/ and tests with concrete drilled from bridges /9/ absolutely confirm detrimental effects of TICC. Doubts that in specimens of young concrete, when exposed to temperature changes, are exposed to the effects of autogeneous healing and faster hydration during "hot" part of temperature cycles, which also were discussed in the literature /10/, have been taken into account: in specimens of young concrete, when exposed to large number of temperature cycles, and in old concrete drilled from bridges, there is no interference of autogeneous healing or faster hydration of cement.

A rewiew of the problem of TICC is given in the literature /11/.

3. MAIN THERMAL PROPERTIES OF COMPONENTS THAT AFFECT TICC

CTE of hardened cement paste varies between 9 and 25.4×10^{-6}/K, which is not large interval /12/. CTE of rocks which are usually used as aggregate in concrete, varies between negative values - contracting when heated - and 16×10^{-6}/K - see /12/.

However, carbonate rocks, which have very low values of CTE, sometime have nonelinear relationship between strains and temperature; they are often nonhomogeneous to a high degree; after cyclic temperature changes they may have residual strains; and often they are more or less thermally anisotropic. All of these properties are important for the phenomenon of TICC, and it is obvious that they have to be studied, and that they make CTE very poor tool to describe thermal volume changes of carbonate (and some other) rocks.

Nonelinear relationship means that inside a temperature range of, say, 100 K, CTE can be lower and higher, for some subintervals, than the average value for the whole range. Usually for the lower temperatures CTE of limestones is lower - which means that damaging effects of TICC could be bigger at lower temperatures.

Nonhomogeneity means that average value of CTE should be measured with as much as possible readings. Special technique has been devised: cube rock specimens have been used to measure temperature strains on each cube face in four directions - 24 readings at each temperature level per specimen (see e.g. /9/).

Residual strains after cyclic temperature changes mean different coefficients of thermal contraction. Since after each temperature cycle new residual strains can appear, this means different CTEs after each cycle - up to a point when these

residual strains between two subsequent cycles reduce to zero!

Thermal anisotropy mostly depends on orientation of calcite minerals - since calcite crystals are thermally anisotropic: they expand in the direction of one crystallografic axis, and contract in the directions of other crystallografic axes. If calcite crystals in the rock are oriented in the same direction, they transfer this anisotropy to the rock. This parallel orientation is often present to some degree, and degree of thermal anisotropy of the rock depends on the degree of parallel orientation of calcite crystals in it. The higher the thermal anisotropy of aggregate rock, the higher are the damaging effects of phenomenon of TICC. It is quite possible that the average value of CTE of a rock is rather near to that of hardened cement paste, but that damaging effects of TICC are high because thermal anisotropy of aggregate rock is high.

4. MECHANISM OF DETERIORATION OF CONCRETE DUE TO THE TICC

Generally TICC do not have to reduce much compressive strength of concrete. However it causes cracks in the concrete, mostly bond between aggregate and hardened cement paste is broken, and then moisture or chlorides penetrate concrete and damage it. So it is quite possible that TICC alone is not able to damage concrete significantly, and that frost action or chloride action is not able to damage concrete alone, but when TICC is combined with one of these two actions, concrete can be damaged. Combination of two or more adverse actions exponentially raises possibilities of damages of concrete.

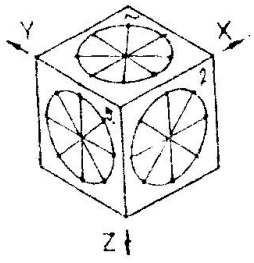

Cube rock specimens measuring temperature strains parallel to the cube edges and in the directions of diagonals

5. TYPES OF CONCRETE STRUCTURES IN WHICH TICC CAN BE DANGEROUS

It is necessary that components of concrete change their volumes differently when exposed to temperature changes. So the structure must be exposed to temperature changes beside having components of different thermal properties. Such types of structures are bridge decks, concrete roadways, concrete airport runways, taxiways and aprons, industrial chimneys, prestressed concrete pressure vessels, cryogenic concretes, roof tiles, and other concretes exposed to temperature changes.

If climatic conditions are severe, like in the Middle East desert regions where daily temperature changes can be large, or in Alaska or Siberia where seasonal temperature changes are large, all concretes exposed to the sun rays could be damaged by TICC. In some cases direct sun rays cause concrete surface to have nearly 30 K higher temperature than the air temperature is.

5.1 Bridge decks

Great surface of bridge slabs is exposed to direct sun rays, and temperature measurments show great differences of slab temperature and temperature of other parts of concrete bridge. This means that concrete of a bridge slab is exposed to rather large temperature changes - larger than the changes of the surounding air's temperature.

Cores drilled from the slab of a ten years old bridge were exposed to the temperature changes between -20°C and +60°C for 28 days - two complete thermal cycles per day. Then four of these cores, and four of reference ones, drilled from the slab of the same bridge - but kept at room temperature, were exposed to water pressure for a week: each day water pressure has been raised for one atmospehere, and kept seven hours per day under pressure. In the first four cores penetrated 72% more water than in the reference ones. It was obvious that new cracks deve-

loped in the specimens which have been heated and cooled in the thermal chamber.

CTE of limestone that has been used as coarse aggregate for this bridge has been measured for the temperature range between -20°C and +65°C, and was found to be about $3x10^{-6}$/K. Such a low CTE of coarse aggregate, and developement of new cracks in the bridge cores, show that TICC considerably contributed to the degradation of the bridge concrete /9/.

5.2 Concrete pavements

Concrete exposed to the direct sun rays reaches considerably higher temperatures than the surounding air. This means that range in which temperature of this concrete changes during one day is higher than diurnal temperature changes of the air. For concrete pavements this is very important because these concretes are exposed to the sun with great area, and TICC effects are to be expected /13/.

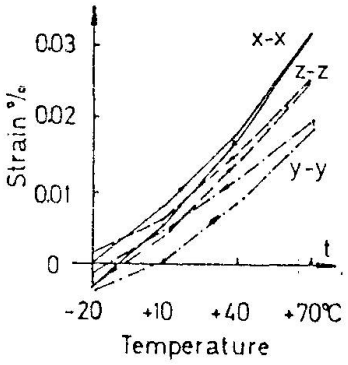

Strains vs temperature for three orthogonal directions shows thermal anisotropy

Contractors prefer to use limestones for concrete pavements because this kind of aggregate usually gives excellent compressive strength, even excellent tensile strength of concrete - and owner of the works require mostly control of compressive strength after 28 days. However limestones are the rock type which can have extremely low CTE - and combination of low CTE of aggregate and large range of temperature changes are essential conditions for detrimental effects of TICC.

Large milage of concrete pavement in Missouri, where it was noted that desintegration characterized initially by a typical map-cracking, occurred only when a specific kind of coarse aggregate has been used in concrete - has been reported by Reagel and Willis in their discussion /2/ of the paper /1/. Detrimental effects of TICC have been suspected, but Reagel and Willis note that it was found that most serious desintegration was always associated with the use of an aggregate having a large CTE. But they also note that this could be explained by more factors and phenomena whose effects overshadow any effect of thermal expansion.

Difficulties in separating effects of TICC and, for example, autogeneous healing, higher rates of hydration during "hot" part of temperature cycle (in experiments with young concrete), or "rim reaction", resulted in contradictory results of tests, and authoritative textbooks on the subject show some reserve when discussing this problem.

In the case of the Missouri pavements, thermal anisotropy of aggregate could also be the reason of desintegration of concrete.

5.2 Prestressed concrete pressure vessels (PCPV)

Since the first nuclear reactor with PCPV came into operation in France in 1959, the normal operating pressures and temperatures for this kind of structure have been gradually rising. Today operating pressures are of the order of 10 MPa, and operating temperatures of concrete reach 100°C - the steel liners reaching 300°C or even more.

Thermal gradient in PCPV requires high amount of prestressing steel around the vessel, but the lower CTE of the concrete, the lower amount of prestressing steel is needed. So often limestone of low CTE is used as crushed aggregate for concrete of PCPV - and problem of TICC is neglected. The same reasons apply for nuclear containment vessels.

To save on prestressing steel in such a way is a dangerous thing because low CTE of concrete is obtained by using aggregate of low CTE, making difference of CTEs

of aggregate and hardened cement paste bigger - and enhancing detrimental effects of TICC. When TICC starts cracking in such concrete, then "gas in cracks" loading problem, arising from leaks in the steel liner, exponentially raises possibilities of leakage of radioactive gasses outside the vessels.

The point is that TICC problem can be solved only by using concrete components of approximately the same CTE, and problem of stresses due to the thermal gradient can be solved by adding more prestressing steel - and not only by using concrete of low CTE. Conclusion should be that using thermally compatible concrete components means more prestressing steel, but it means less trouble during operation of reactor: less shutdowns during operation due to the leakage of radioactive gasses, and less consequent damages to the environment, etc.

5.4 Industrial chimneys

Though modern industrial chimneys have more than one flue in the exterior reinforced concrete shell, and the flue gasses are too hot and need liners, concrete shell still has higher temperature than the surrounding air. The temperature of exterior concrete shell is often changing, especially in higher parts of the chimneys, where constantly changing winds change concrete temperature. If concrete of such a chimney shell is made of thermally incompatible components, the cracks will appear soon.

The problem is rather similar as in PCPV: temperature gradient requires more reinforcement if CTE of concrete is higher - and vice versa. So it happens that some designers and contractors prefer limestone of low CTE for concrete aggregate, because this relults in concrete of low CTE, and save on reinforcing steel. However, this means trouble during operation of the plant - and, possibly, shutdowns and repairs of concrete.

5.5 Roof tiles

Measurements of temperature of roof covers which are exposed to sun rays show sometimes 40 - 50 K higher temperatures than the air. Cloudy weather affect temperature changes: some measurements have shown changes of 17 K in 7.5 minutes. The rain could be the reason of fast temperature changes of surfaces exposed to sun rays: some measurements have shown 8.3 K changes in only one minute, and 37 K in 30 minutes, of the surface hot due to the sun rays, when it was exposed to the rain.

Such severe conditions must destroy composite material if it consists of components with different CTE. If roof tiles are made of sand and cement, the sand should be quartzitic - with high CTE, which is near to the CTE of hardened cement paste.

Replacement of asbestos fibres by polymer fibres should cause trouble, because polymers usually have very high CTE, much higher than the CTE of hardened cement paste.

5.6 Concrete structures at cryogenic temperatures

Concretes exposed to cryogenic temperatures exhibit irregular volume changes when cooled: usually roughly between $-20^{o}C$ and $-70^{o}C$ concrete expands when cooled! Namely hardened cement paste expands when cooled, while nothing similar happens to the aggregate. This means great influence of TICC - and independently of the type of agregate, large tensile stresses and corresponding cracks appear. This is probably one of the main reasons why compressive strength of concrete decreases very much after only few temperature cycles in this range. Type of cement, moisture content, and pore structure are the factors affecting this phenomenon.

6. SOME CONSLUDING REMARKS

The problem is that nobody measures CTE of aggregate which will be used for a concrete. So there is no possibility at all to suspect TICC effects when concrete cracks. And everybody can see moisture or salts, and ascribe cracking to frost or chloride actions, or to something else.

Concrete structures described in Section 5 of this paper could be affected by TICC, but all kinds of concrete structures exposed to temperature changes could be affected by TICC - e. g. industrial floors.

If limestone aggregate is to be used for a structure which will be exposed to temperature changes, CTE of this rock should be measured for the temperature range in question. Also other properties discussed in Section 3 of this paper should be checked.

Practically all climatic conditions similar to the ones prevailing in the desert regions of the Middle East require cautiosness with respect to TICC.

Rocks containing silica minerals should be good with respect to TICC because they have high CTE - near to the CTE of hardened cement paste.

REFERENCES

1. Pearson J. C., A Concrete Failure Attributed to Aggregate of Low Thermal Coefficient. ACI Journal, Sept, 1941.
2. Hornibrook F. B. et al, Discussion of paper /1/, ACI Journal, June 1942.
3. Discussion of papers Nos. 8284 & 8302 by P. G. Fookes & I. E. Higginbottom, Proc. ICE; Part 1, August 1981.
4. Venečanin S. D., Influence of Temperature on Deterioration of Concrete in the Middle East, Concrete (London), August 1977.
5. Venečanin S. D., Durability of Composite Materials as Influenced by Different Coefficients of Thermal Expansion.ASTM STP 691, 1980.
6. Venečanin S., Analysis of Thermal Stresses in Concrete When it is Treated as Nonhomogeneous Three-component Composite Material (in Serbo-Croatian with summary in English). Proc. Symp. Yugosl. Soc. Structural Engineers, Trogir 1980.
7. Al-Tayyib A. J. et al, The Effect of Thermal Cycling on the Durability of Concrete Made from Local Materials in the Arabian Gulf Countries. To be published in Cement and Concrete Research.
8. Baluch M. H. et al, Concrete Degradation due to Thermal Incompatibility of its Components. IABSE Symp. on Durab. of Structures, Lisbon 1989.
9. Venečanin S. D. & Kovačević T. M., Thermal Incompatibility of Concrete Components in Concrete Bridges. Proc. Vol. III, First RILEM Congres, Versailles 1987.
10. Venečanin S. D., Experimental Study of Thermal Incompatibility of Concrete Components. III Int. Conf. on the Durab. of Build. Mat. & Comp., Proc. Vol. III, Helsinki 1984.
11. Venečanin S. D., Influence of Thermal Incompatibility of Concrete Components on Durability. The Arab. Journ. for Science & Engineering, Vol. 11, No., 2, 1986.
12. Venečanin S. D., Stresses in Concrete due to the Thermal Incompatibility of its Components. Int. Conf. on Mat. Science & Restoration, Proc. Vol., Esslingen 1983.
13. Venečanin S., Influence of Thermal Incompatibility of Concrete Components on Durability of Concrete Pavements (in Serbo-Croatian with summary in English). Proc. Int. Conf. on Modern Achievments in Des., Constr. and Maintenance of Concrete Pavements, Portorož 1985.

Influences of the Arabian Gulf Environment on Concrete Durability

Influences du climat du golfe persique sur la durabilité du béton

Einfluss des Klimas am persischen Golf auf die Dauerhaftigkeit von Beton

Abdul-Hamid J. AL-TAYYIB
Dr. Eng.
Research Institute-KFUPM
Dhahran, Saudi Arabia

Abdul-Hamid J. Al-Tayyib, born in 1946, obtained his Ph. D. in Civil Engineering from Texas Tech. University, Lubbock. At present he is Manager of the Materials and Building Technology Program of the Research Institute at King Fahd University of Petroleum and Minerals.

Abdulaziz I. AL-MANA
Dr. Eng.
Research Institute-KFUPM
Dhahran, Saudi Arabia

Abdulaziz I. Al-Mana, born in 1941, obtained his Ph. D. in Civil Engineering from Stanford University. At present, he is Manager of the Metrology, Standards and Materials Division of the Research Institute at King Fahd University of Petroleum and Minerals (KFUPM).

SUMMARY

In an experimental study, the temperature at various depths of concrete slabs exposed in the field environment of the Arabian Gulf countries has been measured. The effect of the temperature of concrete, which has been found different than that of the ambient air temperature, on its durability has been explained. The surface layer of a deteriorated concrete structure has been chemically analyzed to emphasize the role of air suspended particulate matter in concrete durability.

RÉSUMÉ

Des mesures de température ont été faites à différentes profondeurs d'une dalle en béton exposée aux conditions atmosphériques du golfe persique. L'effet sur la durabilité de la différence de température extérieure et dans le béton est discuté. La couche extérieure d'une structure en béton endommagée a été analysée chimiquement afin de déterminer le rôle des particules suspendues dans l'air.

ZUSAMMENFASSUNG

In einer der Witterung ausgesetzten Betonplatte wurden in verschiedenen Tiefen die Temperaturen gemessen. Die Wirkung der von der Umgebungstemperatur abweichenden Betontemperaturen auf die Dauerhaftigkeit wird besprochen. Die oberste Schicht einer geschädigten Betonstruktur wurde chemisch analysiert, um die Rolle der Luft als Träger suspendierter Stoffe zu belegen.

1. INTRODUCTION

The environmental conditions of the Arabian Gulf region are mainly characterized by its hot summer with virtually no precipitation and high evaporation. The daily mean air temperature in the summer usually varies from 30 to 35^{0}C with maximum temperature as high as 50^{0}C. The mean diurnal swing of air temperature is in the range of 10 to 15^{0}C. The relative humidity varies from 40% to 80%. These environmental conditions of the Arabian Gulf countries are considered to be one of the important factors in the rapid deterioration of concrete structures. Some of the other factors are high salt prevalence in ground, ground water and atmosphere, the scarcity of good quality aggregates, and lack of proper specifications. The deterioration of concrete structures within 10 to 15 years of their service life is common in the Arabian Gulf countries [1]. The various deterioration mechanisms identified in the region are reinforcing steel corrosion, sulfate attack, salt weathering and environmental cracking [2].

In this paper, the results of an experimental study are presented in which the actual temperature of concrete has been measured. Some earlier investigators [3,4] have pointed out that the concrete surfaces may have a temperature 30-40^{0}C higher than that of ambient air temperature. This difference between ambient air temperature and concrete temperature is attributed to the fact that the concrete temperature is not only a function of ambient air temperature, but some other factors also. These include solar radiation, thermal characteristics of concrete, wind speed, heat gain or loss from the ground and the occupied space [5]. If the values reported in the above references [3,4] are assumed, the concrete surface temperature in the Arabian Gulf countries may reach as high as 80-90^{0}C during summer days. Such a high concrete surface temperature coupled with a temperature differential along the depth of concrete may induce significant stresses which may even crack the concrete [6-9].

This study was thought to be important because the available literature provides little experimental data on concrete temperature in the Arabian Gulf countries. Such data is needed in quantifying the environmental stresses and assessing their consequences on concrete durability. The cracking of concrete due to its temperature variations, although usually mentioned in literature, has not been thoroughly investigated. Some studies that have been carried out on this aspect are by Illston and Tajirian [6] and Venecanin [7-9].

Data has also been included in this paper from a separate set of experiments which were carried out to determine the chlorides and sulfates accumulated on the concrete surface from the atmosphere. The objective of this work was to demonstrate that the air suspended particulate matter of the Arabian Gulf environment which contains the deleterious chloride and sulfate salts may play an important role in the durability of concrete even if all the precautionary measures are taken to remove these salts during construction.

2. EXPERIMENTAL PROGRAM

For the measurement of temperature at various depths of concrete, two slabs of dimensions 2 m x 2 m x 0.4 m were cast in the field environment of Dhahran. One slab was cast on a 16 cm thick asphalt-sand composite base which in turn was placed on compacted subgrade soil. While the other slab was cast directly on the compacted subgrade soil. The location of the slabs was such that the sun rays reached the slab surfaces without any obstruction. The slab concrete had 28-day compressive and tensile strengths of 387 kg/cm^2 and 49 kg/cm^2, respectively. Thermocouples were embedded at top, middle and bottom of the concrete slabs at different locations. To facilitate the embedding of the thermocouples, they were first mounted on 10 cm x 10 cm x 40 cm precast beams of concrete similar to that

of slab concrete. The mounted concrete beams were then placed on selected locations and concrete was poured.

In the other set of experiment, which was carried out to realize the role of air suspended particulate matter, the dust accumulated on the surface of a deteriorated concrete structure in Dhahran was collected from different locations using a brush. The dust was then analyzed for chlorides and sulfates.

3. RESULTS AND DISCUSSION

Figures 1 and 2 show the temperature at various depths of concrete slab placed on asphalt-sand base during typical days of summer and winter, respectively. The data on temperature of concrete slab placed directly on subgrade soil is not being presented here due to insignificant difference between the temperature of the two slabs. The maximum difference between the temperature of the two slabs has been found in the range of 0.1 to 2.0 ^{0}C at all the depths.

From Figs. 1 and 2, it can be noticed that the difference between the concrete temperature and ambient air temperature is different for different times of the day and different seasons. During the noon time of summer days, the concrete surface temperature is typically 10 ^{0}C higher than that of the ambient air temperature. However, on few occasions of the one year monitoring period, a difference as high as 15 ^{0}C between the concrete surface temperature and ambient air temperature has been recorded. These differences are low as compared to the ones reported in references [3-5]. However, reasonable agreement has been found between the results of this study and the theoretical study of Illston and Tajirian [6]. The concrete temperature predicted by the computer model of Illston and Tajirian [6] for a concrete slab of dimensions 6 m x 6 m x 0.30 m is shown in Fig. 3 for comparison. Their computer model is based on the following equation:

$$k_s \frac{\partial T}{\partial Z} = -H(T - T_A) + gR - se(\bar{T}^4 - \bar{T}_A^4) \quad ..(1)$$

Where T and $\bar{T}$ are concrete temperatures in ^{0}C and ^{0}K, respectively, T_A and $\bar{T}_A$ are ambient air temperatures in ^{0}C and ^{0}K, respectively, Z is the depth

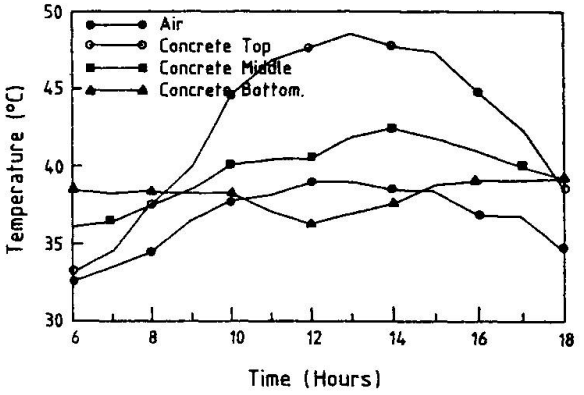

Fig. 1 Variation of ambient air temperature and concrete temperature during a typical summer day in Dhahran

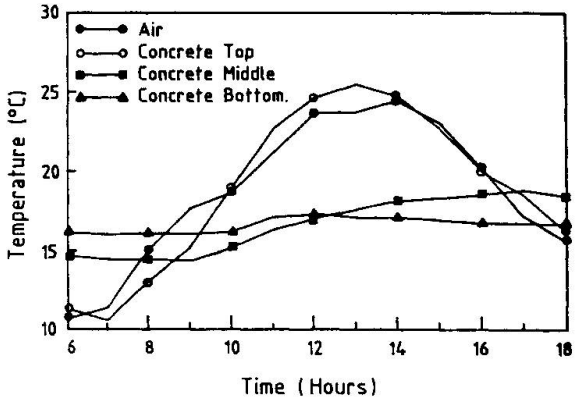

Fig. 2 Variation of ambient air temperature and concrete temperature during a typical winter day in Dhahran

coordinate, k_s is the thermal conductivity of concrete, H is the surface convection factor, g is the absorptivity constant, R is the intensity of solar radiation, s is the Stephan-Boltzmann constant, and e is the emissivity coefficient.

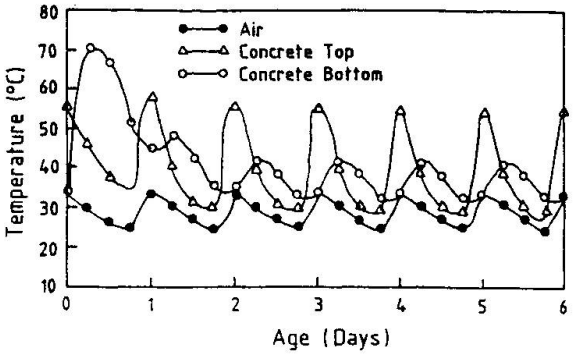

Fig. 3 Concrete temperature predicted by the computer model of Illston and Tajirian (6)

From Fig. 3, it may be noticed that the concrete surface temperature during noon time is approximately 20^0C higher than the ambient air temperature as compared to 10-15^0C in this study. This difference may be attributed to at least two important factors; (a) approximate values of various parameters have been used in equation (1), and (b) the predicted temperatures in Fig. 3 are for a concrete during its first six days of casting when the heat of hydration also contributes in the rise of concrete temperature.

From the results of this study (Figs. 1 and 2), it may also be noted that the typical temperature differential between the top and bottom of slabs during the noon time of summer days is 10^0C, while in winter days it is about 8^0C. During the summer days, temperature differential as high as 15.6^0C has been recorded. The temperature gradient obtained in this study is slightly less than that predicted by Illston and Tajirian [6].

The diurnal change in concrete temperature has been found in the range of 15-20^0C in the summer as well as in the winter. This is higher than the diurnal change in ambient air temperature which is in the range of 10-15^0C.

The large diurnal changes in concrete temperature cause tensile stresses in concrete if the coefficients of thermal expansion of the aggregate and cement paste are significantly different [7-9]. Limestone rock, the commonly available source of coarse aggregates in the Arabian Gulf countries has a coefficient of thermal expansion in the range of 0.9×10^{-6} to $12.2 \times 10^{-6}/^0$C as compared to 10×10^{-6} to $20 \times 10^{-6}/^0$C of hardened cement paste [8]. Venecanin [7] has developed two simple equations that can be used to calculate the stresses in concrete due to daily rise and fall in concrete temperature. These equations include the thermal properties, elastic properties and area of both the aggregate and cement paste along with temperature rise or fall. Considering a coefficient of thermal expansion of $5 \times 10^{-6}/^0$C for aggregates and $15 \times 10^{-6}/^0$C for cement paste along with moderate values of elastic properties and area, tensile stresses that can be generated in the concrete for a temperature change of 15-20^0C are calculated to be 18.75-25.0 kg/cm^2. The magnitude of these type of stresses would decrease with the depth of concrete. As can be seen from Figs. 1 and 2, the diurnal changes in concrete temperature at the middle and bottom of the slab are low as compared to that at the surface. Concrete surfaces subjected to direct sun rays such as airport and road pavements, and bridge slabs are some of the situations where these type of stresses may be significantly high [9].

Another type of stress which may be induced due to temperature is warping stress, particularly in pavement slabs. If there is a large temperature differential along the depth of concrete, the pavement slabs tend to warp and the restraint offered to this warping tendency by the self weight of the slab induces warping stresses. The equations given in reference [10] which are based on Westergaard's analysis and Bradbury's coefficients may be used to calculate such type of stresses. These equations yield a tensile stress of 0.75 kg/cm^2 for the slabs of

this study and for a temperature differential of 15^0C between the top and bottom of the slabs. However, these stresses vary considerably with the dimensions of the slab and its elastic and thermal properties [6]. Keeping the other parameters same, the warping stress in a 5 m x 5 m x 0.4 m slab is calculated to be 13.2 kg/cm^2 as compared to 0.75 kg/cm^2 in the 2 m x 2 m x 0.40 m slab of this study.

The thermal stresses discussed above may not be sufficient to crack a good quality concrete, but in combination with stresses due to loads they may easily do so. Such concrete cracking, which may or may not be structurally dangerous, provides a path for various deleterious salts such as chlorides and sulfates to enter the concrete. These salts initiate or accelerate, if already initiated, the common deteriorating mechanisms, reinforcing steel corrosion and sulfate attack. Even if all the precautionary measures are taken to remove the deleterious salts during the construction phase of concrete, they may come from air suspended particulate matter. This view is supported by the chemical analysis of the surface layer of a deteriorated concrete structure carried out in this study (Table 1). It is believed that the significant amounts of chlorides and sulfates present on the concrete surface are mainly due to high concentration of these salts in the air suspended particulate matter of the Arabian Gulf environment (Table 2).

Location	Cl^- (%)	SO_4^{2-} (%)
1	7.0	21.0
2	8.0	21.0
3	4.5	16.0
4	2.6	18.0
5	5.0	22.0
6	2.0	23.0

Table 1 Chlorides and sulfates on the surface layer of a deteriorated concrete structure in Dhahran

Chemical constituent	Mean concentration ($\mu g/m^3$)		
	Abqaiq	Dhahran	Ras Tanura
Na	13.0	6.0	12.0
K	1.3	1.7	0.9
Ca	21.7	51.8	15.7
Mg	12.7	16.7	7.1
Cl	11.8	18.0	23.2
SO_4	32.6	34.0	23.1
SiO_4	11.9	-	3.9

Table 2 Chemical composition of air suspended particulate matter collected from different parts of Saudi Arabia [reference 11]

4. CONCLUSIONS

This study has revealed that for assessing the influence of temperature on concrete durability, a precise measurement of concrete temperature is necessary. The assessments based on ambient air temperature would be misleading. During the summer days of the Arabian Gulf countries, the concrete surface temperature is 10-15^{0}C higher than that of the ambient air temperature. The diurnal change in concrete temperature is 15-20^{0}C as compared to 10-15^{0}C in ambient air temperature. A temperature gradient as high as 0.4^{0}C/cm has been found along the depth of concrete during summer. In such a temperature regime, significant stresses may be induced in concrete due to thermal incompatibility of concrete constituents. In concrete structures such as pavements, warping stresses may also be present. The thermal stresses in combination with load stresses may easily crack the concrete and once the cracks develop, the chlorides and sulfates

contained in the atmosphere and subsequently settled on concrete surface could enter the concrete and initiate or accelerate the concrete deterioration process.

5. ACKNOWLEDGEMENTS

The authors greatly acknowledge the Research Institute at King Fahd University of Petroleum and Minerals (KFUPM), Dhahran, Saudi Arabia.

6. REFERENCES

1. AL-TAYYIB, A.J. and KHAN, M.S., Concrete Deterioration Problems in the Arabian Gulf- A Review. Durability of Building Materials, Vol. 4, 1987, pp. 287-298.

2. RASHEEDUZZAFAR, DAKHIL, F.H. and Al-GAHTANI, A.S., Deterioration of Concrete Structures in the Environment of the Middle East. ACI Journal, Vol. 81, No. 1, 1984, pp. 13-20.

3. MIRONOV, S.A., MALINSKYI, E.N. and VAKHITOV, M.M., Durability Assessment Criterion for Concrete Exposed to Dry Hot Climatic Conditions. Durability of Building Materials, Vol. 1, 1982, pp. 3-14.

4. DE SERIO, J.N., Designing for Effects of Creep, Shrinkage, Temperature in Concrete Structures. Special Publication SP-27, American Concrete Institute, Detroit, Michigan, 1971, pp. 43-49.

5. ASHTON, H.E. and SEREDA, P.J., Environment, Microenvironment and Durability of Building Materials. Durability of Building Materials, Vol. 1, 1982, pp. 49-65.

6. ILLSTON, J.E. and TAJIRIAN, A., Computer Experiments on Environmentally Induced Stresses in Unreinforced Concrete Pavement Slabs. Magazine of Concrete Research, Vol. 29, No. 101, 1977, pp. 175-190.

7. VENECANIN, S.D., Durability of Concrete Materials as Influenced by Different Coefficients of Thermal Expansion of Components. Durability of Building Materials and Components, ASTM STP 691, P.J. Sereda and G.G. Litvan, Eds., American Society for Testing and Materials, 1980, pp. 179-192.

8. VENECANIN, S.D., Influence of Temperature on Deterioration of Concrete in the Middle East. Concrete, Vol. 11, No. 8, 1977, pp. 31-32.

9. VENECANIN, S.D., Influence of Thermal Incompatibility of Concrete Components on Durability. The Arabian Journal for Science and Engineering, Vol. 11, No. 2, 1986, pp. 157-166.

10. YODER, E.J. and WITCZAK, M.W., Principles of Pavement Design. John Wiley and Sons, New York, Second Edition, 1975, pp. 85-88.

11. Sampling and Characterization of Ambient Air Suspended Particulate Matter in Abqaiq, Dhahran and Ras Tanura. Report, Water Resources and Environment Division, Research Institute, King Fahd University of Petroleum and Minerals, Dhahran, Saudi Arabia, March 1983, 55 pp.

Removal of Concrete by Acidic Water

Usure du béton par de l'eau acide

Betonabtrag durch saure Wässer

Horst GRUBE
Dr.-Ing.
Forschungsinst. Zementindustrie
Düsseldorf, BR Deutschland

Horst Grube, geboren 1938, promovierte als Bauingenieur an der TH Darmstadt. Er leitete 12 Jahre das zentrale Baustofflabor einer Grossbaufirma und ist seit 8 Jahren stellv. Leiter der Hauptabteilung Betontechnik im Forschungsinstitut. Arbeitsschwerpunkte: Ausführung und Dauerhaftigkeit von Betonbauwerken, Durchlässigkeit gegenüber Flüssigkeiten und Gasen, Kriechen, Schwinden, Instandsetzung.

Wolfram RECHENBERG
Dr.-Ing.
Forschungsinst. Zementindustrie
Düsseldorf, BR Deutschland

Wolfram Rechenberg, geboren 1931, promovierte als Chemiker an der TU Hannover. Er war 5 Jahre als Entwickler für Gummiasbest und Klebebänder tätig. Seit 22 Jahren ist er wissenschaftlicher Mitarbeiter des Forschungsinstituts und betreut die chemische Analyse. Zu seinen Aufgabengebieten gehört der chemische Angriff auf Beton und die Erfassung von Zementwerksemissionen.

SUMMARY

The attack of acidic water must be assessed when planning durable concrete structures. The aggressiveness is generally expressed in terms of concentration of attacking acid. A protective layer built up by reaction products and its stability can have a much greater influence on the loss of material than the concentration of the attacking substances. Experiments, based on a calculation model, show how to estimate the loss of material (the amount of affected concrete) to be expected under practical conditions. Parameters are the type and the concentration of the acid solution, the composition of the concrete and the stability of the protective layer.

RÉSUMÉ

Il faut tenir compte de l'attaque possible des eaux acides lors de projet de structures en béton durables. Le degré d'attaque est en général donné par la concentration de l'acide. Une couche protectrice formée par des produits de réaction et sa stabilité peuvent avoir une influence plus importante sur le taux d'usure que la concentration de la solution attaquante. Des expériences basées sur un modèle de calcul montrent comment estimer le taux d'usure dans les conditions réelles de construction. Les paramètres sont le genre et la concentration de la solution d'acide attaquant, la composition du béton et la stabilité de la couche protectrice.

ZUSAMMENFASSUNG

Der Angriff saurer Wässer muss bei der Planung dauerhafter Betonbauwerke berücksichtigt werden. Der Angriffsgrad wird im allgemeinen durch die Konzentration der angreifenden Säure angegeben. Eine aus Reaktionsprodukten gebildete ungestörte Schutzschicht kann einen wesentlich grösseren Einfluss auf die Abtragsrate haben als die Konzentration der angreifenden Lösung. Versuche auf der Grundlage eines Rechenmodells zeigen, wie man die Abtragsrate unter baupraktischen Bedingungen abschätzen kann. Einflussgrössen sind Art und Konzentration der angreifenden sauren Lösung, die Zusammensetzung des Betons und die Stabilität der Schutzschicht.

1. INTRODUCTION

Water which contains diluted acid, e.g. lime-attacking carbonic acid, will affect concrete. The acid dissolves the calcium from its bonds. As a result, the concrete is progressively destroyed from the surface to the inside. The rate at which the hardened cement paste and possibly the aggregate are dissolved mainly depends on the concentration of the attacking acid in the water and on the chmical resistance of the concrete. Many standards determine the degree of attack primarily on the basis of the concentration of the aggressive substances, e.g. ISO standard /1/. Test results show /2,3,6/ that only a very small proportion of the aggressive substances in the running water reacts with the hardened cement paste. Beyond that the chemical resistance of the concrete against a solvent attack can be enhanced by using insoluble aggregates and cement with a higher SiO_2 content /4,5/ and by keeping the water cement ratio low ($w/c < 0{,}60$). The flow rate seems to have very little influence /7/ as long as we stay within the ground water range of flow rates. This behaviour is to be explained by the formation of a protective layer of SiO_2 gel which, with increasing duration of attack, acts as a barrier to the transport of aggressive substance to and removal of dissolved constituents from the concrete. The chemical resistance of the concrete against solvent attacks is thus essentially depending on the existence of that protective layer. Reference to these correlations was made by several authors /8-11/. However, in planning and designing concrete structures they are not yet generally considered. It was therefore the objective of our study to develop a mathematical model for estimating in advance the loss of concrete as a function of the concrete composition, the concentration of the aggressive solution and the stability of the protective layer.

2. COURSE OF REACTION

Tests have shown /11,12/ that carbon dioxide (CO_2) dissolved in water first leads to the formation of a thin layer of calcium carbonate ($CaCO_3$) in the areas of mortar or concrete which are close to the surface. Then additional CO_2 dissolves the $CaCO_3$ to form $Ca(HCO_3)_2$ which is removed by the water. Next in the same process calcium from the calcium silicates is dissolved and removed. What remains is a gel-like layer consisting of hydrous silicon dioxide which also contains iron and aluminium oxide /11,13/. The gel layer becomes thicker with progressing attack. If a solid material forms a protective layer, the rate of dissolution will become essentially independent of the flow rate of the solution. In that case it will only be determined by the thickness and the diffusion resistance of the protective layer. This dissolution process can be slowed down further by reducing the flow rate of the surrounding water towards zero and by increasing the diffusion resistance in the environment of the concrete by a tight soil.

3. DETERMINING THE CaO REMOVAL FROM MORTAR AND CONCRETE

Koelliker measured the rate at which CaO is removed by dissolution from 4 x 4 x 16 cm^3 Portland cement mortar prisms containing about 500 kg of cement per cubic meter and having a water-cement ratio of 0.50 /11,12/. Lime-dissolving carbonic acid was dissolved in the attacking water. The resulting pH value was about 4.4. The surface-related rate of dissolution decreased (following approx. a $1/\sqrt{t}$ law) with increasing exposure time. This indicates that, due to the effect of the lime-dissolving carbonic acid, a protective layer forms which gains in thickness in the course of time and thus increasingly blocks the diffusion of the dissolved CaO.

By means of a model based on Fick's first law equation 1 was developed /14/ which can be used for calculating the thickness d of the destroyed layer after any given exposure time t. The influencing variables are the diffusion coefficient, the mass of soluble matter per volume unit, the area percent of the soluble matter in the area of attack and the difference in $Ca(HCO_3)_2$ concentration:

$$d = \sqrt{\frac{2 \quad D \quad A_l}{m_l \quad A_{ges}} (c_s^* - c_l)} \cdot \sqrt{t} \qquad /1/$$

whereby

d	is the thickness of destroyed concrete layer in cm
D	$Ca(HCO_3)_2$ diffusion coefficient in cm^2/s of the protective layer (gel layer) ($D \approx 1.8 \cdot 10^{-6}$ $cm^2 \cdot s^{-1}$ for SiO_2 gel of hardened Portland cement paste)
m	mass of soluble matter in g of CaO per cm^3 of concrete
c_s^*	CaO-concentration in g/cm^3 in the $Ca(HCO_3)_2$-solution surrounding intact concrete
c_l	CaO-concentration in g/cm^3 in the $Ca(HCO_3)_2$-solution which is unaffected by the concrete
A_l/A_{ges}	ratio of soluble matter area to total area in the cross section
V_l/V_{ges}	ratio of the volume of soluble constituents (if insoluble aggregate is used volume of hardened cement paste) to total volume

$A_l/A_{ges} = V_l/V_{ges}$

Examples of computation including the determination of the concentration difference $(c_s^* - c_l)$ are given in /14/.

The first root in equation 1 represents a constant valid in the respective case. Equation 1 can therefore be simplified to form equation 2.

$$d = a \cdot \sqrt{t} \qquad /2/$$

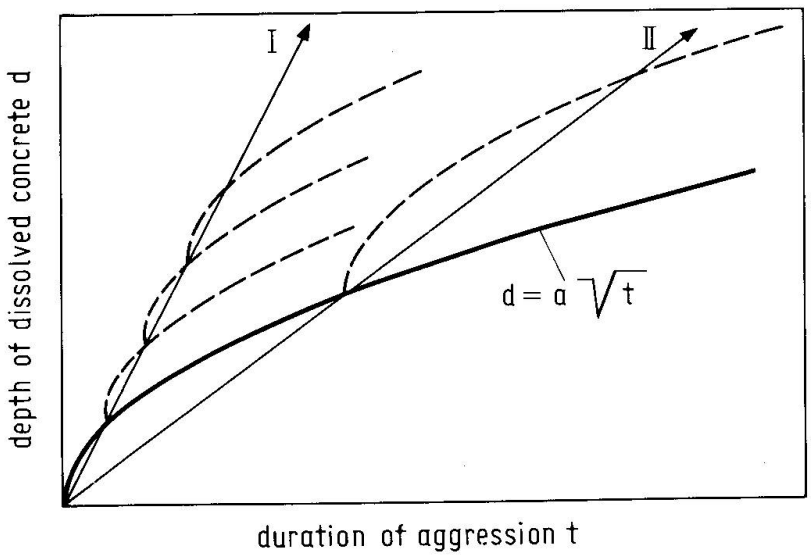

Fig. 1 Acceleration of a solvent attack when removing the protective layer periodically

The loss of mass which occurs with an intact protective layer and follows equation 2 is shown by the full bold line in Fig. 1. It had been assumed earlier that the loss of mass might follow a $\sqrt{t}$ law /6, 8-10/. However, in the past it was not possible to describe different test periods by one function. This was due to the fact that the test specimens were dabbed with a moist cloth before being weighed. In this way part of the gel-like protective layer was removed so that the subsequent reaction occurred much faster than it would have done with an intact protective layer. If the protective layer is removed

regularly it is to be expected that the parabolic function turns to a linear one as shown by the straight lines I and II in Fig. 1. The "linear loss of mass" will be the steeper the more frequently the protective layer is removed (straight line I). It will be the flatter the less frequently the protective layer is removed (straight line II). This "linear loss of mass" has already been observed in connection with long-term tests /3/.

In order to verify this behaviour experimentally 4 x 4 x 16 cm prisms according to DIN 1164 were made with a 35 F Portland cement and a 35 L blast furnace slag cement. They contained 550 kg/m^3 of cement and had a water-cement ratio of 0.50.

The prisms were produced and stored in water by the standard procedure. At the age of 7 days they were placed in tap water which was continuously enriched with CO_2 and renewed every week. The lime-attacking carbonic acid content was about 110 mg CO_2/l, the pH was 6.15 (mean values). The water flow rate was about 4.2 10^{-2} cm/s. The experimental setup is described in detail in /2/.

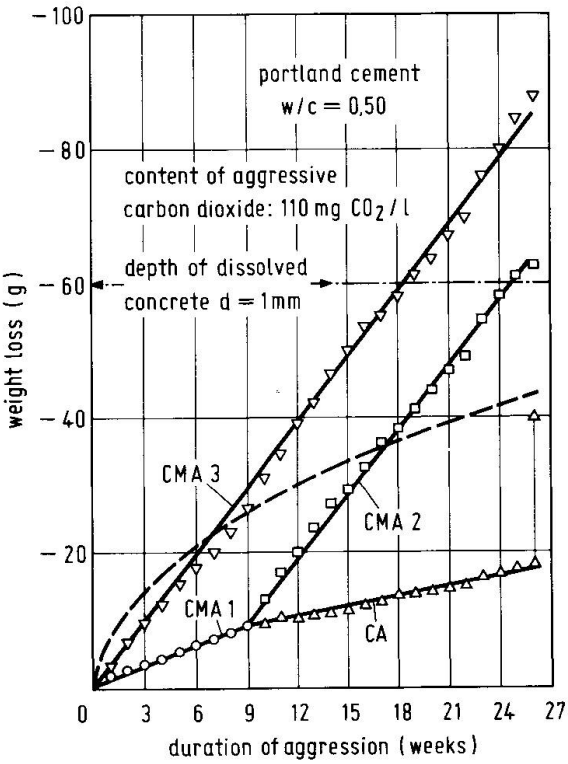

Fig. 2 Weight loss of PC-mortar prisms by aggressive carbon dioxide. Different intervals for removing the protective layer

The results for Portland cement mortar in Fig. 2 show that the weight loss resulting from the uniform chemical attack by 110 mg CO_2/l depends very much on the type and intensity of the additional mechanical treatment. In an initial series of tests the prisms were only dabbed once a week (CMA 1 in Fig. 2). After nine weeks some of the prisms were brushed once a week (CMA 2), the others were not subjected to any further mechanical treatment (CA). The prisms of the second test series were brushed three times per day throughout the test period (CMA 3).

The storage without any further mechanical treatment describes the chemical attack in slowly running water according to ISO DP 9690 /1/ with the diffusion being controlled by the protective layer. Dabbing presents a mild and brushing a vigorous additional mechanical treatment (M) of the protective layer.

The rate of concrete removal for CMA 3 was approx. 1 mm in 18 weeks or about 3 mm/a in the 4 x 4 x 16 cm prisms (a weight loss of 60 g corresponds to about 1 mm of loss of concrete). The rate of concrete loss was lower for the blast furnace slag cement mortars /14/ than it was for the Portland cement mortars. This leads to the assumption that the higher content of silicon oxide and the resulting lower content of calcium oxide in blast furnace slag cement might be an explanation for this behaviour. The question, however, was not studied in greater detail.

The various losses of mass obtained in the tests are below the ones calculated using equation for, e.g., weekly losses, because brushing did not remove all of the SiO_2-gel from the pores. The longer the time period of an undistur-

bed gel layer was the better was the agreement between the calculated and the experimental results /14/. This can be seen from the dotted line in Figure 2, which shows the calculated depth of dissolved concrete according to equation 1. The first brush off at the age of 26 weeks shows the marked value slightly below the calculated value.

4. PRACTICAL APPLICATION

In addition to the construction cost the design engineer should include in his considerations the service life and the repair and maintenance cost of a structure. If concrete is exposed to acids the resulting loss of mass may be irrelevant to its use. This often is the case for structures like foundations or drilled foundation piles. In contrast, the practical use of a container or a water duct where the protective layer may be removed regularly can be considerably impaired by a constant loss of e.g. 0.5 mm of concrete per year. Therefore the design engineer, besides considering the acid concentration in the attacking water, should also pay attention to the external conditions on which the concrete is exposed to the water. For illustration Fig.3 shows the depth of concrete loss in mm after 20 years for different conditions of transport and different content of aggressive CO_2. The conditions of transport are described in Table 1.

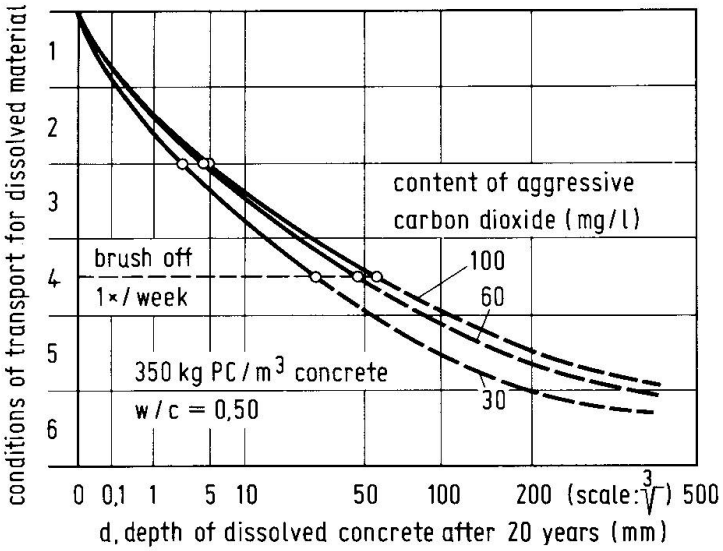

Fig. 3: Depth of dissolved (and removed) concrete after 20 years in different concentration of aggressive carbon dioxide at different conditions of transport (see below) for the products of the reaction

The dots in the figure represent the results of experiments and calculations. The dotted parts of the curves in the areas of TC 5 and 6 are extrapolations that can at present not be validated by test results.

CT 1	Compact deposited soil, permeability $k < 10^{-4}$ cm/s, very slowly moving or stagnant ground water, protective layer, Fick's 2. law.
CT 2	Permeable soil with $k \geq 10^{-4}$ cm/s, ground water moving slowly, protective layer, Fick's 1. law.
CT 3	Flowing free water, protective layer nearly undisturbed, Fick's 1. law
CT 4	Flowing free water, protective layer removed periodically, Fick's 1. law
CT 5	Flowing free water, high velocity of flow, no protective layer, approximation to specific velocity of dissolution.
CT 6	Flowing free water, very high velocity of turbulent flow, cavitation.

Table 1 Conditions of transport (CT) according to Fig. 3

5. CONCLUSIONS

- The diffusion model presented here and the tests described permit to arrive

at a quantitative estimate of the loss of mortar and concrete to be expected in case of a chemical attack by lime-dissolving carbonic acid.

- The exposure to lime-dissolving carbonic acid leads to the formation of a protective layer consisting of gel-like silicon dioxide.

- In the presence of an intact protective layer the loss of mass (the amount of affected concrete) follows a $\sqrt{t}$ law.

- If the protective layer is mechanically destroyed the concrete is removed at an accelerated rate.

- A disturbance of the protective layer, even if it occurs at relatively long intervals, can have a much more damaging effect than an increase in the concentration of the aggressive acid.

- The tests described, i.e. the stripping of the protective layer at regular intervals, and the mathematical model permit a long-term estimate of the loss of mass also caused by other than lime-dissolving carbonic acid. Experiments with other acids can be made in about 3 months.

- It appears possible to consider more completely in future standards the factors which reduce and increase the loss of mass from concrete exposed to attacking acids. This would be to the benefit of concrete structures. It is suggested to define the degrees of attack by solved mass or the affected depth of concrete respectively.

6. REFERENCES

1. ISO-Draft DP 9690 (1987): Classification of environmental exposure conditions for concrete and reinforced concrete structures. ISO-TC 71/SC3.
2. Locher, F.W., und S. Sprung: Die Beständigkeit von Beton gegenüber kalklösender Kohlensäure. beton 25 (1975) H. 7, S. 241/245.
3. Locher, F.W., W. Rechenberg und S. Sprung: Beton nach 20jähriger Einwirkung von kalklösender Kohlensäure. beton 34 (1984) H. 5, S. 193/198.
4. Friede, H., P. Schubert und H.P. Lühr: Angriff kalklösender Kohlensäure auf Beton. beton 29 (1979) H. 7, S. 250/253.
5. Efes, Y., und H.P. Lühr: Beurteilung des Kohlensäure-Angriffs auf Mörtel aus Zementen mit verschiedenem Klinker-Hüttensand-Verhältnis. TIZ-Fachberichte 104 (1980) H. 3, S. 153/167.
6. Friede, H.: Zur Beurteilung des Angriffs kalklösender Kohlensäure auf Beton. Dissertation RWTH Aachen 1983.
7. Gille, F: Über den Einfluß des Kalkgehalts des Zements und des Zuschlags auf das Verhalten des Betons in sauren Wässern. beton 12 (1962) H. 10, S. 467/470.
8. Tremper, B.: The Effect of Acid Waters on Concrete. Journal of the Amer. Concr. Inst., Proc. 28 (1932), S. 1/32.
9. Rombèn, L.: Aspects of Testing Methods for Acid Attack on Concrete. CBI forskning research 1:78 und 9:79, Cement- och betong institutet, Stockholm.
10. Polak, A.F.: Mathematical Model of Concrete Corrosion in Acidic Media. Beton; Zhelezobeton, Nr. 8, (1978), S. 5/6.
11. Koelliker, E.: Über die Wirkung von Wasser und wäßriger Kohlensäure auf Beton. Intern. Kolloquium "Werkstoffwissenschaften und Bausanierung", Berichtsband TA Esslingen, 1983, S. 195/200. E. Moeller GmbH, Filderstadt.
12. Koelliker, E.: Cem. Concr. Res. 15, 100 (1965).
13. Grün, R., und K. Obenauer: Einwirkung von Kohlensäure auf Zementmörtel und Beton. Zement 33 (1944) H. 1, S. 10/12.
14. Grube, H., und W. Rechenberg: Betonabtrag durch chemisch angreifende saure Wässer. beton 37 (1987) H. 11, S. 446/451, und H. 12, S. 495/498.

Anforderungen an Polymerbeton, Eigenschaften und Verarbeitung

Requirements for Polymer Concrete, Properties and Preparation

Qualités requises et préparation du béton de résine synthétique

Peter GRÜBL
Dipl. Bauing.
Dyckerhoff & Widmann AG
München, BR Deutschland

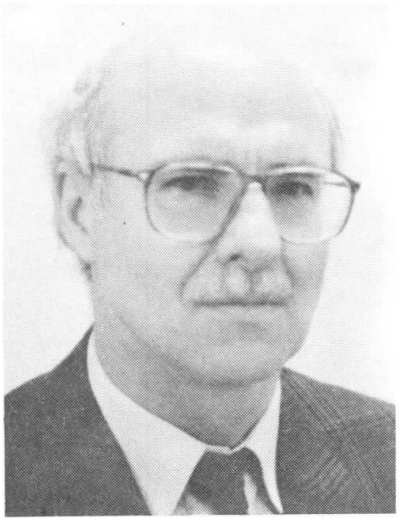

Peter Grübl, geboren 1941, promovierte als Bauingenieur an der Techn. Universität München. Er war mehrere Jahre tätig in der Forschung, Lehre, Konstruktion, Materialprüfung, Instandsetzung und Bauausführung. Seit 1985 ist er Betriebsleiter der firmeneigenen Versuchsanstalt mit Flüssigkunststoffbetrieb sowie verantwortlich für Baustofftechnologie und Qualitätssicherung.

ZUSAMMENFASSUNG

Polymerbeton ist ein relativ junger Ingenieurwerkstoff, der dem Zementbeton technologisch ähnlich ist, gegenüber chemischen Einwirkungen und der Diffusion von Flüssigkeiten und Gasen jedoch einen wesentlich höheren Widerstand als dieser besitzt und deshalb besonders für den Einsatz bei aggressiven Nutzungsbedingungen geeignet ist. Es werden die für einen materialgerechten Einsatz zu beachtenden Anforderungen und massgebenden Eigenschaften dieses Werkstoffes beschrieben und Hinweise für seine Verarbeitung gegeben.

SUMMARY

Polymer concrete is a relatively new construction material, very similar to cement concrete with respect to technological aspects, but with an essentially higher resistance against chemical effects and the diffusion of liquids and gases and is therefore especially appropriate for application under aggressive conditions. This paper describes the main requirements and properties of this construction material decisive for a material technological application and also gives information on preparing this material.

RÉSUMÉ

Le béton de résine synthéthique est un matériau de construction relativement nouveau,semblable du point de vue technologique au béton de ciment. Il a cependant une résistance bien plus grande aux actions chimiques et à la diffusion des liquides et des gaz. C'est pourquoi il convient particulièrement à l'emploi dans des conditions agressives. Cet article décrit les conditions particulières pour une utilisation optimale.

1. EINFÜHRUNG

Unter dem Begriff "Beton" verstehen wir üblicherweise einen Baustoff bestehend aus Zement, Wasser und mineralischen Zuschlägen, ggf. mit Zusätzen. Genau genommen handelt es sich hierbei um Zementbeton. Beim Polymerbeton dagegen besteht das Bindemittel aus einem Polymer, d.h. einem Reaktionsharz, das nach der Zugabe eines Reaktionsmittels durch eine chemische Reaktion erhärtet. Für solche Betone hat sich zur Unterscheidung zum Zementbeton, dem "CC" (= Cement Concrete), die Bezeichnung "PC" (= Polymer Concrete) eingebürgert.

Daneben gibt es noch Mischsysteme bezüglich des Bindemittels, d.h. das Bindemittel besteht aus einer Mischung von Zement und Kunststoff. Ein solcher Beton wird auch als kunststoffmodifizierter Zementbeton oder "PCC" (= Polymer Cement Concrete) bezeichnet.

Gelangt der Kunststoff nicht bei der Betonherstellung in den Beton, sondern wird er erst nachträglich, d.h. nach dem Erhärten des Zementbetons dem Gefüge zugeführt, so spricht man von polymer-imprägniertem Beton "PIC" (= Polymer Impregnated Concrete).

Der Einfluß von Kunststoff auf typische Eigenschaften des Betons geht aus Tabelle 1 hervor.

2. WERKSTOFF POLYMERBETON

Die Idee, ein Polymer als Bindemittel für Beton zu verwenden, ist bereits mehr als 30 Jahre alt. Die ersten Berichte stammen aus den USA. Technologisch ist der Polymerbeton dem Zementbeton sehr ähnlich. Die Eigenschaften des Betons ergeben sich aus den Eigenschaften der einzelnen Bestandteile und ihrem Zusammenwirken.

Eigenschaft	CC	PCC	PIC	PC
Druckfestigkeit (N/mm^2)	45	60	100	120
Zugfestigkeit (N/mm^2)	5	10	10	25
E-Modul (N/mm^2)	35.000	25.000	45.000	35.000
Wasseraufnahme (M.-%)	5,0	1,0	0,5	< 0,1
Säurewiderstand (Erhöhungsfaktor)	1 x	5 x	> 10 x	> 25 x
Frost-Tau-Widerstand (Anzahl der Wechsel/ Verlust in M.-%)	700/25	3000/2	3500/2	1600/0

Tabelle 1 Einfluß von Kunststoff auf typische Eigenschaften des Betons

Beim Polymer lassen sich entsprechend dem makromolekularen Aufbau drei Gruppen unterscheiden:

- Thermoplaste
- Elastomere
- Duromere (= Duroplaste)

Für die Herstellung von Polymerbeton eignen sich nur die härtbaren Duromere. Deren wichtigsten Vertreter sind:

- ungesättigte Acrylharze (PMMA)
- ungesättigte Polyesterharze (UP)
- Polyurethane (PUR) und
- Epoxidharze (EP).

3. EIGENSCHAFTEN VON POLYMERBETON

3.1 Anforderungen

Die Grenzen der Leistungsfähigkeit des Zementbetons liegen hauptsächlich in der begrenzten Widerstandsfähigkeit gegenüber chemischen Einwirkungen insbesondere bei Säuren und in einem begrenzten Diffusionswiderstand gegenüber Flüssigkeiten und Gasen. Verantwortlich dafür ist in erster Linie der Zementstein. Eine Erhöhung des Korrosions- und Diffusionswiderstandes wird durch den Austausch des Bindemittels erreicht. Die auch angewendete Alternative, den Zementbeton durch das Aufbringen einer Beschichtung zu schützen, hat nicht selten zu Schäden geführt (Blasenbildung, Ablösungen), so daß diese Lösung nicht in allen Fällen als ausreichend zuverlässig anzusehen ist.

Unter Korrosionsbeschändigkeit wird die auf die Lebensdauer des Bauwerks bezogene, ausreichend hohe Widerstandsfähigkeit gegenüber der Einwirkung von chemischen Substanzen sowohl organischer als auch anorganischer Art verstanden. Die Forderung nach Dichtigkeit bezieht sich auf die Dichtigkeit des Werkstoffes gegenüber Flüssigkeiten und Gasen. Grundsätzlich beeinflußt eine höhere Dichtigkeit auch die Korrosionsbeständigkeit positiv.

3.2 Dichtigkeit

Die Dichtigkeit wird aufgrund des Diffusionswiderstandes und der Wasseraufnahme des Polymers beurteilt. Das Diffusionsverhalten wird in der Regel am reinen Polymer geprüft und zwar üblicherweise gegenüber Wasserdampf und Kohlendioxid. Für andere Gase liegen keine verläßlichen Werte vor. Die in Tabelle 2 angegebenen Vergleichswerte beziehen sich auf Zementbeton.

Eigenschaft	Zementbeton (CC)	Polymer (EP)
μ (H_2O) / 0 - 50	50 - 100	$0{,}8\text{-}1{,}2 \times 10^6$
μ (H_2O) / 50 - 100	10 - 40	$0{,}4\text{-}0{,}8 \times 10^6$
μ (CO_2)	300 - 400	$2{,}0\text{-}3{,}0 \times 10^6$
Wasseraufnahme	5 %	< 0,2 %

Tabelle 2 Diffusionswiderstandszahlen von Zementbeton und Polymer (Richtwerte)

3.3 Festigkeit

Druck- und Zugfestigkeit liegen wesentlich höher als bei zementgebundenen Betonen. Beide sind abhängig von Harzart und Harzgehalt. Letzterer kann umso geringer ausfallen, je größer das Größtkorn des Zuschlages und je gröber die Sieblinie ist. Optimale Ausnützung ist erreicht, wenn Kornbruch eintritt.

3.4 E-Modul

Beim E-Modul ist der Einfluß des Zuschlages wesentlich stärker ausgeprägt als bei der Zug- und Druckfestigkeit. Der E-Modul des Harzes ist i.a. wesentlich geringer als der des Zuschlages und kann näherungsweise zwischen 5 und 10 kN/mm^2 angenommen werden. Daneben hat auch die Kornform einen nicht zu vernachlässigenden Einfluß. Richtwerte enthält Tabelle 1.

3.5 Kriechen

Die Werte für das Kriechen hängen von der Art der Beanspruchung ab. Unter Zugbeanspruchung zeigt sich eine stärkere Kriechverformung als unter Druckbeanspruchung.

Die Kriechverformungen sind beim Polymerbeton größer als beim Zementbeton. Mit zunehmender Temperatur steigt die Kriechneigung an. Gleiches gilt auch bei Zunahme des Harzgehaltes.

3.6 Schwinden

Bei Polymerbeton ist eine Volumenveränderung bzw. Längenverkürzung die Folge der chemischen Reaktion während des Härtungsvorganges. Man spricht deshalb auch vom Reaktionsschwinden. Es kommt zum Stillstand, wenn die Reaktion abgeschlossen ist, näherungsweise im Alter von 7 Tagen. Wird die Reaktion durch Wärme beschleunigt, kann der Endwert bereits nach wenigen Stunden erreicht sein.

Die Größe des Schwindmaßes hängt von der Art des Kunststoffes ab. Werte für das lineare Schwinden und das Volumenschwinden sind in Tabelle 3 angegeben.

Polymer	Schwindmaße	
	linear	Volumen
ungesättigtes Acrylat	0,5 - 2,0 %	8 - 12 %
ungesättigtes Polyester	2 - 3 %	8 - 12 %
Polyurethan	0,2 - 0,3 %	3 - 5 %
Epoxidharze	0,2 - 0,4 %	3 - 5 %

Tabelle 3 Anhaltswerte für das Reaktionsschwinden von Duromeren

3.7 Temperaturverhalten

Obwohl es sich bei den Kunstharzen der Polymerbetone um Duromere handelt, die durch eine Temperaturerhöhung keine Zurückführung in den plastisch verform-

baren Zustand erfahren, zeigen sie jedoch beim Durchschreiten eines für das jeweilige Harz spezifischen Temperaturbereiches eine Zunahme der Verformbarkeit. Man spricht hier von der Glasübergangstemperatur. Bei gefüllten Harzen und Betonen ist das Abfallen nicht so ausgeprägt wie bei den reinen Harzproben, an denen es üblicherweise geprüft wird.

Die Höhe der Glasübergangstemperatur ist eine entscheidende Kenngröße zur Beurteilung der Brauchbarkeit des Harzes für die Herstellung von Polymerbeton für lasttragende Bauteile. Sie sollte nicht unter 50°C liegen. Durch besondere Härter und Formulierungen lassen sich Werte bis zu 100°C und auch darüber erreichen.

3.8 Wärmedehnung

Die Wärmedehnzahlen der reinen Harze können das 10- bis 20fache der Werte des Zuschlages aufweisen. Sie nehmen i.a. mit steigender Temperatur zu. Durch besondere Wahl der Zuschläge und der Zusammensetzung der Mischung lassen sich Polymerbetone mit Wärmedehnzahlen erhalten, die auch niedriger als die von Zementbetonen sein können.

3.9 Dauerstandfestigkeit

Die Dauerstandfestigkeit der Polymerbetone liegt niedriger als beim Normalbeton. Bei üblichen Epoxidharzen liegt dieser Wert zwischen 50 und 60 % der Kurzzeitfestigkeit. Für andere Harze können vergleichbare Verhältnisse angenommen werden. Durch spezielle Formulierungen des Härters, verbunden mit einer Wärmebehandlung während der Erhärtungsreaktion, läßt sich die Dauerstandfestigkeit auf den Wert des Normalbetons anheben.

3.10 Abriebverhalten

Vergleichbar dem Beton hat auch hier die Art und Beschaffenheit des Zuschlages einen wesentlichen Einfluß auf die Höhe des Abriebes. Günstig wirkt sich eine Zähigkeit des Harzes aus. Durch geeignete Zusammensetzung lassen sich höhere Abriebwiderstände als beim Normalbeton erzielen.

3.11 Korrosionswiderstand

Dieser ist wesentlich höher als bei Zementbeton und läßt sich durch die Wahl des Bindemittels gezielt beeinflussen. Besondere Vorteile gegenüber dem Zementbeton ergeben sich hier im Abwasser- und Umweltschutzbereich aber auch bei Bauteilen mit Frost-Tausalz-Einwirkung.

Durch besondere Formulierungen lassen sich bestimmte Eigenschaften gezielt verbessern ("züchten"), zumeist auf Kosten anderer Eigenschaften. Dies führt dann zur Funktionstrennung, d.h. die raumabschließende Funktion übernimmt ein konventioneller Werkstoff, die schützende Funktion der Polymerbeton.

3.12 Bakterienresistenz

Seitdem bekannt ist, daß Beton durch schwefelsäurebildende Bakterien (Thiobacillus) zerstört werden kann, wird auch für Kunststoffprodukte im Abwasserbereich der Nachweis einer ausreichenden Widerstandsfähigkeit verlangt. Auch bei Schwefelbeton wurde ein Angriff dieser Bakterien beobachtet.

4. VERARBEITUNG

4.1 Herstellung

Um ein dichtes Gefüge zu erreichen, ist ein Mindestgehalt an Bindemittel erforderlich. Darüber hinaus wird ein zusätzlicher Bindemittelanteil für das Erreichen bestimmter Verarbeitungseigenschaften benötigt. Der minimale Gehalt liegt bei ca. 6 %. Die Technologie ist der des Zementbetons vergleichbar.

4.2 Feuchtigkeitsempfindlichkeit

Unter Feuchtigkeitsempfindlichkeit versteht man das Verhalten des Harzes im Gemisch bei Anwesenheit von Feuchtigkeit während der Aushärtung. Sie hängt vom Harz ab. Feuchtigkeitsempfindliche Harze erfordern die Verwendung von getrockneten Zuschlägen. Anderenfalls wird entweder die Haftung am Zuschlag gestört oder es kommt zu einer Schaumbildungsreaktion. Durch Vorbehandlung der Zuschläge mit Silikon läßt sich die Feuchtigkeitsempfindlichkeit reduzieren. Ziel weiterer Entwicklung ist es, die Unempfindlichkeit so zu steigern, daß auch haldenfeuchtes Zuschlagmaterial verarbeitet werden kann.

4.3 Wärmeentwicklung

Bei der Polymerisation und der Polyaddition wird wesentlich mehr spezifische Wärme freigesetzt als bei der Hydratation von Zement. Das erfordert insbesondere bei größeren Bauteilabmessungen besondere Maßnahmen zur Begrenzung des Temperaturanstieges, der Eigenspannungen und der Temperaturverformung des Bauteils. Für die Herstellung von besonders maßgenauen Baukörpern werden verformungsstabile Harze verwendet.

4.4 Gesundheitsschädlichkeit

Je nach Harzart ist die Beeinträchtigung der mit der Verarbeitung betrauten Menschen unterschiedlich groß. In letzter Zeit werden vermehrt Anstrengungen unternommen, um die Verträglichkeit der Kunststoffe zu verbessern. Wenn in der Regel auch keine toxischen Wirkungen vorhanden sind, so kann es doch bei bestimmten Personengruppen zu Störungen des Allgemeinbefindens bis hin zu Allergien kommen. Deshalb sind bei der Verarbeitung im Vergleich zum Zementbeton einige zusätzliche Maßnahmen zu beachten.

5. BEURTEILUNG

Der Einsatz von Polymerbeton ist dort eine Alternative, wo der Zementbeton aufgrund seiner bekannten Eigenschaften nicht ausreichend leistungsfähig ist. Das gilt in erster Linie hinsichtlich des Korrosionswiderstand und der Dichtigkeit von Bauteilen beim Einsatz unter aggressiven Nutzungsbedingungen. Polymerbeton ist auch deshalb eine Alternative im Bauwesen, weil seine Technologie der des Zementbetons sehr ähnlich ist. Eine Vielzahl von Anwendungsbeispielen liegen vor. Der Einsatz war überall dort erfolgreich, wo die erzielten Verbesserungen am Gesamtsystem die erhöhten Kosten für den Werkstoff rechtfertigen.

Adhäsionsfestigkeit von Kunststoffbeschichtungen auf Beton

Improving the Adhesion of Polymer Coatings on Concrete

Amélioration de l'adhérence des revêtements de polymères au béton

Michael FIEBRICH
Dr.-Ing.
RWTH Aachen
Aachen, BR Deutschland

Michael Fiebrich, Jahrgang 1954, studierte Bauingenieurwesen an der RWTH Aachen. Seit 1980 ist er als wissenschaftlicher Mitarbeiter im Institut für Bauforschung der RWTH tätig. 1987 promovierte er zum Dr.-Ing. Sein Forschungsschwerpunkt ist die Adhäsion zwischen Kunststoffen und mineralischen Baustoffen.

ZUSAMMENFASSUNG

Zahlreiche Betonkonstruktionen werden auf ihren Nutzungsflächen mit Beschichtungen auf Kunstharzbasis versehen. Infolge rückwärtiger Durchfeuchtung treten immer wieder Schäden (Blasen, Ablösungen, Risse, u. a.) an den Beschichtungen auf. Mit Hilfe experimenteller Untersuchungen werden die für einen dauerhaften Adhäsionsverbund Kunstharzbeschichtung/Beton wichtigen Parameter analysiert und quantifiziert. Allgemeingültige Grundsätze der Beschichtungstechnologie zur Vermeidung von Beschichtungsschäden werden aufgestellt.

SUMMARY

The surfaces of numerous concrete constructions are protected with polymer coatings. Due to water penetration damage like bubbles, delamination, cracks, etc. may occur on the coating. With the aid of experimental investigations all important parameters for durable adhesion between concrete and polymer coating are analyzed and quantified. General demands on the coating technology in order to avoid any damage to coatings are discussed.

RÉSUMÉ

Les surfaces de nombreuses constructions en béton sont protégées par des revêtements de polymères. La pénétration de l'eau peut provoquer des défauts d'adhérence sur les revêtements tels que décollements, fissures, bulles. Par des recherches expérimentales, tous les facteurs importants pour une adhérence durable entre le béton et le revêtement de polymères sont analysés et quantifiés. Des recommandations générales pour la technologie de revêtements sont formulées.

1. EINFÜHRUNG

Zahlreiche Betonkonstruktionen (Wasserbehälter, Becken von Kläranlagen, Trogbauwerke, u. a.) werden auf ihren Nutzungsflächen mit Beschichtungen auf Kunstharzbasis versehen. Bei eingeerdeten Bauteilen dringt Wasser über ungeschützte (nicht abgedichtete) Bauteiloberflächen in das Innere des Betons und erreicht die Haftzone zwischen der innenliegenden Beschichtung und dem Beton. Es treten immer wieder Schäden wie Blasen, Ablösungen und Risse auf, die mit einer Verminderung oder dem Verlust der Adhäsion in der Grenzfläche Beton/Beschichtung verbunden sind. Die werkstoffwissenschaftlichen Kenntnisse der Adhäsion reichen nicht aus, um die Ursache von Schäden eindeutig zu klären bzw. um Anforderungen an Beschichtungsstoffe und Technologie zu formulieren, die dauerhafte Adhäsion garantieren. Ausgehend von in der Praxis auftretenden Adhäsionsschäden an kunstharzbeschichteten Betonbauteilen, die ständig oder temporär Wassereinwirkungen ausgesetzt sind, wurden experimentelle Untersuchungen zum Adhäsionsverhalten des Verbundsystems Kunstharzbeschichtung/Beton durchgeführt [1]. Die Untersuchungen hatten zum Ziel:

- die für die Adhäsion relevanten technologischen Parameter zu quantifizieren und damit ihre Anzahl auf eine baupraktisch vertretbare Menge zu reduzieren

- die derzeitigen Grundsätze zur Ausführung von Beschichtungsmaßnahmen und Anforderungen an Beschichtungsstoffe zu präzisieren.

2. EXPERIMENTELLE UNTERSUCHUNGEN

Bei den Laboruntersuchungen wurden im einzelnen folgende Faktoren und Ausprägungen betrachtet:

a) Betonuntergrund

- Festigkeitsklassen (B 35/B 55)
- Lage des Untergrundes (horinzontal, HOR/vertikal, VER)
- Untergrundvorbereitung (Wassersandstrahlen, G, keine: stahlgeschalt, N)
- Wassergehalt zum Beschichtungszeitpunkt (trocken, TR, wassergesättigt, NA).

b) Beschichtungsstoff

- 15 Modifikationen auf Basis von EP, PMMA und AY-Dispersionen.

Aus der Vielzahl der für den betrachteten Praxisfall marktüblichen Beschichtungssysteme wurden 11 Modifikationen auf Epoxidharzbasis ausgewählt, die sich u. a. bezüglich Härtertyp, Gehalt an Lösemitteln und reaktiven Verdünnern bzw. Wasseremulgierbarkeit der Harz-/Härtersysteme unterschieden. Darüber hinaus wurden 2 reaktive PMMA-Systeme sowie 2 Acrylharzdispersionen mit in die Untersuchungen einbezogen. Nach der Filmbildung der applizierten Beschichtung (48 h bei 8 °C) wurden die beschichteten Betonflächen 4 unterschiedlichen, in der Baupraxis auftretenden Wassereinwirkungen (Lastfälle 1 bis 4), ausgesetzt. Die Lastfälle unterschieden sich hinsichtlich der Art der Wassereinwirkung (allseitig, partiell) und gezielt eingetragenem Riß in der Beschichtung.

Während der 365 Tage andauernden Betriebsbeanspruchung wurde mittels Haftzugprüfung die Haftzugfestigkeit bestimmt und die zugehörige Bruchform registriert. Unterschieden wurden 3 Hauptbruchformen:

- Adhäsionsbruch zwischen Beton und Beschichtung
- Kohäsionsbruch im Beton
- Polymerbruch der Beschichtung.

Für die Auswertung der Versuchsergebnisse wurden die Haftzugfestigkeit im Adhäsionsversagensfall (β_{HZ}: Adhäsionsfestigkeit), die relativen Häufigkeiten der

Bruchform Adhäsionsversagen (r. $H.^A$), sowie eine aus den beobachteten Merkmalen abgeleitete Rechengröße, den Gütewert, herangezogen [2]. Der Gütewert ergibt sich zu:

$$GW = \beta_{HZ}{}^A \cdot (100 - r.\ H.^A).$$

Der Wert diente zur quantitativen Abschätzung der universellen Brauchbarkeit der untersuchten Beschichtungsstoffe.

3. EINFLUSS DER BETONEIGENSCHAFTEN UND BETRIEBSBEANSPRUCHUNGEN AUF DIE ADHÄSIONSGÜTE VON BESCHICHTUNGSSTOFFEN

3.1 Überblick über Adhäsionsgüte der Beschichtungsstoffe

Einen Überblick über die unterschiedliche Güte der untersuchten Beschichtungsstoffe liefert Bild 1, auf dem die Gütewerte über den untersuchten Stoffmodifikationen dargestellt sind; nicht berücksichtigt sind hier die Einflüsse aus den Beton- und Betriebsbeanspruchungsfaktoren.

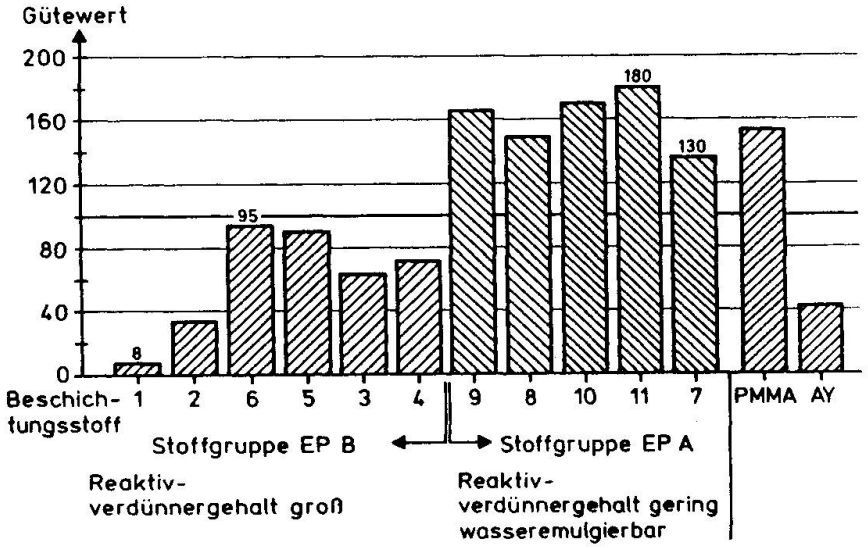

Bild 1: Gütewerte der Beschichtungssysteme

Der vorliegende Wertebereich der Gütewerte trennt die Epoxid-Beschichtungsstoffe in 2 Gruppen, wobei die eine Gruppe einen Gütewertbereich zwischen 8 und 95 überstreicht, während die andere Gruppe Gütewerte deutlich über 100 aufweist. Diesen beiden Gütewertgruppen lassen sich folgende Stoffmerkmale zuordnen: Gehalt an Reaktivverdünnern, Wasseremulgierbarkeit der Harz-/Härtersysteme. Im Mittel weisen Beschichtungsstoffe mit geringen Reaktivverdünnergehalten - wie sie in der Stoffgruppe A vorkommen - gewisse Vorzüge bezüglich der Adhäsionsgüte gegenüber den Stoffen mit großen Reaktivverdünnergehalten - wie sie in der Stoffgruppe B vertreten sind - auf. Ferner erweist sich die Wasseremulgierbarkeit der Harz-/Härtersysteme, die ausschließlich in der Stoffgruppe A vertreten sind, für die Adhäsionsgüte günstig. Die reaktiven PMMA-Systeme lassen sich bezüglich ihres Gütewertes in die Stoffgruppe A einordnen, während die Acrylharzdispersionen lediglich Gütewerte der Gruppe B erreichen.

3.2 Wichtigkeit der Betoneigenschaften und Betriebsbeanspruchungen für Gütewerte

Die Wichtigkeit aller betrachteten Beton- und Betriebsbeanspruchungsfaktoren für die Gütewerte läßt sich unter Vernachlässigung der Beschichtungsstoffeigenschaften quantifizieren. Hierfür werden für alle untersuchten Faktoren jeweils relative Gütewerte gebildet, die die Gütewerte der jeweiligen alternativen Ausprägung (eines Faktors) ins Verhältnis setzen. In Bild 2 finden sich die relativen Gütewerte für alle Faktoren (von der Betonfestigkeit bis zur Betriebsbeanspruchung). Die Ausprägung, auf die sich der jeweilige relative Gütewert bezieht, ist als Fußzeiger in der darunterliegenden Abszissenzeile angegeben.

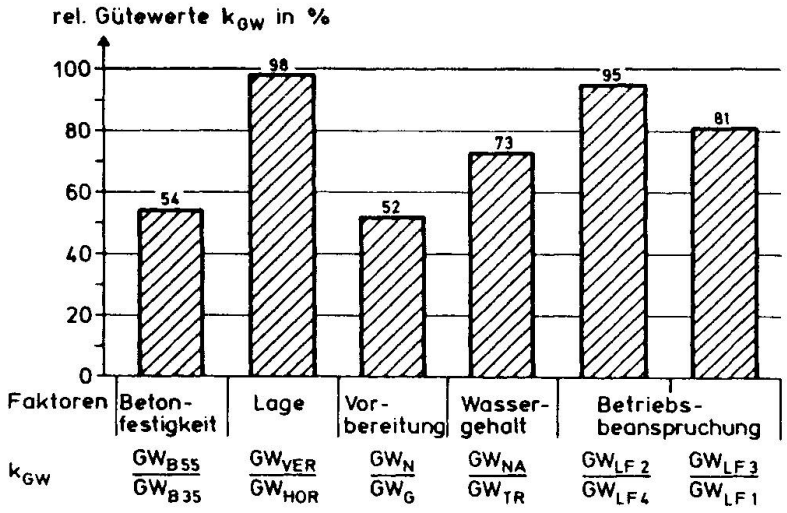

Bild 2: Relative Gütewerte k_{GW} von Epoxidharzbeschichtungsstoffen für Betoneigenschaften und Betriebsbeanspruchungen

Im Mittel gilt bezüglich der quantitativen Wichtigkeit folgendes:

- Die Faktoren "Betonfestigkeit" und "Untergrundvorbereitung" sind für die Adhäsionseigenschaften gleichrangig und weisen im Vergleich zu den übrigen Faktoren den größten Einfluß auf.

- Für den Faktor Untergrundvorbereitung bedeutet dies:
  Im Mittel erreichen die Gütewerte auf nicht abtragend vorbereiteten Untergründen etwa die Hälfte der Gütewerte wie auf abtragend vorbereiteten.

- Analoges gilt für die Betonfestigkeitsklasse: Die Eigenschaften eines hochfesten Betons (repräsentiert hier durch die Betonfestigkeitsklasse B 55) führte zu Gütewerten, die im Mittel etwa 50 % jener Gütewerte betragen, die bei einem niederfesten Beton (repräsentiert durch die Festigkeitsklasse B 35) erreicht werden.

- Die Faktoren Lage des Untergrundes bzw. Betriebsbeanspruchung weisen einen vergleichsweise vernachlässigbaren Einfluß auf die Gütewerte aus.

- Der Einfluß des Faktors "Wassergehalt" ist im Mittel bezüglich seiner Wichtigkeit etwa halb so groß wie die Faktoren "Betonfestigkeit" und "Untergrundvorbereitung".

3.3 Anforderungen an Beschichtungsstoffe

Aus den als relevant erkannten Betonfaktoren "Betonfestigkeit", "Untergrundvorbereitung" und "Wassergehalt" ergeben sich 8 unterschiedliche Betonuntergrundkombinationen (Bild 3).

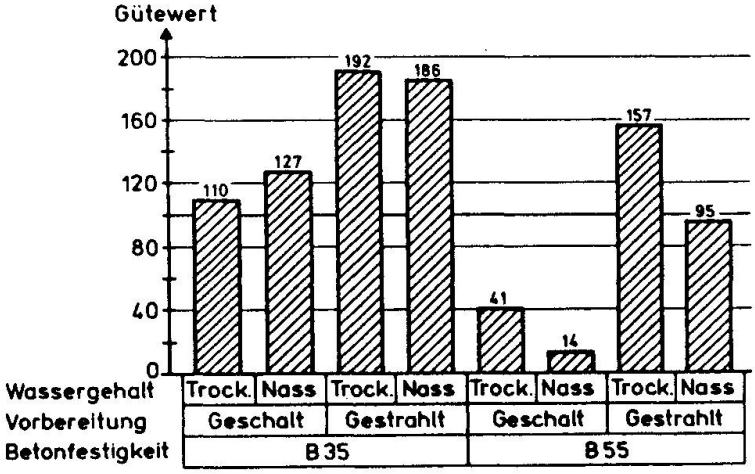

Bild 3: Gütewerte der Epoxidharzbeschichtungsstoffe für unterschiedliche Betonuntergründe

Die mittleren Gütewerte variieren zwischen 14 und 192 als einem Verhältnis von 1:14. Aus der Darstellung wird deutlich, daß die Kombination "B 55 stahlgeschalt" im Mittel die höchsten Anforderungen an die Adhäsionsgüte stellt, während die Kombination B 35 abtragend vorbereitet im Mittel die geringsten Anforderungen an die Adhäsionsgüte stellt. Ferner zeigt sich, daß der Einfluß des "Wassergehaltes" auf die Adhäsionsgüte von der Betonfestigkeitsklasse, d. h. den damit verbundenen Poreneigenschaften, abhängig ist. Auf B 55 abtragend vorbereiteten Untergründen ergibt sich eine Reduzierung des Gütewerts um knapp 40 %, während auf den entsprechenden B 35-Untergründen der Einfluß praktisch vernachlässigbar ist.

3.4 Einfluß der Betriebsbeanspruchungsdauer

Ob und inwieweit die Dauer der Wasserbadlagerung und Betriebsbeanspruchung die Adhäsionsfestigkeit beeinflussen, zeigt Bild 4. Stellvertretend für die untersuchten Beschichtungsstoffe sind dort 4 ausgewählte charakteristische Kurvenverläufe der zeitabhängigen Adhäsionsfestigkeit dargestellt.

Es wird deutlich, daß die Adhäsionsfestigkeit auf hohem bzw. niedrigem Niveau mit zunehmender Beanspruchungsdauer zu- bzw. abnehmen kann und daß die Zu- bzw. Abnahmen der Adhäsionsfestigkeit zwischen 10 bzw. 25 % variieren.

Deutlich wird ferner, daß die Beschichtungsstoffzusammensetzung einen größeren Einfluß auf die Adhäsionsfestigkeit ausübt als die Dauer der Betriebsbeanspruchung.

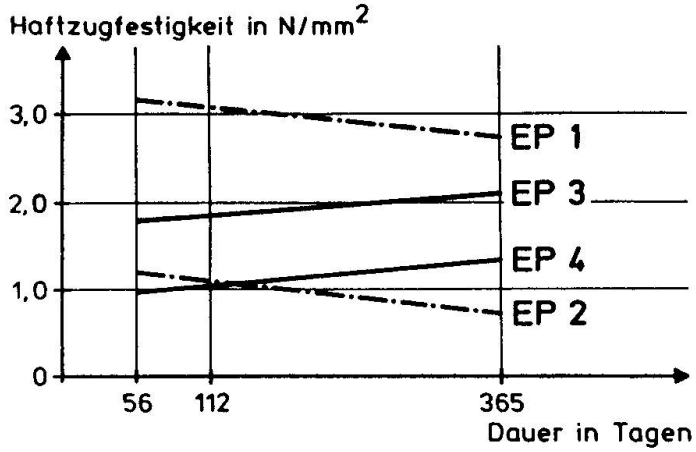

Bild 4: Einfluß der Dauer der Betriebsbeanspruchung auf die Adhäsionsfestigkeit repräsentativer Epoxidharzbeschichtungsstoffe

4. SCHLUSSBEMERKUNG

Mit Hilfe statistischer Regressionsanalysen wurde die quantitative Wichtigkeit der Beschichtungsstoffbestandteile (Härterart, Art und Menge an reaktiven Verdünnern und Lösemitteln, u. a.) bezüglich der Gütewerte untersucht. Dabei ergab sich, daß die Wichtigkeit der Kunstharzbausteine die Größenordnung der Untergrundfaktoren (Betonfestigkeit, Untergrundvorbereitung) erreichen kann [2]. Weitergehende Präzisierungen über den Einfluß der Beschichtungsstoffmerkmale waren nicht möglich. Dies war vorrangig darauf zurückzuführen, daß die chemische Analytik bisher nicht in der Lage ist, konfektionierte technische Härtersysteme hinreichend trennscharf zu detektieren.

Aus den Untersuchungsergebnissen wurden allgemeingültige Grundsätze für den Betonuntergrund, den Beschichtungsstoff und die Betriebsbeanspruchung abgeleitet, die für die beobachteten Zielgrößen (Adhäsionsfestigkeit, Versagens- und Blasenhäufigkeit) relevant sind. Diese Grundsätze, die in [1] niedergelegt sind, geben Hinweise, unter welchen Randbedingungen adhäsionsmindernde Phänomene auftreten, wenn extreme Härtungsbedingungen vorliegen und Wasser auf das beschichtete Bauteil einwirkt. Es darf jedoch nicht gefolgert werden, daß bei Einhaltung dieser Grundsätze überhaupt keine Adhäsionsschäden an Beschichtungen auftreten. Eine Eignungsprüfung der Beschichtungsstoffe erscheint daher zwingend notwendig. Es wurden daher Prüfkriterien für ein Laborprüfverfahren entwickelt, die geeignet erscheinen, das Haftverhalten von Beschichtungsstoffen bei extremen Härtungsbedingungen und temporärer Wassereinwirkung abzuschätzen [1].

LITERATURVERZEICHNIS

1. FIEBRICH, M., Kunststoffbeschichtungen auf ständig durchfeuchtetem Beton. Aachen : Institut für Bauforschung, RWTH Aachen, 1987. - Forschungsbericht F 184.

2. FIEBRICH, M., Zur Adhäsion zwischen polymeren Bindemitteln und Beton unter besonderer Berücksichtigung von Wassereinwirkungen. Dissertation an der Fakultät für Bauingenieur- und Vermessungswesen der RWTH Aachen, 1987.

Factors which Influence Durability of Wooden Structures

Facteurs affectant la durabilité des structures en bois

Einwirkungen auf die Dauerhaftigkeit von Holzbaukonstruktionen

S. K. MALHOTRA
Professor
Techn. Univ. of Nova Scotia
Halifax, NS, Canada

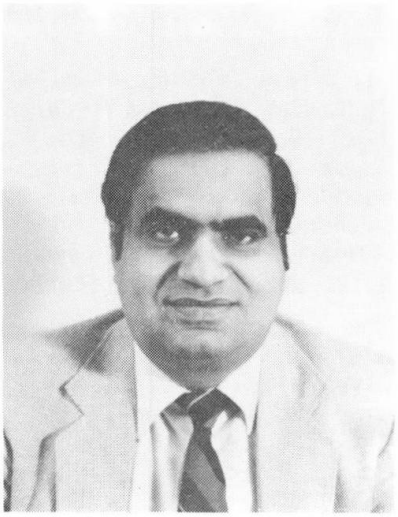

S. K. Malhotra received his Ph. D. from Technical University of Nova Scotia, Halifax, Canada. He has been involved with teaching and research in timber engineering and structural engineering for many years, and has published numerous papers. He holds several appointments on boards and technical committees of professional, research and design code development organizations.

SUMMARY

Various factors affecting the serviceability and durability of wooden structures are briefly discussed. Discussion is focused on the following factors: loading (man-made loads and forces due to natural hazards); time (duration of load, fatigue and creep); cyclic environment; weather exposure; decay due to fungi, insects and marine organisms; chemicals; and fire. A review of the manner in which these factors are accounted for in the current design codes for wooden structures is given.

RÉSUMÉ

Plusieurs facteurs ayant un effet sur l'aptitude au service et la durabilité des structures en bois sont examinés avec soin: charges dues à l'homme et à la nature; durée (durée du chargement, fatigue du bois et retrait); effets saisonniers; effet des conditions climatiques; effet des moisissures, des insectes et des organismes marins; produits chimiques; et feu. L'article présente la façon dont ces éléments sont pris en compte dans les normes pour les constructions en bois.

ZUSAMMENFASSUNG

Verschiedene Faktoren, welche die Gebrauchstauglichkeit und die Dauerhaftigkeit von Holzbaukonstruktionen beeinflussen, werden diskutiert. Es handelt sich dabei um: Einwirkungen (menschliche und natürliche), Zeitdauer (Einwirkungsdauer, Ermüdung und Kriechen), zyklische Beanspruchungen, Bewitterung, Zersetzungen infolge von Pilz- und Insektenbefall sowie durch marine Organismen, Chemikalien und Feuer. Es folgt eine Uebersicht über die Berücksichtigung dieser Faktoren in den heutigen Holzbaunormen.

1. INTRODUCTION

To carry out effectively the task of evaluation, maintenance, rehabilitation or upgrading of wood structures, it is imperative that the influence of various factors on the performance of these structures be understood. The factors discussed in this paper are: loading; time; temperature; moisture content; cyclic environment; weathering; insects, fungi and other organisms; chemicals; and fire.

2. LOADING

A structure must be designed to carry all man-made and natural hazard loads. Man-made loads generally include the dead and live gravity loads, constraint forces and accidental loadings such as from fire and blast. Live loads correspond to the intended use of the structure and to the occasional extrodinary loadings. One should design for possible changes in occupancy that might result in heavier loads than does the intended use. Constraint forces arising from differential settlement and due to temperature, creep, chrinkage, warping and other similar effects, should be considered in the design.

Depending on the location of the structure, loads resulting from hazards for a wood structure generally consist of forces due to wind, rain, snow, flood, earthquake, ponding and expansive soil. Critical areas for damage against wind forces are attachment of cladding and anchorage of the roof to the walls and the walls and floor system to the foundation. Anchorage must resist uplift, overturning and sliding. A dynamic analysis or wind tunnel testing may be needed for a structure potentially very sensitive to wind forces. Aspects to be considered in the design for earthquake forces include ductility in members and connections, limited strength loss with load reversal, compatible ductility between elements, and alignment of the massed and rigidity centers to avoid torsion.

Snow loading is dependent not only on geographical location, but also on local terrain effects and structure geometry. Wind-blown snow can cause large accumulations or drifts to develop which result in loads of intensity far in excess of those normally anticipated from annual precipitation records for a region. A taller structure in the close vicinity to the roof being considered, combined with high winds, will sometimes result in heavy snow loads in limited areas of the roof. The National Building Code of Canada [1] has recognized this phenomenon for several years and has developed guidelines for the designer to consider.

Ponding can be a serious hazard with flat roofs when there is inadequate strength or stiffness and insufficient roof drainage. Roofs should be designed either to ensure adequate drainage or to support the additional loads due to ponding.

3. TIME (DURATION OF LOAD, CREEP AND FATIGUE)

It is well recognized that the ultimate strength of wood decreases as the time of fracture increases, that is wood members can withstand higher loads for a shorter duration of time than the loads for a longer period. Therefore, the effect of duration of load on wood properties is an important aspect to be considered in the design of wood structures. To account for this effect, structural design codes, such as the National Standard of Canada [2] classify loads into a number of categories according to their duration and provide adjustment factors for use in design for these various durations. Presently, research on the influence of duration of load on wood structures is being carried out in Canada, U.S.A. and many other countries to study this phenomenon in depth.

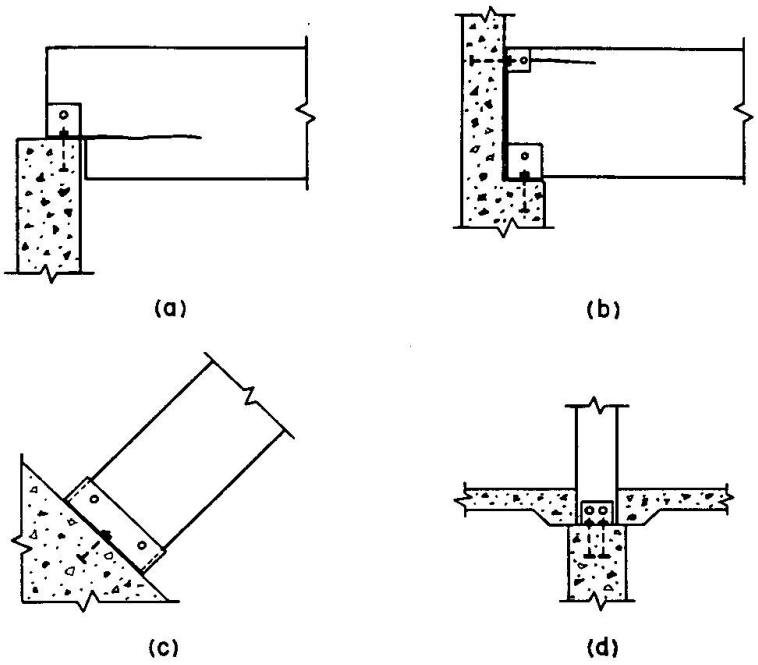

Fig. 1 Some Illustrations of Possible Problem-Type Connections

It has been observed that cyclic relative humidity and temperature affect the relation between loading and time-to fracture. Hearmon and Paton [3] have noted that the time-to-fracture for small, clear wood specimens in bending could be drastically reduced if the specimens were subjected to cyclic changes in relative humidity. Further research by Schniewind and Lyon [8] has shown that this reduction in time-to-fracture is dependent on specimen size. Design for fatigue in wood structures is generally considered to be not so important as in many other structural materials. However, research of fatigue fracture in wood indicates that the possibility of fatigue fracture under cyclic loading conditions should not be ignored in situations when it is anticipated that the structure will be subjected to a very large number of cycles.

4. TEMPERATURE, MOISTURE CONTENT AND CYCLIC ENVIRONMENT

It is commonly accepted that exposure to high temperature for a limited period usually has no permanent effect on strength properties, although strength properties are temporarily reduced while wood is at an elevated temperature. However, high temperatures associated with high moisture content may require a reduction of strength values.
The change in moisture content affects almost all mechanical properties of wood. The generally accepted relation between moisture content and strength is that a reduction in the moisture content of wood results in its higher strength and less deflection at a given stress level [5,6].

Wood is dimensionally quite stable as long as its moisture content is above the fiber saturation point. Wood shrinks as it dries below the fiber saturation point. Shrinkage of wood in structures in service causes several problems, particularly in connection details. As lumber dries more rapidly through the ends than through the sides, more serious splitting occurs at the ends where connections are located. This can cause loosening and failure at joints by splitting between fasteners.

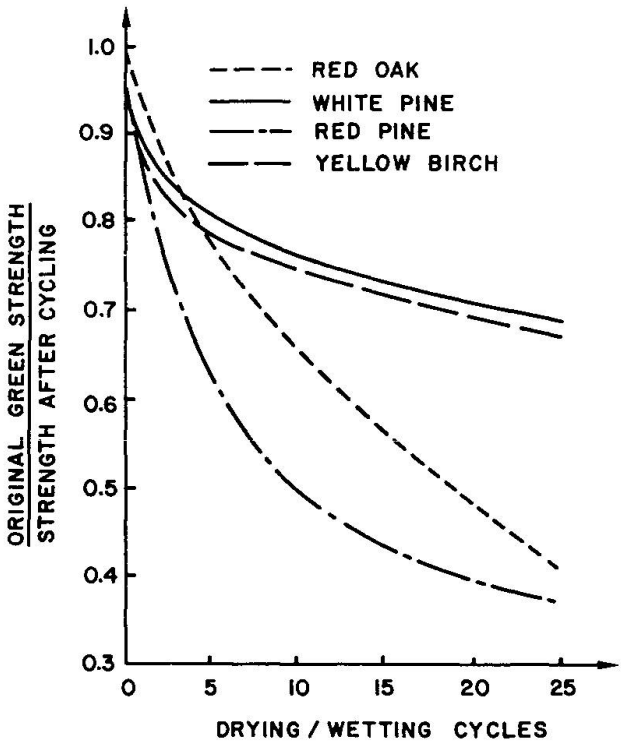

Fig. 2 Influence of Drying-Wetting Cycles on Shear Strength

Good construction practice is to retighten bolts in bolted joints and in joints with split ring connectors after a structure has been in service for some one year or so.

Special care must be taken to avoid problem-type connections. Figures 1(a) and (b) give illustrations of two possible problem-type connections. The clip angles or concealed internal anchors as connected to the beam enhance the formation of a split when wood shrinks, thus reducing the effective strength of the connection and effect shear strength of the member.

It should be mentioned that the strength and stiffness of a nailed joint is reduced if there is a gap caused by shrinkage between the component members [7]. This effect should be considered in the design process.

Wood being rheological material, may behave somewhat differently in each successive cycle when used under cyclic environmental conditions. The effect of repeated wetting and drying cycles can be quite severe on some strength properties of wood and on deflections in trusses. For example, Fig. 2 illustrates the reduction of shear strength measured during 25 drying-wetting cycles for 4 different species of wood [4]. Hearmon and Paton [3] have shown that cyclic exposure to changes in moisture content significantly reduces wood strength. They observed a creep failure at loads only 3/8 the maximum load a matching specimen would sustain if maintained at a constant moisture content. The effect of moisture cycling can be quite significant and should be accounted for in design when structural members are expected to be exposed to cyclic moisture contents.

Another aspect, associated with moisture content effects, that should be considered is the influence on the time-dependent properties of wood when moisture changes occur while wood is under load. When wood is under constant load and a sudden change in moisture content takes place, a large increase in creep deformation can result.

5. WEATHERING, INSECTS, FUNGI AND OTHER ORGANISMS, AND CHEMICALS

Wood exposed outdoors without protection, is subjected to physical and chemical changes as a result of weathering. These changes usually affect only the surface of the wood and the wood under this relatively thin surface is essentially unchanged and unaffected. In the absence of decay, wood exposed to the weather can last for a very long time. Good engineering and construction practices for wood structures to protect them from prolonged wetting and use of finishes to protect them from weathering effects, should eliminate weathering as a cause of serious damage of wood structures.

Wood, a biological material, is susceptible to degradation by organisms, most of which require oxygen, moisture, food and a favourable temperature. Bacteria and fungi induce a bio-chemical attack while insects destroy wood by mechanically biting off bits of wood tissue. The initial effect of bacteria infestation of wood generally results in an increase in permeability. The increase in permeability makes bacterially-degraded wood especially susceptible to increased moisture absorption. Long-term bacterial action may cause significant reduction in wood strength properties.

Critical locations for moisture absorption and decay are connections, exposed end-grain surfaces and splits and checks. Care must be taken to avoid problem-prone connections. Figure 1(c) and 1(d) show, respectively, a connection with wood column (or arch) in closed steel box and a connection where the base of the wood column is concealed by placing concrete around the connection. The problem in Fig. 1(c) can be avoided by providing weep holes in the box and that in Fig. 1(d) can be prevented by setting the column base on a pedestal above the floor slab.

Treatment of wood with preservative chemicals contributes to resistance against wide spectrum of bacteria, fungi and insects. Adequate pressure treatments with preservatives significantly extend the service lives of many species of wood.

Wood is generally considered to possess a high degree of resistance to attack by a wide variety of chemicals. The adverse effect of acids and bases on strength properties of wood is greatly influenced by wood species. Generally, hardwoods are more susceptible to chemical degradation than are coniferous species. Alkaline solutions, which dissolve some of the hemicelluloses and attack lignin in wood, have a greater effect on wood strength than do acids. Acids make the wood more brittle and reduce its strength. Some salts may increase certain strength properties of wood and others may significantly reduce strength.

6. FIRE

The loss of load-carrying capacity of wood components under the action of fire is the result of two major causes: Namely, the formation of charcoal in the outside portion of the member and the weakening of a thin layer that is immediately beneath the charcoal. The basic effects of fire on a wood member are the reduction in cross section (only cold wood core area is effective) and the weakening of metalic fasteners in the member.

Fundamental to the problem of incorporating fire safety in structures is the way in which fire, heat and smoke spread. There could be several building design deficiencies which contribute to the spread of fire, heat and smoke throughout a building or from one building to another. Designing to minimize damage by fire must be incorporated in the architectural planning process as early as possible.

It has been noted that open doors and stairs, together with lack of firestopping in concealed spaces are responsible for spread of fire and smoke in a high percentage of fires in dwellings. Fire spread from one area of a building to another through open concealed spaces is a major problem. The National Building Code of Canada [1] stiplulates requirements on where and how much firestopping

and draftstopping are to be used.

Treatment of wood with fire-retardant chemicals is an effective means of preventing flame spread. Fire resistance of wood structures can also be improved through good design and construction details. In heavy timber construction, fire resistance is provided by massive wood and the avoidance of concealed spaces in which fire may originate and spread undetected. As light-frame wood construction, most residential dwellings belong to this category, do not have the fire resistanace provided by heavy timber construction, special attention should be given to good construction details to delay the spread of fire and reduce hazards to occupants. Firestops should be provided at exterior walls, at each floor level and at the level where the roof connects with the wall.

7. CONCLUSIONS

The effects of various factors which influence the performance of wood as structural material were reviewed in the paper. Current design specifications and codes on engineering design in wood deal with usual service environments (dry condition, wet condition, various durations of loads, etc.), but other extremes in the environment, such as severe variations in temperature, cyclic moisture conditions, changes due to weathering, biodegradation, chemical degradation, are not adequately dealt with. The problem of interaction of various environmental factors needs to be addressed, with respect to their combined effect on wood properties.

Wood, one of the world's principal construction materials, is dependable, versatile, economical and energy-efficient. With the proper understanding of the material behaviour and with the adoption of good engineering design and construction practices, wood structures can be built economically to provide many, many years of durable service life.

REFERENCES

1. ASSOCIATE COMMITTEE ON THE NATIONAL BUILDING CODE, National Building Code of Canada, National Research Council of Canada, Ottawa, Ontario, Canada, 1985.
2. CANADIAN STANDARDS ASSOCIATION (CSA), Engineering Design in Wood (Limit States Design), National Standard of Canada CAN3-086.1-M84, CSA, Rexdale, Ontario, Canada, 1984.
3. HEARMON, R.F.S. and PATON, J.M., Moisture Content Changes and Creep of Wood, Forest Products Journal, Vol. 14, No. 8, 1964, pp. 357-359.
4. KEITH, C.T., Some Effects of Repeated Drying and Wetting on Wood Properties, Forest Products Laboratory of Canada Technical Note No. 23, Ottawa, Ontario, 1960.
5. MADSEN, B., Duration of Load Test for Wet Lumber in Bending, Forest Products Journal, Vol. 25, No. 5, 1975,. pp. 33-40.
6. MALHOTRA, S.K., Buckling Strength of Solid Timber Columns", Ph.D. Thesis, Technical University of Nova Scotia, Halifax, Nova Scotia,. 1969.
7. MALHOTRA, S. K., and THOMAS, B., Effect of Interface Gap on Load-Slip Characteristics of Timber Joints Fabricated with Multiple Nails, Canadian Journal of Civil Engineering, Vol. 12, No. 1, 1985, pp. 104-113.
8. SCHNIEWIND, A.F. and LYON, D.E., Further Experiments on Creep-Rupture Life Under Cyclic Environmental Conditions, Wood and Fiber, Vol. 4, No. 4, 1973, pp. 334-341.

Dauerhaftigkeit hochfester Stangen und Drähte mit Zugbeanspruchung

Durability of High Strength Bars and Wires in Tension

Durabilité des barres et fils à haute résistance en tension

Ulrich MORF
Dr. sc. techn.
EMPA
Dübendorf, Schweiz

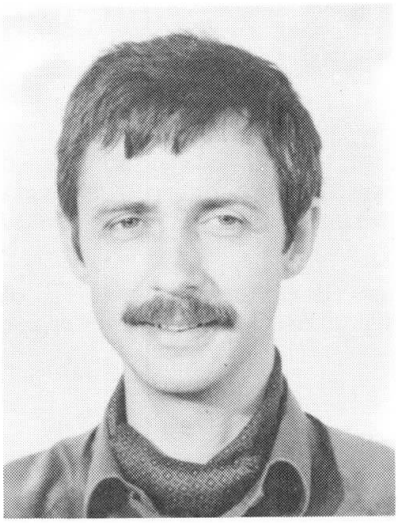

Ulrich Morf, geboren 1942, promovierte als Bauingenieur an der Eidg. Technischen Hochschule in Zürich. Er befasste sich zuerst drei Jahre als Konstrukteur mit Stahlbau und Druckleitungsbau. Seit 1971 ist er Abteilungsleiter an der EMPA (Abt. Metalltechnologie und Konstruktionen) und bearbeitet Prüfaufträge, Forschungsprojekte und Gutachten im Gebiet Metalltechnologie, Bruchmechanik, Tragverhalten und Schweisstechnik.

ZUSAMMENFASSUNG

Die Dauerhaftigkeit von Stählen in Bauwerken kann mit modernen Erkenntnissen über das Bruchverhalten und die Risszähigkeit von Materialien auch baupraktisch besser definiert werden. Dazu werden hier eine Prüfsystematik und ein erweitertes Sicherheitskonzept für Spannstähle und Schrauben als Zugglieder vorgestellt.

SUMMARY

The durability of steels in structures can be defined for practical application by utilizing current knowledge of fracture behavior and fracture toughness. In this paper testing methodology and an extended safety plan are presented for prestressing steels and bolts as tensile elements.

RÉSUMÉ

Les connaissances actuelles pratiques sur le comportement à la ruine et la mécanique de rupture permettent de mieux définir la durabilité des aciers dans les constructions. Dans ce but des méthodes d'essai et un plan de sécurité complémentaire sont présentés pour des aciers de précontrainte et des boulons agissant comme éléments tendus.

1. DERZEITIGER STAND UND ENTWICKLUNG VON STÄHLEN

1.1 Dauerhaftigkeit von Spannstählen, Stangen und Drähten

Durch langjährige Entwicklung von gezogenen Drähten, gewalzten Stangen und Schraubenwerkstoffen zu Zug-Bauteilen konnte bei diesen ein hoher Grad an Zuverlässigkeit erreicht werden. Rückschläge sind oft dann entstanden, wenn Materialeigenschaften und Bauelemente nicht als Ganzes entwickelt wurden. Schädigende Einwirkungen können bereits vom unsachgemässen Transport, von der Lagerung und von der Montage stammen. Bei den Langzeiteigenschaften haben natürlich der Korrosionsschutz, versprödende Betriebseinwirkungen oder dynamische Beanspruchung eine grosse Bedeutung.

In verschiedenen Schaden- und Laboruntersuchungen wurde bereits gezeigt, dass Vorschädigungen und Kerben eine grosse Rolle spielen (Nürnberger [1], der Verfasser [2], S. 10 und 18, 161 bis 164), dass aber auch bei vergüteten Stählen und Stählen mit Überfestigkeiten ein erhöhtes Bruchrisiko auftritt besonders an Spanngliedern mit Lücken im Korrosionsschutz (SRK.-Bericht [3] und Hampeijs [4] sowie Morf u. Mitarbeiter [5].

Viele aktuelle Problemstellungen der Dauerhaftigkeit können heute zahlenmässig am besten mit der hier zusammengefassten bruchmechanischen Methodik untersucht werden (vgl. [2], S. 53).

1.2 Erweiterte Prüfsystematik und Sicherheitskonzept

Für die Anwendung der Bruchmechanik mit entsprechender Relativierung für das Bauwesen werden in dieser Arbeit eine angepasste Prüfsystematik und ein entsprechendes Sicherheitskonzept vorgestellt. Sie sind speziell für Spannstahl und Schrauben ausgelegt.

Prüfsystematik für hochfeste Stähle mit Risszähigkeitsprüfung

Die Art der hochfesten Stähle und die Langzeitanwendungen im Bauwesen führen dazu, dass eine Bruchzähigkeitsprüfung die Oberflächenzone (ca. 5% des Durchmessers) erfassen muss, die oft andere Eigenschaften aufweist als der Kern. Weiter müssen versprödende Einflüsse wie Dehngeschwindigkeit und Temperatur superponiert geprüft werden; für die Voraussage des Langzeitverhaltens, z.B. Korrosion, hat dies in Überlagerung mit geeigneten Medien zu geschehen. Aus Sicherheitsgründen ist oft der Nachweis unter extremen Bedingungen (Langzeit oder Stoss) die massgebende Kontrolle (vgl. Figur 1).

Sicherheitskonzept mit zusätzlicher Bewertung des Bruchverhaltens

Der Tragfähigkeitsnachweis im Bauwesen stützt sich im Fall der Anwendung plastischer Berechnungsmethoden auf die zusätzliche Hypothese, dass plastische Verformbarkeit vorhanden ist. Bei Gebrauchslasten darf bis zum Betriebsende kein Sprödbruch auftreten. Deshalb muss vor allem beim Einsatz hochfester Spannstähle ein materialtechnologischer Nachweis für genügende Duktilität (bei gekerbten Bauteilen: Risszähigkeit) erbracht werden. Im Flussdiagramm in Figur 2 ist ein dreigliedriger Nachweis dargestellt: Auf dem mittleren Block im Flussdiagramm dürfte im Normalfall ein "Bruchnachweis unter vereinfachten Bedingungen" genügen; bei Langzeitextrapolationen auf das Betriebsende von kritischen Bauteilen muss aber auch der dritte Block mit einem "Bruchnachweis mit bekannten Fehlergrössen unter extremen Bedingungen" überprüft werden. Vor allem diese letzte Prüfung für Langzeitextrapolationen wird für die Dauerstandeigenschaften wie Relaxation seit langem angewandt. Sie müsste nur noch mit definiert angerissenen oder/und "bewitterten" K_{ISCC}-Proben durchgeführt werden, um nachzuweisen, dass während der Betriebsdauer keine Brüche oder instabilen Risse auftreten.

2. STAHLEIGENSCHAFTEN UND ANGEPASSTE ZÄHIGKEITSPRÜFVERFAHREN

2.1 Aktuelle Spannstahlprüfung

Die bekannten Festigkeitsprüfverfahren und technologischen Oberflächenprüfverfahren weisen eine Neigung zu Anrissen und zu sprödem Verhalten nur ungenügend nach. Die in Euronorm 138 [7] für Spannstähle gesetzten Grenzen für minimale Biegeradien, Bruchdehnung bzw. Standzeiten für SCC-Versuche in FIP-Richtlinien [6] sind nur brauchbar für Normalfälle.

Die für Schraubenprüfung üblichen Kerbschlagversuche mit innenliegenden Proben nach Norm ASTM A540 sind zur Kennzeichnung des Anrissverhaltens von Spannstangen nicht anzuwenden (vgl. Kap. 3 Prüfprogramm).

Die zusätzlich interessierenden Stahleigenschaften bei extrem beanspruchten Stählen sind aufgrund der erwähnten Arbeit [2] die folgenden:

- Die **Anrisseigenschaften** von Stangen und Drähten sind anisotrop, variabel über die Anrisstiefe und teils auch temperaturabhängig ([2], S. 110).
- Für die Dauerhaftigkeit ist auch die **Rissgeschwindigkeit** zu beachten ([2], S. 29).
- Die Versuche mit den in Kap. 2.2 eingeführten **Scharfkerben** zeigen auch typische Unterschiede zwischen gezogenen Drähten und Stangen. Die dabei abgeschätzten dynamischen **Bruchzähigkeitswerte** K_{ID} liegen im günstigen Fall für Drähte bei 2'000 bis 3'000 $Nmm^{-3/2}$, bei Stangen an der Oberfläche bei 1'500 und und am Fuss von tiefen Konstruktionskerben bei 2'000 $Nmm^{-3/2}$.
- Die typischen **Dehngeschwindigkeiten** entsprechen Stosswirkungen von $d\varepsilon/dt = 5 \cdot 10^{-3}$ bis 1/s, **ähnlich wie sie bei Bauwerken auch auftreten** (= "low blow"-Schlagbiegeversuch).

2.2 Scharfkerbenprüfungen mit guter Korrelation zur Bruchzähigkeit

Zur Bestimmung der kritischen Bruchzähigkeit (Figur 1) eines anrissgefährdeten Bauteils ist die spezifische Anrissenergie, bestimmt mit der J-Integraltechnik nach Norm ASTM E813, oder die Bruchzähigkeit nach ASTM E399 zu ermitteln. Für hochfeste Stangen des Bauwesens wurden hier als Ersatz für die ASTM-Normen verschiedenartige seitengekerbte Rundproben zur Abschätzung der Bruchzähigkeit entwickelt, welche sich für Stossprüfung und Langzeitversuche eignen (Figur 3).

Dank einer progressiv zunehmenden Rissfrontbreite ist mit den neuen Kerbformen eine Risszähigkeitsbestimmung in der Oberflächenzone möglich (Figur 3). Die zugehörigen Spannungsintensitätskorrekturfaktoren Y' für Dreipunktbiegeproben sind als Kurven dargestellt für die speziell geeigneten Sichelkerbprobenformen (SSK, Sichel) und andere Formen. Die Versuchsresultate mit den heiklen Drahtproben zeigen, dass die Versuchstechnik für Stangen und Drähte im "low blow"-Versuch trotz der auftretenden Schwingungen funktioniert. Diese Methode ist für instrumentiere Kerbschlagprüfhämmer bereits Stand der Technik (vgl. [2], S. 174). In diesem Versuch wird die Biegekraft F in Funktion der Zeit aufgenommen, an einer 3-Pkt-Biegeprobe mit wirksamem Hebelarm ℓ.

3. PRAKTISCHE ANWENDUNGEN IN FORM VON PRÜFSPEZIFIKATIONEN

Die vorgeschlagene Prüfsystematik führt bei konsequenter Anwendung des dreigliedrigen Sicherheitsnachweises (Figur 2) zu Prüfspezifikationen mit Einbezug der Risszähigkeit. Für eine Sonderanwendung, bei der der Zeiteinfluss eine Rolle spielt, mit ungünstiger Superposition der Einwirkungen, ist hier eine typische Prüfspezifikation zusammengestellt.

Stabmaterial für Stossbelastung bei Tieftemperatureinsatz

Rohmaterial: Zugstange (Dmr.26) mit gewalztem/gerolltem Gewinde.
Einbauzustand: Ab Werk geschützt, eingebaut und auf Baustelle gegen Korrosion geschützt, im Betrieb kontrollierbar und austauschbar.
Prüfbedingung: Kurzzeitprüfung mit betriebsähnlicher Belastungsgeschwindigkeit und superponierter minimaler Temperatur.
Prüfprogramm: Zugversuch (Dehnung, Einschnürung), Biegeversuch im Baustellenzustand, SSK-Schlagbiegeversuch (ev. Kerbschlagversuch mit Kerbe an der Oberfläche), instrumentiert für "low blow"-Technik zur Ermittlung des K_{ID}-Wertes.
Qualitätssicherung: Aus dem garantierten K_{ID}-Wert des Herstellers kann mit der Beziehung in Figur 3 der zulässige Oberflächenfehler für die Kontrollen festgelegt werden. Die Probeentnahme aus einer Gewindestange ist in Figur 4 dargestellt.

Das Beispiel zeigt eine typische Anwendung des Bauwesens, bei der die statische Betrachtungsweise ohne Untersuchung des Risszähigkeitsverhaltens nicht statthaft ist. Dauerhaftigkeitsnachweise sind mit Vorteil an "repräsentativ geschädigten" Bauteilen durchzuführen.

4. BEZEICHNUNGEN

a	Risstiefe, Kerbtiefe	R_e, R	Streckgrenze, Festigkeit
D	Durchmesser der Probe	Y'	Spannungsintensitätskorr.faktor $= (K_I/\sigma\sqrt{a})(32\sqrt{a/D}/\pi)$
F	Kraft auf Biegeprobe	$d\varepsilon/dt$	Dehngeschwindigkeit
ℓ	Hebelarm der Biegeprobe	σ	mechanische Spannung
K_{IC},K_{ID}	stat., dyn. Bruchzähigkeit		
K_{ISCC}	K_{IC} (Spannungsrisskorrosion)		

5. ILLUSTRATIONEN

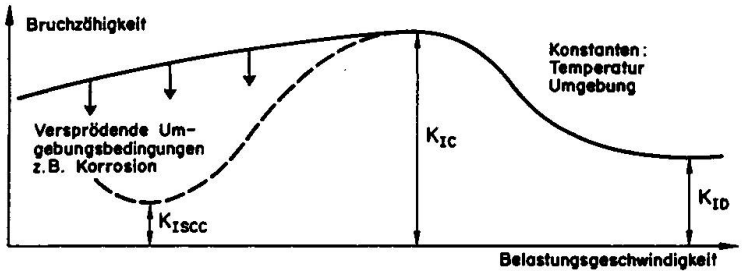

Langzeitgebiet	Quasistatisch	Dynamisch (Stoss)
$d\varepsilon/dt < 10^{-7}/s$	$d\varepsilon/dt \sim 10^{-5}/s$	$d\varepsilon/dt > 10^{-3}/s$
Bauteil oder Probe :		
vorgeschädigte, korrodierte, gekerbte Zugprobe oder Biegeprobe	angerissene oder gekerbte Zug- (Bauteil-) oder Biegeprobe	gekerbte, evtl. angerissene Schlagbiegeprobe, evtl. Zugprobe
Einrichtung :		
Dauerstandversuch - Kriechversuch oder Zugversuch, $\dot{\varepsilon}$ = konstant - Relaxationsversuch	Zugprüfmaschine - elektromechanisch oder - servohydraulisch geregelt	Schlagwerk instrumentiert - Pendel - Fallwerk
Umgebungseinfluss (Konditionierung) :		
- Medium, Temperatur	- Temperatur	- Temperatur

Figur 1:Bruchzähigkeit als Funktion der Belastungsgeschwindigkeit

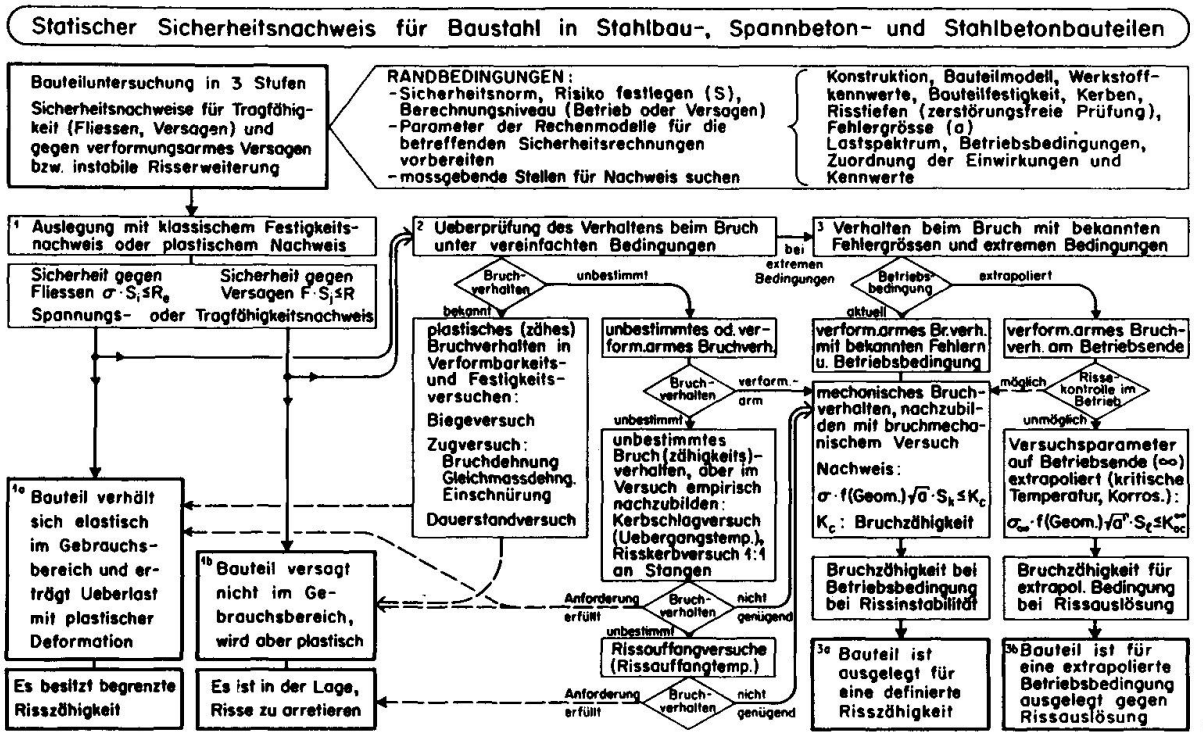

Figur 2: Statischer Sicherheitsnachweis mit Überprüfung des Verhaltens beim Bruch

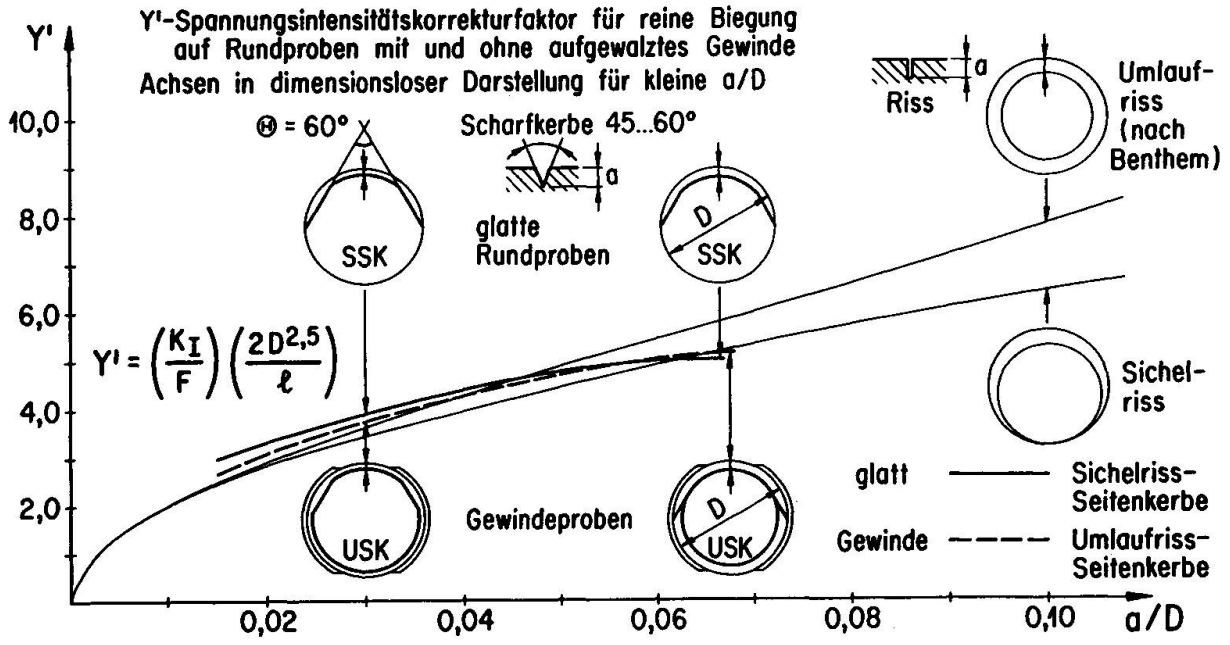

Figur 3: Funktionen für Bereich a/D von 0.02–0.07

$Y' = 250x - 6'426x^2 + 93'400x^3 - 536'000x^4$ für USK-Gewinde

$Y' = 271x - 7'186x^2 + 102'900x^3 - 589'000x^4$ für SSK-Sichel

$Y' = 0.018 + 181.9x - 2'407x^2 + 14'590x^3$ für Umlaufriss

$Y' = 0.023 + 177.5x - 2'463x^2 + 14'300x^3$ für Sichelriss

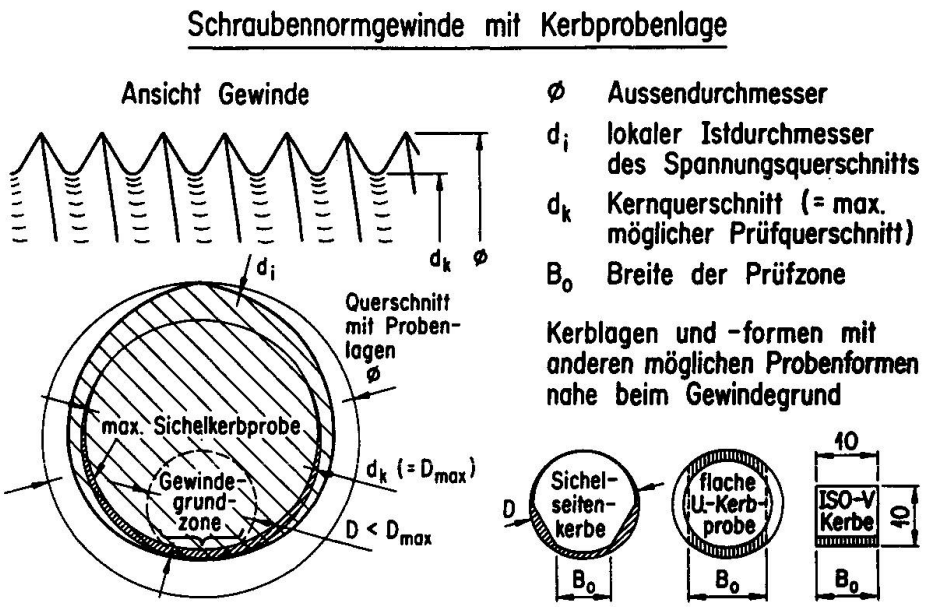

Figur 4:Anordnung von gekerbten Rund- und ISO-V-Proben in Gewindestange

6. LITERATURVERZEICHNIS

[1] U. NÜRNBERGER, "Analyse und Auswertung von Schadensfällen bei Spannstählen". Forschung, Strassenbau BVM BRD 308 (1980).

[2] U. MORF, "Zähigkeitsverfahren für Draht und Stangenmaterial am Stahl". Diss. ETHZ Nr. 8492/EMPA-Publ. Nr. 216 (1988).

[3] VERSCH. AUTOREN, "Spannungsrisskorrosion in Spannbetonbauwerken". Stahleisen mbH, Düsseldorf (1983).

[4] G. HAMPEIJS, "Spannungsrisskorrosion von Spannstählen...". X. Kongress der FIP, New Delhi (1986).

[5] U. MORF UND MITARBEITER, "Korrosionsinduzierte Sprödbrüche an Stangenmaterial". SIA (SVMT) Doku. 98 (1985).

[6] FIP-Report on Prestressing steel Nr. 5, "Stresscorrosion cracking resistance test...". 5/7 (1980).

[7] Euronorm 138-79 "Spannstähle"

Fatigue Strength of Corroded Steel Plates from Old Railway Bridge

Résistance à la fatigue de tôles en acier corrodées d'un vieux pont de chemin de fer

Ermüdungsfestigkeit korrodierter Stahlbleche einer alten Eisenbahnbrücke

Hidehiko ABE
Prof. of Civil Eng.
Univ. of Utsunomiya
Utsunomiya, Japan

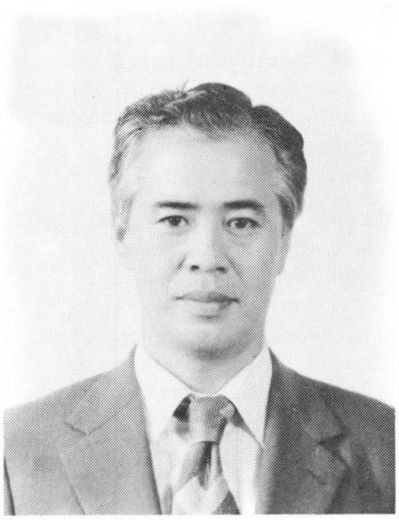

Hidehiko Abe, born 1931, graduated, and received his doctoral degree from the University of Tokyo, Japan. For 30 years he worked for the Japanese National Railways, mainly engaged in design of steel bridges. Since 1984 he has been teaching structural engineering at University of Utsunomiya.

SUMMARY

This paper presents results of fatigue tests for corroded steel plates. The test specimens with various degrees of corrosion were taken from an old bridge which had been used for over fifty years. It also deals with an attempt to predict the remaining fatigue life of steel railway bridges. For this purpose the author conducted fatigue tests of a steel railway bridge, which had been long in use and compared the test result with the analytical one.

RÉSUMÉ

Des essais de fatigue sur des tôles en acier corrodées sont présentés. Les échantillons, présentant différents degrés de corrosion, ont été prélevés sur un pont de plus de 50 ans. Les essais sont exécutés pour prédire la durée de vie restante. Les résultats sont comparés avec des solutions analytiques.

ZUSAMMENFASSUNG

Ermüdungsversuche an korrodierten Stahlblechen werden vorgestellt. Die Versuchskörper verschiedenen Korrosionsgrades wurden einer über fünfzigjährigen Brücke entnommen. Der Versuch wurde unternommen, um die Restlebensdauer vorauszusagen. Zu diesem Zweck werden die Versuchsresultate mit analytischen Ergebnissen verglichen.

1. INTRODUCTION

Steel bridges for railways are apt to suffer from fatigue damages. They are usually designed according to standards which take the fatigue effect into account and structural details which are supposed to have high resistance to fatiegue failure are selected. Nevertheless, many fatigue damages have occurred in actual railway bridges and they are often associated with corrosion. While most available fatigue data for structures are those which are obtained from specimens of non-corroded materials, few data of fatigue tests conducted on steel members which have been corroded under natural circumstances are available.

The authors conducted fatigue test for the steel parts which had been cut off from an old railway truss bridge in use for over fifty years in Japanese National Railways. The test results revealed that the notch shape made by corrosion had a greater effect on the fatigue strength than the decrease of the sectional area due to corrosion, if it was not excessive.

The paper also deals with an attempt to estimate a cumulative fatigue effect analytically and compare it with the result obtained from an experiment on an actual railway plate girder bridge which was used for more than fifty years in one of the busiest trunk lines. The test result suggested, however, that the effect of cumulative fatigue damage was obscured by the effect of corrosion and the wide scatter of the test results in this example. It seems to difficult to predict the remaining life of a bridge accurately in this way in practice.

2. TEST ON CORRODED PLATES

2.1 Test Specimens and Procedures

The bridge from which the test specimens were cut off is Tenryu Bridge, a truss bridge constructed for Tokaido Line, one of the busiest trunk lines. It was erected in 1913 and had been used for about fifty years. In addition to specimens of standard coupon type , riveted specimens and shallow beam type bending specimens using the lower flanges of the stringers were also prepared as shown in Fig. 1. According to the static test conducted for mechanical properties of materials, the tensile strength of lower lateral members were a little inferior to those specified by JIS-SS 41 and ASTM-A 36, while the mechanical properties of other members were in conformity to the specifications. In the fatigue test the load was varied from nearly zero to the maximum tension.

Table 1 shows the outline of test series and summary of the test results.

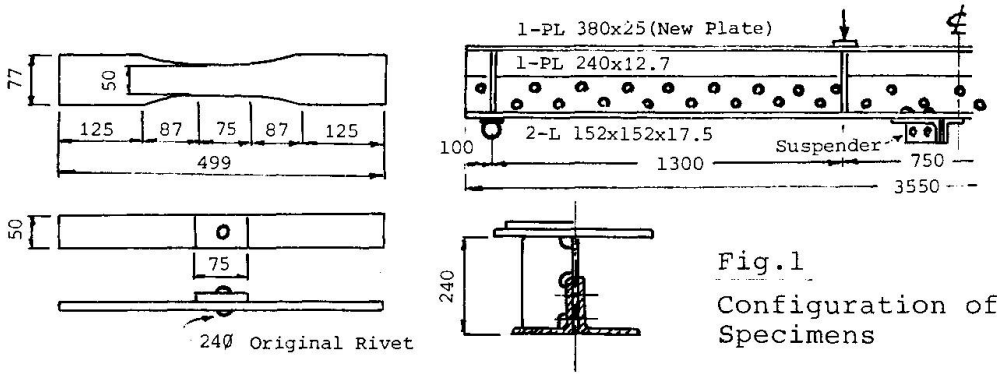

Fig.1 Configuration of Specimens

2.2 Test Results

The test results are presented in Figure 2. As for the expression of the stress intensity for corroded specimens, three different ways were used; 1) the original cross-sectional area, 2) the average remaining cross-sectional area and 3) the area of the cross-section through which the rupture passed were referred to.

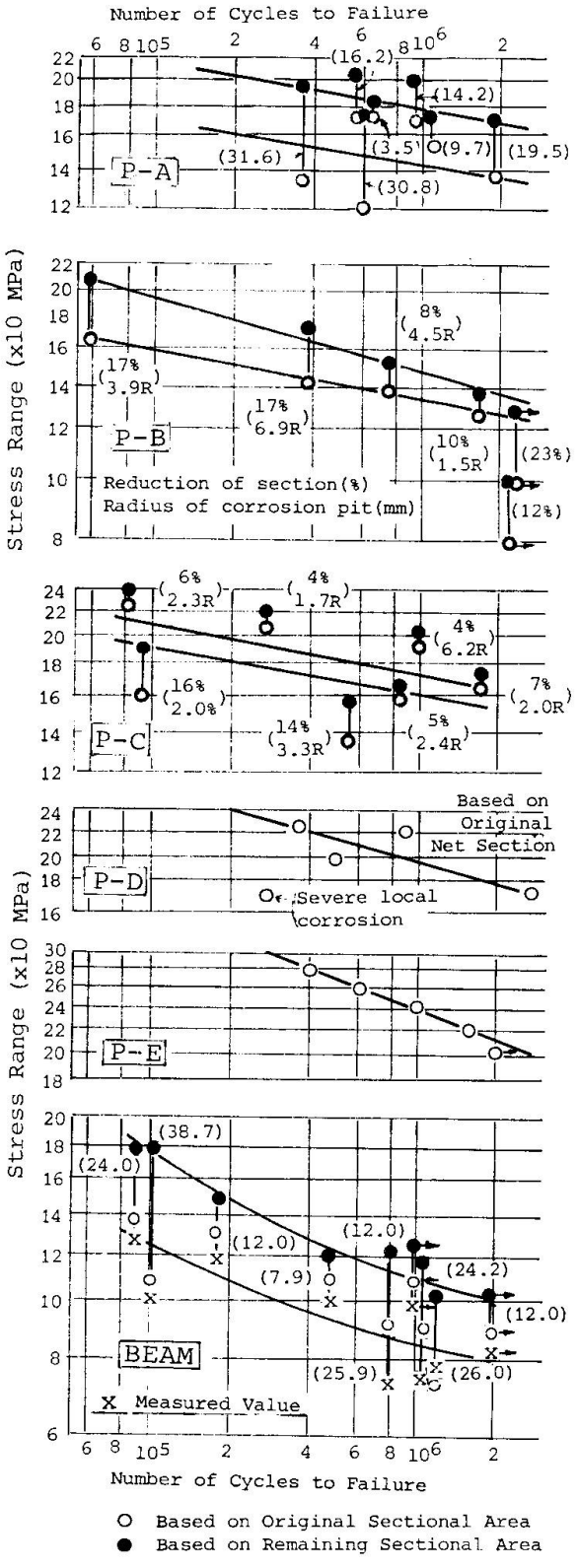

Fig. 2 Fatigue Test Results of Each Series

Furthermore, the radii of the corrosion pits from which the fatigue cracks started are also shown in the figures. For the bending test specimens, the stresses are expressed by three different ways, which are based on 1) the calculation according to the original non-corroded shape, 2) the measurement by wire strain guages and 3) the values in inverse proportion to the reduction in the cross-sectional area due to local corrosion.

While the cracks were initiated at the bottoms of pits formed by corrosion in all the plate type specimens, they started from the edges of rivet holes in the riveted specimens and from the spot of the attachment for suspension of the lower lateral members in the beam type specimens. Several photos of fractured specimens also are shown.

2.3 Discussion

The data plotted in the figures are generally widely scattered. It is felt to be wider than in the cases of usual non-corroded specimens. The zero to tension fatigue strengths at two million cycles are summerized in Table 1. Assuming the fatigue strength of non-corroded plain plate with cut edge of 50 S as 250MPa on average, that of even a slightly corroded specimen is 210MPa (about 85%) and that of a heavily corroded specimen is drastically lowered down to 140 MPa (about 55%) even as expressed in reference to the remaining cross-section. The corroded riveted specimen, however, has a fatigue strength of 180 MPa, which is equivalent to the non-corroded riveted specimen. The reason for this seems that a riveted specimen has stress concentration inherently due to the rivet hole, which has the same degree of adverse effect on the fatigue strength as the surface irregularity due to corrosion and which need not be superimposed with the effect of corrosion.

In the beam type specimens, the fatigue strength is as low as 100MPa. It suggests that the corrosion adjacent to the attachment has a very adverse effect on the fatigue strength. It is natural that if the strength is evaluated in reference to the original cross-sectional area, it should be lowered furthermore. It seems that the

effect of the radius of the corrosion pit on the fatigue strength is insignificant.

Table 1 Specimens tested and fatigue stengths

Series		Corrosion	Location of Specimens	No.	Strength, MPa 1*	2**
Plates	P-A	Severe	Lower flange of stringer	7	170	135
	P-B	Severe	Lower Lateral bracing for truss	6	135	125
	P-C	Slight	Upper lateral bracing for stringer	7	160	150
	P-D	Slight	Lower lateral bracing for truss+	5	180	180
	P-E	Little	Web of stringer	5	210	210
Beam		Severe	Lower flange of stringer	7	100	80

+) Specimens with rivets, *) Strength 1 is based on average cross-sectional area decreased by corrosion and **) Strength 2 is based on original cross-sectional area.

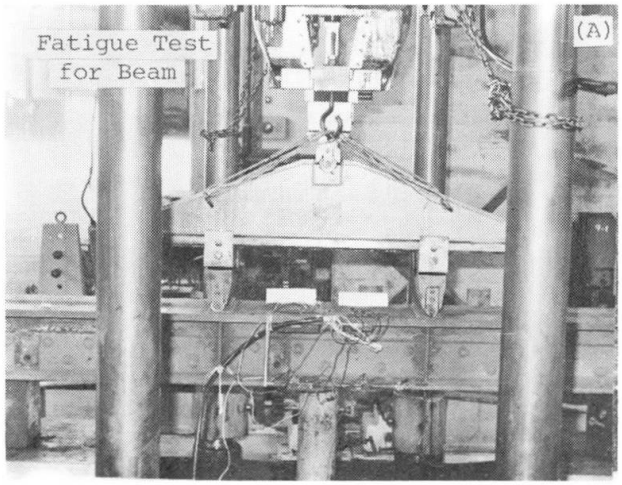

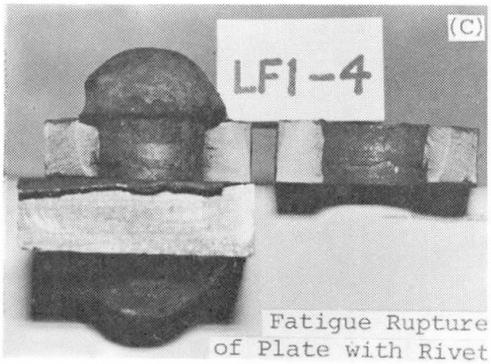

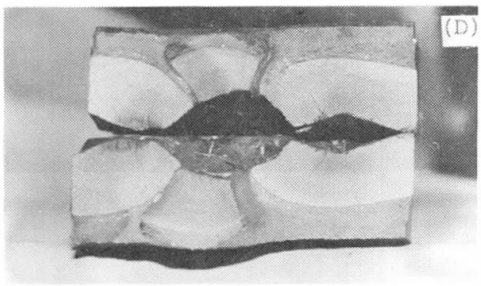

Fatigue Rupture of Heavily Corroded Plate

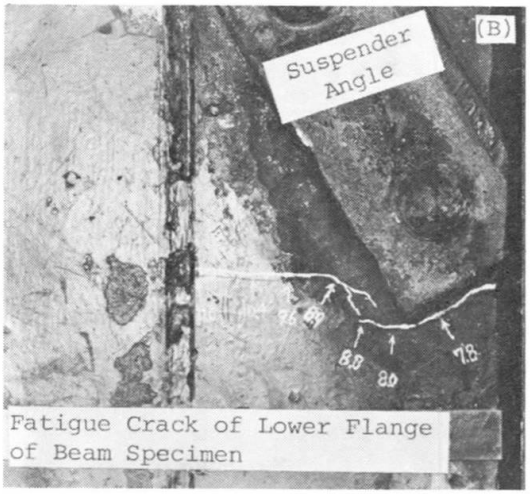

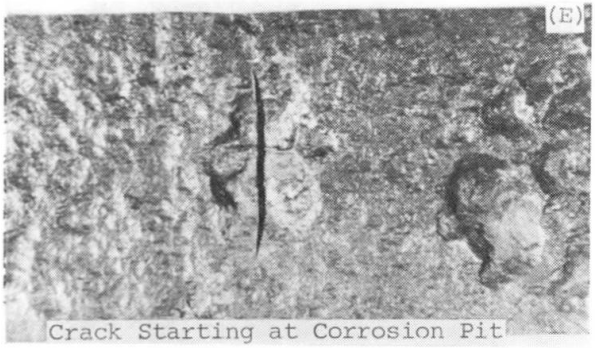

3. TEST FOR CUMULATIVE FATIGUE DAMAGE

3.1 Test Specimens and Procedures

The bridge which was used for investigation of the cumulative fatigue effect was a plate girder bridge of a 12.9 meter long span, used for 54 years in To-

hoku Line, a relatively busy trunk line. It was fabricated in U.S.A. and its material was produced in Carnegie Co. The specimens for fatigue test were cut off from the lower flanges of the plate girder. It was considered that the riveted parts of the lower flanges had suffered from the cumulative fatigue effect more severely than other parts because of the location and the stress concentration. For comparison, specimens were also taken from the less stressed parts and in some specimens the original holes were reamed, so as to remove the zone which was estimated to have been subjected to the most severe cumulative fatigue effect. According to the static test, the materials were in conformity with JIS-SS 41 and ASTM-A 36. The loading was repeated at a rate of 500 cycles per minute from 12 MPa to the maximum tension in the fatigue test.

3.2 Test Results

Fig. 3 shows the comparison of the results of specimens of plain machined plate, and specimens with rivet holes that were supposed to have experienced three different degrees of cumulative fatigue effect. It is natural that the value of plain plate specimens is high. It shows that the difference among the values of specimens of different conditions are very small, as judged from the regression lines of respective series, though the results are widely scattered.

3.3 Calculation of Cumulative Fatigue Effect

Table 2 shows the calculated stress, the number of stress cycles and the estimated cumulative fatigue effect for each of the eras when the types of locomotives crossing the bridge were recorded to be different. The cumulative effect was evaluated according to Miner's Law and the stresses around the rivet holes were assumed to 1.9 times as large as those in the non-riveted parts as seen in Fig. 3. The coefficients of cumulative fatigue effect were, thus, determined as 0.288 and 0.010 for the parts subject to larger stress and those subject to smaller stress, respectively. In Fig. 3, the three theoretical lines thus obtained are drawn together with the test results.

The difference of remaining fatigue life due to the difference of experienced stresses (Series 5 and 6) in the present case is insignificant as seen from the theoretical lines. The effects of corrosion and quality of rivet holes caused the test results to scatter over a very wide range. For those reasons it was found to be practically difficult to clarify the difference of remaining fatigue life due to the cumulative fatigue effect.

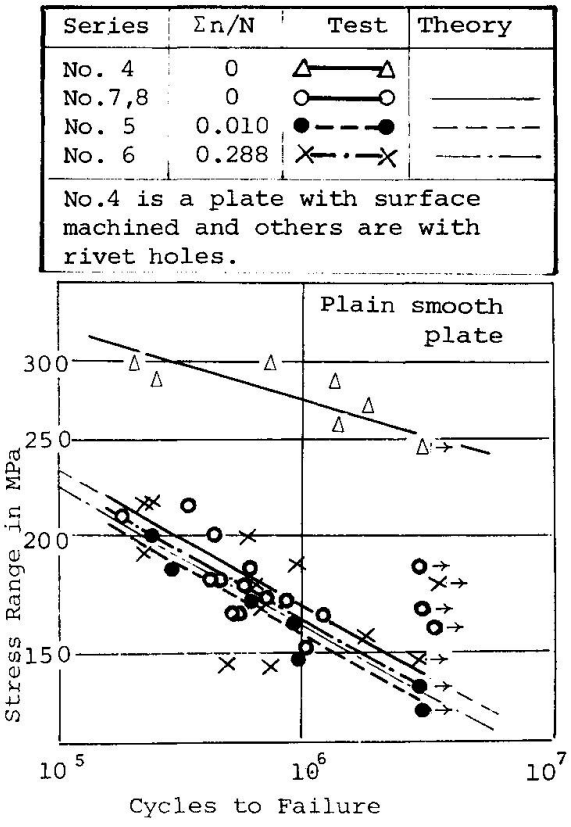

Fig.3 Results of Fatigue test of Cumulative Damage

4. CONCLUSIONS

(1) Even slight corrosion has a significant effect on the fatigue strength, especially in case the original element is smooth, free from stress concentration.

When the allowable fatigue strength is to be determined for the design where such elements are used, care must be taken so as to provide a greater safety margine, assuming a possibility of future corrosion to some extent.

In a heavily corroded steel plate, the fatigue strength is drastically lowered to as low as 140 MPa to 100 MPa in reference to the remaining cross-sectional area, of stress range at two million cycles, because of severe stress concentration at the corrosion pit and because of reduction of the cross-sectional area. But the fatigue strength of elements which involve stress concentration inherently, such as riveted plates, are relatively less influenced by corrosion.

(2) According to an experiment on specimens cut off from a steel railway bridge which had been subjected to even considerably frequent loadings in the past, the cumulative fatigue effect on the remaining life appeared insignificant in practice. One of the reasons for this seems that the corrosion and irregularity in fabrication tend to cause such a vast scatter in the results of fatigue test that it is difficult to clarify the effect of the cumulative fatigue damage. The other reason may be that actually the cumulative effect on the main members or bridges which are carefully designed according to the current specifications is usually insignificant. Most of the actual fatigue failures have occurred at inadequate structural details, parts which have substantial defects in fabrication or hidden excessive corrosion, and have resulted from causes that had not been considered, when designed, such as repetition of out-of-plane deformation and vibration [1][2].

Table 2 Example of Calcaulation of Cumulative Fatigue

	More Stressed Part				Less Stressed Part			
Period (1900)	Stress (M Pa)	n_i (x1000)	N_i	n_i/N_i	Stress (M Pa)	n_i (x1000)	N_i	n_i/N_i
17 -19	112.7	132	2,592	0.051	74.5	132	79,782	0.002
31 -45	129.4	183	1,657	0.110	86.2	183	47,276	0.004
46 -58	120.5	153	2,084	0.073	80.4	153	58,558	0.003
59 -63	103.9	50	3,377	0.015	69.6	50	102,747	0.000
64 -71	103.9	130	3,377	0.038	69.6	130	102,747	0.001
Ditto	51.9	43	32,013	0.001	34.3	43	893,299	0.000
Sum/54		691		0.288		691		0.010

5. REFERENCE

[1] H. ABE and A. TANIGUCHI, Fatigue Damage and Repair of Floor Beam of Steel Railway Bridges, Proc. of ASCE-IABSE Symposium at Morgantown, U.S.A., August 1980, pp 414 to 421

[2] H. ABE et al., Fatigue Damage and Repair of Steel Railway Bridges in Japan, Final Report of IABSE Symposium at Tokyo, September 1986, pp 48 to 51

Aluminizing as a Reliable Method of Steel Corrosion Protection

Protection anticorrosion efficace à l'aide d'un revêtement d'aluminium

Aluminiumbeschichtung als wirksamer Korrosionsschutz

I. A. BOIKO
M. Sc. (Eng.)
TSNIIPSC
Moscow, USSR

I. A. Boiko, born 1938. Graduated from the Moscow Institute of Non-Ferrous Metals. He has been studying the corrosion problems of aluminium coatings of steels in atmospheric conditions.

S. V. MARUTYAN
M. Sc. (Eng.)
TSNIIPSC
Moscow, USSR

S. V. Marutyan, born 1948. Graduate from the Moscow Institute of Aviation Technology. He has been studying the processes of steel aluminizing.

SUMMARY

The technology of hot-dip aluminium coating of steel members has been investigated. The corrosion-resisting properties of the obtained coatings have been studied for the areas of industrial and agricultural installations. A favourable effect of alloying of the aluminium melt with manganese on the coating corrosion resisting properties has been shown. Industrial production of aluminium-coated power transmission line supports has been initiated.

RÉSUMÉ

Une technologie a été développée pour le dépôt de revêtements protecteurs en aluminium sur des éléments de structures métalliques par immersion à chaud. Les propriétés anticorrosives des revêtements obtenus sont étudiées dans les milieux agressifs industriels et agricoles. L'alliage d'aluminium fondu avec manganèse exerce une influence positive sur les propriétés anticorrosives des revêtements. La production industrielle des appuis de lignes à haute tension avec revêtement d'aluminium a été mise au point.

ZUSAMMENFASSUNG

Es wurde ein Schmelztauchverfahren zur Herstellung eines Aluminiumschutzüberzugs für Stahlbauelemente entwickelt. Die Korrosionseigenschaften dieses Überzugs in industriellen Medien und beim landwirtschaftlichen Betrieb wurden überprüft. Es wird eine positive Wirkung des Mangans als Legierungselement in Aluminiumschmelzen auf die Korrosionseigenschaften der Überzüge gezeigt. Die fabrikmässige Herstellung aluminiumüberzogener Freileitungsmaste ist aufgenommen worden.

The preservation of structural steelworks of industrial buildings and structures during their service life contributes to decreasing the service labour expenditure and, at present, is one of the major problems.

The total national economy losses due to corrosion of structures under the effects of corrosive atmospheres are approximately 1.5 thousand million roubles per year.

The metal loss, however, is only a part, and not the main one, of the total loss caused by corrosion. It leads to idle standing of equipment, to failures, to drop in equipment capacity and to products quality deterioration.

The continuous intensification of production and increase in capacity of assemblies resulting in a rise of operational effects on structures, on the one hand, and the desire to reduce the structural or building weight by application of thin-walled structures due to the use of progressive designs and high-quality steels, on the other hand, impose additional and more stringent requirements for corrosion protection of metalworks. In this context, the problem of high-durability protective coatings is nowadays one of the most important problems of the national economy.

At present, coatings of zinc, aluminum and their alloys are widely used for protection of structures against atmospheric corrosion and effects of fresh and sea water.

High corrosive resistance of aluminum, fast growth of its production together with the zinc deficiency steady increase raised a question of aluminum coatings wide application in building and industrial production.

One of the most efficient methods of aluminum coating application is hot-dip aluminizing which consists in dipping of a steel product into aluminum melt.

Hot-dip aluminum coatings provide long-term corrosion protection of steel structures in the atmospheres of weak and mean corrosivity (classification according to the Soviet standards). Aluminum coatings 80-100 m thick provide corrosion protection of steelworks for a period of 20 to 50 years, depending on the service conditions.

The increased corrosive resistance of aluminum which is inferior only to titanium in aerated solutions, is accounted for by the resistance of the oxide film consisting of Al_2O_3 or $Al_2O_3 \cdot H_2O$ and appearing on the aluminum surface,

In industrial atmospheres polluted with sulphur compounds, in particular, hydrogen sulphide and sulphurous anhydride, the aluminized steel has a fairly good resistance to corrosion.

It is common knowledge that, in the majority of environments, zinc protects steel electrochemically being an active anode. The problem concerning the possibility of electrolytic protection of steel by means of aluminum coating applied on its surface is not simple. In soft waters, the aluminum coating is considered to behave as a cathodic one, because, in this case, the potential of aluminum is more positive than that of steel. In sea water and in some fresh waters, particularly, when they contain Cl^- and SO_4^{-2}, the potential of aluminum is shifted to more active area, this

resulting in polarity reversal of the couple Al-Fe. In these cases, the aluminum coating is an anode and provides a sacrificial protection of steel. One should bear in mind that the couple "base metal" - "protective metal coating" only results from disturbance of the coating (coating defects, porosity of edges after cutting-off).

Service conditions	Corrosivity acc. to Soviet standards	Rate of corrosion, m/year		
		Aluminum coating	Zinc coating	Cm3 without any coating
Urban industrial atmosphere	weak	0.3-0.5	1-3	34-40
Integrated chemical plant	mean	1-3	25-30	200-210
Agricultural installations	weak and mean	5-7	15-20	90-100
Integrated iron-and-steel works	mean	1.5-2.0	25-30	130-140

Table Corrosion resistance of Cm3, zinc and aluminum coatings in different service conditions

Proceeding from the assumption that hot-dip coatings are porousless and that the hot-dip process provides coatings without defects, the aluminum coatings protect the base metal primarily mechanically.

A coating formation takes place when there is an interaction between the liquid phase (aluminum and its alloys) and the solid one (steel surface). At the boundary of these two phases, there occur the processes of wetting, interdiffusion, solution, chemical interaction and crystallization in the system Al-Fe, including some alloying elements. The coatings thus obtained have a complex structure. The layer contiguous with steel consists of intermetallic compounds of Al and Fe, and the surface layer determining the coating durability consists of an aluminum alloy with the inclusions of Fe.

In the course of aluminizing, iron accumulates in the aluminum melt and results in decrease of the coating corrosive resistance, particularly, when its content exceeds 2.5%. The iron concentration exceeding 3.0% (the melt temperature being 700 to 730 C), the crystallization of the intermetallic compound of Fe_xAl_y type occurs on the surface of the product aluminized deteriorating its service properties and appearance.

The optimization of the temperature conditions and of the aluminizing duration allows the iron accumulation in the melt to be reduced, and, thus, the corrosive resistance of coatings to be increased. Another way of increasing the corrosive resistance of coatings is alloying of the melt with elements lowering the melt

saturation with iron and neutralizing its adverse effect in the coating.

The full-scale and accelerated corrosion tests of specimens with hot-dip aluminum coatings containing iron, silicon, manganese have shown that hot-dip coatings containing manganese have the greatest durability (Fig. 1).

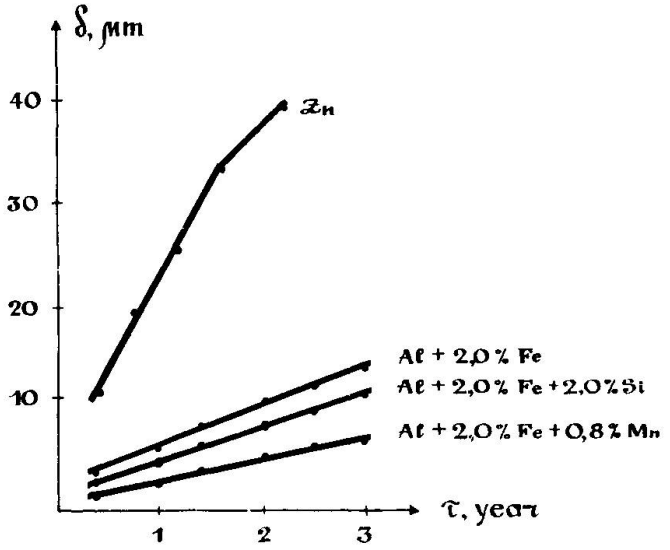

Fig. 1 Dependence of the values of corrosion failure (δ) of aluminum and zinc coatings of steel upon the test period (τ) in conditions of an integrated chemical plant

Alloying of iron-containing aluminum melt with silicon or manganese leads to a change of the electrode potentials of the coating microelements. Manganese neutralizes the effective cathodic action of inclusions $FeAl_3$, whereas silicon forms cathodic inclusions (FeSiAl) and (FeSiAl) in the coating.

The corrosion-resisting properties of aluminum coatings are predetermined by their structure which, in its turn, depends on the conditions of the coating formation. The coating structure is under a great influence of the aluminizing temperature, the steelwork hot-dipping duration, the melt composition and the steelwork cooling conditions after the coating application. Therefore, the observance of technological conditions of aluminizing will allow an aluminum coating to be formed on a steel product surface, this coating having a minimum-thickness intermetallic layer and no cathodic inclusions of $FeAl_3$ and Fe_2Al_5 compounds in the aluminum layer (Fig. 2).

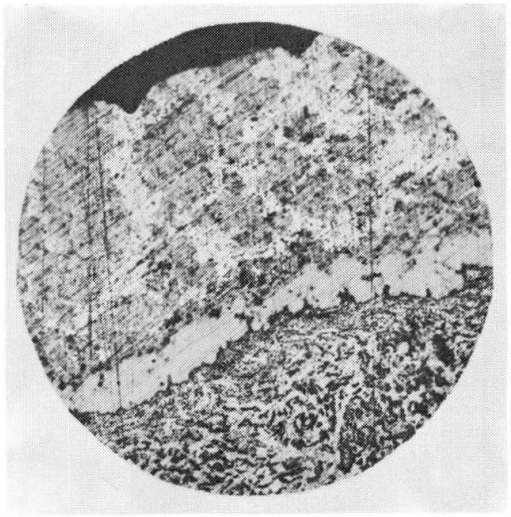

Fig. 2 Aluminum coating microstructure

The aluminizing process has been industrially mastered for corrosion protection of steelworks of power transmission line supports.

Leere Seite
Blank page
Page vide

POSTERS

Leere Seite
Blank page
Page vide

Zur Zeitfestigkeit der Verdübelung bei Verbundträgern mit Profilblechen

Fatigue Strength of Headed Stud Connections for Composite Beams with Profiled Steel Sheeting

Résistance à la fatigue des goujons dans des structures mixtes

H. BODE
Prof. Dr. -Ing.
Universität Kaiserslautern
Kaiserslautern, BR Deutschland

J. KRETZ
Dipl. -Ing.
Universität Kaiserslautern
Kaiserslautern, BR Deutschland

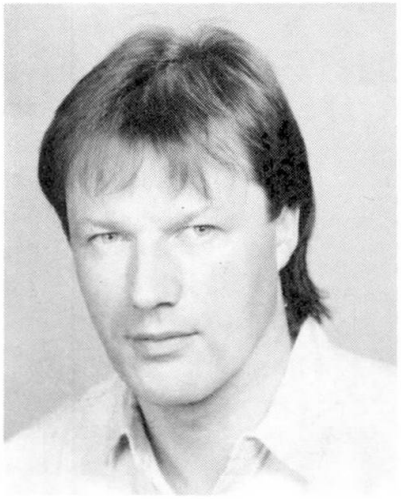

ZUSAMMENFASSUNG

Dieser Beitrag beschäftigt sich mit dem Trägerverbund zwischen Betongurten und Stahlträgern, der durch Verwendung von Stahlprofilblechen beeinflusst wird. Die Untersuchungen betreffen die Tragfähigkeit der Verdübelung unter nicht ruhender oder dynamischer Belastung. Die günstigen Zeitfestigkeiten bei Verwendung von Profilblechen lassen für Verbundträger einen grösseren Anwendungsbereich im Industriebau erwarten.

SUMMARY

This paper deals with the composite action between concrete flanges and steel sections, which is influenced by the use of profiled steel sheetings. The study concerns the connector strength in case of dynamic loading. The relatively high fatigue strengths even in case of profiled steel sheetings crossing the steel section form the basis for a wider use of composite beams for industrial buildings.

RÉSUMÉ

Cet article traite de la liaison entre la section de béton et la poutre métallique. Cette liaison est influencée par l'emploi de tôles profilées. Les essais concernent la résistance des goujons sous charge mobile ou dynamique. L'effet favorable de l'emploi de tôles sur la résistance à la fatigue de la structure mixte permet d'en prévoir une plus grande utilisation dans les bâtiments industriels.

1. TRÄGERVERBUND, DYNAMISCHE FESTIGKEIT

1.1. Allgemeines

Verbundträger und Verbunddeckenkonstruktionen im Industriebau werden nicht immer nur vorwiegend ruhend belastet. Oft treten nicht vorwiegend ruhende Belastungen auf, z. B. aus Gabelstaplerbetrieb, bei Kranbahnen, bei Hänge- und anderen Fördersystemen. Auch stoßartige Belastungen können auftreten.

An der Universität Kaiserslautern wurden 21 Versuche mit dynamischer Einstufenbelastung durchgeführt. Sie waren vom DASt und der AIF gefördert und finanziell unterstützt worden /7/. Die Untersuchungen wurden im Zeitfestigkeitsbereich bei Lastspielzahlen um 100.000 und mit einer hohen Ausnutzung der Verbundmittel bis zu 82 % der tatsächlichen statischen Festigkeit durchgeführt. Dies trägt der hohen Dübelbeanspruchung im Gebrauchszustand bei plastischer Bemessung im Hoch- und Industriebau Rechnung. Im einzelnen handelt es sich um
- 6 Trägerversuche und
- 15 Scherversuche.

1.2 Scherversuche

Für die Scherversuche wurden Versuchskörper nach Bild 1 verwendet.

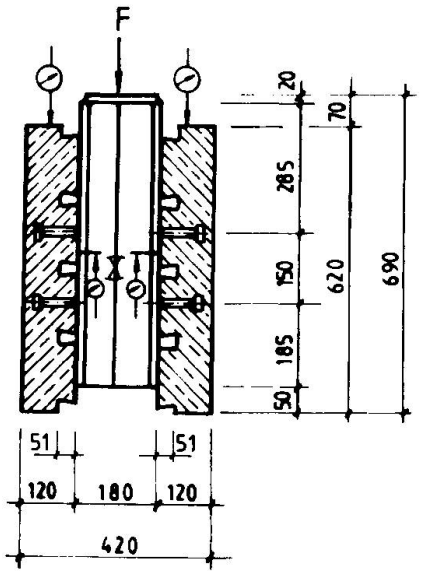

Bild 1: Scherversuchskörper

Die Darstellung in Bild 2 zeigt die auch für die anderen Scherversuche typische Zunahme der Relativverschiebungen zwischen Betongurt und Stahlprofil mit der Lastspielzahl N beim Versuch S 2/5.

Zu Beginn der Versuche betrug der Anfangsschlupf 1.1 mm, dann erfolgte der Bereich stabilen Schlupfwachstums, in dem der Beton vor dem Dübelfuß wegen der konzentrierten Belastung langsam zerstört wurde. Von etwa 10^6 Lastspielen an nahmen die Relativverschiebungen überproportional zu, bis der Bruch der Bolzen oberhalb des Schweißwulstes eintrat.

Um die Wöhlerlinie, die bei doppeltlogarithmischer Auftragung näherungsweise eine Gerade darstellt, zu erhalten,werden die Spannungsdifferenzen und Lastspielzahlen bis zum Bruch aufgetragen und statistisch ausgewertet. Die Neigung der

Wöhlerlinie wird durch den aus den Versuchen berechneten Exponenten k = 8,26 bestimmt und beträgt 1/k.

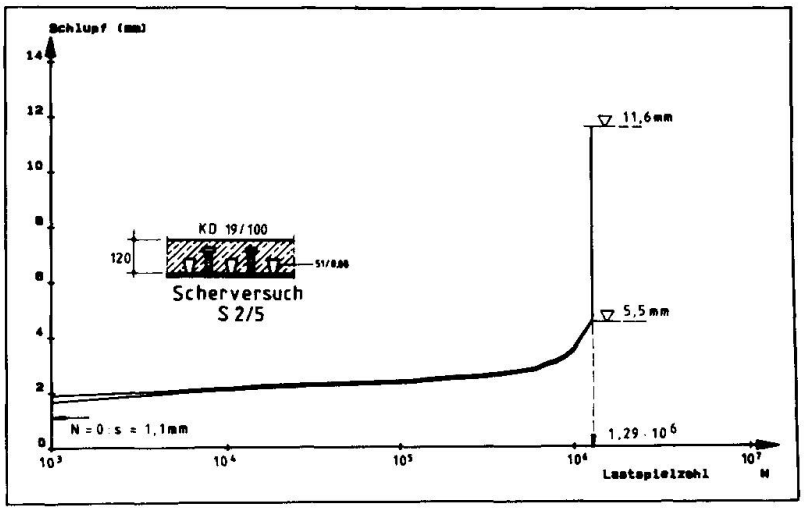

Bild 2: Schlupf im Versuch S 2/5

Im Dübel und in seiner Umgebung stellt sich ein komplexes Kräftespiel ein, was nur global durch ΔD_S oder durch eine Schubspannungsdoppelamplitude $\Delta\tau$ im Bolzenschaft als Maß für die Höhe der Beanspruchung erfaßt werden soll.

Im Vergleich zu den Bochumer Versuchen von Roik /3, 5/ mit massiven Vollplatten liegen die hier mit Profilblechen ermittelten Zeitfestigkeiten niedriger, und zwar um etwa 18 %. Diese Reduktion muß man aber im Zusammenhang mit der statischen Dübeltragfähigkeit sehen, die bei Holoribblechen um ca. 3O % niedriger liegt als bei massiven Vollplatten. Die Kopfbolzendübel verhalten sich - trotz der sehr hohen Ausnutzung der Dübel - in Verbindung mit Profilblechen unter dynamischer Belastung vergleichweise günstiger als bei statischer Beanspruchung.

1.3 Trägerversuche

Trägerversuche haben den Vorteil, daß Betongurt, Dübelzone, Dübel, Schweißung und Stahlträger wie bei einem tatsächlichen Träger wirklichkeitsnah beansprucht werden können. Das gilt in besonderem Maße für die gleichzeitige Beanspruchung von Dübelfuß und Stahlflansch durch Dübelkräfte und Gurtspannungen.

Neben dem Probelm, mit wenigen Trägerversuchen zu statistisch aussagekräftigen Ergebnissen zu gelangen, besteht die Schwierigkeit vor allem in der Ermittlung der tatsächlich auftretenden Dübelkräfte, da diese sich nicht direkt messen lassen. Sie werden deshalb zunächst auf der Grundlage des elastischen Schubflusses mit Hilfe der Q·S/I-Formel berechnet. Zusätzlich wird jedoch eine Versuchssimulation mit einem leistungsfähigen Computerprogramm durchgeführt, welches die nichtlineare Trägeranalyse einschließlich der Nachgiebigkeit der Verdübelung berücksichtigt. Damit kann insbesondere gezeigt werden, daß die Rückrechnung von Dübelkräften über starren Trägerverbund im allgemeinen fehlerhaft ist.

Weiterhin zeigt sich, daß sich durch diese Korrektur der Dübelkräfte, wie sie mit Hilfe der Q·S/I-Formel ermittelt worden sind, die Ergebnisse von Scher- und Trägerversuchen deutlich angleichen lassen.

Bild 3 enthält den Versuchsträger T2/2 der Serie 2 mit Betongurt in der Zugzone. Die drei Träger der Serie T1 waren gleich ausgebildet, aber so angeordnet und belastet, daß der Betongurt in der Druckzone lag. Das Bild enthält auch die Lage der Meßstellen (DMS und Wegaufnehmer).

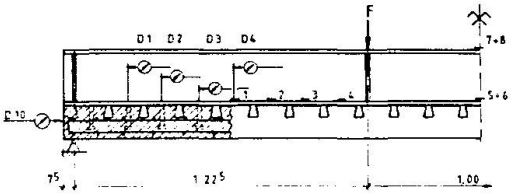

Bild 3: Versuchsträger T2/2

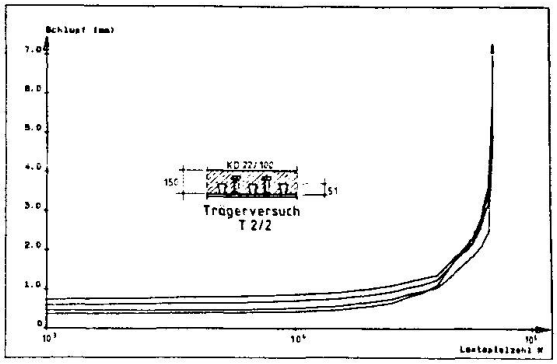

Bild 4: Trägerversuch T2/2; Schlupf bei Oberlast

In Bild 4 wird die Vergrößerung der Relativverschiebung bis zum Bruch gezeigt, während Bild 5 die entsprechenden Dehnungsverläufe wiedergibt.

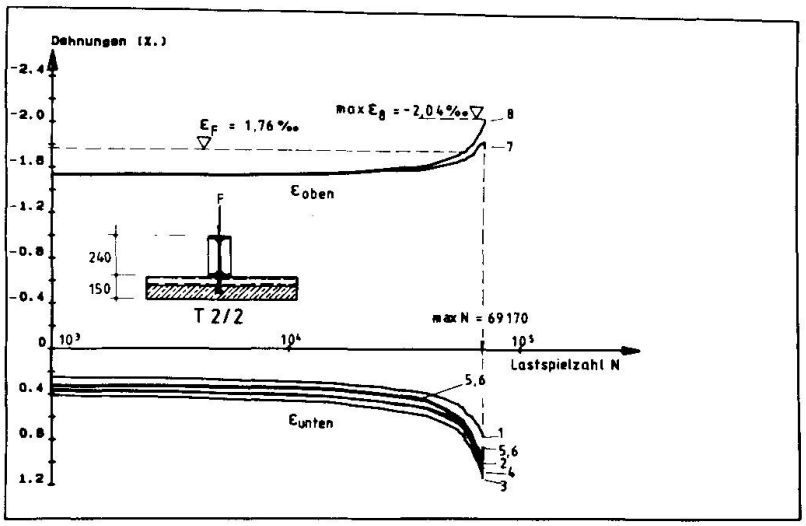

Bild 5: Trägerversuch T2/2; Dehnungen bei Oberlast

Aus diesen Last-Schlupf-Verläufen sieht man, daß die Verdübelung mit der Lastspielzahl N weicher wird. Auch die hier dargestellten Stahlträger-Randdehnungen lassen das erkennen. Infolge der abnehmenden Dübelsteifigkeit wird das Zusammenwirken unvollständiger. Insbesondere nimmt die Biegebeanspruchung im Stahlträger zu, und die vormals elastischen Dehnungen überschreiten die elastische Streckgrenze. Das bedeutet gleichzeitig, daß die wirklichen Dübelkräfte mit der Zeit kleiner werden. Tatsächlich liegt damit nun keine reine Einstufenbelastung der Dübel mehr vor.

Mit dem o. g. Rechenprogramm /6/ wurden dann die rein statischen Vergleichsberechnungen durchgeführt, deren Ergebnisse in den Bildern 6 und 7 dargestellt sind.

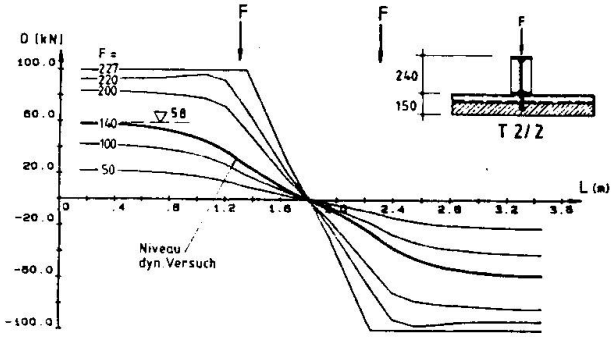

Bild 6: Verlauf der Dübelkräfte

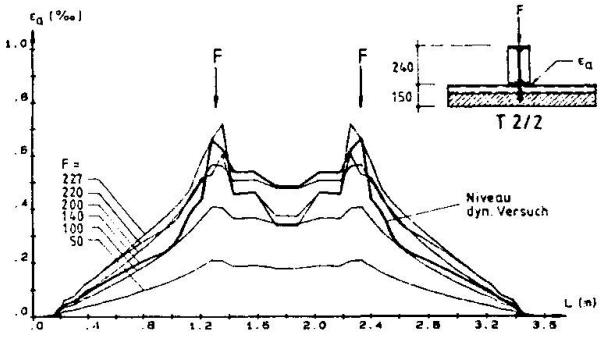

Bild 7: Verlauf der Stahldehnungen

In Bild 6 sind die berechneten Dübelkraftverläufe unter statischer Last bis zur rechnerischen Traglast dargestellt. Auch im mittleren Trägerbereich, in dem die Gesamtquerkraft gleich null ist, treten Dübelkräfte auf.

Die Q·S/I-Formel für starren Verbund bei linear elastischem Verhalten sowie Beton im Zustand I würde den Maximalwert 73 kN ergeben. Infolge des unvollständigen Zusammenwirkens sind die Dübelkräfte mit D_S = 58 kN deutlich kleiner als die mit starrem Verbund berechneten:

Zustand I: Reduktion von 73 auf 58 kN (79 %)
Zustand II: Reduktion von 67,5 auf 58 kN (86 %)

Tatsächlich nehmen die Dübelkräfte außerdem mit der Lastspielzahl ab. Deshalb sind hier über die MINER-Regel schädigungsgleiche Dübelkräfte berechnet. Dadurch ergibt sich eine weitere Reduktion der vergleichbaren Dübelbeanspruchung, und zwar im Fall des Trägers T2/2 von 58 auf 54 kN.

Die Ergebnisse der Trägerversuche sind im Bild 8 in das Diagramm der Scherversuche eingetragen.

Ohne Berücksichtigung der Nachgiebigkeit der Verdübelung liegen die Werte deutlich über dem Streuband der Scherversuche: Trägerversuche scheinen günstigere Ergebnisse zu liefern! Wir haben jedoch gerade zeigen können, wie wir bei der Auswertung des Trägerversuches T2/2 die Nachgiebigkeit rechnerisch berücksichtigt haben.

Bei Versuch T2/2 führt die dadurch verursachte Reduktion um insgesamt 26 % auf eine Lage im Streuband, dasselbe gilt für T1/3 und vermutlich auch für alle anderen Trägerversuche: richtig ausgewertet, werden die Ergebnisse von Scher- und Trägerversuchen wieder miteinander vergleichbar.

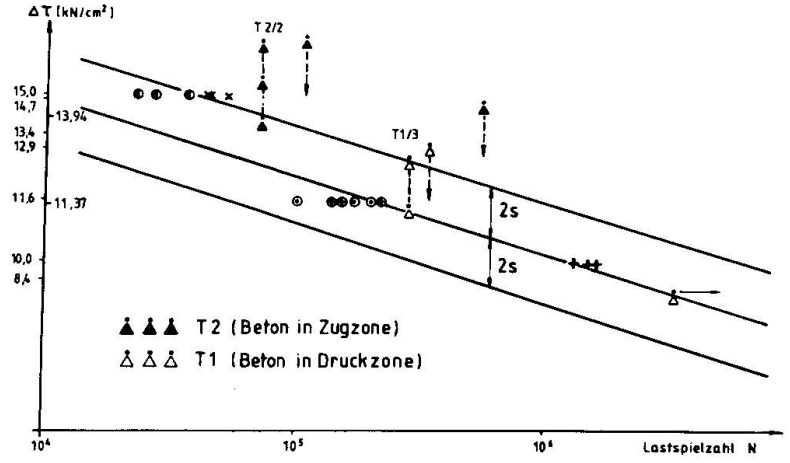

Bild 8: Zeitfestigkeiten der Scher- und Trägerversuche

1.4 Literaturhinweise

/1/ Richtlinien für die Bemessung von Stahlverbundträgern

/2/ H. Bode, R. Künzel: Zur Verwendung von Profilblechen beim Trägerverbund Festschrift Baehre, Karlsruhe 1988

/3/ K. Roik, H.-J. Holtkamp: Untersuchungen zur Dauer- und Betriebsfestigkeit der Verdübelung von Verbundträgern mit Hilfe von Kopfbolzendübeln. Studiengesellschaft für Anwendungstechnik von Eisen und Stahl, P 1O1, Düsseldorf 1986

/4/ R. P. Johnson, R. J. Buckby: Composite structures of steel and concrete. Vol. 2, London 1979

/5/ K. Roik, G. Hanswille: Zur Dauerfestigkeit von Kopfbolzen dübeln bei Verbundträgern Bauingenieur 62/1987

/6/ J. Schanzenbach: NG-Verbund-Programm zur physikalisch nichtlinearen Berechnung von Verbunddurchlaufträgern mit nachgiebiger Verdübelung. Universität Kaiserslautern, 1988

/7/ H. Bode, J. Kretz: Trägerverbund im Industriebau unter nicht ruhender Belastung bei Verwendung von Profilblechen. DASt/AIF-Forschungsbericht (unveröffentlicht), Kaiserslautern 1988

Strength of Freeze-Thaw Deteriorated Concrete

Résistance du béton détérioré par des cycles gel-dégel

Festigkeit von durch Frost und Auftauen beanspruchtem Beton

Jesper KRUS
Civil Eng.
Royal Inst. of Technology
Stockholm, Sweden

Jesper Krus, born 1961, graduated as a Master of Sicence in Civil Engineering at the Royal Institute of Technology in Stockholm in 1987, since then he has been studying for a doctorate at the Dep. of Structural Engineering.

SUMMARY

Tests have been performed in which drilled-out concrete cores were first subjected to an environmental load in the form of freezing-thawing and then to a functional load in the form of a fatigue or static failure load. The aim was to study the combined influence of the deterioration factors on the strength of concrete. Measured results show that a concrete without entrained air which freezes in pure water shows no appreciable loss of strength. In contrast, if salt is present in freezing medium, strength degradation of up to 50 per cent can occur very quickly.

RÉSUMÉ

Des carottes de béton prélevées par forage ont été soumises à des contraintes dues au gel et dégel, puis à des contraintes physiques, sous forme d'essais de fatigue ou statiques, l'objet étant d'étudier l'influence combinée de ces facteurs de décomposition sur la résistance du matériau. Ces essais on montré qu'un béton sans adjonction d'air, qui gèle dans de l'eau pure, ne perd que très peu de sa résistance. Par contre, si le liquide contient du sel, on note une dégradation rapide de la résistance.

ZUSAMMENFASSUNG

Es wurden Versuche an Betonbohrkernen durchgeführt, welche nach einer umweltmässigen Beanspruchung in Form von Einfrieren/Auftauen einer funktionsbedingten Beanpruchung (Ermüdungs- oder Bruchbeanspruchung) ausgesetzt wurden. Ziel war, die kombinierte Einwirkung dieser Zerstörungsfaktoren auf die Festigkeit des Betons zu untersuchen. Die Ergebnisse zeigen, dass die Festigkeit von in sauberem Wasser eingefrorenem Beton ohne Luftzusatz kaum nennenswert nachlässt. In einem Medium mit Salz hingegen kann sich die Festigkeit sehr schnell um bis zu 50% verschlechtern.

1. BACKGROUND

In the survey by Ingvarsson & Westerberg [1], it emerged that the interaction between environmentally and functionally caused deterioration was a subject on which research was considered a matter of importance. In the first instance, this concerned the problem area of fatiguing of salt- and frost-damaged concrete and fatiguing of concrete with embedded, corroded reinforcement steel. As a continuation, tests on the strength and fatigue properties of freeze-thaw deteriorated concrete have been carried out on behalf of the Swedish National Road Administration and the Swedish Transport Research Board. These tests are reported below.

2. TESTS

2.1 Test specimens

The purpose of the tests was to reflect the combined effect of environmentally caused and functionally caused degradation factors and how this effect varies with different concrete mixes. To this end, tests were carried out according to Fig. 1 in three subseries. These were:

I W/C = 0.60, without air entrainment
II W/C = 0.50, without air entrainment
III W/C = 0.50, with approx. 8 % entrained air

In all cases, use was made of pure standard Portland cement and an aggregate with a maximum size of 16 mm. The weight ratio cement:gravel:stone was 1:3.5:1.4 in series I, 1:2.3:1.7 in series II and 1:2.1:1.6 in series III.

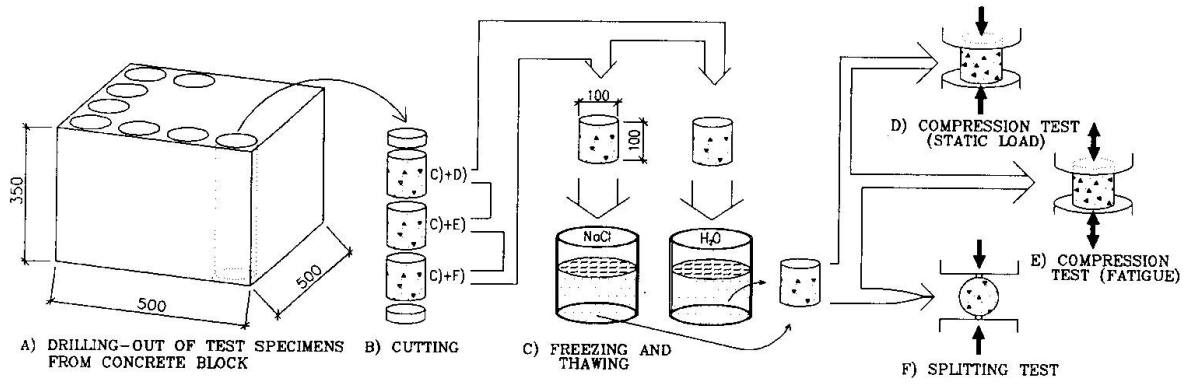

Fig. 1: Test procedure

Cores with a diameter of 100 mm were drilled out of specially cast concrete blocks. The cores were cut into three cylinders with lengths of 100 mm, see Fig. 1:A and 1:B. Each subseries comprised 54 concrete cylinders.

2.2 Environmental load

Half the number of cylinders were frozen in water and half the number in a 3 per cent sodium chloride (NaCl) solution. The 54 cylinders were divided into 9 groups exposed to 0, 7, 14, 28 or 56 freeze-thaw cycles, with or without NaCl in the freezing medium, see Fig. 1:C. After

being cast the cylinders were kept continuously moist, until freeze-loading.

2.3 Functional load

After being subjected to freezing and thawing, the strengths and fatigue properties of the concrete cylinders were tested by means of a static load test until failure in compression (Fig. 1:D), a fatigue test (Fig. 1:E) and a splitting test (Fig. 1:F).

3. TEST RESULTS

3.1 Static load tests

3.1.1 Compressive strength

The static load tests to compression failure were conducted with a constant velocity of 5 μm/sec. The results from these tests formed the basis for the load levels used in the fatigue tests, see Section 3.2 below. The ultimate stresses measured in the static load tests are shown in Fig. 2.

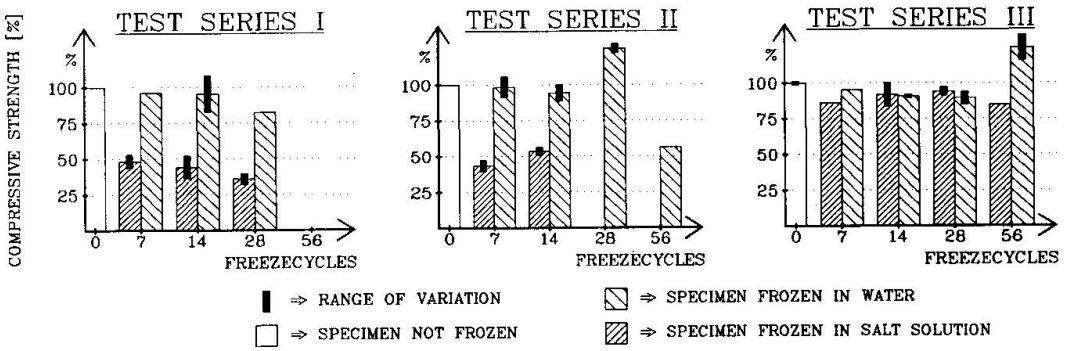

Fig. 2: Results of static compressive strength tests

The measured ultimate compressive strengths of the cylinders are shown in Fig. 2 for the different subseries I, II and III. The results are presented as mean values for each group. The columns are grouped two by two according to the number of freeze cycles. The left-hand columns show the values for the NaCl-frozen cylinders and the right-hand columns those of the water-frozen cylinders. The thick line at the top shows the range of variation for the compressive strength of all cylinders in the group. In some freeze groups one or both columns are missing, the reason being that the specimens did not withstand the freeze-thaw cycles. Cylinders which had passed the fatigue test without rupturing and then were loaded statically to failure are not included in the results shown in Fig. 2.

It is evident from the results that the ultimate compressive strength rapidly decreases on freezing in NaCl solution, if the concrete does not contain an air-entraining admixture. From series I and II it can be concluded that the ultimate strength has fallen to approx. 50 per cent of the original value. On the other hand, the ultimate strength is very good in series III where entrained air was added to the concrete. Measured strengths and deformations also indicated that the moduli of elasticity decreased upon freezing in both water and salt solution. This was valid for all subseries I, II and III.

An interesting observation that can be made is that those strength values which have decreased

at only seven freeze cycles tend to become stabilized at this level, or occasionally even to increase slightly again. See Fig. 2.

3.1.2 Splitting strength

It is evident from the results of splitting tests, as presented in Fig. 3, that the tensile strength of the concrete, as well as its compressive strength, is considerable decreased when the concrete freezes in the presence of NaCl. This applies, according to Fig. 3, in the first instance to subseries I and II where the concrete did not contain entrained air. The results from subseries III instead indicates an increasing splitting strength, probably due to deviations in the concrete itself. Also in series III the strengths of the NaCl-frozen cylinders are slightly inferior.

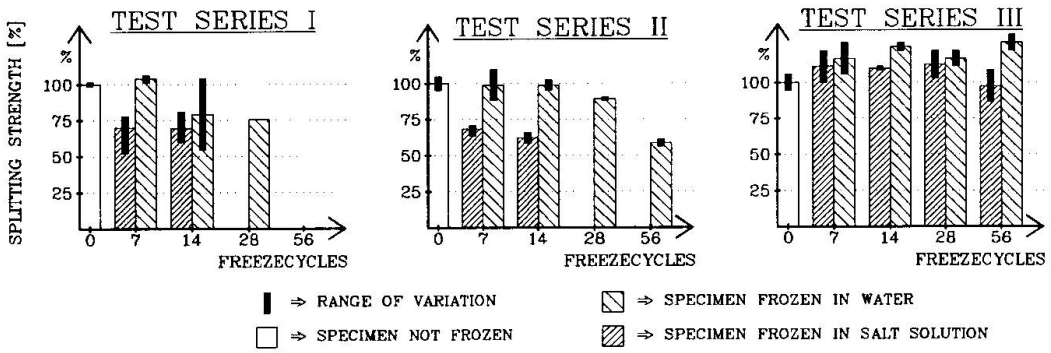

Fig. 3: Results of splitting tests. Designation as per Fig. 2

3.2 Fatigue test

The fatigue tests were performed with a compressive load frequency of 7 Hz at night and 15 Hz during the day. The fatigue test results observed are presented in Fig. 4.

In Fig. 4, σ is used for the maximum stress to which the cylinder was exposed in each load cycle, while f_u designate the ultimate compressive stress measured at the static load tests, see section 3.1.1 above. In each load cycle, the load was varied between 0 and σ. In the diagrams of Fig. 4, the Wöhler curve according to Bennet & Muir [2] is shown in order to make a comparison possible. From this it can be concluded that the fatigue properties of the concrete are affected by freezing and thawing irrespective of whether the freezing medium was provided with NaCl or not. This conclusion is valid for concrete without air entrainment only. With respect to fatigue, concrete cylinders with air entrainment, series III, were not affected at all. These results are somewhat confusing, as they do not correspond to those obtained by Antrim & Mc Laughlin [3]. In this reference concrete cylinders both with and without entrained air are subjected to fatigue. No significant differences in fatigue resistance were detected.

For the cylinders which had not ruptured at $2 \cdot 10^6$ load cycles, the tests were discontinued. Insted these cylinders, which are not included in Fig. 4, were loaded to either static compressive or splitting failure. These cylinders normally showed a higher compressive and lower splitting strength than those not fatigue tested. This tendency however, was not discernible throughout. An explanation may be that these cylinders did not rupture by fatigue due to their high compressive strength. On the contrary, internal cracking due to the fatigue load caused a decrease in splitting strength, i.e. tensile strength.

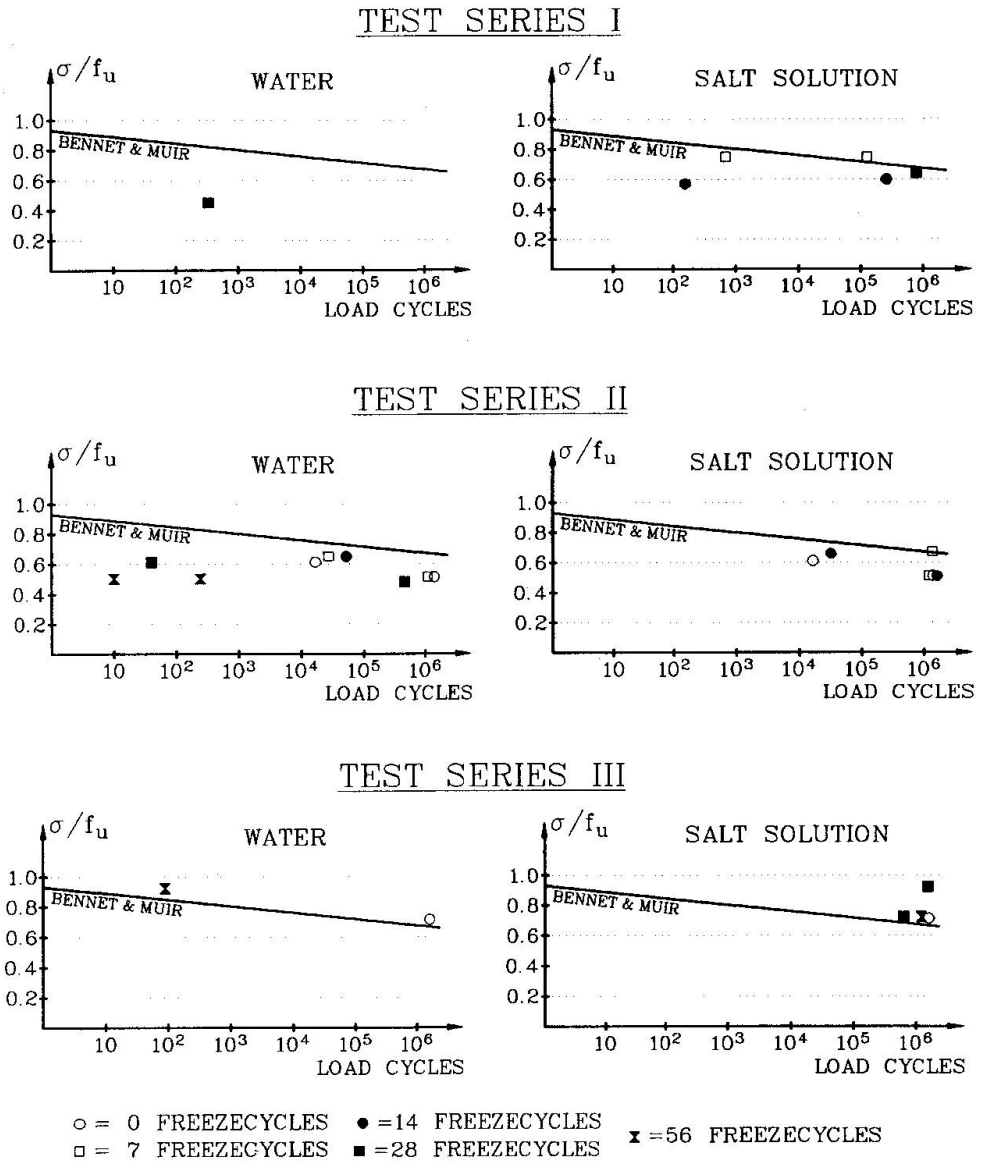

Fig. 4: Results of fatigue tests, series I, II and III

4. CONCLUSIONS

The conclusions from the tests can be summarized as follows:

1. Concrete which freezes in pure water retains its strength properties well.
2. Concrete which freezes in the presence of NaCl very quickly loses its strength properties, unless air is entrained. The strength properties which decrease directly upon freezing in salt solution tend to become stabilized after a small number of freeze cycles.
3. Concrete which freezes in pure water or in salt solution loses some of its fatigue resistance. However, if air is entrained the resistance retains.

Older concrete structures which have regularly been exposed to de-icing salts or seawater may now have deteriorated, resulting in a considerably inferior concrete strength and decreased fatigue resistance. In determining the load-carrying capacity of older structures it is therefore essential to drill cores and to examine the strength and fatigue properties of these. It is thus a doubtful procedure to recalculate older structures in accordance with new codes on the basis of the strength which the concrete had when the structure was built, taking for granted that this strength is retained.

5. FUTURE WORK

In addition to the test series described above, the interaction between functionally and environmentally caused load impacts will be studied. The planned work will embrace both mild (non-tensioned) reinforced concrete beams and prestressed concrete beams. The beams will be exposed either to freeze-thaw cycles or to corrosion of the reinforcement. This will be accomplished by giving the reinforcement a positive electric potential in relation to the concrete. By this means, chlorides will be led in towards the reinforcement and the reinforcement will corrode. When the beams have been exposed to this environmental load, they will be subjected to a functional load in the form of a static load test to failure or a fatigue test.

6. REFERENCES

1. INGVARSSON H., WESTERBERG B., 1986, Operation and maintenance of bridges and other bearing structures, Publ. No. 42 from the Swedish Transport Research Board, Stockholm, Sweden, ISSN 0282-8022.
2. BENNET E. W., MUIR S. E. St J., 1967, Some fatigue tests of high-strength concrete in axial compression, Magazine of concrete research, Vol. 19, No 59, pp 113-117.
3. ANTRIM, J. C. and Mc LAUGHLIN, J. F., 1959, Fatigue study of air-entrained concrete. ACI Journal, May, pp 1173-1182.

Crack Widths and Deformation Behavior of Reinforced Concrete Structures

Largeur de fissures et comportement en déformation de structures en béton armé

Rissbreiten und Verformungsverhalten von Stahlbetontragwerken

Gerd GÜNTHER
Gesamthochschule Kassel
Fachgebiet Massivbau
Kassel, Fed. Rep. of Germany

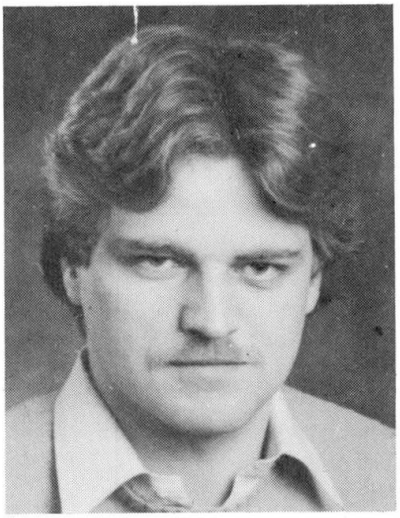

Gerd Günther, born in 1957, 1985 Dipl.-Ing., University of Kassel since 1985 Assistant in the Division of Reinforced Concrete of the University of Kassel.

Gerhard MEHLHORN
Gesamthochschule Kassel
Fachgebiet Massivbau
Kassel, Fed. Rep. of Germany

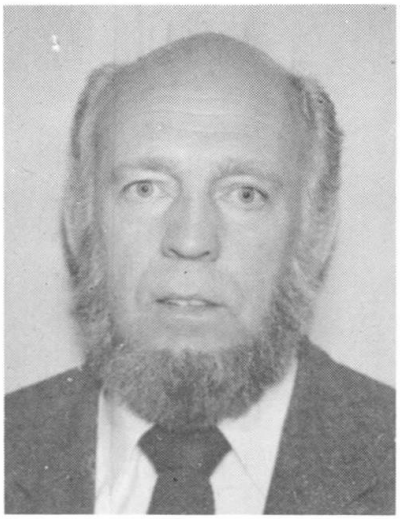

Gerhard Mehlhorn, born in 1932, apprenticeship as steel construction worker, 1959 Dipl.-Ing., TH Dresden, 1959-1965 Design Engineer, 1965-1983 TH Darmstadt, Dr.-Ing. 1970, since 1972 Professor of Civil Engineering, 1982 Visiting Professor University of Toronto, since 1983 Professor of Civil Engineering at University of Kassel, since 1984 also Consulting Engineer at Kassel (until 1984 at Darmstadt).

SUMMARY

In this contribution the results of tests are shown. With the tests the increase of crack widths and deformations in dependence on load duration and number of load cycles was investigated. Especially considered are the consequences of the initial stress state caused by shrinkage on the crack width development. Besides simple tension and bending tests biaxial compression-tension tests were also carried out on reinforced concrete panels.

RÉSUMÉ

Gracê à des essais, l'augmentation des largeurs de fissures et des déformations dépendant de la durée et de la valeur de la charge devait être clarifiée. Les conséquences de l'état d'auto-contraintes créé par le retrait sur l'évolution des largeurs de fissures sont prises en considération. Outre les essais de traction et de flexion, des essais biaxiaux compression-traction on été réalisés.

ZUSAMMENFASSUNG

Mit Versuchen sollte geklärt werden, wie gross die Verformungs- und Rissbreitenzunahmen in Abhängigkeit von der Belastungsdauer und der Anzahl der Lastwiederholungen sind. Die Auswirkungen des durch Schwinden verursachten Eigenspannungszustandes auf die Rissbreitenentwicklung wurden besonders berücksichtigt. Neben den reinen Zug- und Biegeversuchen wurden auch biaxiale Druck-Zugversuche an Stahlbetonscheiben durchgeführt.

1. INTRODUCTION

The durability of reinforced concrete structures mainly depends on crack widths and deformations. The protection against corrosion of the reinforcement is lost when crack widths are large and the stability is endangered. With too large deformation increases owing to long-term loads considerable usage restrictions of the building may result. In this contribution the results of about 120 tests on crack spacing, crack widths, and deformation behavior of reinforced concrete structures under monotonically increasing, cyclic, and long-term loads are presented.

2. CRACK SPACINGS

The average and maximum crack spacings of the reinforced concrete panels [1, 2], the centrically and eccentrically reinforced tension specimens [3, 4, 5], and the reinforced concrete beams [6] are presented in table 1. A dependence of the crack spacing on the concrete compressive strength and on the related rib area was not observed.

Owing to repeated loads and permanent loads no new cracks occured (not considering a few exceptions) with constant top load. As a result of unintentional eccentricities with the regularly and centrically reinforced tension specimens the cracks separated the concrete only partially at initial loading. Thus, the cracks still developed with repeated and permanent loads.

The crack development which occured with the eccentrically reinforced tension specimens (see Fig. 3) and the reinforced concrete beams are to be traced back to the decrease of concrete tensile strength owing to repeated loads.

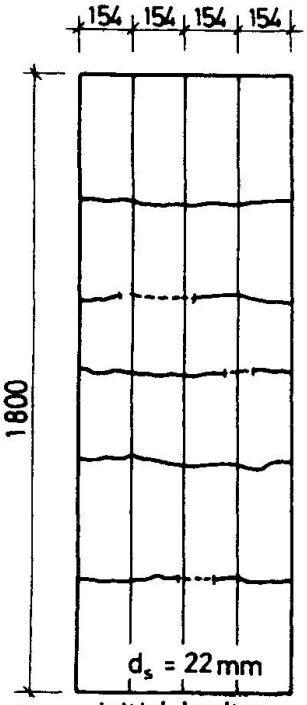

——— initial loading
----- as a result of repeated loads

Fig. 1 Crack pattern of intended centrically reinforced specimen S 22

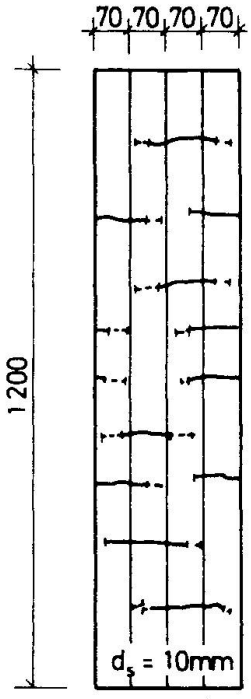

——— initial loading
----- after permanent load of 144 days

Fig. 2 Crack pattern of intended centrically reinforced specimen DAUER 4

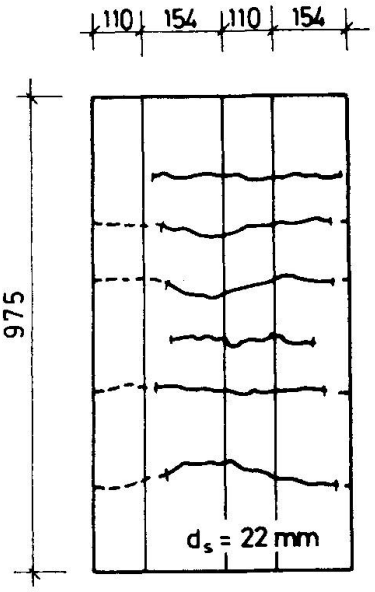

——— initial loading
----- as a result of repeated loads

Fig. 3 Crack pattern of eccentrically reinforced specimen E 11

In the crack patterns of the reinforced concrete panels [2] without transverse compression (see Fig. 4) and with 0,6 β_c transverse compression (see Fig. 5) no dependence of the amount of cracks on transverse compression can be seen.

Specimen		d_s [mm]	ü [mm]	s [mm]	reinforcement	number of specimens	crack spacing [mm] a_m	crack spacing [mm] a_{max}	calculated average crack spacing [mm] $a_m = 2\,(ü + 0{,}1 \cdot s) + 0{,}1\,\frac{d_s}{\mu}$	calculated average crack spacing [mm] $1{,}7 \cdot a_m$
reinforced concrete panels	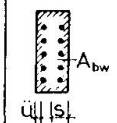	10x8,S	10	50	ribbed bars with transverse reinforcement	2	134	185	105	178
					ribbed bars	5	136	200		
					ribbed mats	2	107	150		
		10x5,5	11	50	ribbed bars with transverse reinforcement	2	126	200	147	249
					ribbed bars	2	103	200		
					ribbed mats	1	102	125		
	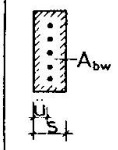	5x16,0	42	100	ribbed bars	2	140	250	183	311
centrically reinforced tension specimens	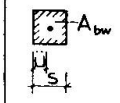	1x10,0	30	70	ribbed bars	10	128	210	135	230
		1x10,0	40	90		2	127	220	200	340
		1x16,0	32	80		3	115	160	131	223
		1x16,0	48	112		2	183	240	219	372
		1x16,0	64	144		2	333	390	322	547
		1x22,0	44	110		20	174	310	180	306
		1x22,0	66	154		27	290	450	300	511
		1x22,0	88	198		16	359	630	442	752
		1x28,0	56	140		2	200	300	229	390
		1x28,0	84	196		2	333	450	382	650
		1x28,0	112	252		2	417	530	563	957
excentrically reinforced tension specimens	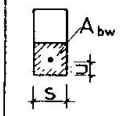	1x22,0	44	110	ribbed bars	8	156	280	180	306
		1x22,0	66	154		4	285	425	300	511
reinforced concrete beams	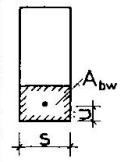	1x22,0	44	150	ribbed bars	3	244	300	214	363
	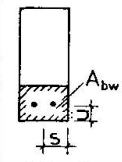	2x22,0	44	75	ribbed bars	2	162	250	151	256
	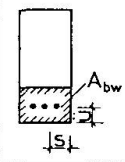	3x22,0	44	54	ribbed bars	2	113	185	131	223

Tab. 1 Crack Spacings

In accordance with the approach in the CEB/FIP requirements [7] for the calculation of the average crack spacing a_m the following equation resulted for ribbed bars and mats:

$$a_m = 2\,(ü + k \cdot s) + 0{,}1\,\frac{d_s}{\mu}\,; \qquad k = 0{,}1 \text{ for ribbed bars}$$

This yields a satisfactory agreement with the experimentally determined crack spacings (see table 1) for design of buildings. The effective zone of the reinforcement was established as in Fig. 6 according to Gergely and Lutz [8] as with the eccentrically reinforced tension specimens no dependence of the crack spacing on the height of the specimen was stated.

Furthermore a differentiation between tensile and flexural load could be neglected with respect to the CEB/FIP requirements so that it can generally be calculated with k = 0,1 for ribbed bars. The average crack spacings multiplied by 1.7 are in approximate accordance with the largest crack spacings of the experiment (see table 1).

With smooth mats the bond strength is generally transferred by the transverse reinforcement only. Cracks always form at the transverse reinforcement because of the smaller concrete cross section in this area. Forces can be transferred into the concrete until only two transverse reinforcement bars are left between two cracks. Thus the maximum crack spacing corresponds to the double spacing of transverse reinforcement. With this spacing only one transverse reinforcement bar is left between two cracks and no more forces can be introduced into the concrete.

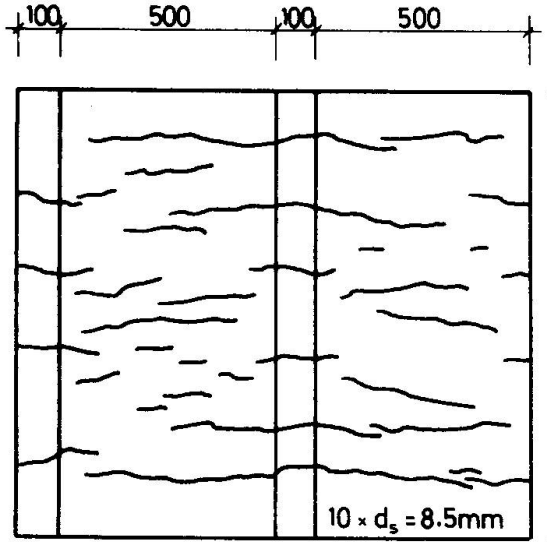

Fig. 4 Crack pattern of reinforced concrete panel B 19 (Q = 0)

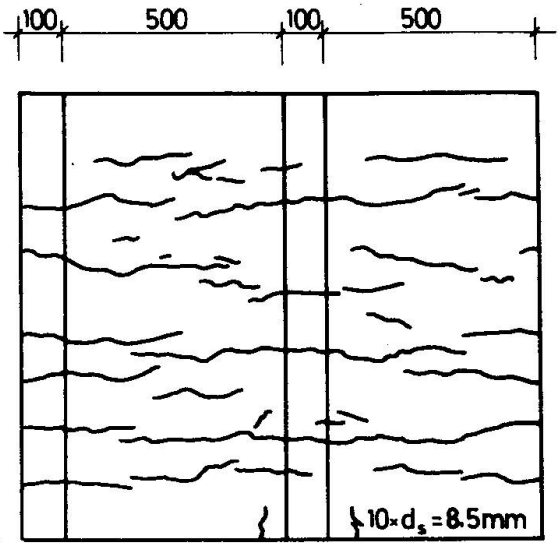

Fig. 5 Crack pattern of reinforced concrete panel B 11 (Q = 0,6 β_c)

3. CRACK SPACINGS

It was shown in [4] that the deformations of a reinforced concrete specimen mainly occur in the cracks and that the average crack w_m widths can be calculated with the equation stated in [7]:

$$w_m = \varepsilon_m \cdot a_m. \tag{2}$$

The maximum crack width results in approximately:

$$w_{max} = 1{,}7 \cdot w_m. \tag{3}$$

4. DEFORMATION BEHAVIOR OF CENTRICALLY AND ECCENTRICALLY REINFORCED TENSION SPECIMENS

The principal correlations between average strain over the cracks and external load related to the steel cross sectional area resulting from monotonically increasing and cyclic loading are shown in Fig. 7.

In order to describe the stress-strain behavior of centrically reinforced concrete specimens loaded in tension neglecting shrinkage of concrete the following idealization for initial loading.

$$\varepsilon_m = \frac{\sigma_s}{E_s} \sqrt{1 - \left(\frac{\sigma_s^1}{\sigma_s}\right)^2} \tag{4}$$

yielded a good agreement. This idealization is also valid for reinforced concrete panels under transverse load and for eccentrically reinforced tension specimens, if the effective concrete cross section according to Fig. 6 and the centrical concrete tensile strength are taken as a basis for the determination of the steel stress σ^1_s. The largest average strain at top load which stabilizes after a certain number of repeated lods can be approximately recorded with:

$$\varepsilon^o_{m,max} = \frac{\sigma^o_s}{E_s}\sqrt{1 - \left(\frac{\sigma^1_s}{\sigma^o_s}\right)^S} \quad (5)$$

At complete unloading a residual strain of about

$$\varepsilon_r = 0{,}2 \cdot 10^{-3} \quad (6)$$

remains in the specimen. This is independent of the number of load cycles.

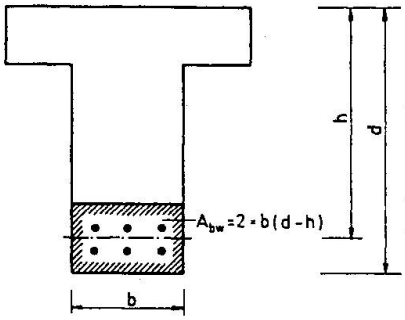

Fig. 6 Effective zone of reinforcement (acc. to [8])

It was stated with all tests that after approximately 5000 load cycles or after a 6-months permanent load no considerable deformation increases occured.

The initial stress state caused by shrinkage results, related to the load beginning, in larger average strains compared with the specimens without shrinkage. The stress-strain behavior of specimen S07 shown in Fig. 8 makes clear that the average strains can exceed those of the pure steel.

In case the shrinkage influence is considered for the determination of the steel stress in the cracked cross section directly after the first crack, the average strain related to the initial load can also be calculated according to Eq. (4) using $\sigma^1_{s,schw}$

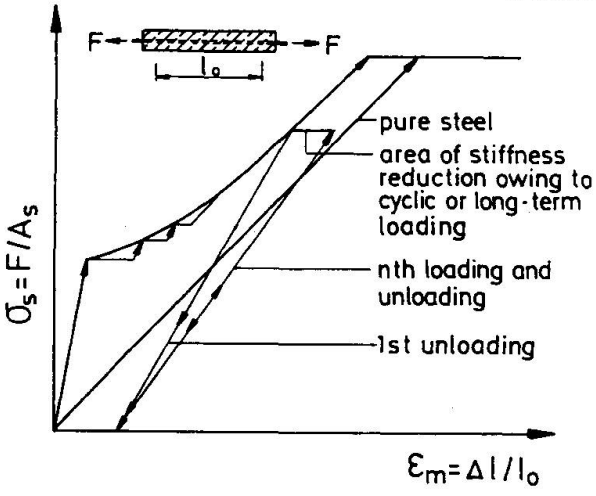

Fig. 7 Stress-strain relationships for axially loaded reinforced concrete

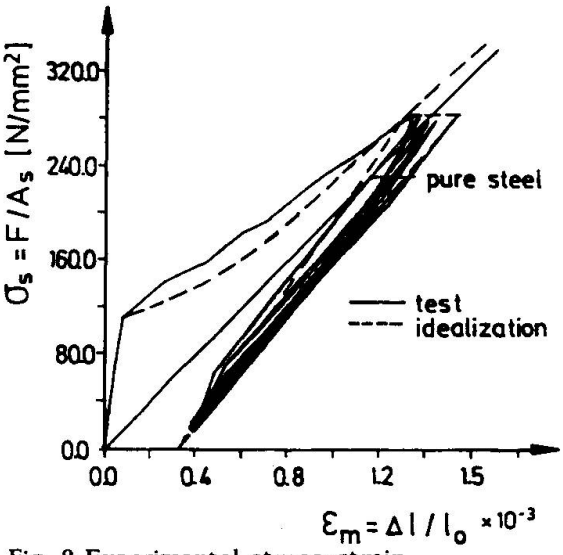

Fig. 8 Experimental stress-strain relationships of specimen S07 under shrinkage and idealization

$$\varepsilon_m = \frac{\sigma_s}{E_s}\sqrt{1 - \left(\frac{\sigma^1_{s,schw}}{\sigma_s}\right)^2} \quad (7)$$

The largest average strain increase at top load which stabilizes after a certain number of load cycles results to approximately

$$\Delta\varepsilon^o_{m,schw} = \frac{\sigma^o_s}{E_s}\left[\sqrt{1 - \left(\frac{\sigma^1_s}{\sigma^o_s}\right)^S} - \sqrt{1 - \left(\frac{\sigma^1_s}{\sigma^o_s}\right)^2}\right] \quad (8)$$

as with specimens without shrinkage.

At complete unloading of the specimens a residual strain of

$$\varepsilon_r = 0{,}2 \cdot 10^{-3} + \varepsilon_m^o + \Delta\varepsilon_{m,schw}^o - \varepsilon_s^o \quad (9)$$

is left.

5. NOTATIONS

b	= width
d	= total height
h	= height from center of gravity of tension reinforcement to compression edge
d_s	= diameter of reinforcement bar
$\ddot{u}$	= smallest concrete cover of reinforcement at pure tension = distance between bottom side of reinforcement bar and tension edge at eccentric tension and flexion
s	= distance of reinforcement bar (see table 1)
A_s	= steel cross sectional area
A_{bw}	= effective concrete cross section (see Fig. 6)
$A_{b,n}$	= area of concrete (net)
μ	$= \frac{A_s}{A_{bw}}$
F	= force
E_s	= modulus of elasticity of steel
β_c	= cylinder crushing strength
σ_s	= steel stress
Q	= lateral pressure
σ_s^1	= steel stress in concrete cross sectional area directly after first crack
σ_s^o	= maximum steel stress at cyclic or long-term loading
$\sigma_{s,schw}^1$	= steel stress in crack cross sectional area directly after the first crack considering shrinkage influence
ε_s^o	= steel strains at top load
ε_m	= average strain
ε_m^o	= average strain at top load
$\varepsilon_{m,max}^o$	= largest average strain owing to cyclic or long-term loading
ε_r	= residual strain in specimen after unloading
$\Delta\varepsilon_{m,schw}^o$	= strain increase owing to repeated loads at top load considering shrinkage influence
a	= average crack spacing
a_{max}	= maximum crack spacing
w_m	= average crack width
w_{max}	= maximum crack width

References

[1] KOLLEGGER, JOHANN; GÜNTHER, GERD; MEHLHORN, GERHARD: Zug- und Zug-Druckversuche an Stahlbetonscheiben. Forschungsbericht Nr. 1 aus dem Fachgebiet Massivbau, Gesamthochschule Kassel, 1986. *

[2] GÜNTHER, GERD; MEHLHORN, GERHARD: Versuche an Beton- und Stahlbetonscheiben unter ein- und zweiaxialer Beanspruchung. Forschungsbericht Nr. 9 aus dem Fachgebiet Massivbau, Gesamthochschule Kassel, erscheint 1989.*

[3] GÜNTHER, GERD; MEHLHORN, GERHARD: Untersuchungen zur Mitwirkung des Betons zwischen den Rissen für monoton steigende und schwellende Belastung. Forschungsbericht Nr. 3 aus dem Fachgebiet Massivbau, Gesamthochschule Kassel, 1987. *

[4] GÜNTHER, GERD; MEHLHORN, GERHARD: Beeinflussung des Spannungs-Dehnungs-Verhaltens von Stahlbetonzugkörpern durch die Art der Rißöffnung und den durch Schwinden verursachten Eigenspannungszustand. Forschungsbericht Nr. 8 aus dem Fachgebiet Massivbau, Gesamthochschule Kassel, 1989. *

[5] GÜNTHER, GERD; MEHLHORN, GERHARD: Langzeitverformungsverhalten von Stahlbetonkörpern. Forschungsbericht Nr. 8 aus dem Fachgebiet Massivbau, Gesamthochschule Kassel, 1989. *

[6] GÜNTHER, GERD; MEHLHORN, GERHARD: Verformungsverhalten von Stahlbetonbalken unter wiederholter Belastung. Forschungsbericht Nr. 5 aus dem Fachgebiet Massivbau, Gesamthochschule Kassel, 1988. *

[7] CEB/FIP-Mustervorschrift für Tragwerke aus Stahlbeton und Spannbeton. Deutscher Ausschuß für Stahlbeton, 1978.

[8] GERGELY, PETER; LUTZ, L.A.: Maximum Crack Width in Reinforced Concrete Flexural Members. In: Causes, Mechanics and Control of Cracking in Concrete, SP-20, American Concrete Institute, Detroit, 1968, S. 87-117.

* Summary, notations, and legends to pictures both in German and in English.

A 12 Year Case Study of a Reinforced Concrete Building

Une étude de cas d'une durée de 12 ans concernant un bâtiment en béton armé

Eine 12 Jahre umfassende Fallstudie eines Stahlbetongebäudes

Leslie PARROTT
Research Engineer
British Cement Assoc.
Slough, UK

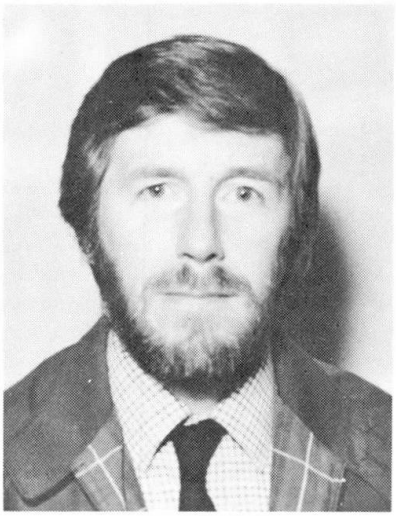

Leslie Parrott received his Bachelor and Doctor degrees in civil engineering from London University. His research on various aspects of concrete performance, including internal moisture, deformation properties, carbonation, durability and high strength, has resulted in about 80 published papers.

SUMMARY

Shrinkage and stress-induced strains in a two-storey office building were measured using vibrating wire gauges embedded in the roof and intermediate floor. The floor dried more quickly than the roof. This contributed to tensile stresses in the floor, differential movements and associated cracking of glazed panels and internal block wall. The bituminous membrane on the flat roof deteriorated after 7 years and water leaked through the carbonated concrete roof slab. This case study shows that service behaviour is greatly affected by concrete moisture conditions.

RÉSUMÉ

Le retrait et les déformations dues aux contraintes dans un bâtiment à deux étages ont été mesurés à l'aide de jauges à fils vibrants noyées dans le toit et le plancher intermédiaire. Le plancher a séché plus rapidement que le toit. Cela a entrainé des efforts de traction dans le plancher, des déplacements différentiels et une fissuration du vitrage et du mur interne en parpaing. La membrane bitumineuse du toit plat a été détériorée après 7 ans et l'eau s'est infiltrée à travers les dalles de toiture en béton carbonaté. Cette étude de cas montre que l'entretien ets largement affecté par les conditions d'humidité du béton.

ZUSAMMENFASSUNG

Mit Hilfe vibrierender, im Dach und in der Gebäudedecke eingebetteter Messstreifen wurden Schwinden und durch Beanspruchung verursachte Verformung in einem zweistöckigen Bürogebäude gemessen. Die Decke trocknete schneller als das Dach. Dies trug zu Zugspannungen in der Decke, Differentialbewegungen und damit verbundenem Platzen von Glasfassadenplatten und innerer Blockwand bei. Die bituminöse Schicht auf dem Flachdach war nach 7 Jahren schadhaft und Wasser drang durch die karbonisierte Betondachplatte. Diese Fallstudie zeigt, dass die Haltbarkeit in starkem Masse von den Feuchtigkeitsbedingungen des Betons beeinflusst wird.

1. INTRODUCTION

Investigations of in-situ movements in concrete structures were initiated by the British Cement Association in the mid-1970's as part of a programme on the prediction of concrete deformation properties. The reported investigation of a two-storey office building has been continued because it is providing valuable information relating to long-term moisture conditions, carbonation and durability in reinforced concrete.

2. DESCRIPTION OF BUILDING

A diagram of the two-storey office building is shown in Figure 1. There are twelve bays each 5.4m long with a stairway at the ninth bay providing some longitudinal restraint. The 4.4m wide offices are accessed by 1.3m wide corridors on the ground and first floors. The longer portion of the building between the stairway and an old stone tower can move longitudinally by virtue of a movement joint at the interface of the tower and office corridors. At this interface and for one bay the width of the structure is reduced to that of the corridor and the walls are fully glazed. The continuous floor and roof slabs were cast in-situ on precast concrete cross beams that were supported by a frame of precast columns and longitudinal beams.

The in-situ and precast concretes were made with lightweight coarse aggregate and a natural sand. 100mm cube strengths at 7, 28 and 182 days were 35.9, 42.4 and 55.0 MPa respectively. The mix constituents per cubic metre were 170kg free water, 350kg Portland cement, 730kg zone 2 sea dredged sand and 600 kg of lightweight aggregate plus about 100kg of absorbed water.

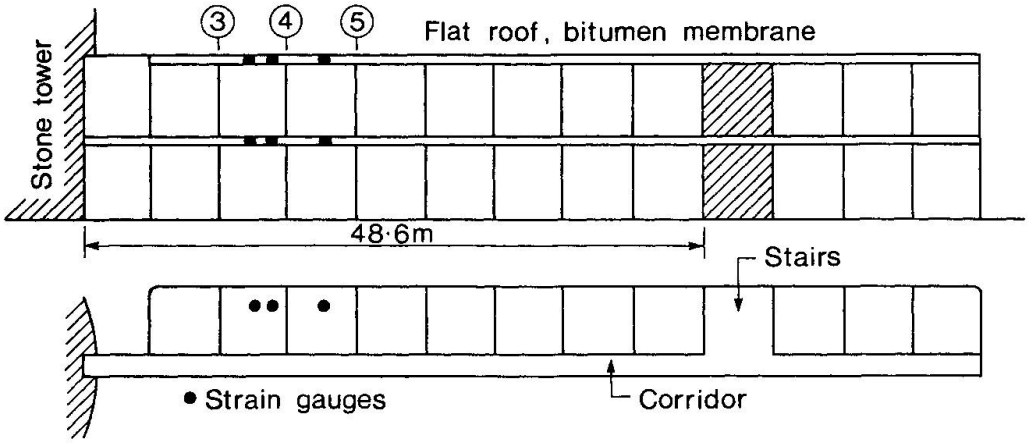

Fig. 1 Elevation and plan of two-storey office structure

3. MEASUREMENT METHODS

The 165mm deep floor and roof slabs in bays 3-4 and 4-5 were instrumented at mid-span with embedded vibrating wire strain gauges set at three depths above the neutral axis. Bays 3-4 of the floor and roof were also instrumented near the neutral axis at quarter-span (i.e. where stresses were expected to be small). The strain gauges were installed horizontally in orthogonal pairs with the longitudinal gauge parallel to the length of the building. This

arrangement of gauges permits separate calculation of shrinkage and stress-induced strains [1].

A small correction was made (2.5 microstrain/^{o}C) to allow for the difference in thermal expansion of the concrete and the steel wire in the strain gauge and was based upon in-situ temperature measurements. The shrinkage and stress-induced strains (Esh and Est) were calculated from the longitudinal and transverse strains (El and Et) using the relations Est = (El - Et)/1.18 and Esh = El - Est. The factor 1.18 derives from the assumption that Poisson's Ratio is 0.18 for short and long-term loading [1]. Contraction and extension are regarded as positive and negative strains, respectively.

Prisms measuring 100 x 100 x 290mm were cast from the in-situ concrete for various site and laboratory tests.

4. RESULTS AND DISCUSSION

4.1 Concrete prisms and measured strains

Six prisms were stored beneath the roof for long-term measurements of shrinkage and weight loss. The shrinkage results in Figure 2 suggest that approximate moisture equilibrium was reached after about 3 years and this was consistent with the weight loss measurements: thereafter the small increase in shrinkage was accompanied by a slight gain of weight that was indicative of carbonation [2].

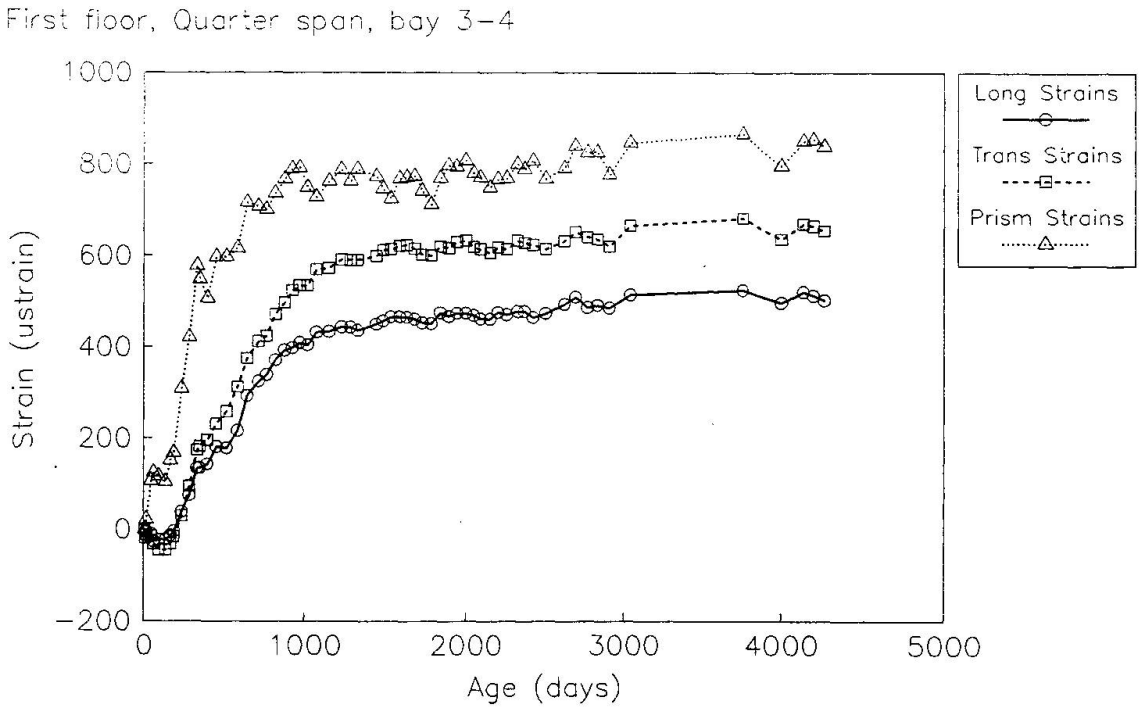

Fig. 2 Strains in prisms; longitudinal and transverse strains at quarter span, bay 3-4 in floor.

Figure 2 shows that initially longitudinal strains are slightly larger than transverse strains at quarter-span in the floor. This is consistent with the expected, small flexural stresses. After about 250 days the transverse strains exceed the longitudinal strains and this indicates that axial tensile stresses develop at later ages. Similar patterns of transverse and longitudinal strain were observed at mid-span in bays 3-4 and 4-5 of the floor.

4.2 Shrinkage and stress-induced strains

The calculated strains for bay 4-5 of the floor slab are shown in Figure 3. There were only small differences in shrinkage between the three instrumented sections. The shrinkage of the floor slab developed more slowly than the prism shrinkage (Fig 2) and appears to be stabilizing at a smaller, final strain. These effects are attributable to differences in drying path length [3]. The stress-induced strains exhibit the expected pattern for flexural loading but they are superposed by the development of tensile strains.

The calculated strains for the roof slab in Figure 3 show that shrinkage developed more slowly than that in the floor. Although the roof slab was similar in thickness to the floor slab drying was retarded by the waterproof layer on its upper surface. The stress-induced strains exhibit the expected pattern for flexural loading but they are superposed by the slow development of small tensile strains. The tensile strains in the roof develop more slowly than those in the floor.

The strain patterns in Figure 3 suggest that longitudinal drying shrinkages of the floor and, to a lesser extent, the roof are restrained and thus cause the development of longitudinal tensile stresses. This is consistent with the similarity in shape and period of occurrence of the shrinkage versus age and stress-induced strain versus age curves. Restraint may have derived from the columns, longitudinal beams, internal block walls and the foundation.

4.3 Movement and cracking

Qualitative corroboration of the more rapid drying shrinkage of the floor compared with the roof and foundation was provided by visible movement between the building and the adjacent stone tower. Furthermore, several glazed panels in the corridor next to the tower cracked at an age of about 5 years due to the shearing action of the floor movement. Cracking of internal block walls provided additional evidence of the relative movement of the floor. The replacement glazing has not shown any sign of distress. A mastic-filled joint was provided between the block wall and the structural components of the building: this has prevented any further cracking of the walls.

4.4 Roof leakage and carbonation

Solar radiation caused local expansion and deterioration of the bituminous roof membrane after 7 years, in spite of a surface layer of white, reflective stone chippings. Consequently the central drainage gully did not function properly and after rainfall it acted as a reservoir for water leaking through the roof slab. Continued deterioration of the roof membrane and leakage of water over a period of five years caused damage to internal finishes and raised the question of reinforcement corrosion. Measurements on a prism stored beneath the roof suggested that the roof slab may be carbonated to a

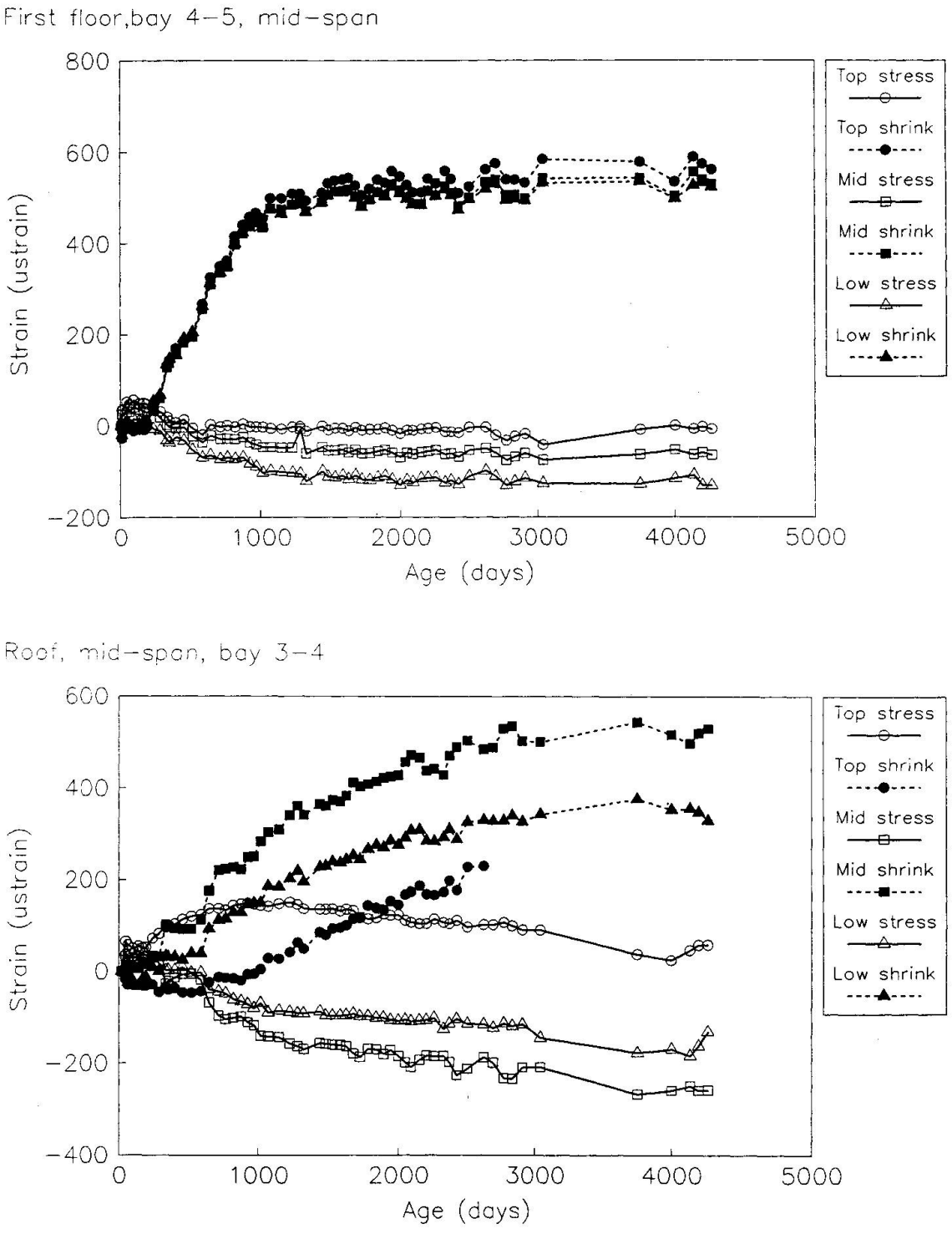

Fig. 3 Shrinkage and stress-induced strains in floor(upper) and roof(lower).

depth of 12mm (standard deviation = 3mm). The specified depth of cover was 20mm and with the standard deviation typically in the range 5 to 15mm [4] there is a risk that some of the reinforcement may be corroding[2]. Further inspection for signs of corrosion is planned.

5. CONCLUSIONS

The reported long-term case study of a two-storey office building showed that moisture conditions can have an important effect upon the service performance of a concrete structure; they can affect building movements, component stresses and durability.

Restraint of drying shrinkage caused the development of an axial, tensile component of stress in the floor and, to a lesser extent, in the roof.

It seems advisable to use carbonation-resistant concrete for flat roof construction to minimise the risk of reinforcement corrosion in the event of leakage.

ACKNOWLEDGEMENT

The long-term support of this project by the British cement industry is gratefully acknowledged.

REFERENCES

1. PARROTT L., A study of some long-term strains measured in two concrete structures. Proc. RILEM Internat.Symp. on Testing in-situ of concrete structures. Budapest 1977 Vol.2, 123-139.

2. PARROTT L., A review of carbonation in reinforced concrete. Cement and Concrete Association Report C/1-0987, July 1987, 126 pages.

3. CEB-FIP., International recommendations for the design and construction of concrete structures. June 1970, 80 pages.

4. Clear C., Review of cover achieved on site. To be published.

Durability of Foundation Concrete in an Aggressive Environment

Durabilité du béton de fondation dans un environnement agressif

Dauerhaftigkeit von Betonfundationen unter aggressiven Bedingungen

D. V. MALLICK
Technical Advisor
National Consulting Bureau
Tripoli, Libya

M. M. TAWIL
Prof. of Civil Eng.
University of El Fateh
Tripoli, Libya

A. A. SHIBANI
Chairman
Nat. Consult. Bureau (NCB)
Tripoli, Libya

Prof. Mallick, born 1936, received his doctorate at Bristol University, U.K. Professor and Consultant for 13 years. Prof. Mallick, now in a consulting firm, is a technical advisor. Fellow ICE (India) and ASCE.

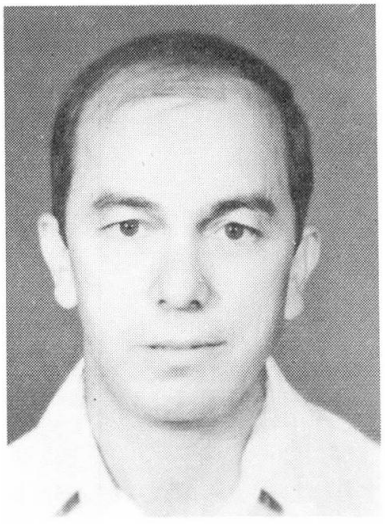

Prof. Tawil, born 1945, received his doctorate at University of Colorado, USA. Prof. Tawil is a University staff member for 13 years. He has also been a part-time technical advisor to the National Consulting Bureau, Tripoli, for the last 11 years.

Dr. Shibani, born 1944, received his doctorate at North Carolina State University, USA. Dr. Shibani, besides his duties at NCB, has been a part-time staff member in the Mechanical Eng. Dep., University of El Fateh, Tripoli for the last 13 years.

SUMMARY

A case study assessing the durability of foundation concrete in the vicinity of the sea where a number of aggressive conditions exist is presented. The use of OPC compared to SRC is preferred when sulphates and chlorides coexist due to its high resistance to chloride diffusion. Durability of foundation concrete can be enhanced by a sacrificial layer all around and applying a waterproof coating.

RÉSUMÉ

L'étude évalue la durabilité d'un béton de fondation dans des conditions extrêmes d'agressivité dues à la proximité de la mer. L'utilisation de l'OPC est préférée à celle du SRC due à sa haute résistance à la diffusion chlorique lorsque des sulphates et chlorides co-existent. La durabilité du béton de fondation peut être augmentée par une "couche de sacrifice", ainsi que par un agent imperméable appliqué sur la fondation.

ZUSAMMENFASSUNG

Vorgestellt wird eine Fallstudie zur Dauerhaftigkeit von Betonfundationen in einer Region mit aggressiven Bedingungen in Meeresnähe. Die Verwendung von OPC ist dem SRC vorzuziehen, wenn Sulfate und Chloride gleichzeitig vorkommen, da Ersterer zu einem dichteren und weniger durchlässigen Beton führt. Die Dauerhaftigkeit der Fundamente kann durch eine "Opferschicht" von mindestens 50 mm Beton und durch einen wasserdichten Anstrich verbessert werden.

1. INTRODUCTION

This study is devoted to the assessment of durability of concrete foundations of overhead transmission line towers constructed in a number of aggressive conditions commonly met in Sebkha region. Environmental aggression to foundation concrete occurs due to: (a) Aggressive compounds in the sub-soil or ground water surrounding the concrete, and (b) Effect of wetting and drying.

For foundation concrete, the effects of aggressive compounds in sub-soil and ground water are more predominant. It is well known that chemicals in the dry state will not attack concrete; this applies particularly to sulphates as these are often found in the form of lenses in soil strata. The tolerable level of sulphate concentration in relatively dry, well drained soils is about four times the acceptable limit when the sulphates are in the form of a solution in ground water. In most soils, it is the concentration of aggressive chemicals in the ground water which decides the type of cement and the quality of concrete to be used.

All portland cement concrete is prone to acid attack. Some of the chemical compounds which may be encountered in ground water of Sebkha region and which are aggressive to ordinary portland cement are described below. Further, their effects on the durability of the concrete are also presented.

2. AGGRESSIVE CHEMICAL COMPOUNDS IN SEBKHA

2.1 Sebkha

The soil in Sebkha in the vicinity of sea is generally aggressive and is very little compacted. The ground water level is very near the surface and contains aggressive chemical compounds like sulphates and chloride in solution, and acids in various proportions. In winter the lowest parts of Sebkha form shallow lakes and in summer the ground dries out and hardens. Aggressive compounds in the subsoil and ground water surrounding the foundation concrete attack it by reacting with hardened cement paste. Attack on cement can thus take place, sulphates reacting with Ca(OH)2 and with calcium aluminate hydrate. The products of the chemicals reactions gypsum and calcium sulpho aluminate, have considerable large volume than the compounds they replace, so that the reaction with the sulphate leads to expansion causing tensile stresses which finally leads to cracking of concrete.

2.2 Sulphates in Solution in Ground Water

The most commonly found sulphates in Sebkha ground water are those of calcium, magnesium and sodium. Calcium sulphate is less soluble at normal temperatures than the other sulphates mentioned above; and the solution is saturated at about 2000 mg/litre of SO3.

Sodium and Magnesium sulphates are very soluble in water and therefore their concentration can be much higher than calcium sulphate. Magnesium sulphate is more aggressive to portland cement concrete than the sulphates of sodium, calcium and pottassium, when in equal concentration. Magnesium sulphate attacks calcium silicate hydrate as well as Ca(OH)2 and calcium aluminate hydrate and, decomposes the hydrated calcium silicates.

The rate of sulphate attack increases with an increase in the strength of the solution, but beyond a concentration of about 0.5% of Mg SO4 the rate of increase in the intensity of the attack slows down. If the w/c ratio is low, the deteriorating effect of sulphate takes much longer time.

The concentration of the sulphates is expressed as the number of parts by weight of SO3 per million (ppm). Conversion of SO4 to SO3 can be made as follows:

$$SO3 = 0.83\ SO4$$

A concentration of 1000 ppm of SO3 is considered moderately severe and 2000 ppm are severe especially if Mg SO4 is the predominant constituent.

In addition to the concentration of sulphate, the speed with which the concrete is attacked depends also on the rate at which the sulphate removed by the reaction with cement can be replenished. Thus in assessing the danger of the sulphate attack the movement of ground water has to be known. Alternating saturation and drying in Sebkha leads to rapid deterioration of concrete.

2.3 Chlorides in Solution in Ground Water

Chloride is generally present in ground water as a solution of sodium chloride (common salt). The chloride solution of high concentration can attack the cement paste. Chlorides in solution react with the calcium aluminate phase in the cement to form calcium chloro aluminate, and although there is a debate as to the precise mechanism involved, it is well known that in certain circumstances where there are high concentrations of chloride expansive disruption of the concrete can occur. However, the chloride salts are highly soluble and can be leacked from the concrete preventing their concentration.

2.4 Sulphates and Chlorides in Ground Water

It is however known that in the case of sulphates co-existing with chlorides in ground water, the latter inhibits the expansion of concrete [1, 2] and the question of sulphate attack is then considered less critical and the chloride attack becomes more alarming. Chlorides in ground water of Sebkha near the sea have a tendency to combine with a part of the C3A forming a "more or less insoluble chloro aluminate" [3].

It has been a common practice and is even today to use cement with low C3A content to overcome sulphate attack in concrete exposed to sulphates either soluble in ground water or present in marine environment. Among these cements are the sulphate resisting cement (SRC) where the C3A content is limited to a maximum of 3.5% by B.S. 4627 and the ASTM Cement V in which C3A is limited to a maximum of 5%. Recent research, however, indicates that concrete made with SRC has less resistance to chloride ingress (or migration).

2.5 Acids in Ground Water

When the pH of subsoil and/or ground water is below the neutral point of 7.0 the water is then acidic and is liable to attack concrete made with any type of portland cement. The severity of the attack depends upon a number of factors. The pH value is a measure of the intensity of the acidity, and by itself does not give any indication of the type or the amount of acid present.

3. DETERIORATION OF FOUNDATION CONCRETE IN SEBKHA

Solid salts do not attack concrete, but when present in a solution they react with hardened cement paste. Disruption of concrete mass may occur by the expansive reaction of voluminous crystalline salt formations, normally caused by the ingression of chloride and sulphate solutions. Erosion of materials by dissolution of the cement mainly due to the action of acids, if present, can take place. Chemical reactions can lead to the type of damage generally known as 'Concrete Corrosion'.

Foundation concrete below or near the ground water table are affected by chemical effects accompanied with alternative cycles of drying and wetting. When the water table is high the concrete becomes saturated and when it goes down, part of the water evaporates from concrete causing salts to crystallize. A subsequent rise in water level causes the concrete to saturate again with water containing higher concentration of salts. The recurrence of such a process in course of time causes crystal growth within the pores, if the concrete is permeable, resulting in swelling action leading to cracking of concrete. There is a limit to the size of cracks allowable for various types of exposure; these limits range from 0.1 mm for very severe environment to 0.4 mm for mild environment.

Maximum precautions must be taken to ensure crack free concrete in order to stop ingression of chlorides. Steel reinforcement is protected from corrosion by the surrounding concrete provided this concrete is dense and of adequate thickness. The corrosion potential of steel due to the presence of soluble chlorides in the ground water is increased in porous concrete which in turn can result from inadequate compaction, high w/c ratio and low cement content. In case of reinforced concrete, the migration of chloride ions from the ground water establishes anodic and cathodic areas, the resulting electrolytic action leads to an accumulation of the corrosion products on the steel which causes its expansion with a consequent rupture of concrete.

As mentioned earlier, the chloride solution of high concentration can attack the cement paste and expansive disruption of the concrete can occur. Fortunately, the chloride salts are highly soluble and can be leacked from cement preventing their concentration.

When sulphates co-exist with chlorides in ground water of Sebkha, the latter inhibits the expansion of concrete and the question of sulphate attack is then considered less critical and the chloride attack then becomes more predominant. The rate of diffusion of chlorides in SRC is more than in OPC. In the circumstances where chlorides coexist with sulphates and are in higher quality, the effect of chloride attack and subsequent corrosion of reinforcement is relatively increased by the use of SRC.

4. MEASURES TO ENHANCE DURABILITY OF FOUNDATION CONCRETE IN SEBKHA

In the light of chemical expansive reactions which are responsible for the deterioration of concrete in Sebkha containing aggressive water soluble salts in ground water as mentioned above, it is necessary to take some special precautions to protect the foundation concrete from cracking and corroding.

Protection against subsoil chemical action has to be preventive in nature because the affected areas of concrete in contact with the soil and the ground water are practically impossible to inspect after construction. The protective

measures should obviate the need for maintenance and repairs and should serve as water proofing. Some of the preventive measures recommended are as follows:

- Use of cement low in C3A. In practice, it has been found that a C3A content of 7% provides an approximate border line between cements of good and poor performance.

- Where chloride and sulphates co-exist with a large quantity of chlorides, use of OPC should be preferred over SRC.

- Use of a dense, impervious and high strength concrete.

5. CASE HISTORY

A doubt regarding the durability of concrete consisting of OPC of overhead transmission towers foundation in Sebkha area necessitated an investigation into chemical aggressiveness of Sebkha. Results of the chemical analysis of a water samples conducted by Raymond International of Deleware Inc. (Tripoli branch) in April 1978 are presented below:

Sample No. 1/W/3.0; Site: Misurata Sebkha.

Chemical Analysis

pH	=	7.3
Chlorides	=	80250 mg/l
Hardness as CaCO3	=	23600 mg/l
Calcium	=	900 mg/l
Magnesium	=	5200 mg/l
Sulphates	=	9200 mg/l

A proper chemical analysis demonstrated that first $CaSO_4$ will be formed consuming 1500 mg/l of sulphates necessary for a saturated solution of calcium sulphate. The remaining sulphate (9200 - 1500 = 7700 mg/l) will react with (7700 x 0.253) 1948.1 mg/l of magnesium forming maximum possible amount of $MgSO_4$. The balance magnesium will either react with the chloride or will remain in the ground water in the form of hardness. Hence, all magnesium available will not react to form $MgSO_4$ which is more aggressive to portland cement concrete than the sulphates of sodium, calcium and pottassium when in equal concentration.

It is well known that in addition to the concentration of sulphates, the speed at which foundation concrete is attacked depends upon the rate at which sulphates removed by reaction with cement can be replenished. Thus the movement of ground water plays a key role since alternating saturation and drying leads to rapid deterioration of concrete. Most of the tower foundations were either in the submerged state or in a dry state, hence the effect of ground water movement with less variation was considered less serious.

Normally, SRC should be used when sulphates in higher concentration are present. But this recommendation is not obligatory when sulphates and chlorides co-exist

in the ground water since the later inhibit the expansion of concrete and the question of sulphate attack is then less critical. Recent research [4] has indicated that SRC has poor resistance to chloride ingression as compared to OPC. Therefore the use of OPC in the present circumstances was considered more acceptable than SRC provided other precautions for concrete in Sebkha are also taken into design consideration.

6. CONCLUSIONS AND RECOMMENDATIONS

- Durability of concrete foundations in Sebkha can be ensured with the following precautions:

  a) Adequate concrete cover to the reinforcement. 50 to 75 mm concrete cover is recommended.

  b) Provision of a sacrificial concrete layer (minimum thickness 50 mm) all around the foundation concrete.

  c) Use of a dense, impermeable and high strength concrete is made.

- Although SRC is generally recommended for use in foundation concrete in Sebkha; but when sulphates and chlorides co-exist, in ground water, the use of OPC can be preferred over SRC due to its higher resistance to chloride ingression.

- A coating of a water proofing material around the foundation concrete will enhance the durability.

REFERENCES

1. NEVILLE, A.M., Properties of Concrete, Pitman, 3rd edition, 1981.

2. MURDOCK, L.J. and BROOK, K.M., Concrete Materials and Practice, Edward Arnold, 5th edition, 1979.

3. CIRIA, the CIRIA Guide to Concrete Construction in the Gulf Region, Construction Industry Research and Information Association, Special Publication 31, London 1984.

4. STUVO, Concrete in Hot Countries, Netherland, 1985.

Porosity and Permeability as Indicators of Concrete Performance

Porosité et perméabilité comme indicateur de comportement du béton

Porosität und Durchlässigkeit als Indikatoren des Betonverhaltens

J. G. CABRERA
Senior Lecturer
University of Leeds
Leeds, England

A. R. CUSENS
Prof. of Civil Eng.
University of Leeds
Leeds, England

C. J. LYNSDALE
Research Fellow
University of Leeds
Leeds, England

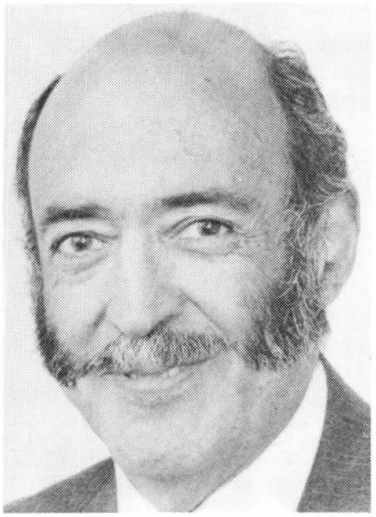

Joe Cabrera has lectured in Leeds since 1967. His main research is performance and durability of engineering materials.

Tony Cusens was appointed to his current position in Leeds in 1979. His main research fields concrete structures, especially bridges. He is Vice-Chairman of the British Group of IABSE.

Cyril Lynsdale has been engaged in concrete research since 1983. His main interests are the study of durability and the use of admixtures in concrete.

SUMMARY

Based on the results of an extensive laboratory study, this paper proposes statistical models which link numerically oxygen permeability to pore structure characteristics, total porosity and compressive strength, water/cement ratio, air content and age. The models are used to predict adequate levels of performance for concrete in bridge structures.

RÉSUMÉ

Fondé sur les résultats d'un essai étendu de laboratoire, cet article offre des modèles statistiques qui lient numériquement la perméabilité à l'oxygène aux caractéristiques de la structure des pores, à la porosité totale, à la résistance à la compression, au rapport eau-ciment, à la teneur en air et à l'âge. Ces modèles sont employés pour prédire des niveaux de comportement suffisants pour le béton dans la construction des ponts.

ZUSAMMENFASSUNG

Basierend auf den Resultaten von umfangreichen Laboruntersuchungen werden statistische Modelle vorgeschlagen, welche die Sauerstoffdurchlässigkeit mit der Charakteristik der Porenstruktur, der Gesamtporosität, der Druckfestigkeit, dem Wasser/Zement-Verhältnis, Luftgehalt und Betonalter verknüpfen. Die Modelle werden zur Prognose des Verhaltens von Betonbrücken verwendet.

1. INTRODUCTION

It is now accepted that the performance of concrete under a particular environment cannot be solely related to its strength but that it is a function of its pore structure and permeability [1, 2]. The new British code of practice for the structural use of concrete [3], for example, specifies strength, cement content and water/cement ratio as criteria for design. This, although not satisfactory, is an attempt to control performance by indirectly controlling porosity. The new draft for the Eurocode [4] in concrete has, however, proposed the measurement of permeability as a sole criterion for durability. Notwithstanding the fact that in recent years a large amount of work has been devoted to this problem [5, 6, 7], there is no accepted method for measuring permeability.

This study presents empirical statistical models which relate the oxygen permeability of concrete to other intrinsic and compositional properties of the material. The models are used as an aid to understanding which properties of concrete have a relevant effect on its permeability and also to predict long-term permeability from measurements made at early ages. The paper proposes the use of these models to set criteria for the design of durable concrete mixes.

2. MIX DESIGN AND MATERIALS

The mix design used in this investigation is based on the criterion of "minimum porosity" [8] which involves the selection of the components of concrete to achieve maximum packing.

The composition of the mix designed by the method indicated gave a mix of the following proportions: 1 part of cement, 2.33 parts of sand and 3.5 parts of gravel. The ordinary Portland cement (opc) content of the mix was 325 kg/m^3. This composition was used to prepare three "control" concretes by varying the water/cement ratio (see Table 1).

Table 1: Mixes investigated and their fresh properties

Mix	w/c ratio	Superplasticiser		PFA	Slump	Flow Table	Air Content
		Type	Dosage*(%)	(%)	(mm)	(mm)	(%)
A	0.65	None	None	None	215	580	0.6
B	0.55	None	None	None	55	390	1.65
C	0.40	None	None	None	0	-	2.8
BN2	0.55	SNFC1	0.2	None	172	550	1.2
BN3	0.55	SNFC1	0.4	None	240	690	0.9
CN2	0.40	SNFC1	1.2	None	50	350	2.6
BM2	0.55	SMFC	0.2	None	155	500	1.3
BM3	0.55	SMFC	0.4	None	225	650	0.9
CM2	0.40	SMFC	1.4	None	50	305	1.60
BP2	0.55	Co-Po	0.08	None	200	545	3.25
BP3	0.55	Co-Po	0.16	None	230	600	5.70
CP1	0.40	Co-Po	0.19	None	50	320	3.9
BSF2	0.55	SNFC2	0.3	None	210	555	3.4
BSF3	0.55	SNFC2	0.45	None	220	600	2.7
CSF1	0.40	SNFC2	0.70	None	50	310	5.4
BLS2	0.55	MLS	0.2	None	200	560	3.5
BLS3	0.55	MLS	0.4	None	215	615	4.3
CLS2	0.40	MLS	0.45	None	65	345	8.4
PFA1	0.50	None	None	30	60	360	1.3
PFA2	0.55	None	None	30	160	485	1.2
PFN	0.40	SNFC1	1.0	30	45	310	2.2
PFM	0.40	SMFC	1.2	30	45	300	1.9
PFL	0.40	MLS	0.45	30	45	320	6.3
PFS	0.40	SNFC2	0.6	30	50	320	4.3
PFH	0.40	Co-Po	0.15	30	50	310	7.0

*Dosage is based on solid/solid weight/weight of cement

Five superplasticisers (see Table 2) were added to the control mixes at different dosages to obtain concretes with a wide range of workabilities up to flowing concrete (see Table 1).

Code	Superplasticiser Description
MLS	Modified lignosulphonate
SNFC1	Sulphonated naphthalene formaldehyde condensate (Powder)
SNFC2	Sulphonated naphthalene formaldehyde condensate (Liquid)
SMFC	Sulphonated melamine formaldehyde condensate
CP	Co-polymer based on acrylic acid and hydroxy-propyl-methacrylate

Table 2: Superplasticisers used in the investigation

Some mixes were also prepared by substituting 30% of the opc with pulverised fuel ash (pfa).

3. PROPERTIES AND METHODS

Air content, slump, flow table (see Table 1) and cube compressive strength were measured according to the relevant parts of BS 1881 [9]. The porosity was obtained by helium pycnometry using a Micromeritics Autopycnometer. Oxygen permeability was measured using the Leeds cell [7].

Although some of the hardened concrete properties were monitored for ages of up to one year, the results used in this paper correspond to ages of 1, 3, 7, 28 and 90 days. The samples were cured in a fog room kept at 20°C and 100% relative humidity. Prior to testing for porosity and oxygen permeability the samples were dried in an oven at 105°C. This method of drying was found not to affect the order of ranking of oxygen permeability values [10, 11].

4. RESULTS AND DISCUSSION

The abundance of data from the 25 mixes studied required the use of statistical techniques for interpretation and evaluation of the effects of the various parameters measured. The data was therefore analysed using a standard statistical package (Statistical Analysis System, SAS). The models presented have a confidence limit of 95%.

4.1 Parameters affecting permeability

Pore structure characteristics directly affect the permeability of concrete, therefore any parameters influencing these characteristics should have an effect on the resistance of concrete to penetration of gases, liquids and ions.

The statistical analysis allowed the evaluation of a large number of properties of concrete with regard to their effects on permeability. From this analysis the most important properties and the extent to which they affected oxygen permeability (K, m^2) were: water/cement ratio (w/c), age (t, days), air content (a, %) and porosity of the fraction of cement paste of concrete (Pp, %). The statistical model (coefficient of correlation $R^2 = 0.80$) which relates these parameters to permeability is:

$$\text{Log } K = -16.853 + 0.077(a)\ (w/c) - 0.012(t)^{0.66} + 0.037(Pp)(w/c)$$

In this model, the air content and the water/cement ratio are considered interactively since (a) is inversely related to (w/c) and its effect on permeability depends on the value of (w/c), i.e. the lower the value of (w/c) the smaller the effect of (a) on the oxygen permeability (10, 12).

4.2 Relation between permeability, strength and porosity.

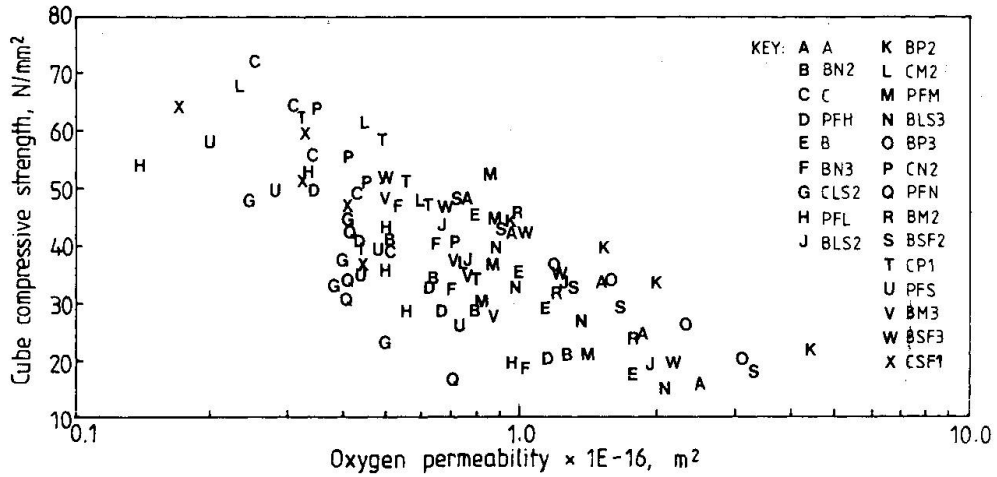

Figure 1: Cloud diagram relating compressive strength to permeability

The compressive strength of concrete is, in most specifications, the dominant parameter used to "control" the quality of concrete. Although there is a good relation between permeability and strength for a particular concrete, the relation cannot be generalised for concretes where the composition is varied either by changing the aggregate-cement ratio or by changing the type of cement or using chemical additives. The results of this investigation confirm the fact that permeability is related to compressive strength for any one mix but when a relationship is attempted for all mixes the result is a cloud diagram as shown in Figure 1. Results reported by Lawrence [13] for concrete mixes made with opc, opc/pfa and opc/slag cured in water at 20°C show similar trends to those shown in Figure 1, i.e. a series of permeability-strength curves within a wide band. Lawrence, [13] however, concludes that there is a single relationship between oxygen permeability and cube strength, despite the fact that his results indicate that at a particular permeability concrete strength varies between 30 and 60 N/mm² depending on the mix.

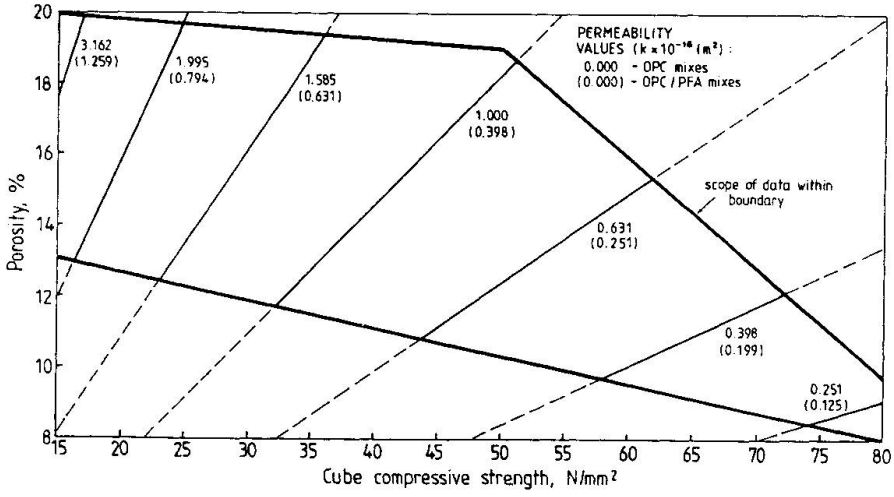

Figure 2: The porosity-strength-permeability model

Statistical analysis of the data gathered in this investigation indicates that oxygen permeability (K) is directly related to porosity (P, %) and inversely related to strength (fcu, N/mm²). The analysis also revealed that the

statistical validity improved by separating the data into two groups; one for opc mixes and one for mixes made with opc/pfa. The models are shown below:

(a) opc concretes:

$$\log K = -15.54 + 1.114 \log \left(\frac{P}{fcu}\right), \quad R^2 = 0.71$$

(b) opc/pfa concretes:

$$\log K = -15.95 + 1.01 \log \left(\frac{P}{fcu}\right), \quad R^2 = 0.85$$

These models are presented in Figure 2, where the cartesian co-ordinates correspond to porosity and compressive strength and parametric space is divided by contour lines of equal permeability.

4.4 Prediction of long-term permeability from early age values

The use of a permeability test as a quality control test would require measurements at early ages during the mix design stage; therefore relations to predict the long-term permeability of concrete from values at early ages would be very useful. From the data collected in this work, a statistical model to predict the permeability of concrete samples up to the age of 90 days from its one-day value (K_1, m^2) has been obtained. The model is:

$$\log K = -3.688 + 0.789 \log K_1 + \frac{0.356}{t} \; ; \; R^2 = 0.89$$

This model can be used to establish tentative one-day permeability values as a criterion for designing for durability at the stage of trial mixes for a particular job, from the knowledge of the permeability of 'good' and 'bad' in-service concrete. In this investigation, oxygen permeability values of in-service 30 year old concretes, both 'good' concrete and 'bad' concrete showing signs of distress and cracking have been obtained; these were 5×10^{-17} (m^2) and 190×10^{-17} (m^2) respectively. If these values are used in the models as the target permeabilities (i.e. K) then the one-day values will be:

For 'good' concrete $K_1 = 1.02 \times 10^{-16}$ m^2

For 'bad' concrete $K_1 = 1.02 \times 10^{-14}$ m^2

These values can be used as a guide to design for durable concrete. It has, however, to be mentioned that for this model to be of general use, the data base has to be expanded to cover a wider range of concrete mixes.

Similar analysis was carried out on chloride permeability and statistical models have also been developed for its prediction [10]. This will be published elsewhere.

5. CONCLUSIONS

(a) The parameters affecting the oxygen permeability of concrete are: air content, water/cement ratio, porosity and age.
(b) Oxygen permeability is related to the porosity/strength ratio. This relationship is influenced by the presence of pfa in the concrete.
(c) Oxygen permeability, porosity and strength influence the performance of concrete in a particular environment, and at least two of these three parameters are required to predict the performance of concrete.
(d) It is suggested that the target value for oxygen permeability, at one day, for design should be 1×10^{-16} m^2.

6. REFERENCES

1. J G Cabrera, "The use of pulverised fuel ash to produce durable concrete", Improvements in Concrete Durability, Thomas Telford, London, 1985, pp 19-35.
2. A R Cusens and J G Cabrera, "Development in Concrete and Related Materials", Institute of Physics, Conference No 89, Session 7, Paper presented on New Materials and their Applications, Warwick, September 1987, IOP Publishing Ltd, 1988, pp 237-249.
3. British Standards Institution, BS 8110:Part 1:1985, Structural Use of Concrete, Code of Practice for design and construction, London, BSI, 1985.
4. European Committee for Standardisation Draft of ENV 206 Concrete - Performance, Production, Placing and Compliance Criteria, CEN, 1988.
5. The Concrete Society, "Permeability testing of site concrete - a review of methods and experience", Report of a Concrete Society Working Party. Permeability of Concrete and its Control, Papers for a one-day conference, London, 12 December 1985, The Concrete Society, 1985, pp 1-68.
6. P B Bamforth, "The relationship between permeability coefficients for concrete obtained using liquid and gas", Magazine of Concrete Research, Vol 39, No 138, 1987, pp 3-11.
7. J G Cabrera and C J Lynsdale, "A new gas permeameter for measuring the permeability of mortar and concrete", Magazine of Concrete Research, Vol 40, No 144, 1988, pp 177-182.
8. J G Cabrera, "Concrete mix design using minimum porosity (in preparation).
9. British Standards Institution BS 1881:1983, Parts 102, 105, 106, 116, London, BSI, 1983.
10. C J Lynsdale, "The influence of superplasticisers on the engineering properties and performance of concrete", PhD Thesis, Dept of Civil Engineering, University of Leeds, in preparation.
11. C Bohring and W Riedel, "Gas permeability of concrete and its influence on the corrosion resistance in salt solution", Proceedings of RILEM/IUPAC on Pore Structure and Properties of Materials, Prague, 1973, pp F95-F118.
12. M F Al-Khoory, "The effect of air entrainment on the permeability of concrete", MSc Dissertation, Department of Civil Engineering, University of Leeds, 1988.
13. C D Lawrence, "Measurements of permeability", Proceedings of the 8th International Congress on the Chemistry of Cement, Rio de Janeiro, 1986, FINEP, Vol V, 1986, pp 29-34.

Retrait de Carbonatation
Karbonatisierungsschwinden
Carbonation Shrinkage

Yves F. HOUST
Chimiste
École Polytechnique Fédérale
Lausanne, Suisse

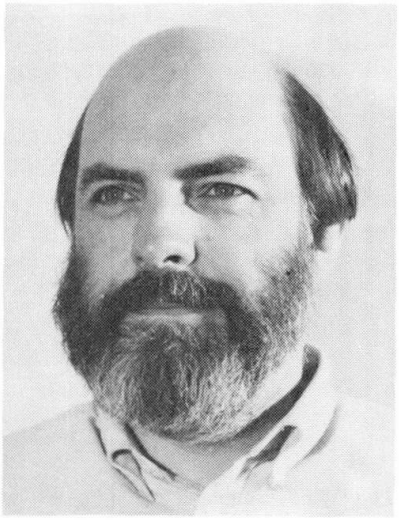

Yves F. Houst, né en 1946, est diplômé de chimie de l'Université de Lausanne. Il travaille dans le domaine des matériaux de construction depuis 16 ans. Il est actuellement chef de la section chimie au Laboratoire des Matériaux de Construction de l'École Polytechnique Fédérale de Lausanne.

Folker H. WITTMANN
Professeur
École Polytechnique Fédérale
Zürich, Suisse

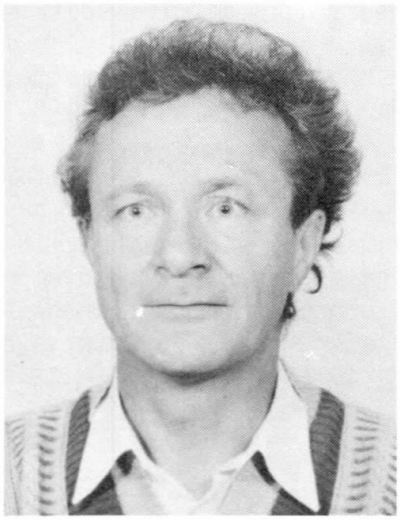

Folker H. Wittmann, né en 1936, est gradué en physique. Il fut 4 ans professeur de matériaux de construction à l'Université technique de Delft (Pays-Bas) et 8 ans à l'École Polytechnique Fédérale de Lausanne. Il est actuellement Professeur ordinaire de matériaux de construction à l'École Polytechnique Fédérale de Zürich.

RÉSUMÉ

Des mesures du retrait de carbonatation ont été effectuées sur des éprouvettes de béton cellulaire de différentes résistances et de la pâte de ciment durcie. L'influence de la teneur en eau et du rapport eau/ciment a été étudiée. Deux mécanismes possibles sont indiqués. La signification du retrait de carbonatation pour la pratique est également discutée.

ZUSAMMENFASSUNG

Das Karbonatisierungsschwinden wurde an Gasbetonproben mit unterschiedlicher Qualität und an Zementsteinproben gemessen. Der Einfluss des Feuchtigkeitsgehaltes und des Wasser/Zement- Wertes wurde untersucht. Zwei mögliche Mechanismen werden vorgeschlagen. Die Bedeutung des Karbonatisierungsschwindens in der Praxis wird diskutiert.

SUMMARY

Carbonation shrinkage of autoclaved aerated concrete with different strengths and hardened cement paste have been measured. The influence of moisture content and of water/cement ratio have been studied. Two possible mechanisms are proposed. The significance of carbonation shrinkage in building practice is also discussed.

1. INTRODUCTION

La carbonatation des bétons et mortiers est un phénomène qui n'altère pas ces matériaux, bien au contraire: la résistance mécanique, le module d'élasticité et la dureté augmentent, la perméabilité aux gaz et aux liquides diminue, les hydroxydes solubles sont transformés en carbonates. Cependant, si le béton est armé, la carbonatation du matériau qui enrobe l'acier d'armature supprime l'immunité dont bénéficie ce dernier. Les aciers peuvent alors se corroder et ainsi limiter la capacité portante des éléments en béton armé. Lorsque les armatures sont proches de la surface du béton, la formation de rouille peut provoquer la fissuration ou l'éclatement du béton superficiel. Ces types de dégâts sont actuellement assez bien connus, parce que malheureusement trop répandus. Il est toutefois un autre inconvénient dont les conséquences négatives sont heureusement plus rares et en général moins graves : c'est le retrait de carbonatation. Lorsque le ciment réagit avec le gaz carbonique, il y a neutralisation des composés basiques et diminution de volume. Cette diminution de volume se traduit par un retrait différentiel entre la surface et le coeur du béton qui est à l'origine de craquelures et de fissures superficielles.

Dans cette communication, on donne les résultats de mesures du retrait de carbonatation du béton cellulaire en fonction de l'humidité relative de l'environnement. Sur des éprouvettes en pâte de ciment durcie on a étudié l'influence du rapport eau/ciment sur le retrait de carbonatation. Les résultats sont comparés avec les données disponibles de la littérature et discutés sur la base des théories proposées.

2. LA CARBONATATION

2.1. La réaction chimique

L'hydratation des deux silicates de calcium du ciment portland conduit à la formation de silicates hydratés et d'hydroxyde de calcium, $Ca(OH)_2$. Les silicates hydratés n'ont pas une composition chimique bien définie et on les symbolise par la formule C-S-H (où C = CaO, S = SiO_2 et H = H_2O). La composition du C-S-H varie et dépend de nombreux facteurs tels que la composition chimique du ciment, la quantité d'eau de gâchage, l'âge, etc... Pour un ciment donné, la quantité de C-S-H et de $Ca(OH)_2$ formés dépend essentiellement du rapport eau/ciment et du temps de réaction. Un calcul simple montre que par exemple dans un m^3 de béton dosé à 300 kg/m^3 d'un ciment portland, plus de 50 kg de $Ca(OH)_2$ sont libérées si l'on admet un degré d'hydratation du ciment de 60%. La teneur en $Ca(OH)_2$ dans le béton peut être réduite de façon importante par l'emploi de matériaux à propriétés pouzzolaniques, comme les pouzzolanes naturelles ou artificielles, les cendres volantes et la fumée de silice condensée (condensed silica fume).

La carbonatation du béton est un phénomène naturel que subit tout matériau à base de ciment. On appelle carbonatation la réaction du gaz carbonique (CO_2) qui est normalement présent dans l'air à raison de 0,03% en volume avec les produits d'hydratation du ciment. Dans les locaux fermés non ventilés, cette teneur peut atteindre 0,1% et même 0,3% dans certaines atmosphères urbaines, des tunnels ou des garages. Les réactions chimiques de carbonatation peuvent être décrites de manière simplifiée par les équations suivantes :

$$Ca(OH)_2 + CO_2 \rightarrow CaCO_3 + H_2O$$
$$C\text{-}S\text{-}H + CO_2 \rightarrow CaCO_3 + SiO_2 + H_2O$$

Ces réactions, qui décrivent des réactions de produits solides avec un gaz, sont très lentes. En réalité, c'est essentiellement le gaz carbonique dissous dans l'eau qui réagit avec $Ca(OH)_2$ en solution et le C-S-H solide, ce dernier étant pratiquement insoluble dans l'eau, tandis que la solubilité de l'hydroxyde de calcium est de 2,5 g/litre à 25 °C. Toutefois, l'eau des pores contient d'importantes quantités d'hydroxydes de sodium et potassium qui sont très solubles et, comme la solubilité de l'hydroxyde de calcium dépend fortement de la présence d'ions OH^-, il n'y a en réalité que de petites quantités de $Ca(OH)_2$ dissous dans la solution des pores du béton. Lorsque le dioxyde de carbone diffuse dans le béton, NaOH et KOH se carbonatent, ce qui augmente la solubilité de $Ca(OH)_2$. Ce dernier doit alors passer en solution pour réagir, ce qui peut prendre un certain temps et expliquer que la propagation de la carbonatation se produit par déplacement d'une zone

qui a une épaisseur variable selon la compacité du béton. Les aluminates du ciment réagissent également pour donner un gel d'alumine [1, p.546].

Une pâte de ciment en équilibre avec l'air ambiant qui a une humidité relative supérieure à 0% contient de l'eau libre (qui s'évapore si l'on diminue l'humidité relative de l'air ambiant). Cette eau est adsorbée à des humidités relatives basses et condensés dans les capillaires pour des humidités plus élevées. Si les pores et les capillaires ne sont pas remplis d'eau, le gaz carbonique peut diffuser dans tout le système poreux [2]. Il se dissout alors dans l'eau condensée où il réagit immédiatement avec les bases.

La réaction de carbonatation principale qui se produit dans le béton peut alors être représentée par l'équation suivante :

$$Ca(OH)_2 + 2H^+ + CO_3^{2-} \rightarrow CaCO_3 \downarrow + H_2O$$

où le $Ca(OH)_2$ doit être dissous avant qu'il puisse réagir. Pour carbonater une couche d'une épaisseur de 1 cm d'un béton contenant 50 kg $Ca(OH)_2/m^3$, on a besoin de.45'000m^3 d'air à 0.033 % de CO_2 par m^3. On comprend mieux ainsi que la carbonatation dans des conditions normales soit un processus lent. $CaCO_3$, le carbonate de calcium qui est le résultat de la réaction existe sous trois formes polymorphes, la calcite, la vaterite et l'aragonite. Bien que la calcite soit la forme la plus stable, les produits initiaux de la réaction de carbonatation naturelle peuvent être l'aragonite ou la vaterite; ces derniers se transforment alors en calcite au cours du temps [1, p.544]. Goodbrake et al. [3] ont trouvé que la principale espèce formée par une carbonatation artificielle était l'aragonite, lorsque les produits d'hydratation peuvent sécher. Toutefois, les conditions de réaction de leur étude étaient bien éloignées de la carbonatation naturelle.

2.2. Variation de volume

La réaction de carbonatation de $Ca(OH)_2$ entraîne une augmentation du volume. Si l'on ne tient compte que des produits solides, l'augmentation de volume de $Ca(OH)_2$ est, selon les produits de réaction formés, la suivante :

	→ calcite ($CaCO_3$)	+ 12 %
portlandite ($Ca(OH)_2$)	→ aragonite ($CaCO_3$)	+ 3 %
	→ vaterite ($CaCO_3$)	+ 19 %

La distribution de la taille des pores d'une pâte de ciment durcie est modifiée par la carbonatation [4]. Elle montre une notable réduction du volume des pores après carbonatation, le phénomène étant plus marqué pour une carbonatation accélérée [5].

La réduction de la porosité entraîne une augmentation des résistances mécaniques. La calcite qui s'est formée consolide la structure de la pâte de ciment durcie. Il est bien connu que le carbonate de calcium qui se forme par carbonatation de $Ca(OH)_2$ est un excellent liant. C'est lui qui assure l'essentiel de la résistance mécanique des mortiers à la chaux. La résistance à la compression et à la flexion de bétons au ciment portland conservés dans une atmosphère de CO_2 peut augmenter jusqu'à 30% par rapport aux mêmes bétons conservés en atmosphère exempte de gaz carbonique [1, p.547]. L'augmentation de résistance est d'autant plus marquée que le rapport eau/ciment du béton est bas [6]. La carbonatation accélérée qui permet l'augmentation des résistances mécaniques entraîne également une diminution du fluage [7] ou une augmentation du fluage si la carbonatation se produit lorsque le béton est sous charge [8]. La dureté, l'imperméabilité et la stabilité de volume sont favorablement influencées par la carbonatation [9].

Les matériaux poreux à base de ciment subissent diverses déformations volumiques que l'on nomme retrait (ou gonflement). Les causes de ces déformations sont multiples et peuvent être classées en quatre catégories[10] :

- retrait thermique lié à une variation de température (causée dans le béton par le refroidissement qui suit l'élévation de température provoquée par l'hydratation du ciment);

- retrait capillaire lié à la formation de ménisques d'eau entre les particules par évaporation superficielle de l'eau de gâchage;
- retrait de dessiccation lié à une diminution de la quantité d'eau dans les pores du matériau;
- retrait chimique (ou gonflement) lié aux réactions chimiques entre le ciment et l'eau ou à la carbonatation par exemple.

Ces divers types de retrait peuvent se produire simultanément, c'est ce qui se passe en général dans la pratique, ou consécutivement. Si l'on élimine le retrait thermique et le retrait de carbonatation qui sera traité plus en détail par la suite, on peut séparer les retraits en *retrait de dessiccation* (sans vieillissement, c'est-à-dire que l'hydratation est bloquée) et en *retrait endogène* d'un béton qui vieillit sans échange d'eau à l'extérieur [11]. Lorsqu'un béton vieillit et sèche en même temps, son retrait n'est pas la somme du retrait de dessiccation et du retrait endogène. Dans la pratique, il faut donc tenir compte de l'interaction de ces phénomènes.

3. PARTIE EXPERIMENTALE

3.1. Béton cellulaire

Des prismes de béton cellulaire 20/20/150 mm ont été prélevés par sciage dans des parpaings de trois qualités courantes du commerce. Ces bétons cellulaires se distinguent essentiellement par leur résistance à la compression et leur masse volumique apparente après séchage à 105 °C, qui est respectivement de 307, 386 et 501 kg/m^3 pour les types L, N et H. Ces prismes ont été placés immédiatement après sciage à différentes humidités relatives dans une enceinte climatique à 25 °C. Les variations de longueurs ont été mesurées au moyen d'un capteur inductif placé sur le prisme posé verticalement. Dès l'obtention de l'équilibre (plus de variation notable de longueur), les prismes ont été mis en contact avec de l'air contenant 2 % de CO_2, ceci toujours à la même humidité relative. Les variations de longueurs ont été mesurées au moyen de capteurs déjà décrits jusqu'à stabilisation.

3.2. Pâte de ciment

3.2.1. Echantillons cylindriques

Les échantillons cylindriques de diamètre 3 mm et de longueur 80 mm ont été obtenus en coulant de la pâte de ciment dans un moule constitué de deux plaques fixées ensemble et percées dans le plan de leurs surfaces communes. Le diamètre et la longueur des trous définissent les dimensions de l'échantillon. Les pâtes de ciment sont injectées au moyen d'une seringue. Les échantillons ont été conservés 28 jours dans l'eau.

A cause de leur fragilité, les échantillons ont été montés sur des bâtis. Ils ont été placés verticalement au sommet d'un triangle équilatéral et collés sur une plaque métallique. Une autre plaque a été collée sur les échantillons. Un appareil simple permet de les positionner correctement et de les tenir en place et parfaitement verticaux pendant le collage. Le dispositif permet de mesurer une moyenne des variations dimensionnelles au moyen d'un seul capteur inductif placé sur la plaque supérieure. Les bâtis ont ensuite été placés dans une chambre climatisée à 25 °C et 55 % h.r. Après obtention de l'équilibre hydrique, on a introduit dans l'enceinte du CO_2 pur.

3.2.2. Echantillons prismatiques

Nous avons utilisé des prismes de pâte de ciment de dimension 3/3/9 mm, prélevés par sciage dans des cylindres de 160 mm de diamètre. La méthode de fabrication de ces cylindres, dont le rapport eau/ciment varie entre 0.3 et 0.8, est décrite dans une autre communication à ce symposium [12]. Ces échantillons ont été montés sur les mêmes bâtis que ceux déjà décrits pour les échantillons cylindriques, mais après au moins une année de conservation dans l'eau. Ensuite, les bâtis ont été placés dans une chambre climatique à 30 °C jusqu'à obtention de l'équilibre. On a alors introduit dans l'enceinte de l'air contenant 2 % de CO2. Le retrait de carbonatation a été mesuré au moyen des capteurs déjà décrits.

4. RESULTATS ET DISCUSSION

Le retrait de carbonatation, mesuré sur les échantillons de béton cellulaire en fonction de l'h.r., est montré à la figure 1. On constate que le retrait a un maximum autour de 80 % h.r. et il diminue brusquement à des humidités plus basses que 70 % h.r. Le béton cellulaire ne contient que très peu de $Ca(OH)_2$. Le retrait est donc à attribuer à la réaction des silicates calciques hydratés avec le CO_2. Vu la grande porosité du béton cellulaire, l'eau libérée pendant la carbonatation ne change pas autant l'h.r. du matériau que dans une pâte de ciment durcie. Il est à remarquer que la densité (type de béton cellulaire) n'a qu'une très faible influence sur le retrait.

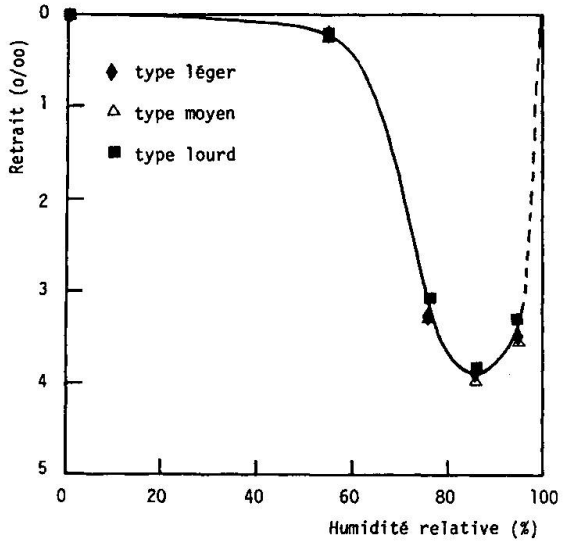

Fig. 1 Retrait de carbonatation de trois types de béton cellulaire autoclavé préalablement équilibré à différentes h.r.

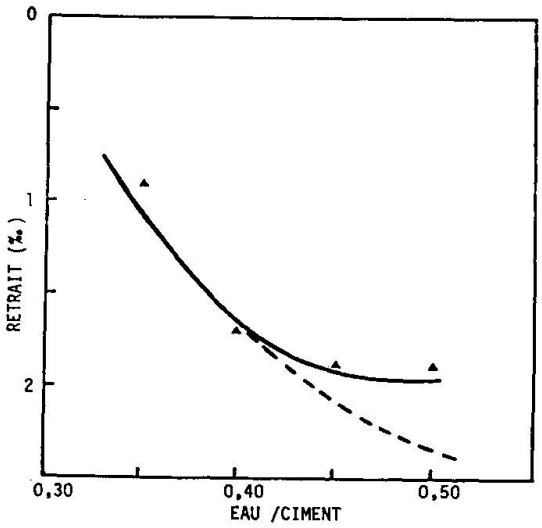

Fig. 2 Retrait de carbonatation de pâtes de pâtes de ciment en fonction de e/c à 55% h.r.

A la figure 2, le retrait de carbonatation mesuré sur des éprouvettes de pâte de ciment durcie équilibrées à 55 % h.r. est montré en fonction du rapport eau/ciment. On constate que le retrait augmente avec le rapport e/c. Il est bien connu que le degré d'hydratation et donc la quantité de produit d'hydratation y inclus le $Ca(OH)_2$ sont plus élevés dans les pâtes avec un rapport e/c plus grand. Pendant la fabrication des échantillons cylindriques avec un rapport e/c plus élevé que 0.4, on n'a pas pu éviter une certaine décantation. Ceci signifie que les valeurs de e/c réelles sont plus basses qu'indiquées à la figure 2 (voir courbe traitillée). Afin d'éviter ce problème, nous avons préparé les échantillons prismatiques décrits ci-dessus. Actuellement, le retrait de carbonatation n'a pas pu être mesuré à cause de la longue période d'équilibrage. Toutefois, les résultats seront présentés au symposium.

A première vue, il est étonnant qu'une réaction chimique qui est associée à une augmentation de volume puisse provoquer du retrait. Il y a plusieurs hypothèses de ce phénomène décrites dans la litérature [13-16]. On sait qu'une partie du $Ca(OH)_2$ est bien cristallisée; on l'observe facilement à l'aide des rayons X. Cependant, environ 20 % du $Ca(OH)_2$ se trouve sous forme colloïdale.

Les cristaux ne subissent pas de retrait de dessiccation, tandis que le gel de C-S-H qui les entoure et la partie du $Ca(OH)_2$ amorphe se rétrécissent. Les cristaux sont donc sous contrainte dans la pâte de ciment durcie partiellement séchée et ils empêchent le retrait. La carbonatation nécessite la dissolution des cristaux et les contraintes peuvent être ainsi libérées. Ce phénomène permet un retrait supplémentaire de la pâte qui entoure les cristaux.

D'autre part, en mesurant l'isotherme d'adsorption, on a constaté qu'à une h.r. donnée la pâte de ciment durcie carbonatée ne contient qu'une fraction de l'eau d'équilibre d'une même pâte non carbonatée. Cette perte d'eau s'explique par le fait que la microstructure des produits d'hydratation devient plus grossière [4]. Ce deuxième mécanisme accroît le retrait de carbonatation.

5. CONCLUSION

Nous avons élaboré une méthode de mesure du retrait de carbonatation. Il est indispensable d'équilibrer les échantillons avant la carbonatation avec des h.r. différentes, si on veut comprendre les mécanismes du phénomène. Etant donné que le retrait de carbonatation est de l'ordre de 1 %, il faut s'attendre que la couche carbonatée soit fissurée. Le risque pour la pratique n'est pas dramatique pour autant qu'il s'agisse d'un béton de bonne qualité. Les techniques modernes de traitement des surfaces du béton permettent de freiner considérablement la carbonatation et les conséquences néfastes.

BIBLIOGRAPHIE

1. LEA F.M., The Chemistry of Cement and Concrete (2nd Ed.), Edward Arnold, London (1970).
2. HOUST Y.F., WITTMANN F.H., The diffusion of carbon dioxide and oxygen in aerated concrete, in (F.H. Wittmann Ed.), Materials Science and Restoration, Technische Akademie Esslingen, Ostfildern (1986) 629-634.
3. GOODBRAKE C.J., YOUNG J.F. and BERGER R.L., Reaction of hydraulic calcium silicates with carbon dioxyde and water, J. Amer. Ceram. Soc., 62 (1979) 488-491.
4. PIHLAJAVAARA S.E., Some results of the effect of carbonation on the porosity and pore size distribution of cement paste, Mat. Constr., 1 (1968) 521 -526.
5. BIER Th.A., KROPP J. and HILSDORF H.K., Carbonation and realcalinisation of concrete and hydrated cement paste in Durability of Construction Materials (J.C. Maso Ed.), Chapman and Hall, London-New York (1987) Vol. 3, pp. 927-934.
6. FREY R. und GOERKE, H.-J., Derzeitiger Stand der Kenntnis des Einflusses der Carbonatisierung auf die Festigkeitseigenschaften von Betonen, TIZ-Fachberichte, 106 (1982) 184-187.
7. ALEXANDRE J., Influence de la carbonatation sur le fluage en compression du béton, Rev. mat. Constr., No 684 (1973) 22-30.
8. PARROTT L.J., Increase in creep of hardened cement paste due to carbonation under load, Mag. Concr. Res., 27 (1975) 179-181.
9. KAMIMURA K., SEREDA P.J. AND SWENSON E.G., Changes in Weight and Dimensions in the Drying and Carbonation of Portland Cement Mortars, Mag. Concr. Res, 17 (1965) 5-14.
10. FERRARIS C.F. et WITTMANN F.H., Retrait de la pâte de ciment durcie, Chantiers/Suisse, 18 (1987) 289-292.
11. BARON J., Les retraits de la pâte de ciment in Le béton hydraulique, Presses de l'ENPC, Paris (1982), chap. 27.
12. HOUST Y.F., WITTMANN F.H., Diffusion de gaz et durabilité du béton armé, Communication à ce symposium.
13. POWERS T.C., A Hypothesis on Carbonation Shrinkage, J. PCA R. & D. Lab., May 1962, pp. 40-50.
14. HUNT C.M. and TOMES L.A., Reaction of blended Portland Cement Paste with Carbon-Dioxide, J. Res. Nat. Bur. Stand., 66A (1962) 473-481.
15. SWENSON E.G. and SEREDA P.J., Mechanism of the Carbonation Shrinkage of Lime and Hydrated Cement, J. Appl. Chem., 18 (1968) 111-117.
16. VERBECK G., Carbonation of Hydrated Portland Cement, ASTM Spec. Techn. Publ. No 205 (1958) 17-36.

Effect of Aggregates on Concrete Properties

Effet des granulats sur les propriétés du béton

Wirkung von Zuschlagstoffen auf die Eigenschaften von Beton

Yoshiaki HIRONAKA
Civil Engineer
Sato Kogyo Co., Ltd
Tokyo, Japan

Y. Hironaka graduated in 1975 as a Civil Engineer from Tokai Univ. He is researching into Acoustic Emission characteristics of concrete structures.

Keizo SAKOTA
Lecturer
Tokai Univ.
Shizuoka, Japan

K. Sakota graduated from Keio University. He is researching into materials of concrete, especially aggregates.

Sadao KIMURA
Civil Engineer
Sato Kogyo Co., Ltd
Tokyo, Japan

S. Kimura gratuated in 1984 from Toyo Univ. and received his M. E. degree in Civil Eng. He is researching into Acoustic Emission characteristics of concrete structures.

Tetsu ISHIBASHI
Civil Engineer
Sato Kogyo Co., Ltd
Tokyo, Japan

T. Ishibashi graduated in 1985 as a Civil Engineer from Kyushu Univ. He is researching into Acoustic Emission characteristics of concrete structures.

SUMMARY

This paper presents a study on the characteristics of concrete with aggregates of inferior quality (low gravity and high absorption). Acoustic emission measurements were performed during uniaxial compressive testing of concrete specimens. According to the results, the quality of aggregates appear more clearly in the static Young's modulus than the compressive strength of concrete. These are simply phenomena caused by the quality of aggregates, but the difference of the fracture process of concrete due to the quality of aggregates is directly indicated by acoustic emission measurements.

RÉSUMÉ

Ce document présente les résultats d'une étude sur les caractéristiques du béton à granulats de qualité inférieure (faible gravité et haute absorption). Les mesures d'émission acoustique ont été exécutées durant l'essai compressif uniaxial d'échantillons de béton. Les résultats on révélé que la qualité des granulats se manifeste plus clairement dans le module de Young statique que dans la résistance du béton à la compression. Ces phénomènes sont causés par la qualité des granulats, mais la différence dans le processus de fissuration du béton due à la qualité des granulats est directement indiquée par les mesures d'émission acoustique.

ZUSAMMENFASSUNG

Diese Arbeit untersucht die Eigenschaften von Beton mit Zuschlagstoffen minderwertiger Qualität (niedriges Gewicht und hohe Absorption). An Betonproben wurden im Verlauf einachsiger Druckprüfungen Schallemissionsmessungen durchgeführt. Die Ergebnisse zeigten, dass sich die Qualität von Betonzuschlagstoffen am deutlichsten im Elastizitätsmodul und nicht in der Druckfestigkeit von Beton zeigt. Anhand der Schallemissionsmessungen war es jedoch möglich, das unterschiedliche Bruchverhalten von Beton in Abhängigkeit von der Qualität der Zuschlagstoffe direkt zu bestimmen.

1. INTRODUCTION

Deterioration of aggregates caused by exhaustion of sound aggregates has become a widespread problem. It is generally known that physical quality of aggregate effects the strength, Young's modulus and durability of concrete. The factor of these effects is considered to be the lower strength of aggregate compared to the strength of mortar or cement paste matrix. So, it is assumed that because of excessive load or repeated load, destruction occurs inside or on the surface of aggregates before it occurs inside mortar or cement paste matrix.Therefore, reduction of water cement ratio of concrete in order to make compensation for the low strength of aggregate is a generalized method. However, the fracture process of concrete with inferior aggregates not yet elucidated must be clarified in order to use such aggregates for concrete. In this paper, the fracture process of concrete with water cement ratio varying from 30 to 70% and with several kinds of aggregates contained is studied by AE measurement and observation with a microscope.

2. PROPERTIES OF AGGREGATES AND MIX PROPORTIONS OF CONCRETE

Table-1 shows the properties of aggragates used for the experiments. Sound aggregates are River Sandstone and River Sand. Inferior coarse aggregate is Crushed Andesite. And inferior fine aggregate is Scoria. Mix proportions of concrete are shown in Table-2. Water cement ratios are 30,50, and 70%. The volume of each material is fixed in order to make clear comparison of effect of aggregates. Table-3 shows the combination of coarse and fine aggregates.

3. PROCEDURE OF EXPERIMENTS

Fig-1 shows the AE measurement system employed during the uniaxial compressive testing of the specimens. The diameter of the specimen is 10cm and the height is 20cm. AE measurement system includes the one-dimensional location system using two transducers installed on the side of the specimen in the axial direction. Determination of AE source location was performed only at the center portion (10cm) of the specimen in the axial direction in order to eliminate the effects of noise generated by the friction between the specimen and the loading plates. Table-4 shows the conditions of AE signal detection. Compressive loading test was carried out using a teflon sheet laid between the loading plate and the specimen to minimize the generation of noise. Loading rate was set at 500N/sec. Three specimens for each combination were used for the observation of cracks either inside or on the surface of aggregates.At first, 30% of the breaking load was applied and removed. The specimen was cut and polished after loading, then inspected with a microscope. In this way, 50% and 100% of the breaking load was applied and observation was performed respectively.

4. RESULTS AND CONSIDERATION OF THE EXPERIMENTS

4.1 Compressive strength and Young's modulus

Figs-2,3 show the compressive strength and the Young's modulus of concrete containing several kinds of coarse aggregates. The compressive strength of the concrete with inferior coarse aggregate was lower than that of the concrete with sound aggregate. However, according to the result of the experiment, the compressive strength showed a variation of 10%. Therefore, there will be some cases where the quality of aggregate cannot be accurately evaluated by the compressive strength of the concrete. According to Fig-3, the difference of Young's modulus caused by the quality of aggregate was more conspicuous than

TABLE-1 PROPERTY OF AGGREGATES

	Specific gravity	Absorption (%)	Kind of stone
Sound Coarse Aggregate	2.62	0.81	Sandstone
Inferior Coarse Aggregate	2.26	4.66	Crashed Andesite
Sound Fine Aggregate	2.59	1.02	Sandstone
Inferior Fine Aggregate	1.94	15.11	Scoria

TABLE-2 MIX PPOPORTION OF CONCRETE

W/C (%)	s/a (%)	W (kg/m³)	C (kg/m³)	S (ℓ/m³)	G (ℓ/m³)
30	40.8	189	630	249	361
50	44.9	189	378	310	381
70	48.8	189	270	354	371

TABLE-3 COMBINATION OF AGGREGATES

Fine Aggregate	Coarse Aggregate	W/C (%)		
		30	50	70
Sound	Sound	SS3C	SS5C	SS7C
Sound	Inferior	SI3C	SI5C	SI7C
Inferior	Sound	IS3C	IS5C	IS7C

TABLE-4 CONDITIONS OF AE DETECTION

Wave Speed	3500-4500	(m/sec)
Attenuation	35	(dB/m)
Pre-gain	40	(dB)
Main-gain	40	(dB)
Threshold Level	1.0	(V)

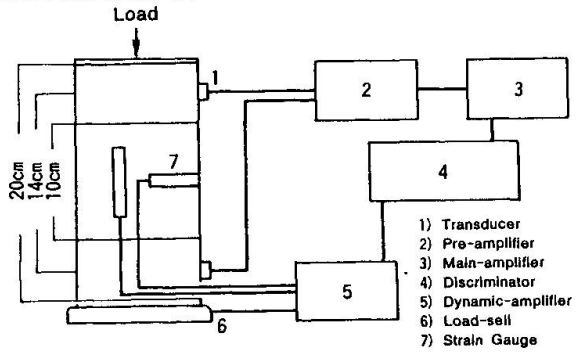

FIG-1 AE MEASUREMENT SYSTEM

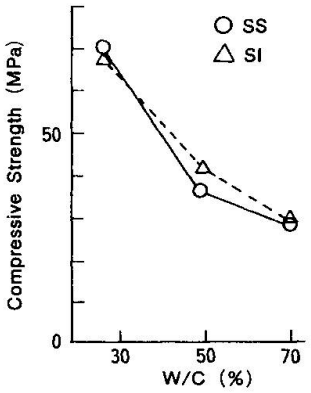

FIG-2 COMPRESSIVE STRENGTH OF SI SERIES

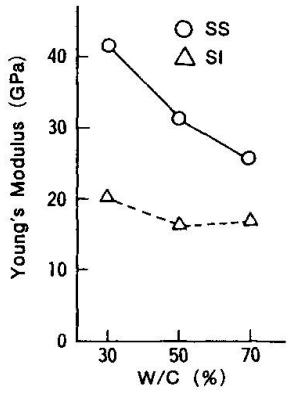

FIG-3 YOUNG'S MODULUS OF SI SERIES

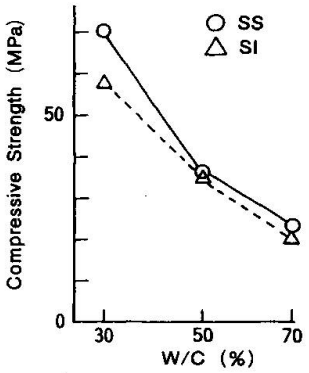

FIG-4 COMPRESSIVE STRENGTH OF IS SERIES

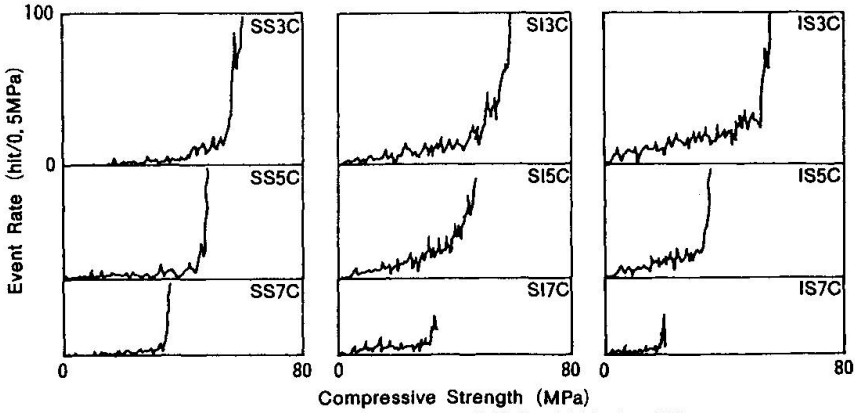

FIG-5 RELATION BETWEEN COMPRESSIVE STRESS AND EVENT RATE OF AE

that of compressive strength. Fig-4 shows the results of compressive test of concretes which contained several kinds of fine aggregates. These results also show that the compressive strength of concrete with inferior sand was lower than that of concrete with sound sand.

4.2 Compressive stress and AE events

Fig-5 shows the relationship between compressive stress and event rate of AE detected from the concrete with sound aggregate (SS series), sound fine aggregate and inferior coarse aggregate (SI series) and inferior fine aggregate and sound coarse aggregate (IS series). The event rate means the number of AE per loading stress of 0.5MPa. These results show that, in the case of the SS series, most AE signals occured at the stress near the breaking point without reference to the water cement ratio. On the other hand, in both cases of the SI and IS series, a large amount of AE signals occured from the low stress level stage, and this phenomenon was obvious in the concrete with a low water cement ratio of less than 50%. The difference of AE characteristic is assumed to be caused by the quality of aggregate. It is considered that the sound aggregate can accumulate the strain energy,so that the generation of micro cracks inside or on the surface of aggregate are restrained at a low stress level. In addition, at the stress near the breaking point, a precipitious destruction occur. This tendency is considered to be remarkable in the concrete with low water cement ratio because the effect of breeding or vacant spaces around the aggregate become negligible in such concrete. But the effect of water cement ratio was not confirmed in the experiments on the SS series. On the contrary, in the case of concrete with inferior coarse aggregate, the stiffness of coarse aggregate is the same or lower than that of mortar. Accordingly, it is assumed that many micro cracks inside or on the surface of aggregate are generated at a low stress level because of the small capacity of strain energy accumulated in aggregate and the stress concentration on them. In the concrete with inferior fine aggregate, the stiffness of mortar is much lower than that of coarse aggregate, therefore, the inside or on the surface of fine aggregate is considered to be easily destructed because of the stress concentration on the mortar.

4.3 Peak amplitude distribution of AE

Fig-6 shows the relationship between the peak amplitude and event counts of AE signals. Specimens are the SS series, the SI series and the IS series concrete with water cement ratio of 30%. In the figure, the stress level i.e. the percentage of compressive stress to the compressive strength, is divided into 2 ranges (0-50%, 0-100%), and the amplitude distribution curve for each range is shown respectively. The solid line is the approximation of the amplitude distribution curve. At the stress level of 0-50%, in the case of SS3C, the event counts of AE were generally small, regardless of amplitude. However, in the case of SI3C or IS3C, many AE signals with small amplitude of 0.1-1.0mv were detected. Then at the stress level of 0-100%, the event counts of AE detected from every specimen increased, but the amplitude distribution showed a tendency to vary with the quality of aggregate. In the case of SS3C, a considerable number of AE with large amplitude, apx. 10mv, were detected. On the contrary, in the case of SI3C or IS3C, most AE signals showed small amplitude of 0.1-1.0mv. This phenomenon is considered to be caused by the quality of aggregate, that is, the difference of the capacity of strain energy accumulated in the aggregate as mentioned in 4.2. Therefore, the fracture process of the concrete with inferior aggregate is different from that of the concrete with sound aggregate.

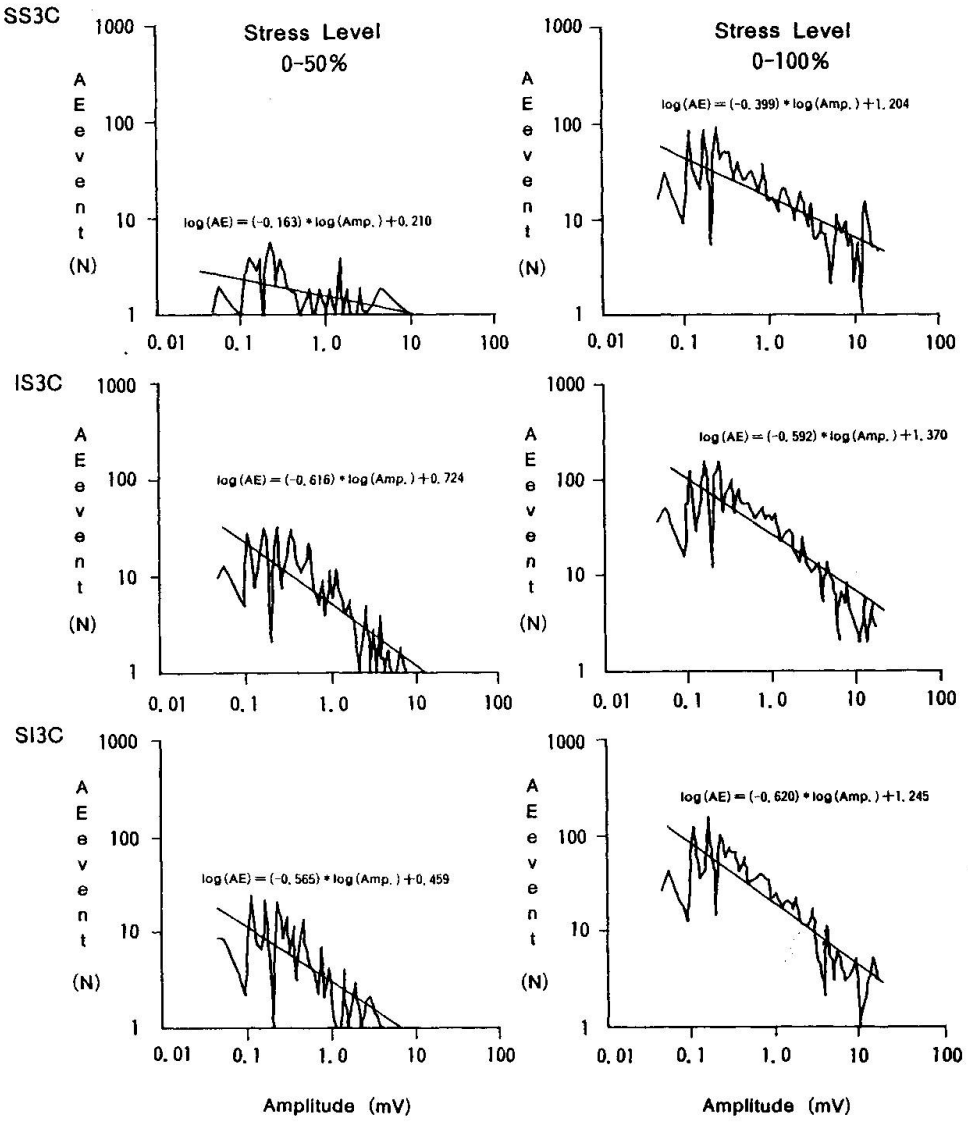

FIG-6 RELATION BETWEEN THE MAXIMUM AMPLITUDE AND EVENT COUNT OF AE

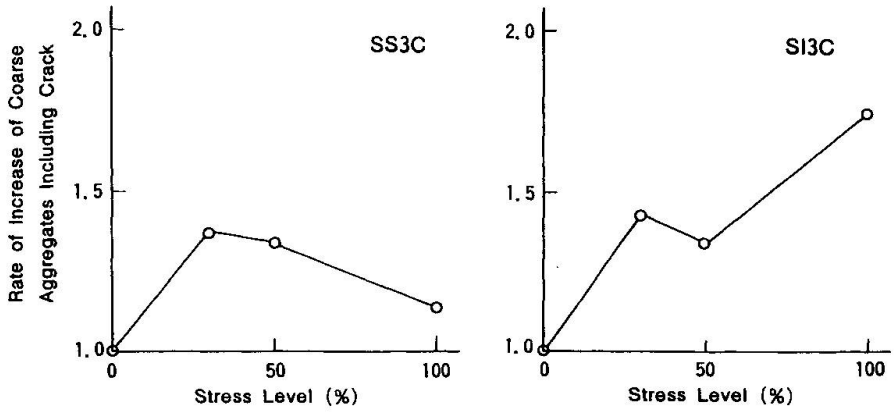

FIG-7 RELATION BETWEEN THE STRESS LEVEL AND THE RATE OF THE INCREASE OF COARSE AGGREGATES WITH CRACK INSIDE THEM

4.4 Micro cracks inside aggregates

Fig-7 shows the relationship between the stress level and the rate of increase of coarse aggregate with crack inside them. The rate of increase of coarse aggregate with crack was obtained by the following process.

1) To obtain the rate of destruction of coarse aggregate in the section of the specimen by observation with a microscope.

$$R = Gc/Go$$

where, R : the rate of destruction of coarse aggregate
Gc : the number of coarse aggregate with crack inside of them
Go : total number of coarse aggregate in the section of the specimen

2) To obtain the rate of increase of coarse aggregate with crack using the following equation.

$$C = Ra/Ro$$

where, C : the rate of increase of coarse aggregate with crack
Ra : the rate of destruction of coarse aggregate at the stress level of a %
Ro : the rate of destruction of coarse aggregate before loading

The results show that the number of inferior coarse aggregate with crack increased in proportion to the stress level while the number of sound aggregate with crack didn't indicate such a tendency. But, the fracture process of scoria which includes many voids in it, could not be confirmed clearly.

5. CONCLUSION

We conclude from the experiment as follows.

(1) Both compressive strength and static Young's modulus of the concrete containing inferior aggregates with low gravity and high absorption are lower than those of the concrete with sound aggregates. But because of the variation of compressive strength, there will be some cases where the quality of aggregate cannot be evaluated accurately by the compressive strength of concrete.
(2) During the uniaxial compressive testing of the concrete with sound aggregates, most of AE signals occur at the stress level near the breaking point. However, in the concrete with inferior aggregates, a large amount of AE are generated from the low stress level stage because of destruction inside or on the surface of aggregates.
(3) During the uniaxial compressive testing, many AE signals with relatively large amplitude are generated from the concrete with sound aggregates. On the contrary, amplitude of AE signals generated from the concrete containing inferior aggregates are generally small. This phenomenon is considered to be caused by the quality of aggregate including capacity of strain energy accumulated in them.

Accordingly, the quality of aggregate appears more clearly in the static Young's modulus than the compressive strength of the concrete containing them. These are simply the phenomena caused by the quality of aggregate and can by no means indicate the difference of the fracture process of the concrete. However, the difference of the fracture process of concrete due to the quality of aggregate is obviously indicated by the resuls of AE measurement during uniaxial compressive testing.

Durabilité du béton à haute résistance

Dauerhaftigkeit von Beton mit hoher Festigkeit

Durability of High Strength Concrete

Guy TACHÉ
Ing. CNAM
CEBTP
Paris, France

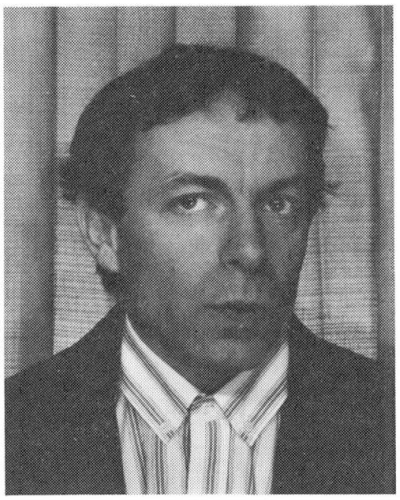

Jacques TRINH
Dr. Ing.
CEBTP
Paris, France

RÉSUMÉ

Cette communication traite de la durabilité du béton à haute résistance en présentant une étude expérimentale réalisée au CEBTP. Deux solutions de poutre fléchie sont comparées, une en béton de résistance courante, et l'autre en béton à haute résistance permettant une réduction de 25% de matière. Elles ont montré une durabilité comparable après avoir été exposées en atmosphères corrosives pendant deux ans.

ZUSAMMENFASSUNG

Dieser Beitrag behandelt die Dauerhaftigkeit von hochfestem Beton durch die Darstellung der im CEBTP durchgeführten experimentellen Forschungsarbeiten. Zwei Lösungen für Biegebalken, einer aus Normalfestigkeitsbeton, der andere aus Hochfestigkeitsbeton — wodurch eine Werkstoffeinsparung von 25% möglich wird — wurden verglichen. Sie zeigten eine vergleichbare Dauerhaftigkeit, nachdem sie zwei Jahre aggressiven Umweltbedingungen unterworfen worden waren.

SUMMARY

The paper deals with the durability of high strength concrete by presenting an experimental study carried out by the CEBTP. Two solutions for flexural beams are compared, one using concrete of normal strength and the other with a high strength concrete allowing a material saving of 25%. They have shown a comparable durability under corrosive atmospheres over a period of two years.

1. INTRODUCTION

L'accroissement de la résistance du béton ($f_{cm} \simeq 85$ MPa) entraîne une amélioration certaine de la compacité du matériau, par rapport à ce qui existe dans du béton de résistance plus usuelle ($f_{cm} \simeq 50$ MPa). C'est une meilleure garantie de la pérennité, que le béton à haute résistance offre avantageusement. Il reste cependant à la vérifier au niveau structural, du fait que dans le béton armé normal et le béton partiellement précontraint la fissuration peut induire la corrosion des armatures.

Toutefois de nombreuses études expérimentales ont été entreprises dans le monde aux fins d'étudier l'influence des fissures sur le développement de la corrosion des armatures. Citons les suivantes, parmi les plus importantes.

- CARPENTIER et SORETZ [1], en examinant des poutres en béton armé à la fois soumises à un chargement statique ou cyclique, et exposées à diverses aspersions agressives pendant une période de 2 ans, ont conclu que :
. l'effet de pompage ("respiration" des fissures) favorise la corrosion des armatures ;
. les fissures parallèles aux barres d'armature sont plus néfastes que celles qui leur sont transversales ;
. avec un enrobage suffisant en béton de bonne qualité, des fissures d'ouverture 0,3 mm n'induisent que des piqûres de corrosion peu dommageables.
- SCHIESSL [2] a étudié le comportement des poutres en béton armé exposées pendant 10 ans dans diverses atmosphères (urbaines, industrielles et marines). Les ouvertures des fissures étaient entre 0,15 et 0,4 mm. L'auteur a relevé que si dans les premiers temps (1 an) le taux de corrosion est fonction croissante de la largeur des fissures, au bout de 10 ans il n'existe plus de corrélation directe.
- Par l'examen de poutres conservées pendant 2 ans dans une ambiance de brouillard salin, ATIMTAYE et FERGUSON [3] ont indiqué que les facteurs primordiaux du phénomène, sont:le rapport eau/ciment ; l'épaisseur de l'enrobage des armatures; et le diamètre des barres. La fissuration semble n'avoir guère d'influence directe.
- MAKITA, MORI et KATAWAKI [4] ont observé, sur des poutres en béton armé, laissées pendant 3 ans dans la baie de Tokyo, qu'avec du béton gâché à l'eau douce, le taux de corrosion croît avec l'ouverture des fissures. Avec de l'eau de mer, les attaques se produisent indifféremment à proximité ou hors des fissures. Les auteurs ont recommandé de limiter la largeur des fissures du béton en surface de l'armature à 0,1 mm !

Ces quelques exemples et d'autres [par ex. 5, 6], concourent à forger l'opinion selon laquelle la largeur des fissures en surface du béton n'est pas un facteur primordial au développement de la corrosion des armatures. Mais toutes ces recherches sont difficilement comparables entre elles. Par ailleurs, il manque encore des références pour des poutres en béton à haute résistance d'une part, et d'autre part, la précontrainte partielle (b.p.p.) à cause du risque de corrosion de l'armature de précontrainte.

2. ETUDE EXPERIMENTALE ENTREPRISE

Dans le cadre du programme général d'études sur la durabilité des structures en précontrainte partielle [7], deux des corps d'épreuve sont réalisés avec du béton de résistance moyenne en compression d'environ 85 MPa. Ce sont des poutres en Té isostatiques (fig. 1), identiques à des poutres associées confectionnées avec du béton de résistance ($f_{cm} \simeq 50$ MPa) à l'exception que l'épaisseur de l'âme et du hourdis est diminuée de 25 %. Les principales informations sur les bétons sont portées au tableau 1.

Un examen préliminaire sous chargement mécanique a montré que l'on est arrivé à obtenir pour les deux solutions, un comportement tout à fait comparable en

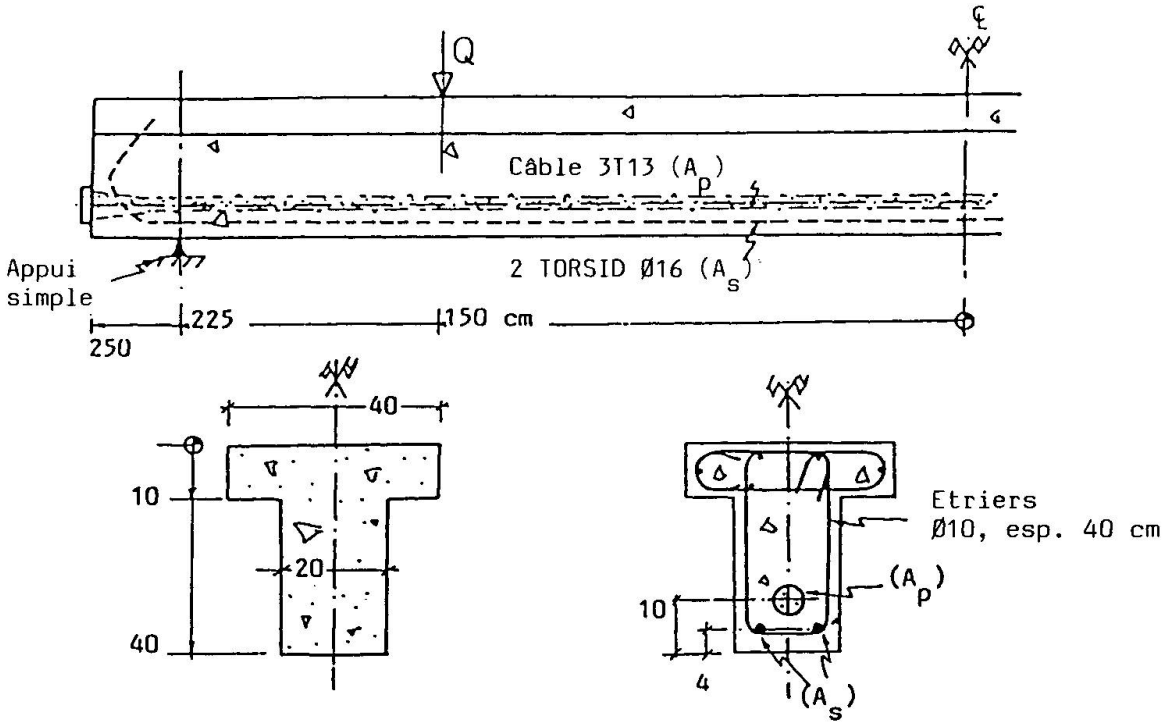

a) Poutres pour béton à résistance 50 MPa

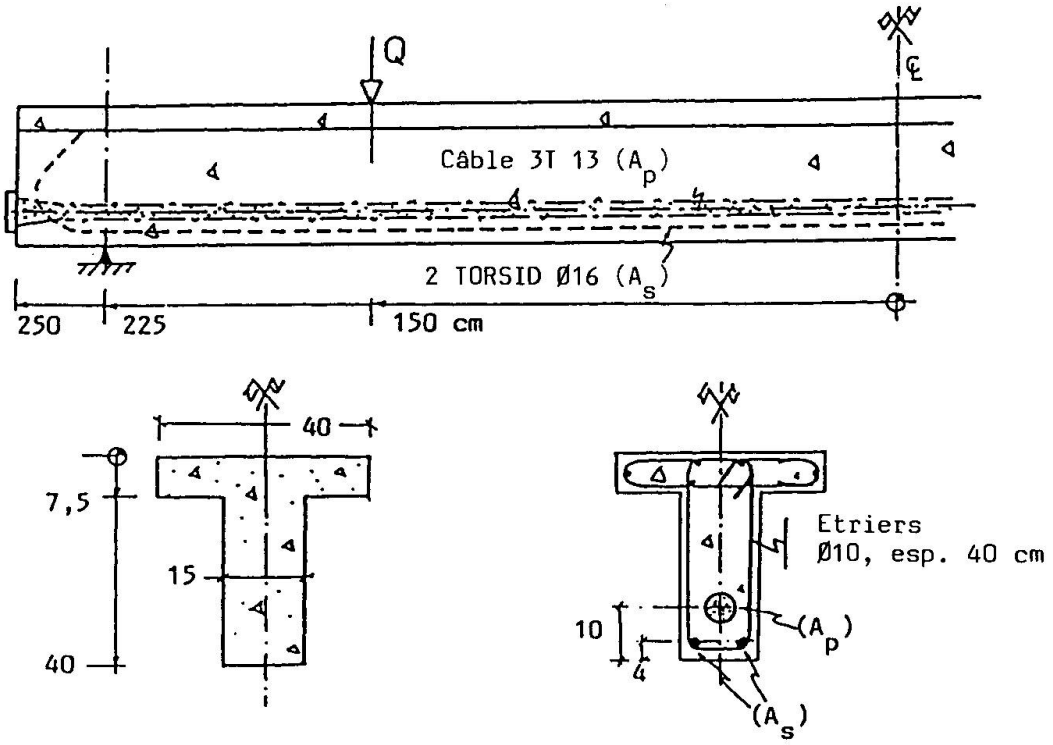

b) Poutres pour béton à résistance 85 MPa

Fig. 1 - Poutres d'essai

		Béton à	
		performance usuelle	haute résistance
(kg/m³)	Granulats (5/20 mm).....	1 080 (1)	1 267(2)
	Sable (0/5 mm).....	720 (1)	326(2) + 326 (1)
	Ciment.....	CPA HP : 350	CPA HP : 425
	Eau.....	190	145
	Plastifiant Sikafluid.....	/	6,37
	Affaissement (mm).....	60	50
	Age à l'essai (jours).....	52	53 et 58
(MPa)	Résistance en compression f_{cj} (3)..	50	85
	Résistance en traction f_{tj}.....	3,7	4,5
	Module de Young E_c	34 000	51 000

(1) Matériaux silico-calcaires de Seine.
(2) Calcaire du boulonnais (concassé).
(3) Essais sur cylindres standards (Ø = 16, h = 32 cm) en compression simple ou en fendage.

TABLEAU 1
Composition des bétons et principales propriétés mécaniques
(recherches NY et OL)

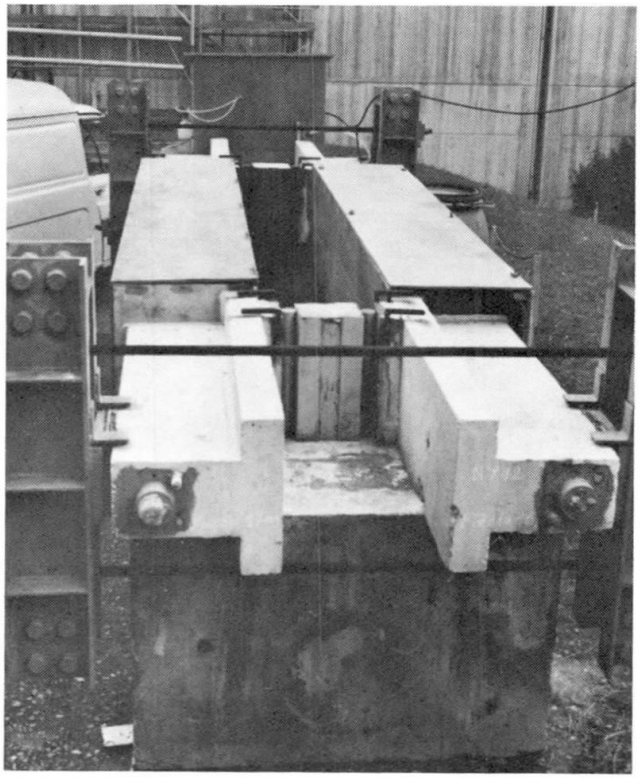

Fig. 2 - Dispositif d'exposition

service selon les règles françaises de calcul BPEL 83 [8].

Chacune des poutres est ensuite conservée durant 2 ans: .dans l'état fléchi atteint à l'application au départ du chargement correspondant à la limite de la précontrainte partielle suivant le BPEL 83. Ainsi les fissures en surface ont une ouverture permanente d'environ 0,15 mm et 0,20 mm, respectivement à la hauteur de l'armature de précontrainte et de l'armature passive ;

. dans une enceinte contenant une atmosphère agressive (fig. 2). Les deux environnements retenus sont, soit une atmosphère constituée d'un mélange gazeux à 50 % d'air et 50 % de CO 2 ; soit une aspersion intermittente (1/4 heure à chaque heure) d'une solution à 35 g de NaCl/litre.

Les conditions thermiques sont celles normales extérieures de Saint Rémy lès Chevreuse (France).

Le suivi pendant l'exposition des poutres est principalement orienté vers :

. la corrosion des armatures, par la mesure du potentiel électrochimique du ferraillage ;
. la pollution du béton, par prélèvement aux fins d'analyses chimiques (détermination des chlorures totaux, et de silice soluble).
Les corps d'épreuve sont aussi examinés périodiquement pour faire la constatation de taches de rouille, d'éclats de béton d'enrobage, des ouvertures de fissures, etc.

Au terme du temps d'exposition, il était prévu de faire un chargement statique des corps d'épreuve pour évaluer la capacité portante résiduelle, et permettre l'examen de l'état des armatures.

3. RESULTATS

3.1 Suivi de la corrosion des armatures

Les diagrammes de la figure 3 montrent l'évolution de la valeur moyenne du potentiel électro-chimique en fonction du temps pour les deux conditions d'exposition retenues.

On y constate qu'en exposition saline, la passivation des aciers survient très vite. De même qu'apparaissent des gradients importants localisés près des fissures où des coulures de rouille sont observées. Avec le temps la dépassivation générale persiste, avec toutefois une tendance à la repassivation à la fin de la 2e année. les gradients tendent également à diminuer mais leur localisation est conservée.

En atmosphère chargée en gaz carbonique, la valeur moyenne n'évolue pratiquement pas, c'est caractéristique de la passivité de l'acier d'armature. Des gradients locaux existent au départ,notamment aux fissures du milieu de la poutre, mais ils s'estompent avec le temps. Ce corps d'épreuve ci a conservé au bout des 2 ans, un aspect parfaitement sain.

3.2 Rupture finale

Seule la poutre conservée en milieu salin ayant montré certaines dégradations (coulures de rouille aux fissures, quelques éclats de l'enrobage) est ensuite soumise à l'essai de chargement jusqu'à rupture. Il n'a pas été constaté toutefois de perte de résistance, ni de ductilité.

L'armature passive présente quelques zones corrodées correspondant à des sections fissurées, de même que les cadres transversaux qui peuvent s'y trouver. Mais aucune corrosion particulière n'est apparue sur la gaine métallique du câble de précontrainte.

Ces résultats sont très analogues à ceux acquis sur des poutres associées confectionnées avec du béton de résistance plus courante.

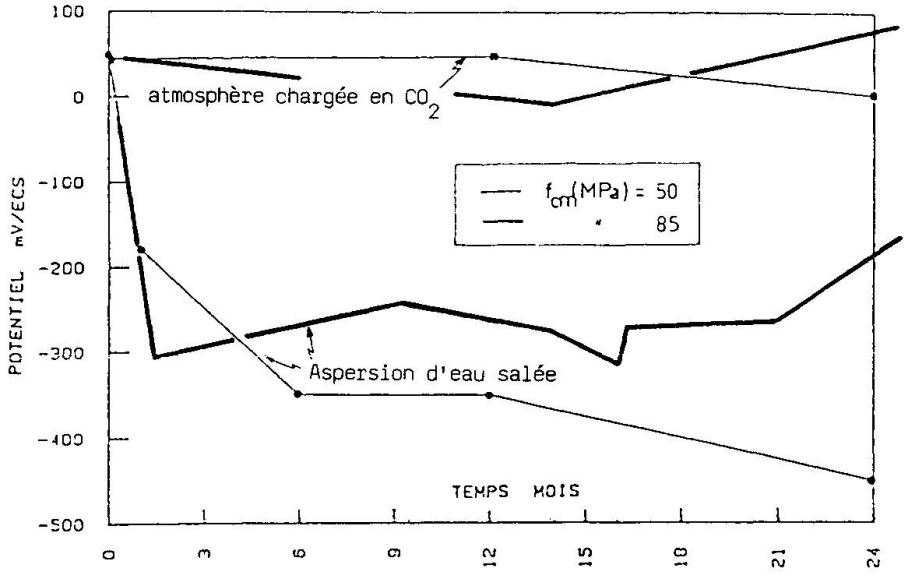

Fig. 3 - Evolution du potentiel électro-chimique.

4. PREMIERE CONCLUSION

Ces essais apportent des références de durabilité de pièces partiellement précontraintes en béton à haute résistance. On peut donc, au vu de ces résultats, escompter une pérennité, comparable au béton de résistance plus usuelle, bien que la solution permet une réduction de béton (≃ 25 %). Toutefois il est encore souhaitable de disposer de résultats d'observations à plus long terme (que 2 ans)

BIBLIOGRAPHIE

1. CARPENTIER L. & SORETZ M.S., Contribution à l'étude de la corrosion des armatures dans le béton armé. Annales de l'ITBTP N° 223-224, Paris, Juillet-Août 1966.
2. SCHIESSL P., Admissible crack-Width in reinforced concrete structures. Colloque inter-Associations "Comportement en service des ouvrages en béton", Liège, Juin 1975.
3. ATIMTAYE & FERGUSON P.M., Early chloride corrosion in reinforced concrete. ACI Journal 55, nov. 1973.
4. MAKITA M, MORI T. & KATAWAKI, Marine corrosion behaviour of reinforced concrete. ACI S.P 65, 16.
5. BEEBY A.W., Corrosion of reinforcing steel in concrete and its relation to cracking. The Structural Engineer, N° 3, Vol. 56 A, Mars 1978.
6. TACHE G. & TRINH J., Fissuration et durabilité du béton partiellement précontraint. Compte rendu du Symposium AIPC, Paris-Versailles 1987.
7. FOURÉ B & TRINH J., Quelques résultats de recherches appliquées au calcul pratique des structures en béton. Annales ITBTP, N° 469, Paris, Nov. 1988.
8. HOANG L.H. & TRINH J., Experimental behaviour in bending of high strength concrete beams. Symposium "Use of High Strength Concrete", Stavanger, mars 1987.

Verbundmittel in spritzbetonverstärkten Stahlbetonbalken

Bond anchors in Shotcrete Reinforced Beams

Goujons d'adhérence dans des poutres renforcées par du béton projeté

Horst G. SCHÄFER
Prof. Dr.-Ing.
Universität Dortmund
Dortmund, BR Deutschland

H. G. Schäfer, geb. 1936, promovierte als Bauingenieur an der TH Darmstadt. Er arbeitete bei der Baufirma Wayss & Freytag und im Ingenieurbüro BGS in Frankfurt. Er lehrte an der TH Darmstadt, war vier Jahre für die GTZ in Dar es Sallam (Tanzania) tätig, bevor er 1985 einem Ruf an die Universität Dortmund folgte.

Gerhard BÄÄTJER
Dr.-Ing.
Universität Dortmund
Dortmund, BR Deutschland

G. Bäätjer, geboren 1941, studierte Bauingenieurwesen an der TU Hannover. Er arbeitete vier Jahre bei der Baufirma Philipp Holzmann im Technischen Büro in Köln. Anschliessend war er an der Ruhr- Universität Bochum tätig, promovierte dort und wechselte 1986 an die Universität Dortmund.

ZUSAMMENFASSUNG

Die Biegetragfähigkeit von Stahlbetonbalken kann vergrössert werden, indem Zulagebewehrung in eine Spritzbetonschicht eingebettet wird. An zwei Versuchsbalken wird der Einfluss von Verbundankern in der Verbundfuge auf das Tragverhalten untersucht. Bis nahe an die Bruchlast verhalten sich spritzbetonverstärkte wie monolithisch hergestellte Balken. Mit Verbundankern versagen die Träger mit Vorankündigung, ohne Verbundanker gehen sie schlagartig zu Bruch.

SUMMARY

The flexural bearing capacity of reinforced concrete beams can be increased by embedding additonal reinforcing bars in a layer of shotcrete. The influence of adhesive anchors crossing the interface between concrete and shotcrete is being studied on two test beams. Up to near failure load the bearing behaviour is the same as for monolithically cast beams. With the application of bond anchors, however, there are evident signs of failure beforehand, whereas the absence of bond anchors leads to an abrupt collapse.

RÉSUMÉ

La résistance à la flexion de poutres en béton armé peut être augmentée par encastrant de l'armature additionelle dans une couche de béton projeté. L'influence de goujons d'adhérence traversant la surface entre le béton original et le béton projeté est étudiée à deux poutres d'essai. Jusqu'au près de la charge de rupture le comportement est le même que pour des poutres en réalisation monolithe. Par l'application de goujons d'adhérence la rupture s'annonce à temps, tandis que l'absence d'un ancrage a pour conséquence une rupture subite.

1. PROBLEMSTELLUNG

Zur nachträglichen Verstärkung von Stahlbetonbalken ist die Spritzbetontechnik besonders geeignet [1, 2]. Nach den deutschen Richtlinien [3] und Normenentwürfen [4] sind zur Übertragung der Schubkräfte in der Verbundfuge "Verbundmittel" anzuordnen. Dieses Bemessungskonzept führt bei nur unterseitig verstärkten Stahlbetonbalken auf Verbundmittelquerschnitte, die häufig nicht untergebracht werden können. Aus diesem Grunde wird an der Universität Dortmund ein Forschungsvorhaben durchgeführt mit dem Ziel, den tatsächlich erforderlichen Bedarf an Verbundmitteln zu ermitteln.

2. VERSUCHSKÖRPER

Um die Grenzen auszuloten, wurden bisher zwei Balken untersucht (Fig. 1). Die beiden Balken waren so ausgelegt, daß die Bügel im Altbeton ausreichende Reserven zur Aufnahme der erhöhten Schubkräfte nach der Verstärkung der Biegezugbewehrung aufwiesen. Über Versuche an Balken mit zugelegter Biegezug- und Schubbewehrung berichtet Eibl [5]. Die beiden Versuchsbalken (VB) unterschieden sich in der Anzahl der Verbundmittel:

- VB1 wurde mit 29 HILTI-Verbundankern M 16 in gleichmäßigen Abständen von 15 cm in versetzter Anordnung vorschriftengemäß ausgelegt;
- in VB2 wurden nur an den Enden der Spritzbetonverstärkung je 2 HILTI-Verbundanker M 10 eingebaut.

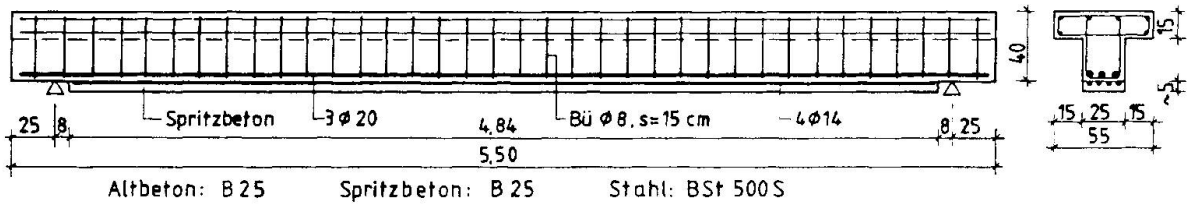

Fig. 1 Abmessungen und Bewehrung der Versuchsbalken (Verbundmittel n. dargest.)

Der Spritzbeton wurde in zwei Lagen im Trockenspritzverfahren aufgetragen; der Altersunterschied zwischen Altbeton und Spritzbeton betrug bei VB1 42 Tage und bei VB2 36 Tage.

3. VERSUCHSDURCHFÜHRUNG

Die Stützweite der Balken wurde im ersten Versuchslauf zu l = 5 m gewählt (Fig. 2). Im zweiten Versuchslauf an der intakten Hälfte wurden die Balken um die Vertikalachse gedreht und so in die Prüfmaschine eingebaut, daß sich die Stützweite auf l = 3 m verkürzte und der Prüfzylinder in der Feldmitte stand.

Erster Versuchslauf (l = 5,00 m):

- Zunächst wurde die Belastung stufenweise etwa bis zur festgelegten Gebrauchslast gesteigert. Die Belastung erfolgte kraftgeregelt mit 126 N/s.
- Nach Erreichen der Gebrauchslaststufe wurden 9000 Lastwechsel aufgebracht (Frequenz 1 Hz; Oberlast/Unterlast = 1,0/0,7-fache Gebrauchslast).
- Anschließend wurden die Balken bis zur Grenztragfähigkeit belastet, wobei die Last weggeregelt mit 1,2 mm/min gesteigert wurde.

Zweiter Versuchslauf (l = 3,00 m):

- Die intakten Restbalken mit 3 m Stützweite wurden zunächst kraftgeregelt mit 126 N/s etwa bis zur Gebrauchslast belastet.
- Nach vollständiger Entlastung wurde die Last weggeregelt mit 1,2 mm/min (VB1) bzw. 0,8 mm/min (VB2) bis zur Grenztragfähigkeit gesteigert.

Bei allen Versuchen wurden Meßdaten für Längsstabdehnungen, Bügeldehnungen, Durchbiegung und Rißbreiten aufgenommen (Fig. 3).

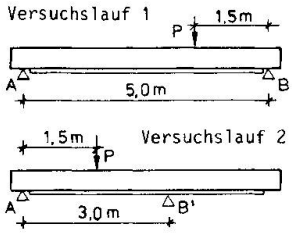

Fig. 2 Systemskizzen

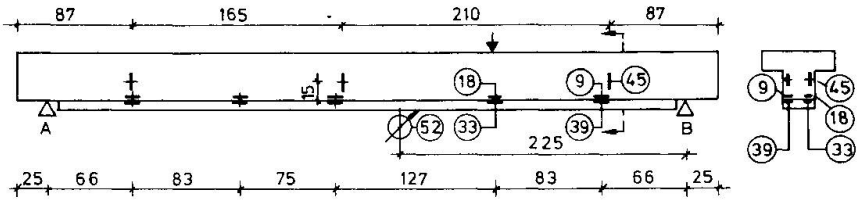

Fig. 3 Lage der Meßstellen

4. VERSUCHSERGEBNISSE

4.1 Tragverhalten

Bei VB1 traten unter höheren Lasten feine horizontale Risse in der Verbundfuge auf. Er zeigte jedoch wie ein monolithisch hergestellter Balken ein ausgeprägtes duktiles Bruchverhalten. Die Tragfähigkeit war erst erschöpft, als sich unterhalb der Einzellast ein Biegeriß weit öffnete und die weggeregelte Last nicht weiter gesteigert werden konnte. Der Versuch wurde abgebrochen als sich in der Betondruckzone unterhalb des Prüfzylinders erste Risse aufgrund der großen Rotation entwickelten. Die Bruchlast betrug 310 kN, was dem $\gamma = 2{,}33$-fachen der rechnerischen Gebrauchslast entspricht.

Bei VB2 traten kurz vor Erreichen der Bruchlast sehr flach geneigte Risse in Höhe der Verbundfuge auf. Das Versagen erfolgte durch schlagartiges Aufreißen der Verbundfuge im gesamten Querkraftbereich zwischen Einzellast und nahem Auflager. Die Zulagebewehrung konnte sich nicht mehr an der Lastabtragung beteiligen. Die weggeregelte Last ging dabei vom Höchstwert $P_u = 303$ kN auf 169 kN zurück und mußte allein vom Altbetonbalken aufgenommen werden. Die Bruchsicherheit bei VB2 betrug gegenüber der rechnerischen Gebrauchslast $\gamma = 2{,}27$. Alle relevanten Daten sind in den Tabellen 1 bis 3 zusammengestellt. Im Versuchslauf 1 ($l = 5$ m) ergaben sich für beide Balken und im Versuchslauf 2 ($l = 3$ m) für Balken VB1 die gleichen Sicherheiten. Im Versuchslauf 2 bei Balken VB2 war sie geringer. Bei VB2 trat das Versagen schlagartig ein, so daß hier nach deutschen Vorschriften eine Sicherheit von 2,1 eingehalten werden müßte. Dieser Wert wurde im Versuchslauf 1 nahezu erreicht, im Versuchslauf 2 dagegen nicht. Beide Balken wiesen bis direkt vor Erreichen der Bruchlast von VB2 nahezu gleiche Durchbiegungen auf (Fig. 4).

Nenndurchmesser [mm]	Istquerschnitt [mm²]	Streckgrenze [MN/m²]	Zugfestigkeit [MN/m²]
6	28,8	490,1	573,1
8	52,3	478,2	539,1
14	159,9	534,1	624,9
20	317,1	532,4	625,7

Tabelle 1 Querschnitts- und Festigkeitswerte der Betonstähle

Balken	Betonalter [Tage]	Druckfestigkeit β_{ws} [MN/m²]
VB1	28	34,6
	104 1)	40,5
	110 2)	36,9
VB2	28	28,7
	96 1)	33,6
	98 2)	30,4

1) Versuchslauf 1 2) Versuchslauf 2

Tabelle 2 Betonfestigkeiten

Versuchs-lauf	Balken	Gebrauchslast [kN]			Bruchlast	Bruchsicherheit	
		unverstärkt	verstärkt				
		nom P_o	nom P_1	ef P_1	P_u [kN]	P_u/nom P_1	P_u/ef P_1
1	VB1	76	133	148	310	2,33	2,09
	VB2	76	133	145	303	2,27	2,09
2	VB1	120	200	222	464	2,32	2,09
	VB2	120	200	218	374	1,87	1,72

Tabelle 3 Gebrauchslasten, Bruchlasten und Bruchsicherheiten

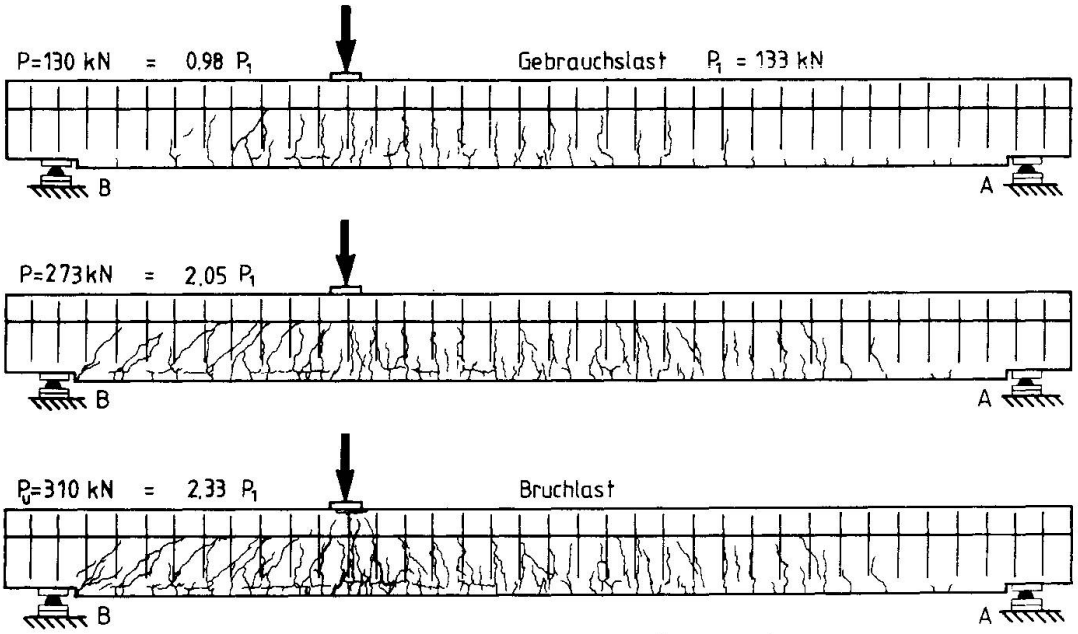

Fig. 5 Rißbilder Balken VB1, Versuchslauf 1 (l = 5 m)

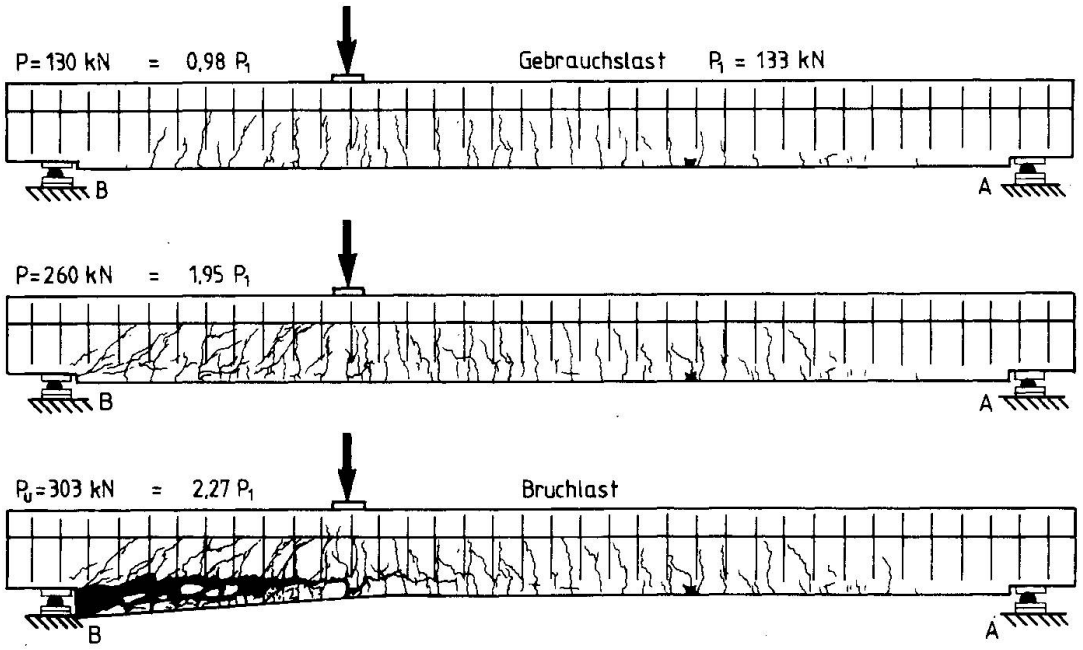

Fig. 6 Rißbilder Balken VB2, Versuchslauf 1 (l = 5 m)

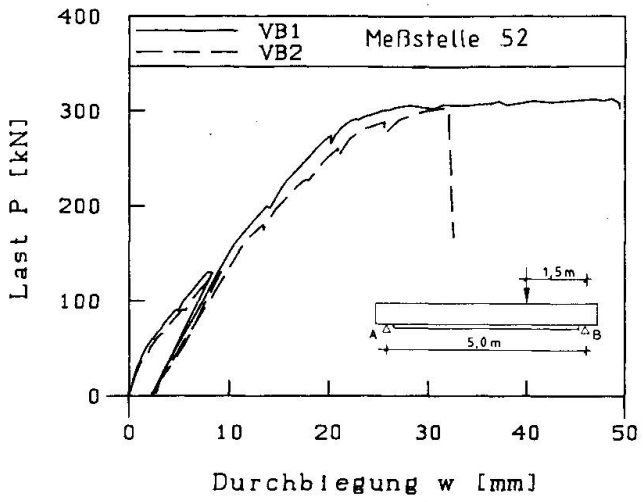

Fig. 4 Last-Verformungs-Diagramme

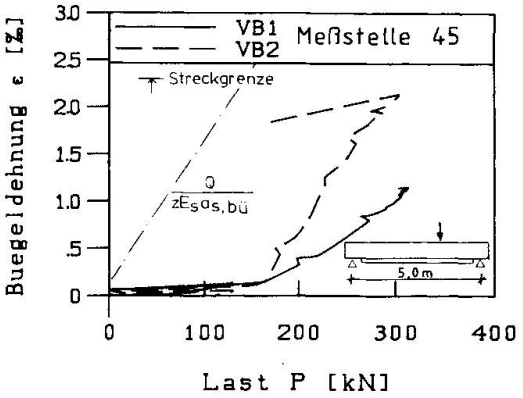

Fig. 7 Bügeldehnungen (VB1 und VB2, Meßstelle 45)

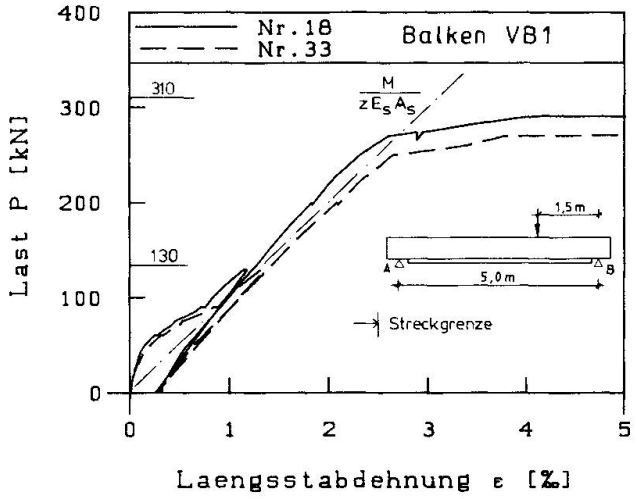

Fig. 8 Längsstabdehnungen (VB1, Meßstellen 18 und 33)

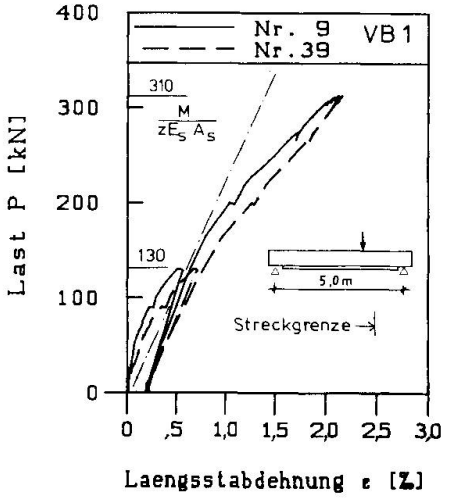

Fig. 9 Längsstabdehnungen (VB1, Meßstellen 9 und 39)

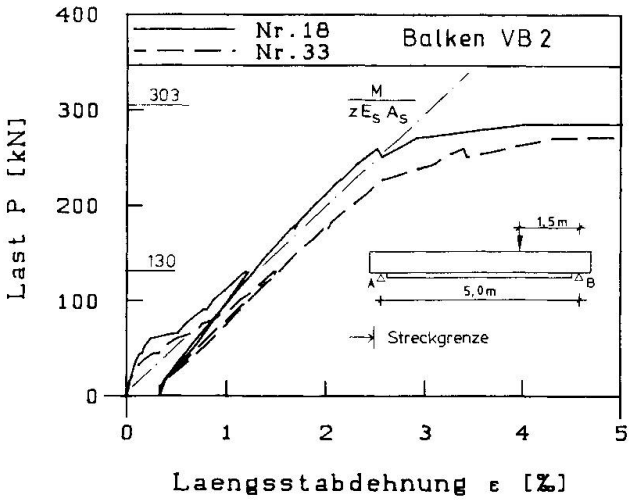

Fig. 10 Längsstabdehnungen (VB2, Meßstellen 18 und 33)

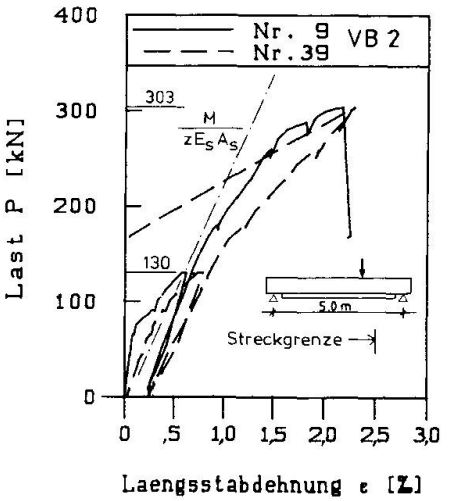

Fig. 11 Längsstabdehnungen (VB2, Meßstellen 9 und 39)

4.2 Rißbild

Die Rißbilder sind in Fig. 5 und Fig. 6 für den jeweils ersten Versuchslauf dargestellt. Beide Balken wiesen im Gebrauchslastbereich ein völlig "normales" Rißbild auf. Die gemessenen Rißbreiten lagen durchweg unter 0,1 mm. Die 9000 Lastwechsel umfassende Schwellbeanspruchung führte nur zu unbedeutenden Veränderungen. Schubrisse bildeten sich erst weit oberhalb der Gebrauchslast.

4.3 Beanspruchung der Bügel

Für VB1 und VB2 mit l = 5 m sind in Fig. 7 die gemessenen Dehnungen eines Bügelschenkels aufgetragen. Es stellte sich bei beiden Balken der typische Dehnungsverlauf ein: erst mit Beginn der Schubrißbildung, im vorliegenden Fall oberhalb der Gebrauchslast, stellte sich das die Bügelbeanspruchung bestimmende Fachwerktragverhalten ein. Die Streckgrenze wurde unter Bruchlast nicht erreicht.

4.4 Beanspruchung der Längsstäbe

Der Verlauf der Längsstabdehnungen ist für VB1 in Fig. 8 und 9 und für VB2 in Fig. 10 und 11 dargestellt. Das Dehnungsverhalten beider Balken ist bis kurz vor Erreichen der Bruchlast das gleiche. Für die Zulagestäbe wurden deutlich größere Dehnungen gemessen als für die Stäbe im Altbetonbalken. Unter der Einzellast überschritt der Stahl die Streckgrenze und erreichte Dehnungen von mehr als 10 ‰. Während bei VB1 die Zulagebewehrung auch unter der Höchstlast noch voll mittrug, fiel bei VB2 als Folge des Verbundfugenversagens die Dehnung auf Null ab. Gleichzeitig stieg die Dehnung der Biegezugbewehrung im Altbeton - obwohl die Last zurückging - etwas an, da die noch vorhandene Last nunmehr allein vom ursprünglichen Stahlbetonquerschnitt übertragen werden mußte. Die Übereinstimmung der rechnerischen mit den gemessenen Werten ist gut, wenn man beachtet, daß sich die berechneten Werte in Fig. 9 und 11 bei Berücksichtigung des Fachwerktragverhaltens entsprechend dem Versatz der Zugkraftlinie gegenüber der M/z-Linie in Richtung der gemessenen Werte verschieben.

5. AUSBLICK

In weiteren Versuchen, die vom Deutschen Beton-Verein unterstützt werden, soll systematisch erkundet werden, welche Mindestmenge an Verbundmitteln erforderlich ist, ohne daß das gutartige duktile Tragverhalten darunter leidet. Es ist zu erwarten, daß künftig die Verbundmittelquerschnitte gegenüber [4] erheblich reduziert werden können.

LITERATURVERZEICHNIS

1. HOLZ K., Anschlüsse, Verstärkungen und Konstruktionsänderungen - flexibel bauen auch mit Stahlbeton. Beton- und Stahlbetonbau 79 (1984), S. 293-298 und S. 322-327.
2. RUFFERT G., Ausbessern und Verstärken von Betonbauteilen. 2. Auflage, Beton-Verlag, Düsseldorf, 1982.
3. Richtlinien für die Ausbesserung und Verstärkung von Betonbauteilen mit Spritzbeton. Fassung Oktober 1983. Deutscher Ausschuß für Stahlbeton.
4. DIN 18551; Spritzbeton. Entwurf 1989.
5. EIBL J., BACHMANN H., FATH F., Abschlußbericht zum Forschungsvorhaben: Nachträgliche Verstärkung von Stahlbetonbauteilen mit Spritzbeton. Universität Karlsruhe, Institut für Massivbau und Baustofftechnologie, 1988.

Frost Resistance of Fibre Reinforced Concrete Containing Microsilica

Résistance au gel de béton renforcé de fibres de micro-silice

Frostbeständigkeit von faserverstärktem Beton mit Flugasche-Zusatz

Sergio LAI
Civil Engineer
University of Cagliari
Cagliari, Italy

Sergio Lai, born in 1954 has a degree in Civil Engineering and for 14 years has been engaged in materials testing at the University of Cagliari (Italy). He has carried out numerous investigations on the durability of concretes, participating in various International Congresses and has published more than 25 papers on the subject.

SUMMARY

This paper presents the results of extensive laboratory investigations aimed at determining the freeze-thaw resistance of conglomerates containing silica fume and polypropylene fibres. Particular attention has been focussed on the influence of mode of preparation on freeze-thaw resistance, as well as on the prediction of such resistance on the basis of tests of short duration.

RÉSUMÉ

Cet article présente les résultats d'une longue série d'essais de laboratoire cherchant a déterminer la résistance au gel-dégel des conglomérats contenants de la micro-silice et des fibres de polypropylène. Une attention particulère a été portée aussi bien à l'influence des méthodes de préparation sur la résistance au gel-dégel qu'aux prévisions de cette résistance avec des essais de courte durée.

ZUSAMMENFASSUNG

Anhand eines Langzeitversuches wurde die Frostbeständigkeit von faserverstärktem Beton mit Flugasche-Zusatz ermittelt. Besondere Aufmerksamkeit wurde dem Einfluss der Verarbeitungsmethode sowie der Korrelation zu Kurzzeitversuchen gewidmet.

1. INTRODUCTION

Condensed silica fume, a by-product of the ferro-silicon industry, is used as a partial replacement o in addition for cement in concrete and mortar. First investigation indicated improved frost resistance (1), (2), (3). When admixed with a conglomerate, silica fume (micronized silica) acts as a filler and its pozzolanic action is enhanced. The addition of polypropylene fibres to the cement mix, serves to check the formation of cracks caused by shrinking. Superplasticizing admixtures allow to balance the larger requirement of mixing water caused by the micronized silica and polypropylene fibres.
The purpose of this paper is to study the frost resistance of concretes containing condensed silica fume and polypropylene fibres when tested in accordance with UNI 7087-72, and with ASTM C666, procedure A, modificate.

2. EXPERIMENTAL PROCEDURES

2.1 Material and proportion

The cement used was Portland 525. The fine aggregate (specific gravity: 2,70, absorption: 2,65 %, fineness modulus: 2,90) was river sand and coarse aggregate (specific gravity: 2,54, absorption: 3,58 %, fineness modulus: 6,40, maximum size: 20 mm) was crushed gravel. Superplasticizer (naphthalene-sulphonate condensed with formaldehyde) was used as admixture. Mix proportion are shown in table 1. Water cement-silica ratios of the specimens were selected as 30, 35, 40, 45 and 50 percent for all freeze-thaw tests (slow and rapid freeze-thaw test up to 30 cycles, and standard test in accordance with UNI 7087-72).
The mix designation are shown in table 2.

2.2 Preparation of specimens

Eight 100x100x400 mm prism and eight 100 mm cubes were cast from each mix. After casting, the molded specimens were covered with a plastic sheet and left in the casting room at 20° C for 24 hours.
After demolding they were cured in 20° C water for 14 days (ASTM C666, procedure A, modificate); for UNI test they were cured in 20° C climatic room for 45 days and 20° C water for another 15 days.

3. TEST METHODS

3.1 UNI 7087-72

The freeze-thaw cycle consist of:
-lowering the temperature of the specimens in air from +5° to -25° C;
-keeping temperature at -25° C;
-elevating the temperature to +5° C with the specimens in water;
-keeping the temperature at +5° C.
The elastic modulus, length and mass of the specimens are measured periodically. The test continues for 300 cycles; it can be stopped when the conglomerate undergoes either a reduction in dynamic elastic modulus of 60 %, an expansion of 0,2-0,3 % or else a mass loss of more than 3 %.

3.2 ASTM C666, PROCEDURE A MODIFICATES (RAPID F-T TEST)

This test method covers the determination of the resistance of concrete specimens when subjected to rapidly repeated cycles of freezing and thawing in water. A freezing-and-thawing cycle consist of alternately lowering the temperature of the specimens from +5° C to -18° C (3 hours) and raising it from -18° C to 5° C (1 hour). The modification consist in considering temperatures varying between +5° and -20° C with different gradients in accordance with figure 1. The relative moduli of elasticity of the test specimens, in thawed condition, are determined.

3.3 Slow F-T tests

The slow freezing-thawing tests by two cycle a day were performed in air and with temperature simulated in agreement with figure 2.

4. TEST RESULT FOR RAPID AND SLOW FREEZE-THAW

Result of the rapid freeze-thaw test up to 30 cycle are shown in figures 3-4, which illustrates the relation between the number of cycles and relative dynamic modulus of elasticity for W/C+SF=0,50 and 0,45. After freeze-thaw test up 30 cycles, relative dynamic modulus dropped to about 70-85 and 75-83 percent respectively.
Results for slow freeze-thaw test up 30 cycles is shown in figure 5, which shows the relation between the number of cycles and relative dynamic modulus of elasticity after 7 days and 28 dayd curing at water/cement-silica ratio of 45 percent. The slow freeze-thaw test is not the most suitable for prediction long term behaviour as temperature gradients are too small and temperature ranges are not very wide.

5. TEST RESULT FOR UNI 7087-72 METHOD

The freeze-thaw tests were performed for 300 cycles and some of the results are shown in figure 6. The diminution in dynamic modulus fluctuates considerably, from between 40 % (C50,0) and 20 % (C45,20). It is shown that performance in freeze-thaw cycles improves both with increasing silica fume additions and decreasing W/C+SF ratio. Along with dynamic modulus measurements, the specimens were also tested, every certain number of cycles, to determine the decline in compression properties. Figure 7 shows dynamic modulus versus compressive strength for some W/C+SF ratios, keeping SF content constant at 20 % (80 kg/cu m).

6. CONCLUSIONS

Test results are summarized as follows:

1) Concretes containing silica fume were observed to perform better in freeze-thaw cycles; in certain cases the diminution is of the order of 20 %, against 38 % observed in the controls.
2) With fast freeze-thaw cycles the reduction in dynamic elastic modulus is 20, 24 and 28 % for the conglomerates with W/C+SF of 0,5 and silica fume addi-

ns of 20, 10 and 5 % by weight of cement.

3) The C50,20 series showed, with the UNI test, a reduction after 300 cycles of 25 % compared to 20 % with the rapid test.
4) The C50,0 series showed a diminution in dynamic elastic modulus of 39 % with the UNI test compared to 26 % with the rapid test.
5) Although not all the data necessary for a statistical analysis are available (the experiments are still in progress) the results so far suggest that for the conglomerates containing silica fume and for the controls, the freeze-thaw resistance can be predicted by means of the rapid test, since the UNI test yields a diminution in dynamic modulus greater by between 25 and 55 %.

REFERENCES

1. TRAETTEBERG A., Frost Action in Mortar of Blended Cement with Silica Dust.Durability of Buiding Materials and Component, ASTM, STP-691, Philadelphia, 1980, pp.536-548.

2. CARETTE T. and MALHOTRA V.M., Mechanical Properties, Durability and Drying Shrinkage og Portland Cement Concrete Incorporating Silica Fume. ASTM Cement, Concrete and Aggregates, Vol.5, No. 1, 1983, pp.3-13.

3. YAMOTO T., EMOTO Y. and SOEDA M., Strength and Freezing-and-Thawing Resistance of Concrete Incorporating Condensed Silica Fume. Proc. 2nd International Conference on Fly-Ash, Silica Fume, Slag and Natural Pozzolans in Concrete, Madrid, Spain, SP 91-54, 1986, pp.1095-1118.

4. LAI S., Sulla messa a punto di un conglomerato fibroso con microsilica resistente ai cicli di gelo-disgelo. Atti delle Giornate AICAP, Napoli, Italy, 4-6 Maggio 1989.

5. LAI S., On the use of Silica Fume, Polypropylene Fibres and Superplasticizers in the preparation of Highly Durable Concretes. Proc. of 2nd NCB International Seminar on Cement and Building Materials, New Delhi, 30 Jan.-3 Feb.1989.

W/C+SF	Slump	Unit Weight (kg/cu m)					
	(cm)	W	C	S	G	SF	Superplast.
.30-.35						20	
.40-.45	10	variab.	400	700	998	40	variable
.50						80	

Table 1 Mix proportion

	W/C+SF	SF	Fibres
C30,0	.30	0	0
C30,5	.30	20	1
C30,10	.30	40	1
C30,20	.30	80	1
.....	...	..	.
C50,0	.50	0	0
C50,5	.50	20	1
C50,10	.50	40	1
C50,20	.50	80	1

Table 2 Mix designation

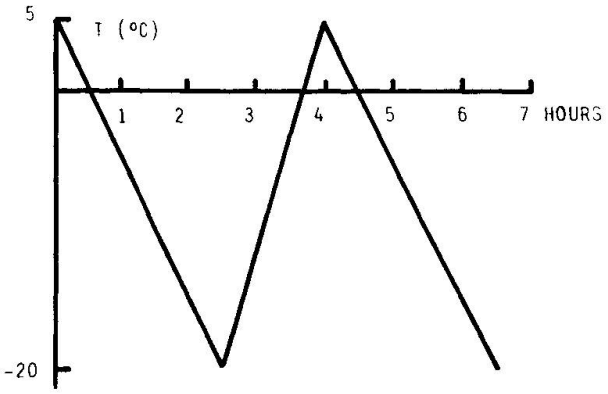

Fig.1 Rapid F-T test (gradients)

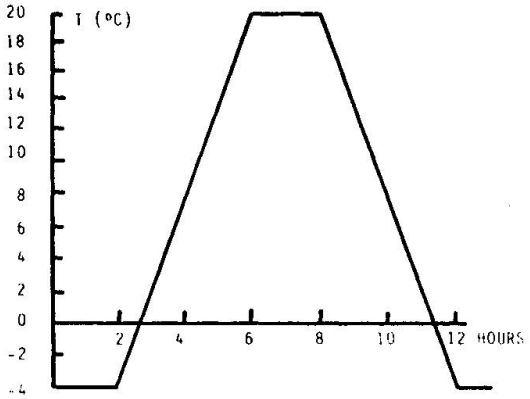

Fig.2 Slow F-T test (gradients)

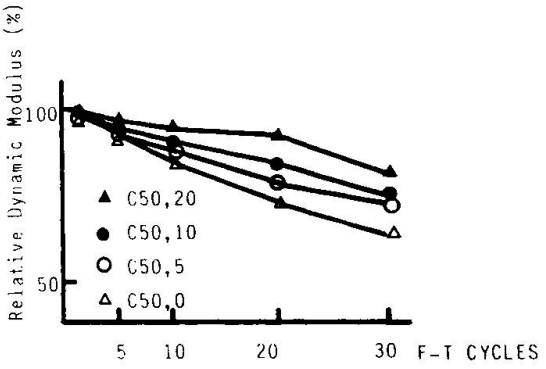

Fig.3 F-T cycle and relative dynamic modulus (W/C+SF=.50)

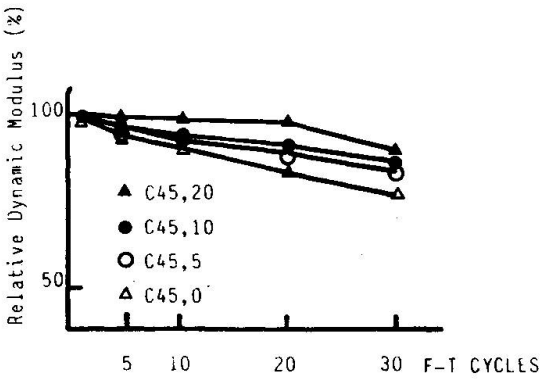

Fig.4 F-T cycle and relative modulus (W/C+SF=.45)

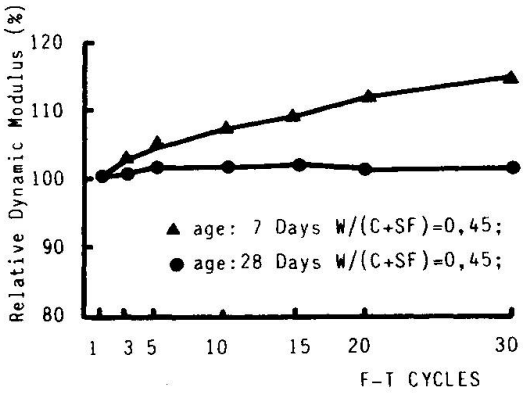

Fig.5 F-T cycle and relative dynamic modulus (slow test)

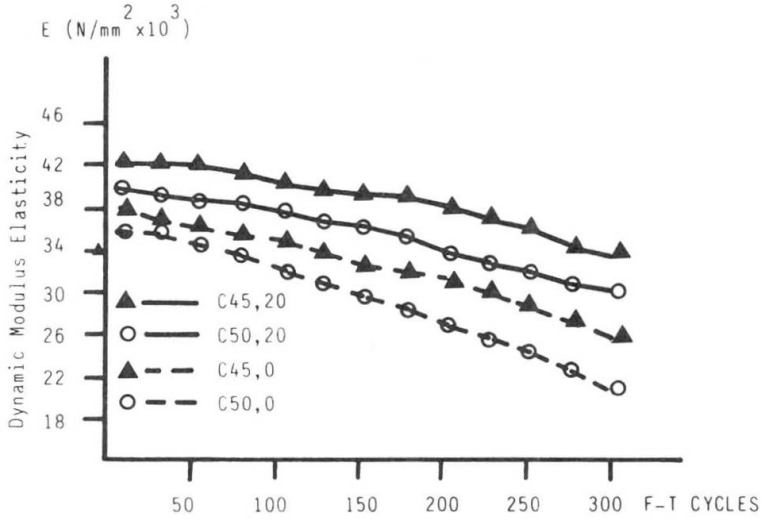

Fig.6 F-T cycle and relative dynamic modulus of elasticity

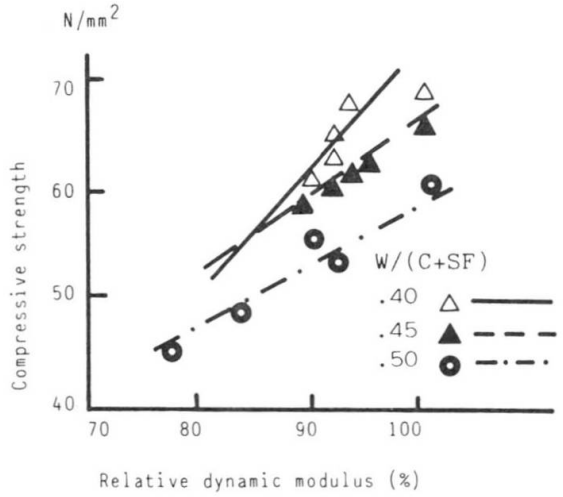

Fig.7 The relation between dynamic modulus and compressive strength

Fig.8 Distribution of fibers in hardened concrete

Creep and Durability of Wood-Joist Floor Systems

Fluage et durabilité du système de poutres dans les planchers en bois

Kriechen und Dauerhaftigkeit von Holzträgerdeckensystemen

I. Robert KLIGER
Research Ass.,
Chalmers Univ. of Technology
Göteborg, Sweden

Robert Kliger, born 1950, graduated from Chalmers University of Technology, Göteborg, Sweden, with a M. Sc. in civil engineering. For three years he was head of design at a company marketing timber-framed houses.
Robert Kliger is currently active in research into various problems related to timber structures.

SUMMARY

Experimental work is presented on the creep properties and durability of both the component parts and complete wood-joist floor structures consisting of wood, wood based materials and steel sheet. The discussion of the use of this type of structure has been limited to floors used above foundations with a crawl space in wooden houses.

RÉSUMÉ

Le travail expérimental démontre les caractéristiques de fluage et de durabilité aussi bien des éléments constitutifs que du système de poutres dans les planchers composés en bois, en matériaux à base de bois et en tôle. La discussion sur l'usage d'une telle construction est limitée au plancher qui est situé sur la fondation avec espace intermédiaire, dans des maisons en bois.

ZUSAMMENFASSUNG

Eine experimentelle Arbeit wird beschrieben, in welcher die Kriecheigenschaften und die Dauerhaftigkeit von Teilmaterialien und von ganzen Holzdeckenkonstruktionen (aus Holz, Holzwerkstoff und Stahlblech) untersucht werden. Die Diskussion der Verwendung dieses Konstruktionstyps wird auf Decken über einem Kriechkeller beschränkt.

1. INTRODUCTION

1.1 Foundations with crawl space in wooden buildings

The conventional crawl-space basement has foundation walls made of materials, such as lightweight concrete blocks, often resting on concrete base foundations. The floors are usually made of prefabricated elements made of either wood and wood-based materials or lightweight concrete. The distance between the ground and the underside of the floor structure is small, but should be a minimum of two feet (∿ 600 mm) to permit inspection.
Climatic studies of cold crawl spaces with an airtight, well-insulated floor structure and ventilated by the outside air have revealed that the relative humidity can be as high as 85-95% [1], especially in the summer, even if all the sources of moisture such as damp and water leakage are eliminated. This is due to the fact that warm outside air with a temperature of about 17°C or higher and a relative humidity of about 70% is chilled in the basement by the ground which is still cold from the winter. The relative humidity will therefore increase and it is then possible for wood and wood-based materials to mould or even rot, despite the degree of ventilation. For this reason a design using steel sheet with a zinc oxide coating on the underside of the floor structure could be advantageous.

1.2 Design of wooden floors

The design of floors is traditionally based on the assumption that the dead load and the applied load are carried entirely by the joists and that the effect of the sheeting on the behaviour of the floor system is negligible. The stresses, moments and deflections are calculated using simple beam equations in which possible composite action is ignored.

1.3 Stressed-skin panels

A stressed-skin panel can be an example of a wood-joist floor system where the interactions between joists and sheeting are included in the design. The advantage of using these panels is the high ratio between strength and weight and the fact that the choice of materials can be optimised with regard to structural, functional och durability requirements.

1.4 Aims and scope

In this paper the application of stressed-skin panels as a prefabricated element above the crawl space is discussed only for "cold" basements, i.e. basements which are not heated and are only ventilated by the outside air.
The main aim of this paper is to study the design and creep characteristics of stressed-skin panels containing wooden joists, chipboard and steel sheet. A simple theoretical model which takes account of the slip modulus between the component parts is used to compute the initial deflection and predict creep. In order to verify the model, four stressed-skin panels were constructed and subjected to long-term loading. The creep properties of the component parts and joints were studied in order clearly to define these properties which were to be used as input for theoretical calculations using the above-mentioned model. The limitations which applied to all the tests were that the sustained load should correspond to a low stress level and that all the tests should be carried out in a constant climate (20°C and 65% RH).

2. LONG-TERM STRENGTH AND DURABILITY OF COMPONENT PARTS AND ADHESIVE JOINTS

2.1 Aims

The experiments on component parts and adhesive joints were conducted primarily to produce information about the strength and creep properties of materials *matched* with those used to build four stressed-skin panels. This information was then used as input to a simple computer program based on a modified theory of elasticity for built-up structures.

2.2 Tests on component parts

The experimental studies included the long-term bending and shear characteristics of wooden beams (stringers in stressed-skin panels), the compression characteristics of chipboard (the compression flange in stressed-skin panels) and the shear properties of glued joints between wood and chipboard and wood and steel. In order to compare long-term deformation for different materials and joints loaded in different modes and varying stress levels, the results were expressed in values of relative creep, ϕ, i.e. creep deflection (deformation) related to an initial deflection. All the relative creep data taken from measurements during some 670 hours (4 weeks) was then fitted to two different mathematical expressions in order to predict creep after 1,000 and 10,000 hours. The power function (Eq.1) probably fits a regression curve, which represents the available creep data, as well as any other mode, even if it tends to overestimate creep after a long time [2].

$$\phi = \beta_0 + \beta_1 \, t^{\beta_2} \qquad (1)$$

where relative creep $\phi = \delta_t/\delta_0$ and δ_0 is the "initial deflection " (deformation) obtained after one minute ± 5 seconds (after the application of the load), which is the time corresponding to t = 0.
β_0, β_1 and β_2 are constants, t is the time (in hours).

The results of these tests show that the relative creep values were higher at the lowest stress level for both wooden beams loaded in bending and chipboard loaded in compression.

Three different types of adhesive (polyurethane, PVA with isocyanate hardener and elastomeric silicone), which join wood to wood and wood to steel, were tested in shear to obtain the short-term strength and deformation. However, in these tests the two PVA and silicone adhesives were chosen for purely scientific purposes, namely as examples of virtually rigid and somewhat flexible joints. The duration of load effect for the different types of adhesive used in timber joints showed that the shear strength decreases the least for resorcinol, followed by polyurethane and PVA with isocyanate hardener [3]. The type of adhesive, as well as the state of the metal surface, are important parameters for the *durability* of a bonded steel joint. Sandblasting the metal surface has the best effect on the durability of steel joints. The rate of degradation in steel joints exposed to humid environments is dependent on the temperature, on the water concentration in the glue- or bond-line and on the type of coating on the steel sheet surface glued to the timber [4]. An accelerated long-term test on joints between wood and steel sheet with polyurethane adhesive [5] revealed that joints did not fail during 8,000 hours' exposure to a shear stress of 0.8 MPa at 100% relative humidity and 50°C. These joints had an ultimate shear stress of 4.3 - 6.5 MPa at a temperature of 20°C.

3. DEFLECTION AND CREEP OF STRESSED SKIN-PANELS

Four specimens (Fig.1) were subjected to a 4-point constant load for nine months. The level of the concentrated loads corresponded to stresses smaller than or equal to the permissible stresses according to the Swedish Building Code SBN 80 [6]. The tests were carried out in a constant climate (20°C and 65% RH).

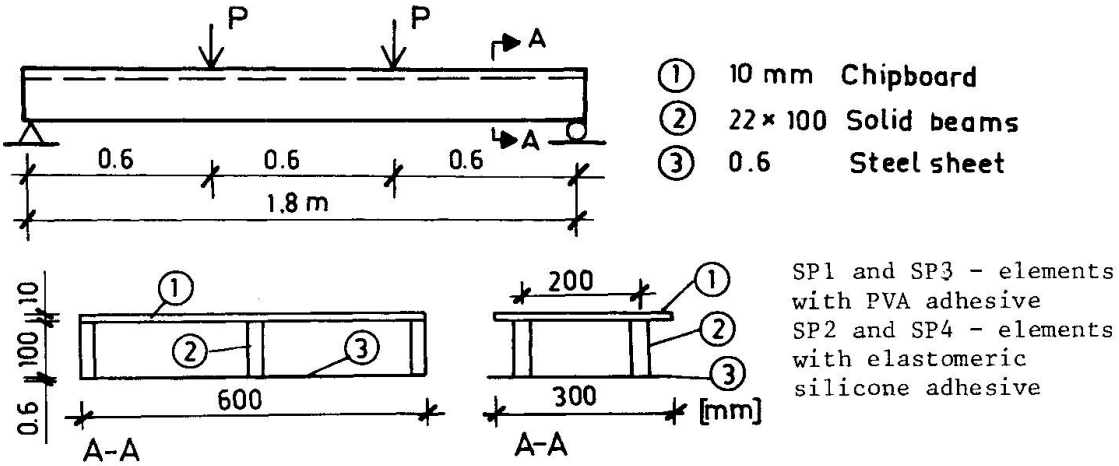

Fig. 1 Loading arrangement and cross-section of stressed-skin panels

The theoretical magnification factor for the mid-span deflections of stressed-skin panels, which includes the effects of interlayer slip, was calculated by using the solution of a differential equation [7] and based on the assumption that the slip modulus is the same in the entire joint and that no variation exists between the joints. In the case of the stressed-skin panels tested here different slip moduli were found for different interlayer joints. This difference was taken into account by calculating the magnification factor for the first two layers (inverted T-beams) and modifying the bending stiffness of these layers. The calculation was then repeated by regarding the first two built-up layers as one unit (rigidly connected) when adding the third layer. This procedure was embodied in a simple computer program.

The creep and creep rate of elements are described by different parameters which are included in the power function, Eq.1, for the creep of each of the component parts and joints. Using the sensitivity analysis of the parameters in the creep functions for each of the submaterials and allowing each of the stiffness variables of interest to change due to creep, it was possible to study the influence of these variables on deflection and creep. When using rigid glued joints with a low tendency to creep, the creep of the entire specimen was similar to that obtained due to combined creep in the stringers and the compression flange.

The creep curves show good agreement between the measured and predicted results for all the specimens which were tested (Fig.2). We must bear in mind the large scatter typical of the input data for wood-based materials and glued joints.

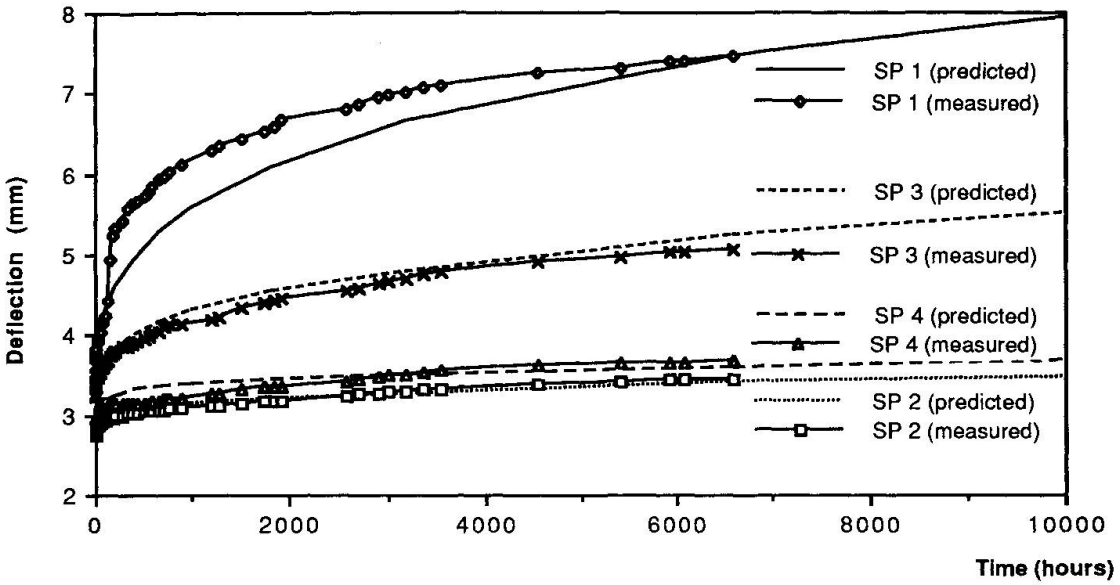

Fig.2 Comparison between theoretically obtained creep curves and the experimentally measured deflections

4. PRACTICAL EXPERIENCE OF THIS TYPE OF STRUCTURE

In order to produce cheap houses with low energy consumption, eighteen houses were built in Täby (Sweden) during the winter of 1984-85. In these houses the floor structure above the crawl-space basement consisted of simply-supported prefabricated elements (stressed-skin panels). Supports made of pressure-impregnated ground plates were placed at the long exterior walls of each house (span of 7.6 metres). The floor elements consisted of 22 mm chipboard on the compression side, 400-mm I-beams with a spacing of 600 mm as stringers and 0.6 mm steel sheet (plywood was used in one house as a reference) on the tension side. In four of these houses the moisture content was measured for one year [8]. The results of these measurements showed that the highest moisture content inside the elements was 14% on the compression side (corresponds to 62% RH) and 17% on the tension side (corresponds to 70% RH). Although the floor structure had a relatively long span, it did not show unacceptable deformation during the test period. Some condensation was discovered in the crawl space during the summer; this was predicted, but no condensation occurred inside the structural floor elements.

5. CONCLUSIONS AND SUGGESTIONS FOR IMPROVEMENTS

It appears to be extremely advantageous to use thin steel sheet as a tension flange in order to reduce deflections and creep in wood-joist floor systems. Specimens with fairly stiff glued joints (PVA adhesive) would show a 20% increase in initial deflection and a 10% increase in creep deflection after 10,000 hours if 12 mm plywood were used instead of 0.6 mm steel sheet in the tension flange. The experimental work discussed here shows that it should be possible to use the same technique to predict the long-term deformation of stressed-skin panels exposed to a varying load or varying climate, provided that one has data for the corresponding properties of the component materials and joints. The durability of steel-to-wood joints exposed to high relative humidity is a very important design consideration. One way of improving the design of this type of structure would be to add extra insulation to the underside of the steel sheet, thus in-

creasing the temperature of the steel surface (this would prevent condensation forming). The best way of protecting timber structures from the harmful influence of moisture is to use a "correct" design. This involves creating an appropriate climate (RH lower than 70%) around timber and timber-based materials. A perforated steel ground plate could be used to support a wood-joist floor system above a crawl-space basement instead of a pressure-impregnated one which could mould in the high humidity which occurs in such areas.

REFERENCES

1. ELMROTH A., Kryprumsgrundläggning (Crawl-space basements). National Swedish Building Research R12:1975 (in Swedish).

2. KLIGER I.R., Determination of creep data for component parts of stressed-skin panels. Proc. CIB-W18/IUFRO S5.02, Paper 19-9-5, 1986.

3. LUNDGREN K., Ny konstruktionslimning. BFR Rapport R85:1985 (in Swedish).

4. KINLOCH A.J., Durability of structural adhesives. Applied Sci. Publ. Ltd. London, 1983.

5. DOLK Å., JANSSON J-F., Accelererad långtidsprovning av polyuretanlim för bärande konstruktioner av trämaterial och stålkomponenter. Träteknik-Centrum P:16, 1984 (in Swedish).

6. The Swedish Building Code. SBN 80. Statens Planverk 1980 (in Swedish).

7. KLIGER I.R., Experimental study of stressed-skin panels under long-term loading. Proc. IUFRO S5.02, Turku, Finland 1988.

8. LINDSKOOG A., ROOS R., Studie av fuktproblem i högisolerade träkonstruktioner. Träteknik-Centrum Rapport P 8702014, 1987 (in Swedish).

Long-Term Properties of Arapree

Comportement à long terme du matériau composite arapree

Langzeiteigenschaften des Verbundwerkstoffes Arapree

Arie GERRITSE
Civil Engineer
Hollandsche Beton Groep nv.
Rijswijk, The Netherlands

Jürgen WERNER
Civil Engineer
Akzo nv.
Wuppertal, F. Rep. of Germany

Leon GROENEWEGEN
Civil Engineer
Hollandsche Beton Groep nv.
Rijswijk, The Netherlands

Arie Gerritse, born in 1929, graduated in Civil Engineering at Rotterdam Technical College, the Netherlands. He is a staff member of the R&D department of Hollandsche Beton Groep (HBG), an international contractor based in the Netherlands, supervising since 1984 the Akzo/HBG development project on the practical use of aramides in concrete.

Jürgen Werner, born in 1939, obtained his Civil Engineering degree at the Technical University of Braunschweig (Fed. Rep. of Germany) in 1966. He is an Akzo project manager in the field of application of fibre reinforced materials in civil engineering.

Leon Groenewegen, born in 1961, obtained his Civil Engineering degree at the Technical University of Delft (the Netherlands) in 1986. He is currently a research engineer at the R&D department of HBG.

SUMMARY

Arapree is a composite made up of aramide fibres and an epoxy resin. It is used as a prestressing material in concrete structures. Apart from some general information on Arapree and its short term properties, the durability aspects are discussed. The paper ends with some impressions of two projects in which Arapree has been applied.

RÉSUMÉ

L'arapree est composé de fibres d'aramide et de résine époxy. Il est utilisé comme matériau de précontrainte dans des structures en béton. Après une information générale sur l'arapree, son comportement à court et long terme est discuté. Enfin deux projets sont décrits, au cours desquels l'arapree a été employé.

ZUSAMMENFASSUNG

Arapree ist ein Verbundmaterial aus Aramidfasern und einem Epoxyharz. Es wird als Vorspannmaterial in Betonkonstruktionen gebraucht. Neben einigen allgemeinen Informationen über Arapree und seine Kurzzeiteigenschaften werden die Langzeitaspekte diskutiert. Am Schluss werden zwei Projekte besprochen, in denen Arapree angewandt wurde.

1. Introduction

In the past few years interesting developments have emerged in the field of non-metallic tensile elements. More and more successful applications of such new materials are reported [1], [2], [3], [4].
The use of these materials will become common practice to structural engineers in the near future. This development necessitates the need for reliable data for these non-metallic elements especially with respect to their long-term behaviour.
In this paper the main long-term properties of Arapree, one of these new materials, will be discussed. The phenomena associated with these properties are well known since they must also be taken into consideration for materials like steel and concrete. However, other -less familiar- characteristics, such as stress-rupture behaviour can be decisive in designing constructions with these new materials. A thorough understanding of the characteristics will be needed for structural engineers who are faced with the problem of assessing constructions in which such new materials are applied.
The products belonging to this new generation of non-metallic tensile elements are based on high strength fibres like glass, carbon and aramid. In this paper the discussion on long-term properties is limited to an overview of the most important characteristics of Arapree, a composite made up of an epoxy resin and Twaron, the aramid fibre produced by Akzo.

2. General information Arapree

Arapree is the result of an ongoing research program of the Dutch/German chemical company Akzo and the Dutch contractor HBG. Arapree is produced as endless elements composed of bundles of non-twisted Twaron-fibres. The elements are produced by passing the fibres through eyelets and combs and subsequently impregnating the bundles with an epoxy resin. To ensure a good bond of the elements with concrete the surface of the elements is provided with a pattern of nobs.
An essential step in the production process is the impregnation of the Twaron bundles. A number of reasons have lead to the decision to impregnate the bundles with resin:

- By impregnating the bundles with an epoxy resin shear stresses fibre to fibre can and will be transmitted in the anchorage zone and in the vicinity of an incidental fibre rupture.

- Transmission of shear stresses of the bundle to the concrete regulated by tuning the surface structure.

- Handling of the elements

- Improvement of the resistance to extreme alkaline and acid environments.

- UV-protection. If applied in concrete this aspect can be neglected. Only in case of external prestressing this might be significant, but can be prevented by the use of additives to the resin deterioration.

- Optimal use of fibre strength. Thanks to the ability of the resin to transfer shear stresses the effect of fibre rupture is limited to a small area.

In table 1 the presently available types of Arapree are summarised.

TABLE 1: Available types of Arapree

Shape rectangular round	Cross-section [mm²] [mm]	Number of filaments	Fibre-cross-section [Twaron HM] [mm²]
rectangular	0,5*20	30 000	3,3
	1,4*20	100 000	11,1
	2,8*20	200 000	22,2
	5,6*20	400 000	44,4
round	2,5	20 000	2,2
	5	100 000	11,1
	7	200 000	22,2

Figure 1 shows a picture of a rectangular Arapree-strip and an Arapree-wedge anchor that is used as a temporary anchorage device. In concrete elements the prestressing force in the elements is transmitted to the concrete by bond.
In figure 2 the stress strain relation of Arapree is compared with common reinforcing and prestressing steel.

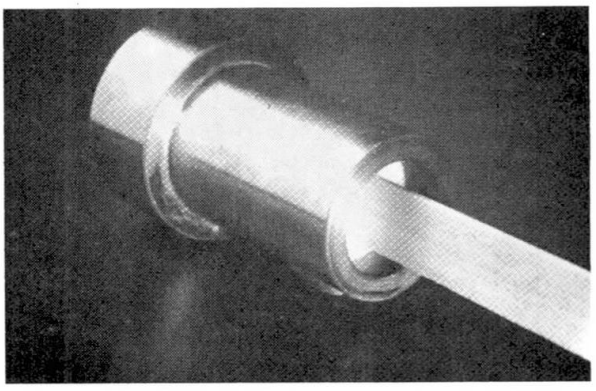

figure 1

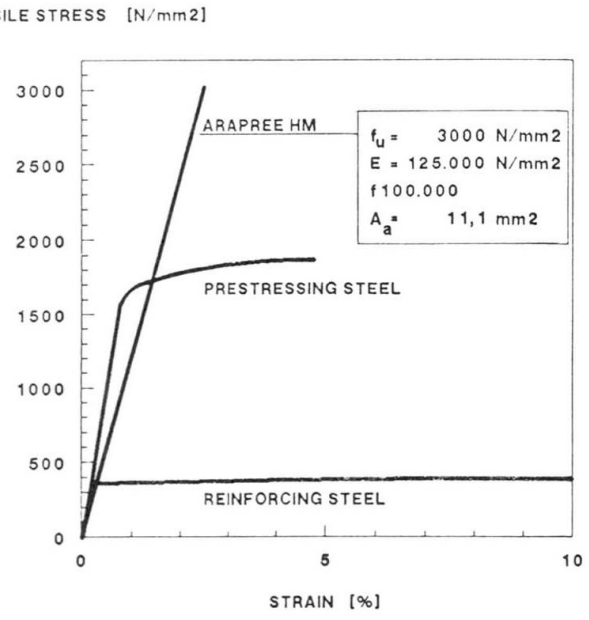

figure 2

The most significant short term mechanical properties of Arapree are given in table 2.

TABLE 2: Short-term properties of Arapree

Properties	Values	Dimension
Arapree bar-strip		
axial tensile strength	3000 (**)	N/mm² (*)
modulus of elasticity	125-130 (***)	kN/mm² (*)
failure strain	2.4	%
density	1250	kg/m³
transverse compressive strength	ca. 150	N/mm²
interlaminar shear strength	ca. 45	N/mm²
poisson ratio	0.38	-

*) Values related to the effective fibre cross-section.
**) Characteristic value: 2800 N/mm².
***) Modulus based on measurements in the range between 10 % to 50 % of the ultimate strength.

3. Durability

Apart from properties like an extremely high strength and considerably high stiffness of these new materials, the most interesting characteristics generating the interest of structural engineers have reference to the long-term behaviour.
Tensile elements based on aramid are non-corrosive, exhibit an excellent resistance to chlorides, are insensitive to electromagnetic currents and prove to have an outstanding fatigue behaviour. In case of reinforcing or prestressing steel all of these characteristics generally lead to requirements to ensure the durability. If aramid is applied there will be no need for such measures.
However, the stress-rupture behaviour and the sensitivity of glass- and - to a lesser degree - aramid fibres to an alkaline environment will give rise to new requirements. This is illustrated in figure 3.
The stress-rupture line given in figure 3 represents the relation between the stress in a tensile element and the time that passes before the material fails under a specific sustained stress-level. It is therefore a different property than the 'long-term-strength', which can be defined by the maximum constant load which can be present over a (very) long period. The long-term strength is also presented in figure 3. It can be seen that the residual strength of an unloaded strip after 100 years exposition in an alkaline environment like concrete is about 85 % of the short term strength. This value has been obtained by means of an extrapolation using the Arrhenius principle, that decribes a relation between the residual strength, temperature and time. Tests at elevated tempatures thus give indications about the residual strength level under normal circumstances.

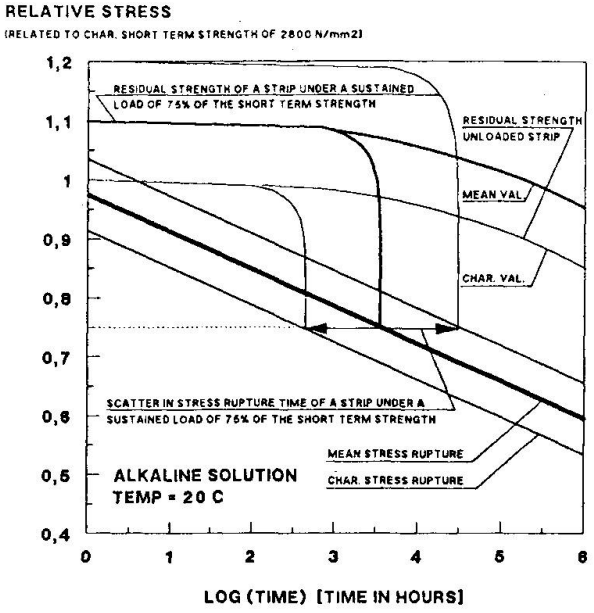

figure 3

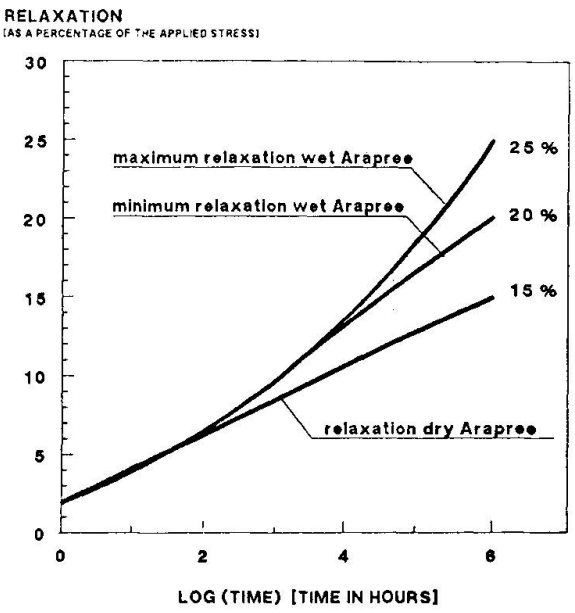

figure 4

The residual strength of a loaded strip hardly depreciates until just before stress rupture. This is illustrated in figure 3 by the residual strength of a strip to which a sustained load of 75 % of its short term strength was applied.

In assessing the structural safety one should estimate the final prestressing level, taking into account all losses caused by concrete deformations and relaxation of Arapree (figure 4). This value must be compared with the characteristic stress-rupture curve taking into consideration a partial factor for Arapree that has been set at 1.15 .
More information about Arapree is given in [5],[6].

4. Arapree in practice

Two projects have already realised in which Arapree was used as prestressing material. An impression of these projects is given in figure 5 and 6. In both cases relatively small prestressed (pretensioned) concrete elements have been produced. This first application of Arapree (1988) concerns concrete posts in a traffic noise barrier along a motorway near Rotterdam (figure 5). Ninety elements of about 4.5 m were prestressed with Arapree.
The second application of Arapree is illustrated in figure 5. Ten concrete hollow core floor slabs with a span of ca. 6 m were prestressed with Arapree (1988/1989). In both cases no additional steel reinforcement was used. The aim was to produce non-magnetic durable pretensioned elements without any steel.

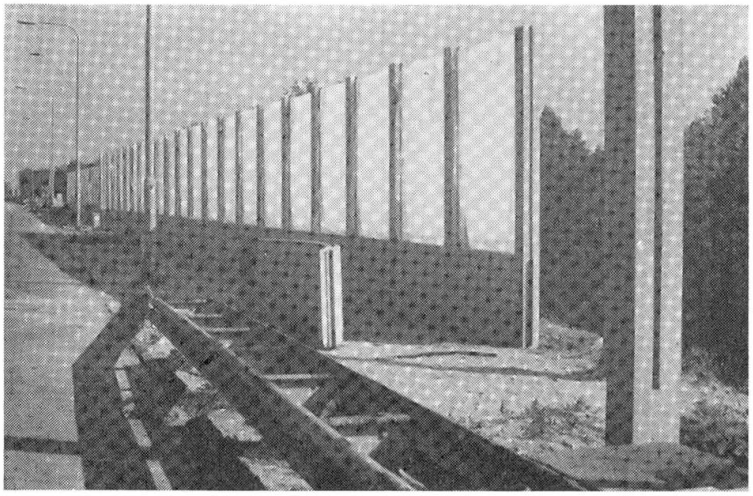

figure 5.

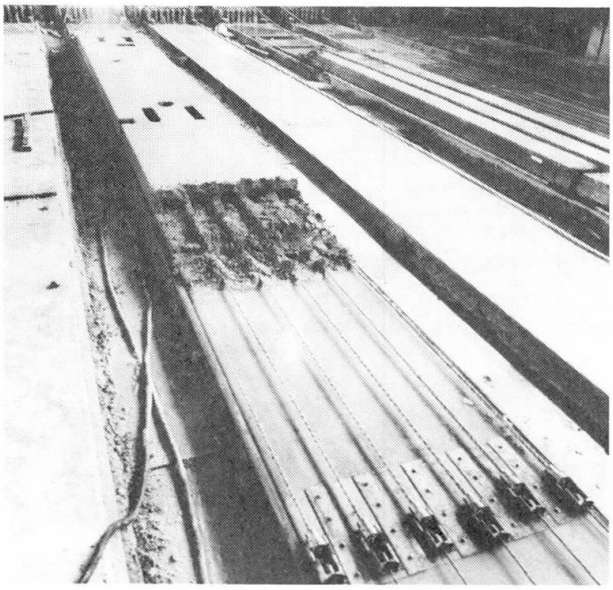

figure 6.

5. References

1: FUJISAKI T., MATSUZAKI Y., SEKIJIMA K., OKAMURA K.; New Materials for Reinforced Concrete in place of Reinforced Steel Bars; IABSE-symposium, Paris Versailles 1987.

2: Dr. WOLFF; Prestressing of Heavy Structures; Ecole Nationale des Ponts et Chaussées, Les Materiaux Nouveau pour la Precontrainte et le Renforcements d'Ouvrages d'Art; Paris, 25-26 october 1988.

3: OKUDA K.; Pitch-based Carbon Fibres; Seminar on the Future of Advanced Composite Materials, May 1987.

4: BURGOYNE C.J. e.a.; Proceedings of the Symposium on Parafil Ropes; Imperial College of Science and Technology, London 1988.

5: GERRITSE A., SCHÜRHOFF H.J.; Prestressing with Aramid Tendons. Technical Contribution to FIP 10-th Congress, Nee Delhi, 1986.

6: GERRITSE A., WERNER J.; Arapree, The Prestressing Element composed of Resin Bonded Twaron Fibres, HBG-Akzo brochure, september 1988.

Proper Use of High-Alumina Cement Concrete

Utilisation correcte d'un béton avec un ciment à haute teneur en aluminates

Korrekte Verwendung eines Betons mit Hochtonerdezement

Kesete GABREKIDAN
Professor
Garyounis University
Benghazi, Libya

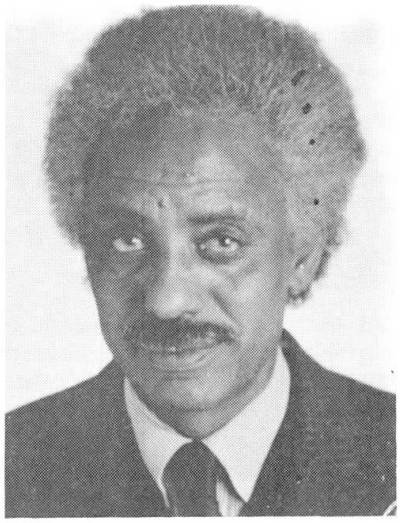

Kesete Gabrekidan, born in 1937 obtained his first degree in Civil Engineering, Addis Ababa University Ethiopia, M. Sc. University of Cincinatti U.S.A. and PhD, University of Bradford, UK. He was involved in special railway-highway bridge design for Atkins & Partners and was senior structural engineer for George Wimpeys Laboratories, UK and for a long period of time on the Addis Ababa University staff.

SUMMARY

After a two year period of storage, the reduction in HACC (High-Alumina Cement Concrete) compressive strength, indicated zero and 50% for normal and dry curing conditions respectively. Full conversion after 7 days hot water storage produces a 25% strength reduction. Under normal curing conditions, the flexural strength developed increased at a curing temperature of 22.5 °C as compared to the standard 18 °C. Shrinkage in HACC is of the same order as that of PCC (Portland Cement Concrete) for similar storage periods, while swelling is independent of storage temperature. In slow converted specimens, creep is dependent on the mineralogy or morphology of the hydrates, while full conversion leads to the same order of creep as PCC.

RÉSUMÉ

Après un temps de stockage de deux ans, la réduction de résistance à la compression du béton HACC a atteint zéro et 50% pour des conditions de conservation du béton normales, respectivement à sec. Un changement complet après 7 jours de stockage en eau chaude donne une réduction de résistance de 25%. Dans des conditions normales de conservation la résistance à la flexion qui se développe a augmenté à une température de conservation de 22.5 °C, comparée à la température normale de 18 °C. Le retrait dans le béton HACC est du même ordre que celui observé dans le béton CP pour un même temps de stockage, alors que le gonflement n'est pas affecté par la température de stockage. Pour les spécimens à changement lent, le fluage dépend de la minéralogie ou morphologie des hydrates alors qu'un changement complet mène au même ordre de fluage que le béton CP.

ZUSAMMENFASSUNG

Nach einer Lagerungszeit von zwei Jahren , erwies sich der Abfall der Druckfestigkeit von Hochtonerdezement als Null und jeweils 50% für normale wie trockene Erhärtungsbedingungen. Vollständige Umwandlung nach 7 Tagen Warmwasserlagerung erbringt eine 25%ige Festigkeitsreduktion. Unter normalen Erhärtungsbedingungen nahm bei einer Erhärtungstemperatur von 22.5 °C im Vergleich zu der Standardtemperatur von 18 °C die entwickelte Biegefestigkeit zu. Bei ähnlichen Lagerungszeiträumen erfolgt Schrumpfung des Hochtonerdezements in gleichem Umfang wie für Portlandzementbeton, während die Quellung von der Lagerungstemperatur unabhängig ist. Bei langsam erstarrenden Proben ist die Kriechdehnung von der Mineralogie oder Morphologie der hydraulischen Bindemittel abhängig, während das vollständige Erstarren zu gleichen Kriechdehnungen wie bei Portlandzementbeton führt.

1. INTRODUCTION

High-alumina cement is produced by heating a mixture of limestone and bauxite to fusing, which quickly attains a very high strength and is in its original form sulphate resistant. At hydration meta-stable aluminates are found at normal temperature and humidity crystalizing in hexagonal form which in turn transforms into a stable cubic compound. Such chemical transformation, depending on intensity of temperature and humidity, induce reduction in volume of gel and increase porosity, termed as "conversion", resulting in strength reduction.(1)
Research that went into high-alumina cement (HAC) was rather unimpressive, to say the least, and consequently code provision accorded by CP114, CP116 and CP110 to HAC in buildings was rather unsatisfactory and misleading. The highlight of this, among other things, was the collapse of two beams of the roof over the swimming pool of Sir John Cass Red Coat School at Stepney, London.(2). Consequently, the part relating to HAC in CP110 was deleted in 1974. With this realization the author conducted intensive studies from 1975 onwards on the subject with special emphasis to prestressed concrete out of which a portion is hereby presented.

2 CONCRETING AND INSTRUMENTATIONS

Short and long-term studies of standard tests running to maximum two and a half years on cylinders, cubes and flexural prismatic beams were made using destructive and non destructive tests. To simulate different environmental conditions, the following curing storages were procured: normal curing (21.5°C and 90-95%RH), dry curing (18°C and 45%RH) and hot-water curing (45°C and 100%RH). One day after cast in an open laboratory area (temperature varying from 7°C to 27°C) the specimens were carried to respective storage regimes.
A 100mm x 100mm x 1000mm prismatic beam steel moulds, fabricated at the School of Civil and Structural Engineering Dept., University of Bradford, UK, were prepared for making shrinkage and/or swell and creep specimens. Shrinkage and creep rigs, fitted with electrical and mechanical measuring devices to avoid instrumentation breakdown, were also designed and fabricated to suit storage conditions.
A mix design, 1:1.6:3, with free W/C ratio of 0.35, aggregate cement ratio of 4.6, compaction factor of 0.78 and cement content of 4100 n/m^3 of concrete was employed throughout the experimental period. The overall grading of aggregates, as suggested by Newman (3), conformed to zone No 2. d.t.a. tests were run periodically to determine the degree of conversion for the various storage regimes. Petrological analysis on sands, for possible presence of soluble alkalis, and spot checks on British brand HAC chemical composition were also performed.

3 TEST-RESULT ANALYSIS AND CONCLUSIONS

3.1 Compressive strength.

The 24-hour strength was nearly the same for all concrete cast, with mean strength of 82.8N/mm^2. Fig.1 indicates the strength - storage time curves for all regimes.

3.1.1 Normal storage: specimens stored in wet room, with indicated ambient conditions, reveal an increase in strength development except in a situation where slow conversion

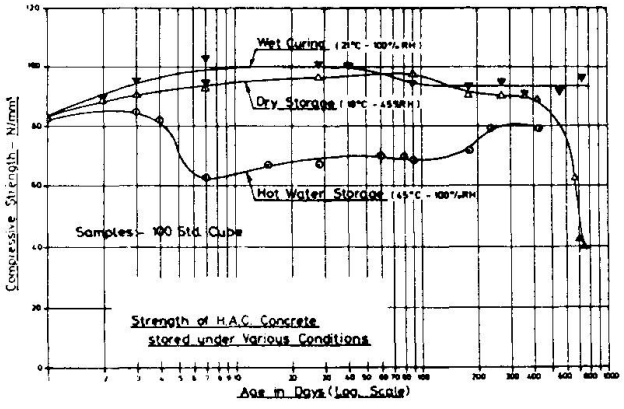

FIG. 1

takes place the fall is followed by strength recovery emanating from rehydration of the unhydrated cement. Such phenomenon persists for a length of time until the chemical reaction is complete. That is to say a cyclic behaviour, characterised by sag and hop; dominates until the hexagonal aluminates (CAH_{10}) complete transformation into the more stable cubic aluminates (C_3AH_6) is restored. It follows that such sluggish conversion does not lend itself to appreciable reduction in strength; evidently not lower than the 24-hour strength.

3.1.2 Hot water storage: specimens stored in hot-water tanks indicate slight increase in strength up to 3 to 4 days and a rapid fall is recorded after 7-8 days. Full conversion time can be estimated using Fig.2, curing temperature versus time required for specimens to reach full conversion. The curve is (Fig.1) then picks up strength gradually, a clear indication of rehydration followed by conversion of the fresh hydrated cement. The maximum observed loss of strength is in the range of 25% of the 24 hour strength. Hence steam curing could offer the best solution if HAC is employed in buildings for tropical climate.

FIG. 2

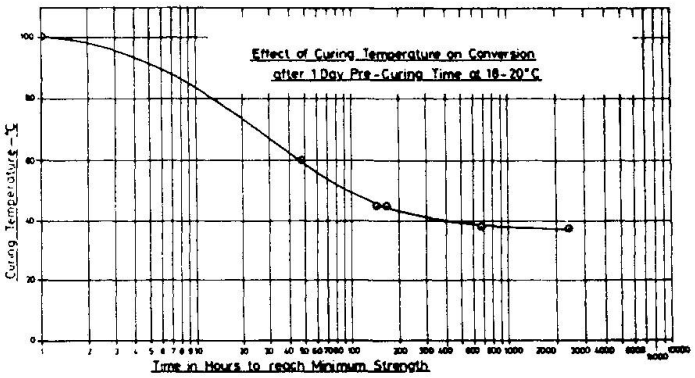

3.1.3 Dry storage: Specimens stored in dry conditions, Fig 1, received the most damage. After 400-day storage in dry room rapid deterioration without sign of strength recovery is observed. After 750 days the compressive strength was reduced to 50% of the 24 hour strength. Deterioration of high-alumina cement concrete, as some researchers claim, cannot always be attributed to conversion. In this particular case, after one day curing in an open laboratory area, specimens were stored in dry room. It is expected that, with the harsh mix the specimens received and denied of the proper curing for the crystals to mature, strength development to full capacity would be far remote. It is also possible, due to severe specimen exposure they may have lost some of the water of hydration vital to matured crystal formation. Destructive tests showed that bond between paste matrix and gravel was exceedingly weak with subsequent loss in strength. The degree of conversion obtained for these specimens also supports that conversion alone had little to play in the deterioration.

3.2 Flexural strength of Standard Prismatic Beams.

Fig.3 shows flexural strength versus time curves for all storage regimes. These curves are similar in shape as that given by Fig.1. The significant change occurs for normal storage condition in which strength development is more pronounced than the remaining storage regimes. This leads to the conclusion that normal curing temperature for HACC can best be established at about 22°C in lieu of the accepted standard of 18°C.
The trend of the curve for normal storage for indirect tensile strength, other things being equal, has a diminishing character than the 24-hour strength. This is contrary to the flexural strength development under similar storage conditions. However such reduction of strength does not raise alarm as there is appreciable strength reserve for design purposes. It is is also interesting to note that the mean Poisons' ratio falls
in the range of 0.15.

3.3 Shrinkage

To assist, compare and contrast, Fig.4 is prepared based on total length. When specimens are stored at low relative humidity, 45%, the shrinkage time curve is smooth and continuous up to 295 days; similar shape as in Fig.1 for the same storage regime. Strength reduction is followed by shrinkage reduction as indicated in Fig.4. Such behaviour affords the following explanations:

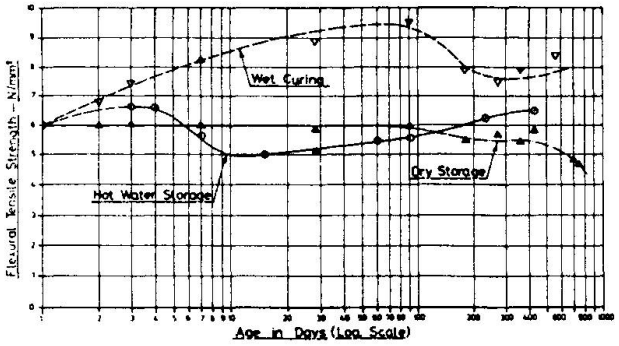

Flexural Strength of H.A.C. Concrete stored under Various Conditions

FIG. 3

1. In the absence of proper curing to achieve crystal maturity, the bond between paste matrix and gravel is weakened thereby partly relieving the restrain; offered by gravel in the shrinkage mechanism.

2. The occurence of conversion, depending on exposure conditions, allows similar mechanism as that of item 1. It can safely be concluded that, unlike Portland cement concrete (PCC) where conversion prevails or proper curing is denied for crystals to mature, shrinkage is not only retarded by also reduced by some margin. The maximum shrinkage value obtained in this research project after 500 days storage was in the vicinity of 350×10^{-6}. If we assume 66 to 85% of the 20 year shrinkage occurs in one year, this will yield 413×10^{-6} in 20 year period comparable to PCC.

FIG. 4

3.4 Swell

Consider for instance specimens stored in hot water tanks (Fig.4). The diminution of strength (Fig.1) is met to some extent by corresponding increase in swelling. As the strength recovery gradually takes charge swelling starts to retard. Second cycle of conversion will induce corresponding increase in swelling until the reaction ceases and the curve levels. The same reasoning is afforded to normal curing depending on rate of conversion. In general it can be concluded that while conversion reduces on one hand the net value of shrinkage, it promotes swelling on the other. The magnitude of swelling is irrespective of storage temperature and stands in the vicinity of 450×10^{-6}; greater than shrinkage value which runs contrary to L'Hermite's' research data on PCC.

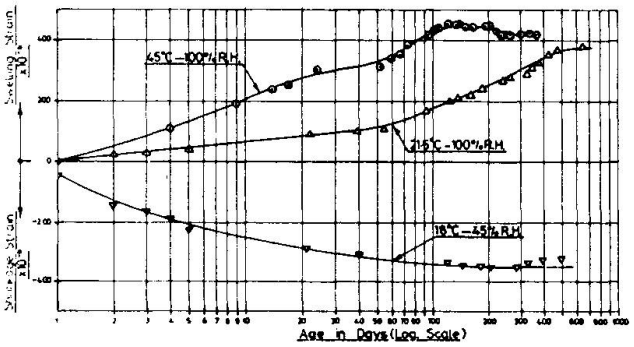

Shrinkage-Time Relationship for Samples stored under Various Conditions

3.5 Creep

Unlike PC, the subject of creep in HAC is the most neglected area of research. A limited amount of research investigations(4) had been published. Glanville showed that the age of loading, other things being equal, has large effect on creep; slower start at earlier stage and an increasing trend at latter stage. This was also confirmed by the author for dry storage conditions.

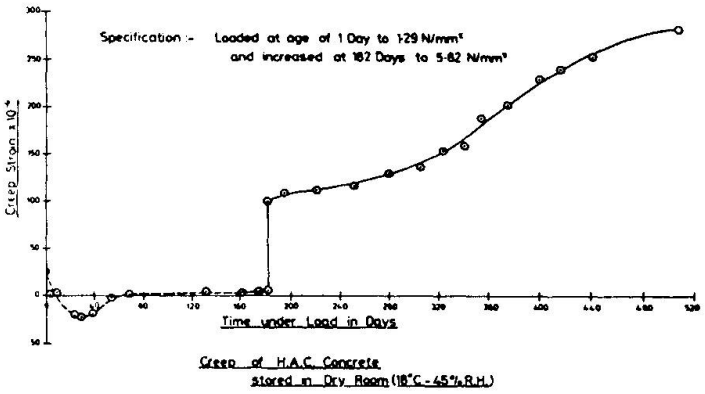

FIG. 5

3.5.1 Dry storage (Fig.5): The specimen was loaded to 13640N (1.29N/mm^2) until the age of 182 days. The curve in Fig.5 shows that creep becomes lower than the elastic deformation confirming Glanville's findings. At the age of 182 days, the sustained load was brought to 61340N (5.82 n/mm^2). The rate of creep progress is again sluggish up to 250 to 280 days and from there on creep increased at higher rate. After 400 days, creep deformation tends to achieve final value.

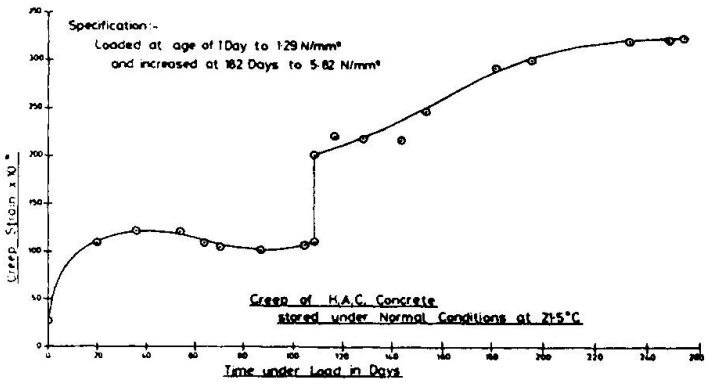

FIG. 6

3.5.2 Normal storage (Fig.6): specimens in this storage conditions were loaded to 13640N after one day cast and increased to 61340N at the age of 110 days. There appears a tendency for creep in dry storage to be less than in wet condition confirming Glanville's findings that the behaviour is organismically different from PCC. After 240 days, a slow increasing trend is observed.

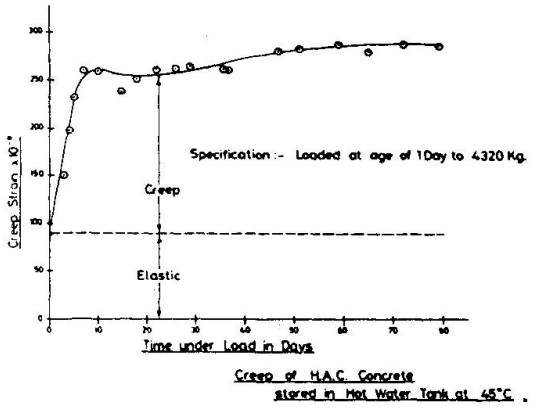

FIG. 7

3.5.3 Hot water storage (Fig.7): specimens were loaded to 43200N at the age of one day. The curve is more uniform than those discussed earlier admitting similarities to PCC creep behaviour.In other words full conversion from meta-stable compound (CA H10) to the stable compound (C_3AH_6) alters the behaviour in the creep-time curve. It follows that while porosity is a function of strength diminution, creep is dependent on the mineralogy or morphology of the hydrates formed. On the other hand at slow conversion HAC is organismically different from creep behaviour of PC while accelerated full conversion, before loading at best, offers similar behaviour as that of PC.

4 REFERENCES

1. Midgley, H.G., "Mineralogy of set HAC", transactions, British Ceramic Society, Vol.66, No4, 1967, pp 161-187.
2. Department of Environment, "HACC in Buildings", BRA 11068/2, 2nd January 1975, 3pp.
3. Newman, K., "Design of concrete mixes with HAC", R/c Rev., vol.5, No 5, March 1960, pp269-294.
4. Glanville, A.M., Glanville, Etal, "Creep or flow of concrete underload", S.I.R., London, Building research Technical Papers Nos 12 and 21, 1930 and 39, pp 39 and 34.

Role of Cement in Sulphate Attack of Reactive Aggregate Mortars

Rôle du ciment dans l'attaque de mortiers à aggrégats réactifs par les sulfates

Rolle des Zementes beim Sulfatangriff auf reaktive Mörtel

A. de SOUSA COUTINHO
Civil Engineer
LNEC
Lisbon, Portugal

Sousa Coutinho, born 1919, obtained his civil engineering degree at the Technical University of Lisbon, and is now Senior Research Officer and Head of the Building Materials Department of the National Laboratory for Civil Engineering.

Arlindo GONÇALVES
Civil Engineer
LNEC
Lisbon, Portugal

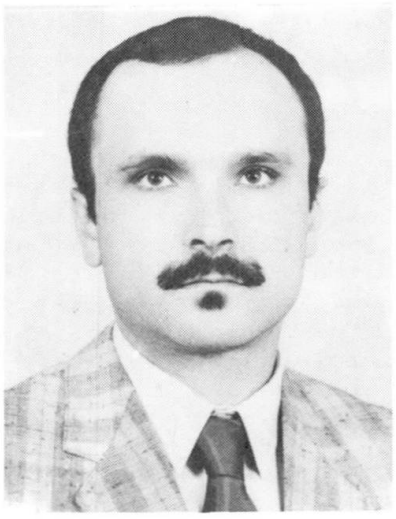

A. Gonçalves, born 1953, obtained his civil engineering degree at the Technical University of Lisbon, and is now Research Officer of the Concrete and Binders Division of the National Laboratory for Civill Engineering.

SUMMARY

This paper presents results of the influence of cement type on the durability of mortars made with sulphate reactive aggregates in a calcium hydroxide saturated medium, and kept under sea water after different curing periods. The observations, some of them over a period up to 20 years have enabled the authors to classify the resistance of the different cement types to sea water attack, when reactive aggregates are used.

RÉSUMÉ

On présente des résultats concernant l'influence du type de ciment sur la durabilité des mortiers préparés avec des agrégats réactifs aux sulfates dans un milieu saturé d'hydroxyde de calcium, et maintenus immergés dans l'eau de mer après différents temps de cure. L'observation, qui en quelques cas s'est prolongée pendant 20 ans a permis de classer la résistance des différents types de ciment à l'attaque de l'eau de mer lorsqu'on utilise des agrégats réactifs.

ZUSAMMENFASSUNG

Dieser Beitrag behandelt den Einfluss der Zementart auf die Beständigkeit des Mörtels mit sulfatreaktiven Zuschlagstoffen in einem mit Kalkhydroxid gesättigten Medium. Die untersuchten Bauelemente wurden dem Meerwasser ausgesetzt. Es wurden verschiedene Behandlunsperioden mit Beobachtungszeiten bis zu über 20 Jahren durchgeführt. Es war möglich, die verschiedenen Widerstände der untersuchten Zemente und der reaktiven Zuschlagstoffe bezüglich der Angriffigkeit des Meerwassers festzustellen.

1. INTRODUCTION

All research in the area of sulphate attack is based on formation of ettringite as a result of reaction between sulphates and C_3A present in portland cements. The ettringite formation can, however, take place without the presence of C_3A, if the reactive alumina for the formation of ettringite is provided by the aggregate [1]. When an aggregate contains kaolinized feldspar, the alumina from the aggregate reacts with sulphates, forming ettringite. The ettringite formed will be expansive as long as the reaction of alumina with sulphate takes place in a medium oversaturated with calcium hydroxide [2].

A concrete dock structure of Leixões Harbour, in the north of Portugal, built in 1940, suffered large expansions and cracking 6 months after the original installation. It was not until 15 years later that a proper explanation for the failure could be found in reactions involving sea water and the weathered feldspar of the aggregate.

With the same aggregates used in that structure, a study was undertaken to compare the resistance of different types of cements to the formation of expansive ettringite, on mortar prisms maintained under sea water in laboratory, after previous curing which varied from 2 days to 1 year. The specimens were subjected to visual inspection for detecting fissures and to length change measurements. The correlation between the Fratini test results and the behaviour of the mixes of portland cement and pozzolan are also discussed.

2. EXPERIMENTAL

The chemical analysis and some physical characteristics of cements and pozzolanas used are described in tables 1 and 2. There are no elements about the portland cement type V, according to ASTM, with exception to C_3A content that was 4.5%. The pozzolanic cement used was a ferric-pozzlanic one, from Italy. The compressive and flexural strengths were determined using prisms with 4 cm x 4 cm x 16 cm; the strength of pozzolanas was measured in pastes of standard consistency with 1 part of lime and 3 parts of pozzolan, by mass.

The pozzolana named Cape Verde is a natural one, existing in the Republic of Cape Verde. Kaoline and diatomite were activated by calcination at 850°C.

The granite, composition of which is presented in table 3, was sieved between 0.8 and 0.4 mm, the grading that has already shown to produce the most rapid alteration of the mortars.

The mortars consisted of 1 part of cementious material, 5 parts of crushed weathered granite sand and 1 part of water, by mass. When using pozzolanas, the cementious material was composed of portland cement and different percentages of pozzolana, varying from 0% to 50%. The mortars were hand mixed and the prisms with 4 cm x 4 cm x 16 cm were also hand consolidated. For each condition, 2 prisms were molded.

The prisms were kept in the molds, in a fog room, for 48 h, and then were either immediately immersed in small plastic tanks filled with sea water, or they were air-cured in the laboratory for 7 d, 28 d, 90 d and 360 d, before immersion. As sea water was encrusting, the protective layer of calcium carbonate was frequently

removed. In the same way, as the pH of the water went up quickly after the contact with the prisms, specially when the prisms were not air-cured, the sea water was also replaced. All the procedures are fully described in an earlier publication [3].

The Fratini test [4] was carried out on pozzolanic cement and on mixes of portland cement and pozzolana.

Cements	SiO_2	Al_3O_3	Fe_2O_3	CaO	MgO	SO_3	K_2O	Na_2O	I.loss
Portland	20.0	6.9	3.5	62.9	2.4	2.1	0.7	0.0	1.5
High alumina	5.5	40.4	16.0	36.6	0.6	Vest.	---	---	0.9
Pozzolanic	29.2	17.0		44.1	2.0	1.1	0.9		5.0
Natural	22.2	6.0	2.6	53.3	3.2	3.6	---	----	7.5
Slag	28.1	7.3	2.1	52.0	4.1	2.3	0.8	0.2	1.6

Pozzolanas	SiO_2	Al_3O_3	Fe_2O_3	CaO	MgO	SO_3	K_2O	Na_2O	I.loss
Cape Verde	49.5	20.2	2.3	1.9	1.7	0.3	5.2	6.2	12.8
Kaoline	52.3	33.2	1.3	0.0	Vest.	0.0	3.6	1.1	8.2
Diatomite	81.0	3.1	4.8	0.5	0.0	0.9	0.4	0.8	10.0

Table 1 Chemical analyses of cements and pozzolanas

Cements and Pozzolanas	45 μm sieve residue %	Surface area Blaine cm^2/g	Mortar or paste strength, MPa			
			Compressive 7 d	28 d	Flexural 7 d	28 d
Portland	----	4270	25.2	35.4	5.3	6.9
High alumina	----	3250	65.5	69.6	6.7	7.4
Pozzolanic	21.1	4430	6.7	19.5	2.0	4.4
Natural	----	4930	4.1	7.5	1.3	2.3
Slag		3800	20.7	33.8	5.2	7.9
Cape Verde	48.0	4270	4.6	10.3	2.0	3.8
Kaoline	15.3	10472	0.6	7.7	0.3	3.6
Diatomite	10.1	23100	2.5	12.6	1.0	3.0

Table 2 Physical characteristics of cements and pozzolanas

Constituents (% by mass)				
Plagioclase	Alkaline feldspar	Quartz	Muscovite	Other minerals
36.6	20.4	31.5	13.0	0.7

Table 3 Composition of weathered granite

3. RESULTS AND DISCUSSION

Results and their discussion will be mainly based on the number of prisms not disrupted, once it was observed that the measured expansion was not a good reference: some prisms cracked under little expansion, others did not crack under high expansion levels.

3.1 Cements

Table 4 presents, for each cement, the number of prisms not disrupted, as a function of the curing time, as well as the time of disruption of the others, that is, the time when a visible crack was recorded.

As shown, the best performance was achieved with natural cement, followed by the pozzolanic one from Italy. According to the theory set out in an earlier publication [2], expansive sulphoaluminate forms only in the presence of calcium hydroxide oversaturated solutions. Therefore, natural cement, with a composition close to that of hydraulic lime, without C_3S and C_3A, does not originate that kind of solutions and so expansive ettringite. The pozzolanic reaction explains the performance of the pozzolanic cement.

The most surprising results were obtained with high alumina cement, usually considered as resistant to sulphate attack. The results are yet more surprising, because other prisms made with not weathered granite evidenced fissuration earlier. It is difficult to find an explanation; maybe this cement does not work well with aggregates of acid nature. Curing time did not change the performance of the cement owing to absence of lime to be hydrated.

Slag cement seems to have excellent performance, on account of results until 7 years, which are compared in fig. 1 with those of a mix of portland cement and 50% of pozzolana, by mass, which showed very good behaviour, as will be seen later. In the two cases the prisms were immersed in sea water 48 h after casting.

3.2 Mixes of portland cement and pozzolana

Table 5 shows, in the same way, the number of prisms disrupted and time until disruption, depending on time of curing and percentage of pozzolana added to cement.

Increasing the percentage of pozzolana, the durability of mortars is also increased: with 40% or 50% of pozzolana, total protection from sulphate attack is obtained, even with 48 h curing. Nevertheless, with other less reactive pozzolanas, the curing time may have to be increased in order to get similar results.

Diatomite was the best pozzolana used, maybe owing to its great surface area. One of the prisms made with the pozzolana of Cape Verde, cured for 7 d, cracked after 6 years approximately, which is thought to be an exceptional result.

3.3 Curing time

The idea behind the consideration of different times of curing was determining the minimum period of cement hydration or pozzolanic reaction to obtain the necessary chemical resistance. As shown in tables 4 and 5, this period depends on the type of cement or on the percentage of pozzolana: it is possible to get good results with only 48 h curing, though increase to 7 or 28 d is always beneficial.

The most salient aspect was total protection obtained when the cure had a duration of 1 year, even for portland cement. As a matter of fact, after 6 months all prisms were completely carbonated, without free calcium hydroxide, which avoided the formation of expansive ettringite. At 7 d, 28 d and 90 d, the depth of carbonation was 2 mm, 7 mm and 14 mm, respectively.

Cements	Prisms not disrupted					Time of disruption, years				
	48 h	7 d	28 d	90 d	360 d	48 h	7 d	28 d	90 d	360 d
Portland	0	0	0	0	2	0.4	2.2	1.2	6.0	>22
High alumina	0	0	0	0	0	4.4	4.3	4.0	2.1	3.1
Pozzolanic	0	0	2	2	2	5.7	6.2	>22	>22	>21
Natural	0	0	2	2	2	12.4	16.3	>22	>22	>21
Slag	2*	-	-	-	-	>7.0	---	---	---	---
Type V	0	-	-	-	-	0.8	---	---	---	---

Table 4 Behaviour of cement mortar prisms as a function of curing time

Pozzolanas	Time of curing	Prisms not disrupted					Time of disruption, years				
		10%	20%	30%	40%	50%	10%	20%	30%	40%	50%
Cape Verde	48 h	0	0	0	1	2	0.9	2.9	5.9	8.9	>23
	7 d	0	0	2	2	1*	3.8	5.2	>23	>23	6.6*
	28 d	0	0	0	2	2	4.0	5.2	5.9	>23	>23
	90 d	0	2	2	2	2	7.2	>23	>23	>23	>23
	360 d	2	2	2	2	2	>22	>22	>22	>22	>22
Kaoline	48 h	0	0	0	2	2	0.5	0.5	13.2	>18	>18
Diatomite	48 h	0	0	2	2	2	1.5	4.2	>17	>17	>18

Table 5 Behaviour of cement and pozzolana mortar prisms as a function of the percentage of pozzolan

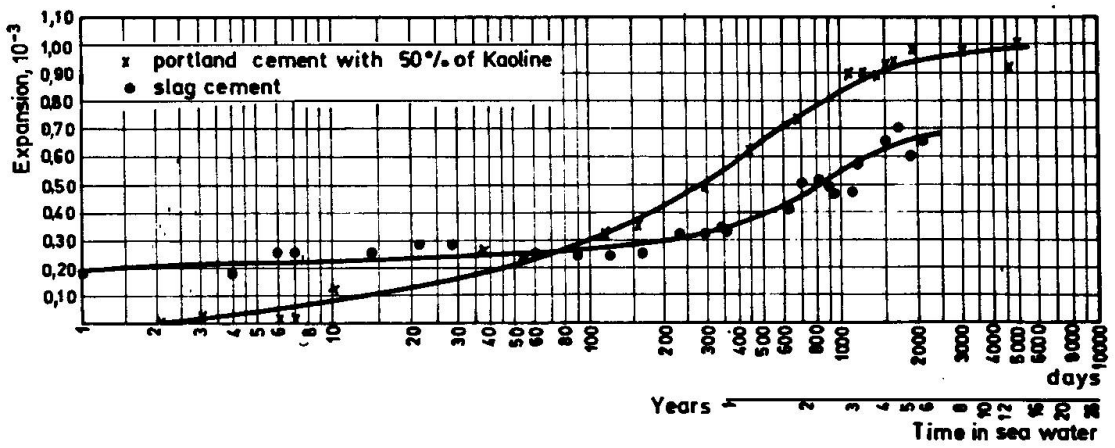

Fig. 1 Expansion of prisms made of two cementious materials

3.4 Fratini test

The Fratini test results were not conclusive to foresee the behaviour of the mixes of cement and pozzolana. Clearly pozzolanic mixes, according to this test, did not show good performance with short curing time. It is believed that the pastes for test should be kept at the same temperature of mortars and tested at the age of their contact with the aggressive medium, so that correlation can be possible. In the standard test the pastes are kept at 40°C for 7 d, which gave rise to an acceleration of the pozzolanic reaction.

4. CONCLUSIONS

The cement that exhibited better performance was the natural one, followed by the ferric-pozzolanic cement: a curing period of 28 d gives total protection against sulphate attack, with this kind of aggregates. With a short cure, 48 h, only slag cement seems to give this protection. High alumina and type V cements did not show good performance.

With an adequate percentage of pozzolan in the mix with portland cement, it is possible to get total protection, even with only 48 h of cure. In the pozzolanas tested, this percentage varied from 30% to 50%.

A curing period of 48 h may be enough for total protection, but increasing it is always advantageous.

The Fratini test does not give information about the behaviour of mixes of portland cement and pozzolana: clearly pozzolanic mixes did not provide total protection with the shorter curing period.

REFERENCES

1. COUTINHO, A. S., Influence de la Nature Minèralogique de l'Agrègat sur la Dècomposition des Mortiers et Bètons de Ciment Portland Exposès à l'Eau de Mer. Cahiers de la Recherche, nº27, Ed. Eyrolles, Paris, 1968.

2. COUTINHO, A. S., Aspects of Sulfate Attack on Concrete. Cement, Concrete and Aggregates, vol. 1, nº 1, 1979.

3. COUTINHO, A. S., Studies on the Resistance of Cements and Pozzolanas to Sea Water Attack. Ed. by LNEC, in Portuguese, Lisbon, 1982.

4. FRATINI, N., Controllo Chimico dei Cementi Pozolanici. An. di Chim., vol. 44, September 1954.